

CONTRACT NAS 1-14000

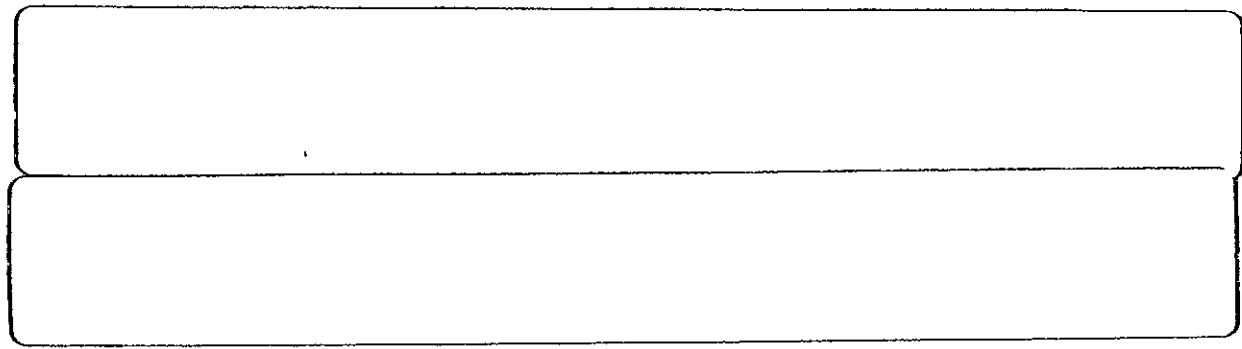
# FLIGHT SERVICE EVALUATION OF AN ADVANCED COMPOSITE EMPENNAGE COMPONENT ON COMMERCIAL TRANSPORT AIRCRAFT

(NASA-CR-144986) FLIGHT SERVICE EVALUATION OF AN ADVANCED COMPOSITE EMPENNAGE COMPONENT ON COMMERCIAL TRANSPORT AIRCRAFT. PHASE 1: ENGINEERING DEVELOPMENT Final Report, 9 Jun. - 31 Dec. 1975 (Lockheed-California	N78-23080	Unclas 17137
---	-----------	-----------------

## PHASE I - FINAL REPORT ENGINEERING DEVELOPMENT

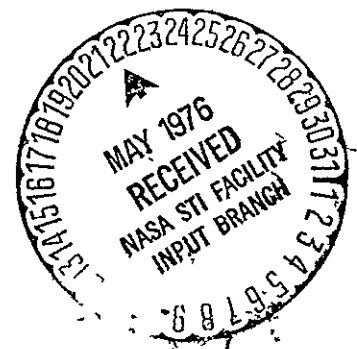
This report is for the period 9 June through 31 December 1975

Lockheed Aircraft Corporation  
Lockheed-California Company  
Post Office Box 551  
Burbank, California 91520



May 1976

Prepared for Langley Research Center



1 REPORT NO. NASA CR-144986	2. GOVERNMENT ACCESSION NO.	3. RECIPIENT'S CATALOG NO
4. TITLE AND SUBTITLE Flight Service Evaluation of an Advanced Composite Empennage Component on Commercial Transport Aircraft: Phase I - Final Report Engineering Development		5 REPORT DATE May 1976
		6. PERFORMING ORG CODE
7 AUTHOR(S) A. Ary, C. Axtell, L. Fogg, A. Jackson, A. James, B. Mosesian, J. Vanderwier, J. Van Hamersveld		8 PERFORMING ORG REPORT NO. LR 27543
9 PERFORMING ORGANIZATION NAME AND ADDRESS LOCKHEED-CALIFORNIA COMPANY P O. BOX 551 BURBANK, CALIFORNIA 91520		10 WORK UNIT NO
		11. CONTRACT OR GRANT NO NAS 1-14000
12 SPONSORING AGENCY NAME AND ADDRESS National Aeronautics and Space Administration Langley Research Center Hampton, Virginia 23665		13. TYPE OF REPORT AND PERIOD COVERED Contract Report 9 June 1975-31 Dec 1975
		14 SPONSORING AGENCY CODE
15. SUPPLEMENTARY NOTES None		
16 ABSTRACT This is the final report of technical work conducted during the first phase of a multiphase program having the objective of the design, development, and flight evaluation of an advanced composite empennage component, manufactured in a production environment, at a cost competitive with those of its metal counterpart, and at a weight saving of at least 20 percent. The empennage component selected for this program is the vertical fin box of the L-1011 aircraft. The box structure extends from the fuselage production joint to the tip rib and includes the front and rear spars. Various design options such as stiffened covers and sandwich covers were evaluated to arrive at a configuration which would offer the highest potential for satisfying program objectives. The preferred configuration selected consists of a hat-stiffened cover with molded integrally stiffened spars, aluminum trussed composite ribs, and composite miniwich web ribs with integrally molded caps. Material screening tests were performed to select an advanced composite material system for the Advanced Composite Vertical Fin (ACVF) that would meet the program requirements from the standpoint of quality, reproducibility, and cost. Preliminary weight and cost analysis has been made, targets established, and tracking plans developed. Plans for subsequent phases were also developed in this phase. These include FAA certification, ancillary test program, quality control, and structural integrity control plans.		
17. KEY WORDS (SUGGESTED BY AUTHOR(S)) Composites                      Testing Materials                        Fabrication Preliminary Design          Manufacturing Structural Analysis          Transport Aircraft		
19. SECURITY CLASSIF (OF THIS REPORT) Unclassified	20 SECURITY CLA Unclassified	

CONTRACT NAS 1-14000

**FLIGHT SERVICE EVALUATION OF AN ADVANCED  
COMPOSITE EMPENNAGE COMPONENT ON  
COMMERCIAL TRANSPORT AIRCRAFT**

**PHASE I – FINAL REPORT  
ENGINEERING DEVELOPMENT**

This report is for the period 9 June through 31 December 1975

Lockheed Aircraft Corporation  
Lockheed-California Company  
Post Office Box 551  
Burbank, California 91520

May 1976

Prepared for Langley Research Center

## FOREWORD

This report was prepared by the Lockheed-California Company, Lockheed Aircraft Corporation, Burbank, California, under Contract NAS1-14000, Flight Service Evaluation of an Advanced Composite Empennage Component on Commercial Transport Aircraft. It is the final report of Phase I - Engineering Development activity covering work completed between 9 June 1975, the effective date of this contract, and 31 December 1975. This program is sponsored by the National Aeronautics and Space Administration (NASA), Langley Research Center. The Program Manager for Lockheed is Mr. Robert L. Vaughn. Mr. Louis F. Vosteen is Project Manager for NASA, Langley. The Technical Representative for NASA is Mr. R. Ronald Clary.



## TABLE OF CONTENTS

Section	Page
FOREWORD	iii
LIST OF FIGURES	vii
LIST OF TABLES	xiii
SUMMARY	1
LIST OF SYMBOLS	2
1.0 INTRODUCTION	5
2.0 TASK 1 - CONCEPT DEVELOPMENT	11
2.1 PRELIMINARY DESIGN	11
2.1.1 Trade-Off Studies	11
2.1.2 Weight Status	41
2.1.3 Cost Status	41
2.1.4 Test Specimen Design	41
2.1.5 Loft and Interface Drawings	41
2.2 STRUCTURAL ANALYSIS	47
2.2.1 Analytical Approach	48
2.2.2 Preliminary Design Allowables	48
2.2.3 Design Criteria	53
2.2.4 Hat Stiffened Cover Analysis	55
2.2.5 Honeycomb Cover Analysis	67
2.2.6 Analysis of Honeycomb Tip Runout	68
2.2.7 Spar Analysis	69
2.2.8 Rib Analysis	74
2.2.9 NASTRAN Model	83
2.2.10 FAA Certification Plan	86
2.3 PRELIMINARY ANCILLARY TEST PLAN	88
2.4 STRUCTURAL INTEGRITY AND QUALITY CONTROL PLANS	89
2.4.1 Structural Integrity Control Plan	89
2.4.2 Quality Control Plan	99

TABLE OF CONTENTS (Continued)

Section	Page
2.5	CONCEPT EVALUATION TESTS 100
3.0	TASK 2 MATERIAL SELECTION 105
3.1	CANDIDATE MATERIALS 105
3.2	MATERIAL SELECTION - ANALYSIS AND TEST RESULTS 106
3.2.1	Qualitative Analysis 106
3.2.2	Screening Test Results 107
3.3	SELECTED MATERIAL 119
3.3.1	Material Specification 120
3.3.2	Qualification of T300/5209 120
4.0	TASK 3 - FABRICATION 124
4.1	PRODUCIBILITY CONSIDERATION STUDIES 124
4.1.1	Skin Cover Concepts 124
4.1.2	Spar Concepts 134
4.1.3	Rib Concepts 134
4.2	PRELIMINARY FABRICATION PLANS 138
4.2.1	Skin Covers 138
4.2.2	Spars and Ribs 141
4.3	ASSEMBLY 141
4.4	TEST SPECIMEN 141
4.4.1	Skin Covers 141
5.0	TASK 4 - TOOLING DEVELOPMENT 151
5.1	TOOLING CONCEPTS 151
5.2	TOOL DESIGN AND FABRICATION 157
5.2.1	Skin Covers 157
5.2.2	Spars 168
5.2.3	Ribs 170
5.3	FINAL ASSEMBLY 170
6.0	PRELIMINARY DESIGN REVIEW (PDR) 177
	APPENDIX A MATERIAL SELECTION AND EVALUATION PLAN 179
	LIST OF REFERENCES 187

## LIST OF FIGURES

Figure		Page
1	L-1011 Advanced Composite Vertical Fin Program - Program Master Schedule	6
2	Program Responsibilities	7
3	L-1011 Advanced Composite Vertical Fin Program - Detail Schedule Phase I	10
4	L-1011 Vertical Fin Box Structure	12
5	Composite Fin Geometry	13
6	Concept Evaluation	15
7	Honeycomb Skin Panels	18
8	Alternate Rib Attachments Blade Stiffener Configuration	20
9	A-Frame Stiffener Cover Configuration	20
10	Rib Attachment I-beam Stiffener Configuration	20
11	I-beam Stiffened Skin Panel	20
12	Stiffener Configuration	21
13	Hat Section Stiffener	21
14	Skin Stiffener Spacing	22
15	Rib to Cover and Hat Section Joint	22
16	Stiffener Runout	23
17	Spanwise Cover Thickness Variation	25
18	Hat Stiffened Cover Concept	26
19	Study Concepts - Spars	27
20	Integrally Stiffened Design	28

LIST OF FIGURES (Continued)

Figure		Page
21	Spar Stiffener Configuration	29
22	Miniwich Spar Design	30
23	Spar Weight and Cost Summary	31
24	Selected Spar Configuration	33
25	Fin Rib Locations	34
26	Hinge/Actuator Rib Concept	36
27	Hinge Rib Truss Concept	36
28	Hinge and Intermediate Stiffened Web Rib Concept for Lower Seven Ribs	37
29	Hinge and Intermediate Miniwich Rib Concept for Lower Seven Ribs	37
30	Hinge and Intermediate Miniwich Rib Concept for Upper Three Ribs	38
31	Hinge and Intermediate Stiffened Web Rib Concept for Upper Three Ribs	38
32	Advanced Composite Vertical Fin Configuration	44
33	Weight-Time History	44
34	Hat Section Specimen	46
35	Structural Analysis Flow Chart	48
36	Sample Run of HYBRID Computer Program	56
37	Design Loads and Stiffener Spacing	59
38	Typical Cover Area	60
39	Skin-Stiffener Section	61
40	Honeycomb Cover Tip Runout	69
41	Shear Buckling Coefficients of Simply Supported, Orthotropic Plates	70

LIST OF FIGURES (Continued)

Figure		Page
42	Spar Web Tee Stiffener	71
43	Spar Tie Cap Cross Section	72
44	Design Net Strength of Graphite/Epoxy Laminates With Holes	73
45	VSS 145.71 Hinge Rib 2D Model	75
46	Metal Rib Cap Cross Section	78
47	Preliminary Composite Rib Cap Concept	79
48	Rib Cap Load Application	79
49	Resized Composite Rib Cap	81
50	Idealized Rib Cap Flange	82
51	Fin Structural Model	84
52	NASTRAN Model Left Surface	84
53	NASTRAN Model Element Numbering System	85
54	Development Test Coverage	89
55	Structural Integrity Control Plan	98
56	Joint Test Specimens	101
57	Stiffener Root Joint Tension Test	103
58	Location of Strain Gages	103
59	Tension Test Load Strain Gage Plots	104
60	Mechanical Properties Comparison	112
61	$O_4/90_4$ Warp Panel Comparison	115
62	Autoclave Cure Cycle Comparison	117
63	Ortho Grid Blade Stiffened Skin Cover	124
64	A-Frame Section Stiffened Skin Cover	126
65	I-Beam Section Stiffened Skin Cover	127

LIST OF FIGURES (Continued)

Figure		Page
66	Hat Section Stiffened Skin Cover - Male Tool Concept	128
67	Hat Section Stiffened Skin Cover - Female Tool Concept	129
68	Hat Section Stiffened Skin Cover - Root End Flare Out	130
69	Honeycomb Skin Cover - Continuous Core	131
70	Honeycomb Skin Cover - Runout at Rib Station	133
71	Baseline Tooling Concept-Miniwich Ribs	135
72	Baseplate Tooling Concept-Truss Rib Caps	137
73	Cover Fabrication	140
74	Spar Fabrication	142
75	Truss Rib Cap/Clip Fabrication	143
76	Composite Vertical Fin Box Assembly Sequence	144
77	Hat Stiffener Tooling	146
78	Cover Fabrication Tool Types	152
79	Spar Fabrication Tool Types	153
80	Thermal Expansion of Elastomeric Tooling for Spars	154
81	Miniwich Rib Fabrication Tool Types	155
82	Truss Rib Fabrication Tool Types	156
83	Drilled Tooling Modification for Composite Assembly	158
84	Flat Table Layup Block	160
85	Layup Block	160
86	Skin Bonding Tool	160
87	Broad Goods Layup Tool	161
88	Aluminum Hat Tool	162
89	Bag and Bleeder Arrangement for Hat Section	162

LIST OF FIGURES (Continued)

Figure		Page
90	Cured Hat Section	163
91	Hat Stiffener for Fin Cover	163
92	Bond Surface of Hat Flanges	165
93	Hat Section Closeout Tool	165
94	Hat Section Fabrication Development	166
95	Fabrication of Hat Section with Integral Closeout	166
96	Hat Section with Integral Closeout	167
97	Four-Ply Thickness Transition Area on Inner Surface of Skin	167
98	Typical Bonding Development Specimen	168
99	Manufacturing and Tooling Considerations - Spars	169
100	Hand Hole Reinforcement Shear Web Test Specimen	169
101	Prototype Spar Tool	171
102	Spar Tooling	172
103	First Molded Spar Section	173
104	Assembly Flow Miniwich Ribs	174
105	Assembly Flow Truss Ribs	175
106	Final Assembly Fixture	176

LIST OF TABLES

Table		Page
1	Weight Summary - Metal Fin	14
2	Cost Summary - Metal Fin (250 Aircraft)	14
3	Fin Study - Cost/Weight Summary	17
4	Hat Section Stiffener Configuration Comparison	24
5	Cover Panel Comparison	25
6	L-1011 ACVF Spar Concept Selection Configurations	32
7	L-1011 Composite Vertical Fin - Rib Weight Trade Summary	39
8	Weight Status Report	42
9	Summary of Weight Changes	43
10	Projected Production/Maintenance Cost	45
11	Preliminary Design Properties for Dry Graphite/Epoxy For Linear Programs	49
12	Preliminary Estimate of Environmental Reduction Factors	51
13	Calculated Environmental Effects on Laminates	52
14	Gt and Et Matching	62
15	Initial Skin and Crown Information	63
16	Skin-Stiffener Element Loadings	66
17	EI and Et Comparison	67
18	Beam Element Loads	76
19	Axial Element Loads	77
20	Beam Element Stresses	80
21	Stresses in Beam Elements 9 and 10	81



LIST OF TABLES (Continued)

Table		Page
22	Critical Load Conditions	85
23	Material Qualification - Ancillary Test	90
24	Design Data - Ancillary Test	91
25	Concept Verification - Ancillary Test	93
26	Fabrication and Assembly Procedure Verification - Ancillary Test	96
27	Candidate Materials	105
28	Qualitative Material Screening	106
29	Physical Properties	108
30	Material Screening Test Results	110
31	Effect of Thermal Residual Stresses on Strength	118
32	Status of Materials and Engineering Process Specification	121
33	Qualification Testing Results T300/5209	122
34	Producibility Rating, Rib Configurations	139
35	Manufacturing Estimates; Rib VSS 145.71 (10 Ribs)	139
36	Bleeder Ply Test Panel Characteristics	150



## SYMBOLS

Measurement values used in this report are stated in SI units followed by customary units in parentheses.

<u>Symbol</u>	<u>Definition</u>
A	Area
[A]	In-plane stiffness matrix
$A_i$	Area of element i
$A_{ij}$	Terms of the A matrix
A1	Axial element area
A2	Axial element area
ALFA	Coefficient of thermal expansion
$C_{max}$	Distance from neutral axis to extreme fiber of rib cap
D	Diameter
[D]	Bending stiffness matrix
$D_{ij}$	Terms of the D matrix
E	Youngs modulus
E1	Longitudinal ply stiffness
E2	Transverse ply stiffness
$E_i$	Youngs modulus of element i
$E_x$	Laminate longitudinal modulus
EI	Bending stiffness
EPSU	Ply strain allowable
Et	Youngs modulus times thickness
F	Stress allowable
$F_{x,cr}$	Buckling stress
G	Shear modulus

<u>Symbol</u>	<u>Definition</u>
$G_{xy}$	Laminate shear modulus
GJ	Torsional stiffness
Gt	Shear modulus times thickness
GW	Gross weight
H	Distance between rib caps
$I_{xx}$	Moment of Inertia about the XX axis
L	Rib spacing or length
L'	Effective column length
$L_e$	Effective length
M	Moment or Mach number
N1	Node 1
N2	Node 2
$N_0$	Number of $0^\circ$ plies
$N_{45}$	Number of $(+45)_s$ plysets
$N_{x,i}$	Load per element i
$N_x$	Applied load, axial loading
$N_{x,cr}$	Column buckling load or buckling load
$N_y$	Applied load in Y direction
$N_{xy}$	Applied shear load
$N_{xy,cr}$	Shear buckling load
NU	Ply Poisson's ratio
P	Force
$S_y$	Applied external load in Y direction
T	Skin thickness
V	Velocity

<u>Symbol</u>	<u>Definition</u>
W	Stiffener spacing or width
a	Panel length or stiffener crown width
b	Panel length or panel width between stiffeners
$b_i$	Width of element i
b'	Effective width between stiffeners
c	Ratio of column length to critical column length
$f_{b,max}$	Bending stress
h	Thickness, height, or distance from spar cap centroid to box centerline
$\bar{h}$	Mean distance from the skin to box centerline
$k_s$	Shear buckling coefficient
p	Pressure
r	Flange radius
t	Thickness
$t_i$	Thickness of element i
y	Distance from neutral axis
Y	Ratio of flexural rigidity of stiffener to rigidity of plate
$\delta_F$	Flap angle
$\delta_{sp}$	Spoiler angle
$\epsilon$	Strain allowable
$\sigma$	Stress

Superscripts

cu	Compression ultimate
tu	Tension ultimate

<u>Symbol</u>	<u>Definition</u>
Superscripts	
su	Shear ultimate
ty	Tension yield
Subscripts	
L	Longitudinal
LT	Longitudinal - Transverse
T	Transverse

## 1.0 INTRODUCTION

This is the final report of technical work conducted during the first phase of a multiphase program which provides for the design, development, and fabrication of three advanced composite empennage components. One component will be static and fatigue tested, and two components will be installed on commercial aircraft for 5-year flight evaluations. This NASA contract was awarded to Lockheed-California Company, Burbank, California, in the amount of \$6 510 000. The Program Manager for Lockheed is Mr. Robert L. Vaughn. Mr. Louis F. Vosteen is Project Manager for NASA, Langley. The Technical Representative for NASA, Langley, is Mr. R. Ronald Clary.

The objective of this program is the development and flight evaluation of an advanced composite empennage component, manufactured in a production environment, at a cost competitive with those of its metal counterpart, and at a weight saving of at least 20 percent. The empennage component selected for this program is the vertical fin box of the L-1011 aircraft. The box structure extends from the fuselage production joint to the tip rib and includes the front and rear spars; it is 7.62 m (25 ft) tall with a root box chord of 2.74 m (9 ft) and represents an area of 13.94 m<sup>2</sup> (150 ft<sup>2</sup>).

The duration of this program is 106 months, with completion scheduled for March 1984. The master schedule for this program is shown in Figure 1. The dotted line in this figure represents the critical path.

The Lockheed-California Company has teamed with the Lockheed-Georgia Company and the Los Angeles Aircraft Division of Rockwell International (LAAD) in the development of the Advanced Composite Vertical Fin (ACVF). Team member responsibilities are shown in Figure 2. The California Company, as prime contractor, has overall program responsibility and will design and fabricate the covers, conduct the full-scale ground tests, install the flight

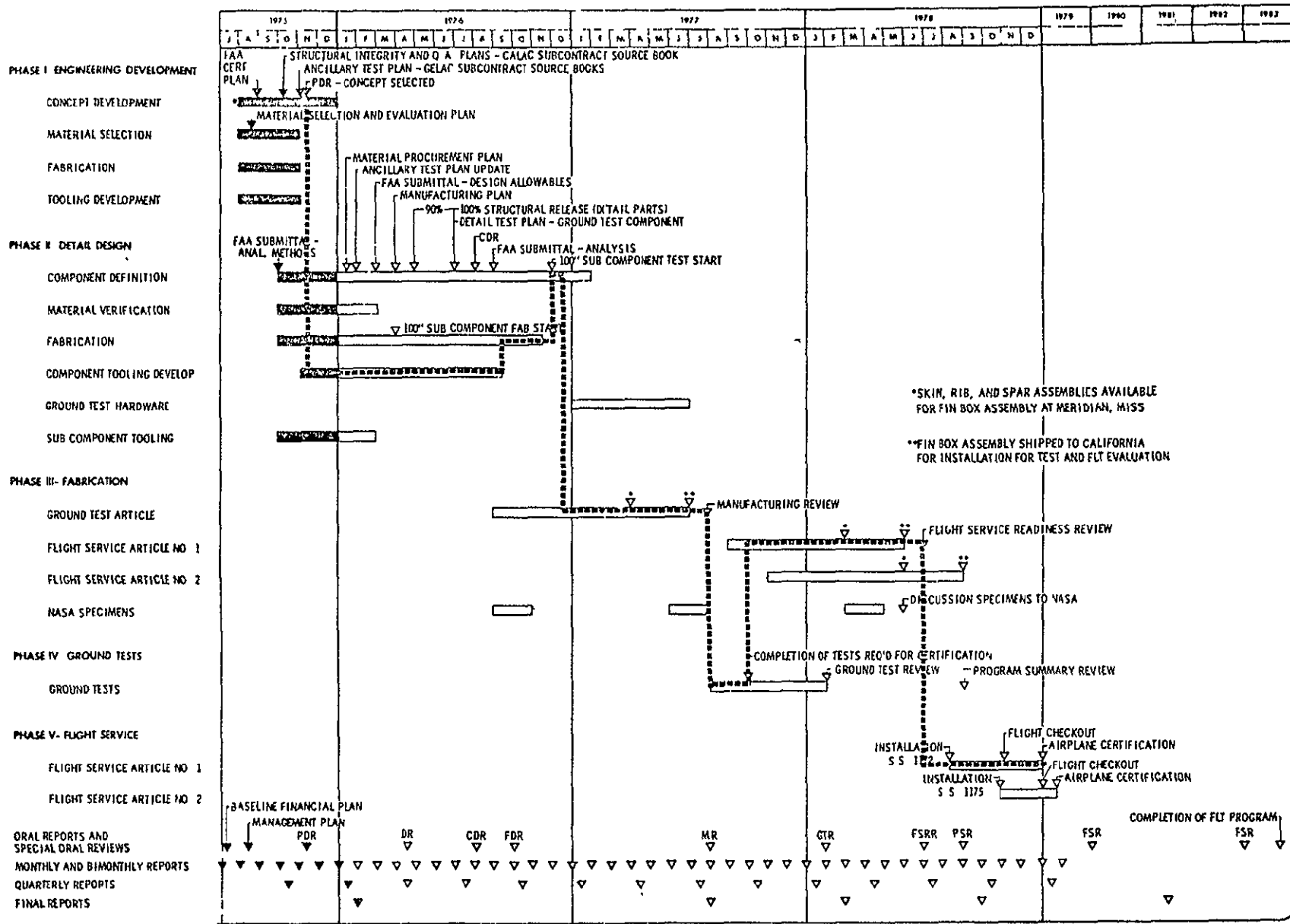


Figure 1. L-1011 Advanced Composite Vertical Fin Program - Program Master Schedule

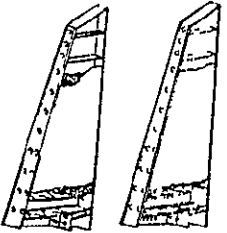
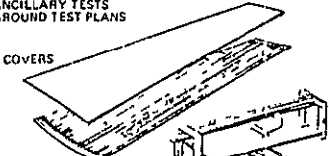

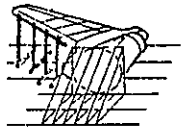

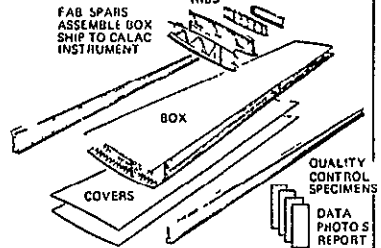
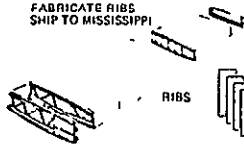

	PHASE I ENGINEERING DEVELOPMENT	PHASE II DETAIL DESIGN	PHASE III FABRICATION	PHASE IV GROUND TESTS	PHASE V FLIGHT SERVICE
LOCKHEED CALIFORNIA CO	PRELIMINARY DESIGN DESIGN DOCUMENTATION PROGRAM PLANS CONCEPT EVALUATION TESTS COST WEIGHT ESTIMATES 	DESIGN AND ANALYSIS OF COVERS DESIGN AND FABRICATE TOOLING MANUFACTURING PLANS ANCILLARY TESTS GROUND TEST PLANS COVERS  COVER PANEL SUB COMPONENTS TORQUE BOX BROAD GOODS DISPENSING MACHINE DATA PHOTOS REPORT	FABRICATE COVERS SHIP TO MISSISSIPPI  QUALITY CONTROL SPECIMENS DATA PHOTOS REPORT	GROUND TESTS VIBRATION FATIGUE ULTIMATE FAIL SAFE, RESIDUAL STRENGTH  DATA PHOTOS REPORT	FLIGHT TEST STORE METAL FINS PERIODIC INSPECTIONS  INSTALL METAL FINS SHIP COMPOSITE FINS TO NASA DATA PHOTOS REPORT
LOCKHEED GEORGIA CO	FURNISH PERSONNEL TO CALAC	DESIGN AND ANALYSIS OF SPARS DESIGN AND FABRICATE TOOLING MANUFACTURING PLANS ANCILLARY TESTS FRONT SPAR AUX SPAR REAR SPAR SPAR SUB COMPONENTS DATA PHOTOS REPORT	FAB SPARS ASSEMBLE BOX SHIP TO CALAC INSTRUMENT  QUALITY CONTROL SPECIMENS DATA PHOTOS REPORT	WITNESS TESTING	NO EFFORT
LOS ANGELES AIRPLANE DIV / ROCKWELL	FURNISH PERSONNEL TO CALAC	DESIGN AND ANALYSIS OF RIBS DESIGN AND FABRICATE TOOLING MANUFACTURING PLANS ANCILLARY TESTS RIBS SUB COMPONENTS DATA PHOTOS REPORT	FABRICATE RIBS SHIP TO MISSISSIPPI  QUALITY CONTROL SPECIMENS DATA PHOTOS REPORT	WITNESS TESTING	NO EFFORT
AIRLINES FAA	CONSULTING-LIAISON	CONSULTING ANALYSIS APPROVAL	LIAISON	LIAISON COMPONENT CERTIFICATION	FLIGHT EVALUATION  L 1011 FLY 5 YEARS

Figure 2. Program Responsibilities

ORIGINAL PAGE IS  
OF POOR QUALITY



articles, and evaluate service experience; the Georgia Company will design and fabricate the front, rear, and auxiliary spars, and assemble the component at their plant in Meridian, Mississippi, where the present L-1011 vertical fins are assembled; and LAAD will design and fabricate all ribs.

Prior to the initiation of Phase I technical activity, a Program Management Plan was prepared and subsequently approved by NASA for implementation. The plan covers the assignments and responsibilities of the prime contractor and the subcontractors. The overall responsibility of each contractor is defined in relationship to a work breakdown structure with emphasis placed on methods to be employed in controlling technical, schedule, and cost performance. In addition, the plan sets forth the program objectives, scope, and a statement of work by work breakdown structure elements.

As part of the cost and scheduling system being used on this program, time phased logic flow diagrams with appropriate graphic displays to depict program status was also developed. The program status is presented as a movable display on a patented wall board (PLANALOG) in the program office at Calac. This display is also duplicated in the project office at NASA, Langley.

During Phase I, various design options such as stiffened covers and sandwich covers were evaluated to arrive at a configuration which would offer the highest potential for satisfying program objectives. The preferred configuration was selected in November 1975. Material screening tests were performed to select an advanced composite material system for the ACVF that would meet the program requirements from the standpoint of quality, reproducibility, and cost. Preliminary weight and cost analysis has been made, targets established, and tracking plans developed. Plans for subsequent phases were also developed in this phase. These include FAA certification, ancillary test program, quality control, and structural integrity control plans. The majority of the Phase I effort was concluded when the results of Phase I activities were presented to NASA at a Preliminary Design Review (PDR) held on 12 November 1975. All technical effort associated with Phase I tasks was concluded on 31 December 1975.

Phase II covers the main engineering effort. Detail design, analysis, and development testing will be accomplished. One significant test which will be accomplished will be on a subcomponent consisting of a major portion of the box structure. This component will be fabricated from representative production tooling and consists of 2.54 meters (100 in.) of the rear spar and 0.914 meters (36 in.) of the box chord and will include the fuselage/box joint. Limited production tooling will be designed and fabricated, and plans for the fabrication of the full-scale components will be written. Phase III provides for the fabrication of the full-scale ground test component and the two components to be used for flight service evaluation. Fabrication of the flight service articles will not begin until after certification tests on the full-scale ground test component have started. During fabrication, actual costs will be documented and components weighed to develop the weight update for the assembled structures.

Ground tests will be conducted on a full-scale vertical fin box beam structure mounted on a fuselage afterbody structure during Phase IV. The test plan will include vibration to determine modal response characteristics, static tests, spectrum fatigue tests to two lifetimes, ultimate load, damage tolerance and fail-safe, and residual strength tests. Repair techniques and procedures established for inservice maintenance and inspection will be employed throughout these tests, if necessary. The test results will be used to verify the analytical, design, and fabrication procedures, and are an essential input to the FAA for certification of the aircraft with the ACVF installed. Certification will be based on satisfying both static strength and fail-safe requirements. Phase V provides for the installation of two ACVF's on commercial aircraft for flight service evaluation for a period of 5 years. Inspection procedures and inspection intervals will be established in conjunction with the participating airlines. Prior to delivery and introduction into regular service, each aircraft will be processed through normal predelivery and other flight tests if required by Engineering and the FAA.

Throughout this program, technical information gathered during performance of the contract will be disseminated throughout the industry and Government. The methods used to distribute this information will be through Technical Highlight Bulletins, to be distributed bimonthly throughout the entire program; Quarterly Reports, which will coincide with calendar quarters; Final Reports, to be distributed at the completion of each phase; and Flight Service Reports. All test data and fabrication data will be recorded on Air Force Data Sheets for incorporation in the Air Force Design Guide and Fabrication Guide for Advanced Composites. Of particular interest are the Special Oral Reviews to be conducted at NASA, Langley, to acquaint industry and the Government with the progress of the program. These reviews follow soon after the Preliminary Design Review (PDR), the Critical Design Review (CDR), and the Flight Service Readiness Review (FSRR). Specific information about the design reviews will be distributed later in the program.

This report describes all the technical work associated with Phase I - Engineering Development, in addition to summarizing program management plans. This work was accomplished during a period extending from 9 June 1975, the effective date of this contract, and 31 December 1975. The detail schedule of Phase I technical activity is shown on Figure 3. This report is structured according to the tasks and subtasks identified on this schedule. All of the tasks, subtasks, milestones, reports, etc. identified on Figure 3 have been completed and/or met.

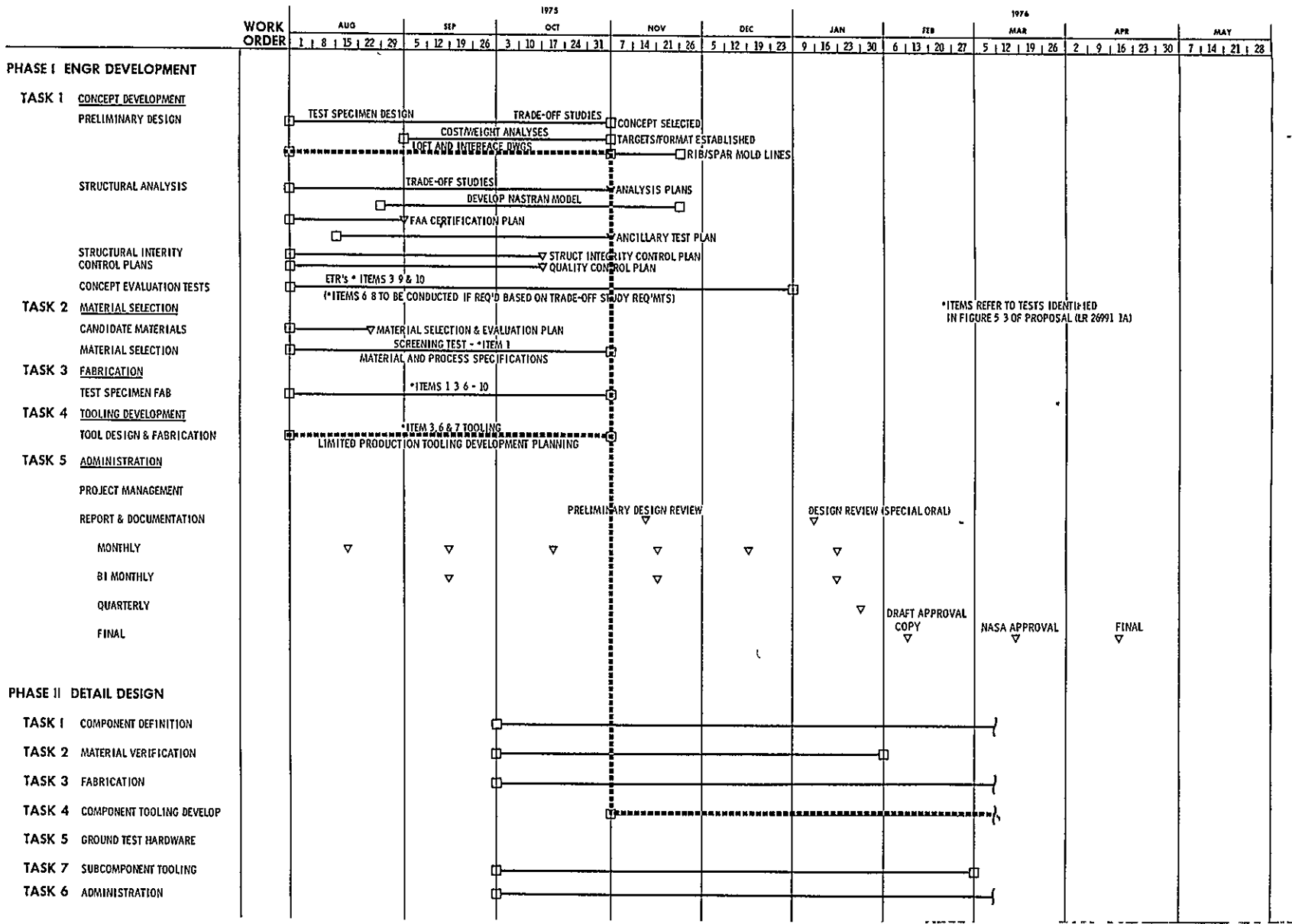


Figure 3. L-1011 Advanced Composite Vertical Fin Program - Detail Schedule Phase I

## 2.0 TASK 1 - CONCEPT DEVELOPMENT

The primary objective of the Phase I activities was to design and select a composite material fin box configuration as a replacement for the all-metal vertical fin box currently in service on the L-1011 aircraft. This replacement is to be accomplished by meeting specific cost/weight goals, functional and structural criterion, and fabrication, assembly, and in-service guidelines.

The team members were located at Lockheed's Burbank, California, facility to conduct the design activities of Phase I which included: (1) design of selected test specimens, (2) design trade-off studies, (3) weight/cost trade-offs, and (4) loft and interface definition. These activities were initiated 28 July 1975 and terminated 31 December 1975.

### 2.1 PRELIMINARY DESIGN

The existing vertical stabilizer box shown in Figure 4 is a conventional all aluminum structure consisting of two main spars, front and rear, one auxiliary spar, five rudder hinge support ribs, ten intermediate ribs, two stub ribs, and eight angle stiffened cover assemblies. The primary structural material is 7075-T6 aluminum alloy. The structural geometry as shown in Figure 5 is approximately 7.62 m (25 ft) long at the rear spar and has chord dimensions of approximately 2.7 and 1.2 m (nine and four ft) respectively at the root and tip. The current weight and cost data for the existing metal structure are given in Table 1 and Table 2 respectively.

A replacement design philosophy generally imposes some restrictions on the redesign of a component. The primary restrictions imposed on the fin box design are the retention of the fuselage/root attachment interface, and retention of the rudder hinge locations which of necessity dictated five rib locations. The implications of these restrictions will be discussed later in the report in the trade-off design studies.

#### 2.1.1 Trade-Off Studies

Figure 6 depicts a matrix of primary and alternate candidates considered in the design concept evaluation. The final concept definition requires the integration of the trade-off studies in the areas of cover panel, spar, and rib design; however, the presentation of the trade-off data is more readily accomplished with separate discussions of the covers, spars, and ribs.



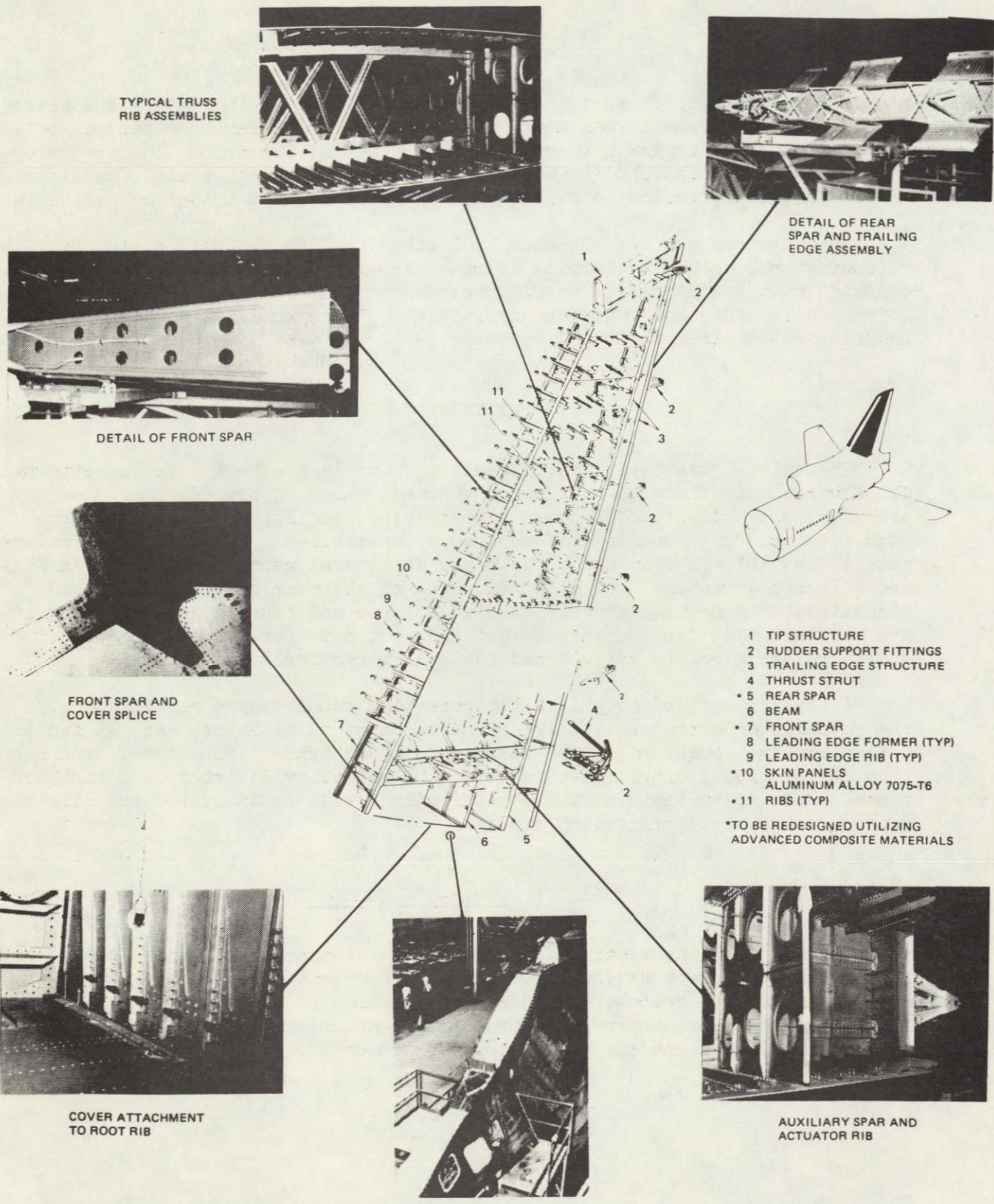


Figure 4. L-1011 Vertical Fin Box Structure

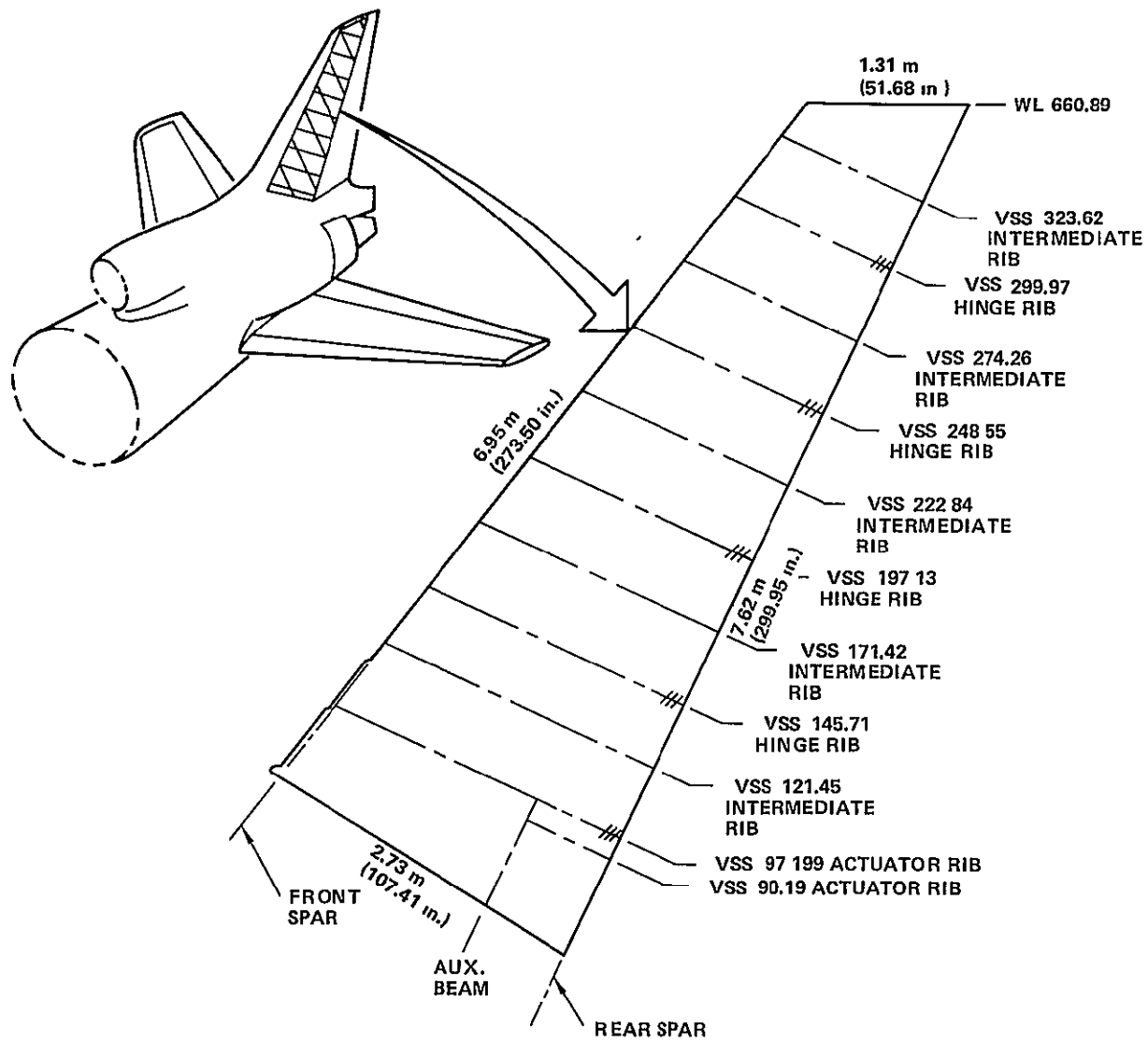


Figure 5. Composite Fin Geometry

TABLE 1. WEIGHT SUMMARY ~ METAL FIN

	Weight	
	kg	(lb)
Covers	208.8	(460.4)
Front Spar	43.9	(96.8)
Rear Spar	42.0	(92.6)
Auxiliary Spar	3.0	(6.6)
Actuator Ribs	18.8	(41.4)
Hinge Ribs	15.2	(33.4)
Intermediate Ribs	28.8	(63.4)
Rib Fittings	8.2	(18.1)
Assembly Hardware	16.1	(35.4)
Protective Finish	4.4	(9.6)
Total Torque Box	389.0	(857.7)

TABLE 2. COST SUMMARY ~ METAL FIN (250 AIRCRAFT)

	250 Aircraft		
	Material \$	Labor \$	Total \$
Covers	2960	14 467	17 427
Spars	1259	9656	10 915
Ribs	992	10 154	11 046
Rib Fittings	301	283	584
Assembly	5752	17 185	22 937
Total	11 164	51 745	62 909

	COVERS (STIFFENED)	COVERS (HONEYCOMB)	FUSELAGE JOINT (STIFFENED)	FUSELAGE JOINT (HONEYCOMB)	RIBS (STIFFENED)	RIBS (HONEYCOMB)	SPARS	ASSEMBLY SEQUENCE
PRIMARY CONCEPTS	<p>CONSTANT SPACING</p> <p>THICKNESS TAPER</p> <p>HAT STIFFENER (HAND LAY UP)</p>	<p>POTTING</p> <p>C RIB</p> <p>PRECURED FACE SHEETS</p> <p>CONTINUOUS CORE</p>	<p>MOLDED TRANSITION</p>	<p>MOLDED GRAPHITE INSERT</p> <p>BALANCED TRANSITION</p>	<p>MOLDED MINIRICH</p> <p>(AND)</p> <p>GR/EP CAPS</p> <p>ALUM DIAGONALS</p> <p>TRUSS RIB</p>	<p>MOLDED MINIRICH</p> <p>(AND)</p> <p>GR/EP CAPS</p> <p>ALUM DIAGONALS</p> <p>TRUSS RIB</p>	<p>MOLDED MINIRICH</p>	<p>ACCESS PROVIDED THRU FRONT SPAR APERTURE</p>
ALTERNATE CONCEPTS	<p>(a) CONSTANT CROSS SECTION PULTRUSION</p> <p>HAT STIFFENER</p> <p>(b) TAPERED THICKNESS HEIGHT AND WIDTH</p> <p>HAT STIFFENER CONVERGING SPACING</p> <p>(c) CONVERGING PULTRUSION</p> <p>A STIFFENER</p> <p>(d)</p> <p>I STIFFENER</p>	<p>(a) PRECURED SKINS</p> <p>C RIB</p> <p>PAN DOWN AT RIBS</p> <p>(b) INNER SKIN COCURED</p> <p>(c) BOTH SKINS COCURED</p> <p>C RIB</p> <p>(d) INNER SKIN COCURED</p> <p>(e) BOTH SKINS COCURED</p> <p>POTTING</p> <p>C RIB</p>	<p>(a)</p> <p>MACHINED RUNOUT</p> <p>(b)</p> <p>SECONDARY BONDED REINFORCEMENT</p>	<p>(a)</p> <p>FACE SHEETS TRANSITION INTO JOINT</p>	<p>(a)</p> <p>BEADED TRUSS</p> <p>A-A</p> <p>(b)</p> <p>STIFFENED WEB</p> <p>B-B</p> <p>(c)</p> <p>BUILT UP MINIRICH</p> <p>C-C</p>	<p>(a)</p> <p>BEADED TRUSS</p> <p>A-A</p> <p>(b)</p> <p>STIFFENED WEB</p> <p>B-B</p> <p>(c)</p> <p>SINE WAVE WEB</p> <p>C-C</p>	<p>(a)</p> <p>STIFFENED WEB</p> <p>A-A</p> <p>(b)</p> <p>STIFFENED WEB</p> <p>B-B</p> <p>(c)</p> <p>SINE WAVE WEB</p> <p>B-B</p>	<p>(a)</p> <p>REMOVEABLE TRUSSES TO PROVIDE ACCESS FROM ROOT RIB</p> <p>(b)</p> <p>SPANWISE SPLICE</p> <p>FASTENERS IN AFT PANEL ACCESSIBLE THRU HOLES IN REAR BEAM</p>

Figure 6. Concept Evaluation



### 2.1.1.1 Cover Panels

Two basic concepts were considered in the trade-offs conducted on the cover design; honeycomb panels versus stiffened laminate panels. The variables considered in the design trade-off studies are shown in Table 3.

Honeycomb Panels.- Configuration 1 featured a honeycomb structure with precured inner and outer skins and a core recess at each rib location. The version was configured for a 1.27 m (50 in.) rib spacing (existing support for rudder hinges) and thus eliminated the two intermediate ribs between each hinge location. This extreme spacing was eliminated from further consideration when early analysis indicated an excessive weight penalty for the design. All subsequent rib spacings were set at approximately 0.635 m (25 in.) eliminating two intermediate ribs and replacing them with one intermediate rib.

The remaining honeycomb panel versions were either full depth with potting at rib locations versus recessed core at rib locations (see Figure 7). Both configurations were analyzed for weight and cost utilizing three fabrication variables: (1) precured inner and outer skins, (2) inner and outer skins cocured, and (3) outer skin precured and inner skin cocured.

The honeycomb designs incorporated a graphite laminate insert at the root end to eliminate load path eccentricities. Figure 7 also shows the root end configuration and joint concept at the fuselage interface. With the selection of the 0.635 m (25 in.) rib spacing, all panels incorporated a 4.8 mm (3/16 in.),  $64 \text{ kg/m}^3$  (4 lb/ft<sup>3</sup>) HRP Glass Phenolic Reinforced honeycomb. The core thickness was varied from approximately 8.6 mm (0.34 in.) at the root end to 22.9 mm (0.90 in.) at the tip. Inner and outer skin thicknesses varied from 1.1 mm (0.45 in.) at the root end to 0.9 mm (0.035 in.) at the tip. Configuration 2B was selected as the best of the honeycomb panel configurations analyzed. The continuous core eliminated load path eccentricities and reduced fabrication complexity, thus reducing weight and cost respectively. Two root end joint specimens were fabricated and tested during preproposal activities to evaluate this configuration. Both specimens exceeded the design requirements for the joint.

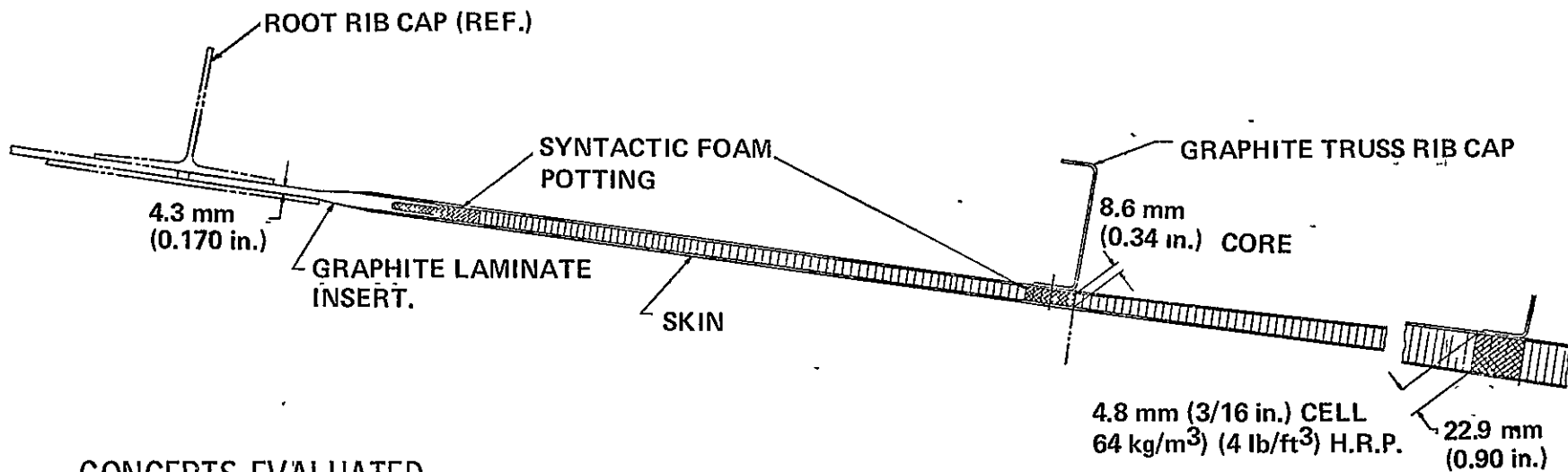
Stiffened Cover Configurations.- The stiffened laminate panel configurations incorporated four basic stiffener cross sections. The four sections were blade stiffeners, A-frame stiffeners, I-beam stiffeners, and hat section stiffeners (three configurations). The blade and A stiffener cross-sections are shown in Figures 8 and 9 with possible rib attachment alternatives. The blade stiffener is simplest to manufacture, however, is inefficient for a compression surface. The blade stiffener has an inherent rolling instability mode resulting from initial waviness and imperfections and lateral support is required at rib locations. The blade would normally consist mainly of 0° oriented plies and the skin mainly  $\pm 45^\circ$  plies. This combination and the geometry would cause high transverse shear deformations and result in a high-risk design. Because of the foregoing, this stiffener configuration was dropped from consideration.

TABLE 3. FIN STUDY-COST/WEIGHT SUMMARY

Cover Concepts		Skin Configuration	Skin Weight		Rib. Spacing		Material* Cost	Manufacturing* Cost	Total Cost (Inc. QA)	
Honey- comb	Stiffened Skins		kg	(lb)	mm	(in.)				
✓		1A	Fiberglass honeycomb/graphite skins - closeout pads	224.5	(494.9)	1270 mm	(50)	\$30 178	\$32 925	\$68 053
✓		2A	Fiberglass honeycomb/graphite skins - precured - closeout pads	187.5	(413.4)	↓ 635 mm	(25)	24 766	39 250	69 916
✓		3A	Fiberglass honeycomb/graphite skins - precured outer skin/cocured inner skin-closeout pads	199.9	(440.8)		(25)	26 800	32 825	64 550
✓		4A	Fiberglass honeycomb/graphite skins - cocured - closeout pads	212.4	(468.2)		(25)	28 998	28 250	61 498
✓		2B	Fiberglass honeycomb/graphite skins - precured - continuous core - closeout pads	175.2	(386.2)		(25)	23 836	32 975	61 761
✓		3B	Fiberglass honeycomb/graphite skins - precured outer-cocured inner skins continuous core - potted pads	187.6	(413.6)		(25)	26 562	29 025	59 967
✓		4B	Fiberglass honeycomb/graphite skins - continous core - cocured potted pads	200.0	(440.9)		(25)	28 974	24 850	57 369
	✓	5	Graphite stiffened skins - precured - parallel "Hat" section	168.6	(371.7)		(25)	27 646	29 050	61 046
	✓	7	Graphite stiffened skins - precured - parallel "I" section	165.8	(365.6)	635 mm	(25)	23 842	38 175	67 742

\* First Unit Cost

ORIGINAL PAGE IS  
OF POOR QUALITY



### CONCEPTS EVALUATED:

FOR BOTH POTTED AND CLOSEOUT PADS,

- COCURED SKINS
- PRECURED SKINS
- PRECURED OUTER SKIN,  
COCURED INNER SKIN

Figure 7. Honeycomb Skin Panels

The A-frame stiffener design in Figure 9 is efficient in pure compression; however, when bending is also imposed, the canted legs tend to roll away from each other resulting in potential fatigue problems. It is a difficult section to stabilize and requires large cutouts in the ribs. For these reasons, the configuration was eliminated from consideration.

The I-beam cross section (see Figure 10 and 11) is more efficient than the blade section, but still imposes a problem with the rolling instability mode. Attachment to the rib caps and shear ties to the skin present some design problems; however, the configuration was considered potentially attractive, and a concept was sized for cost and weight analysis (ref. Configuration 7, Table 3). Two root-end joint specimens were fabricated and tested during preproposal activities to evaluate the I-beam section concept. Both specimens exceeded the design requirements.

The results of the initial consideration of stiffened laminate covers indicated that the closed hat sections appeared to be the most favorable approach, and this configuration was explored in greater detail. Four panel configurations were traded-off to assess the influence of stiffener cross sections, spacing, and internal support on weight and cost.

The variables considered are shown in Figure 12. The basis for comparison included panel size and similar structural loading criteria. The results of the initial screening are shown in Table 4 and would indicate a selection of configuration A based on the lowest weight and a cost equivalency with configuration B. However, the configuration that evolved represents a compromise that incorporates additional requirements such as rib cutout constraints, geometrical constraints, and load transfer requirements.

The hat section that evolved when realistic design constraints were imposed is shown in Figure 13. This hat section in conjunction with the stiffener spacing shown in Figure 14 provides the basis for the current design concept cost and weight analyses. The forward nine stiffener locations geometrically intercept the front spar. However, because of the small angle of intersection, stiffener runout onto the spar is not feasible. The stiffeners along the front spar will terminate at the rib location below the spar intersection point. (See Figure 14.) The aft four stiffener spacings were dictated by the rib load transfer capability which requires four fasteners between stiffeners. (See Figure 15.) The balance of the stiffeners were located to accommodate the remaining chord length and will terminate at the upper closeout rib.

The runout of the stiffeners at the fuselage interface joint is of major concern in the redesign approach. In order to accommodate the existing joint design most readily, the stiffeners were flared and terminated adjacent to the root rib splice tee as shown in Figure 16. This approach does not interfere with the locations of the double row of fasteners through the root rib tee which must be maintained to assure interchangeability between the metal and composite fins.

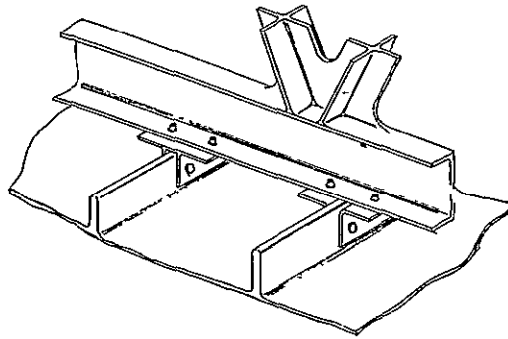


Figure 8. Alternate Rib Attachments Blade Stiffener Configuration

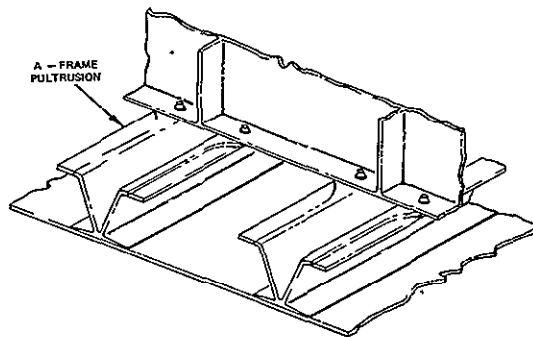


Figure 9. A-Frame Stiffener Cover Configuration

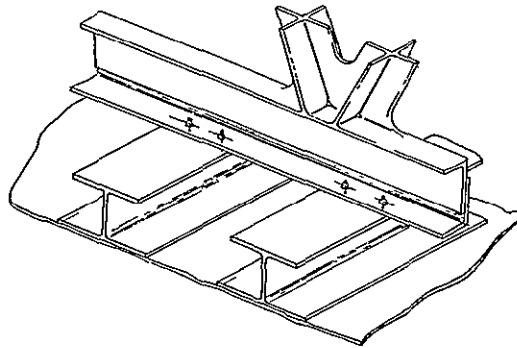


Figure 10. Rib Attachment I-Beam Stiffener Configuration

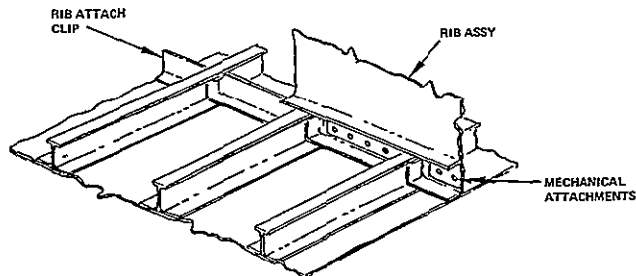


Figure 11. I-Beam Stiffened Skin Panel

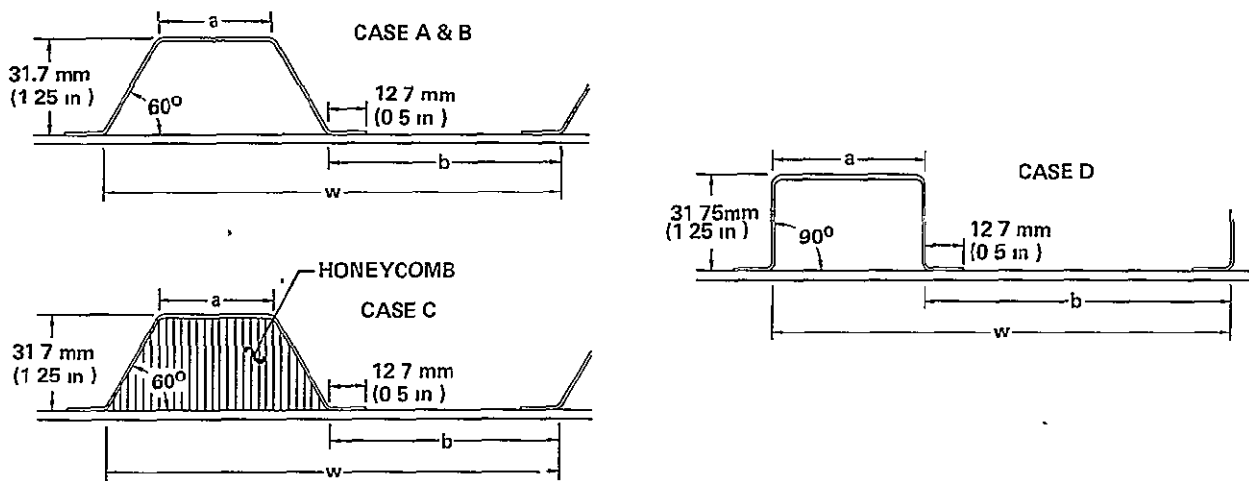


Figure 12. Stiffener Configuration

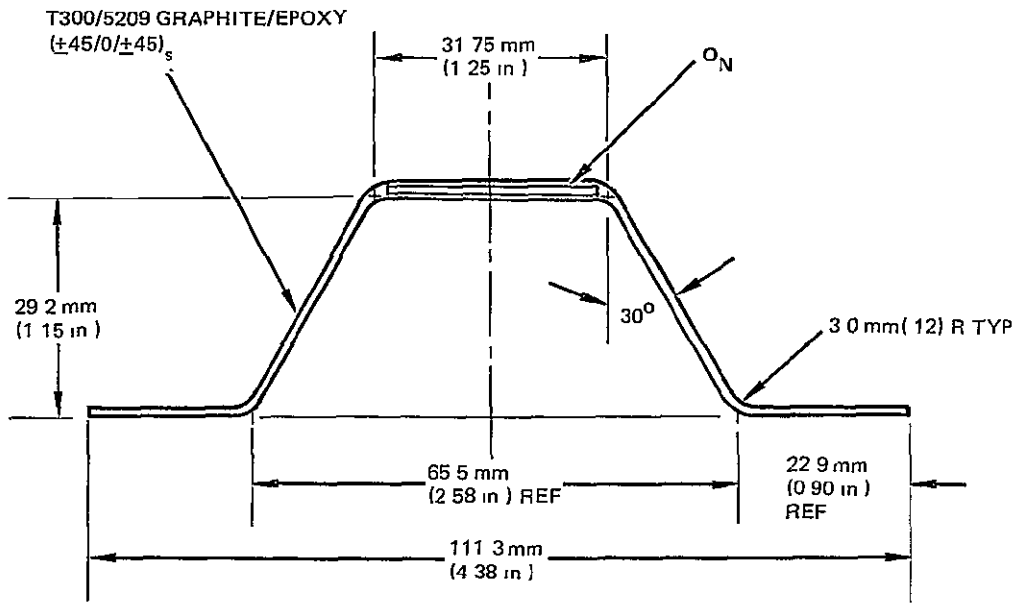


Figure 13. Hat Section Stiffener

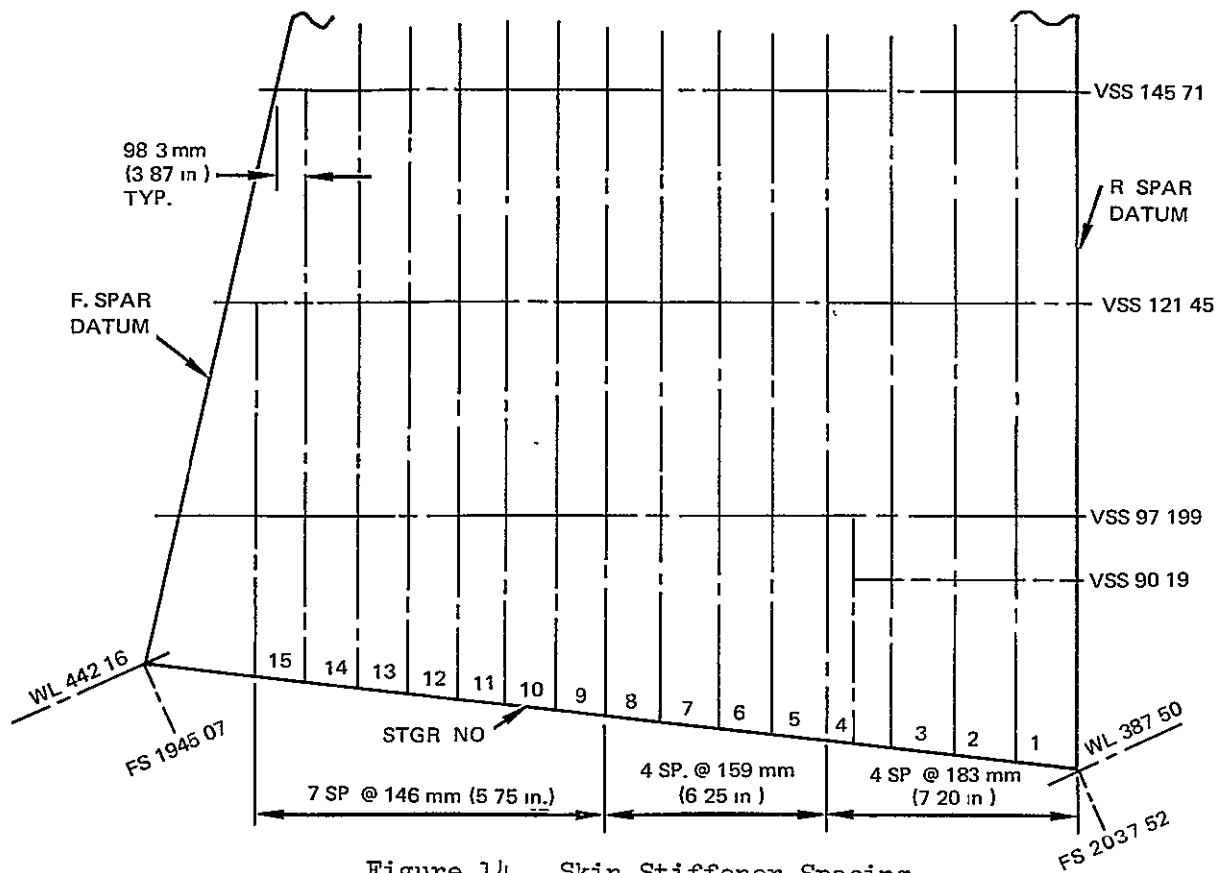


Figure 14. Skin Stiffener Spacing

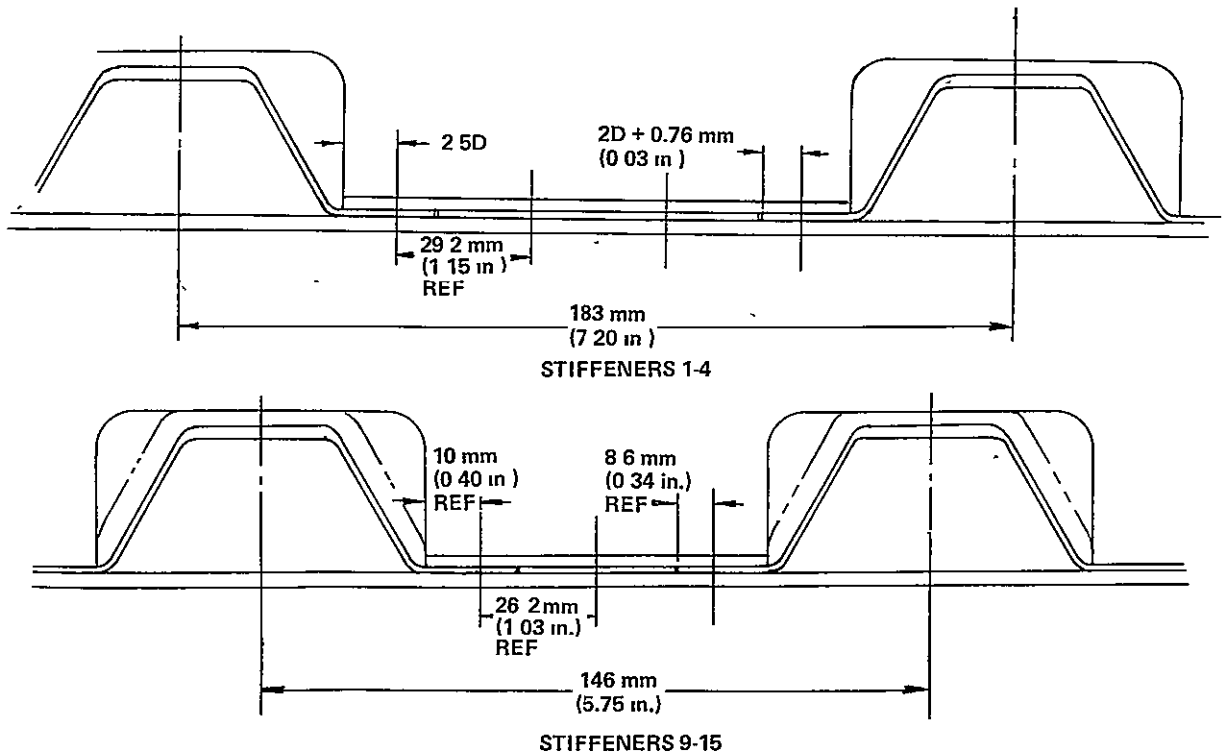


Figure 15. Rib to Cover and Hat Section Joint

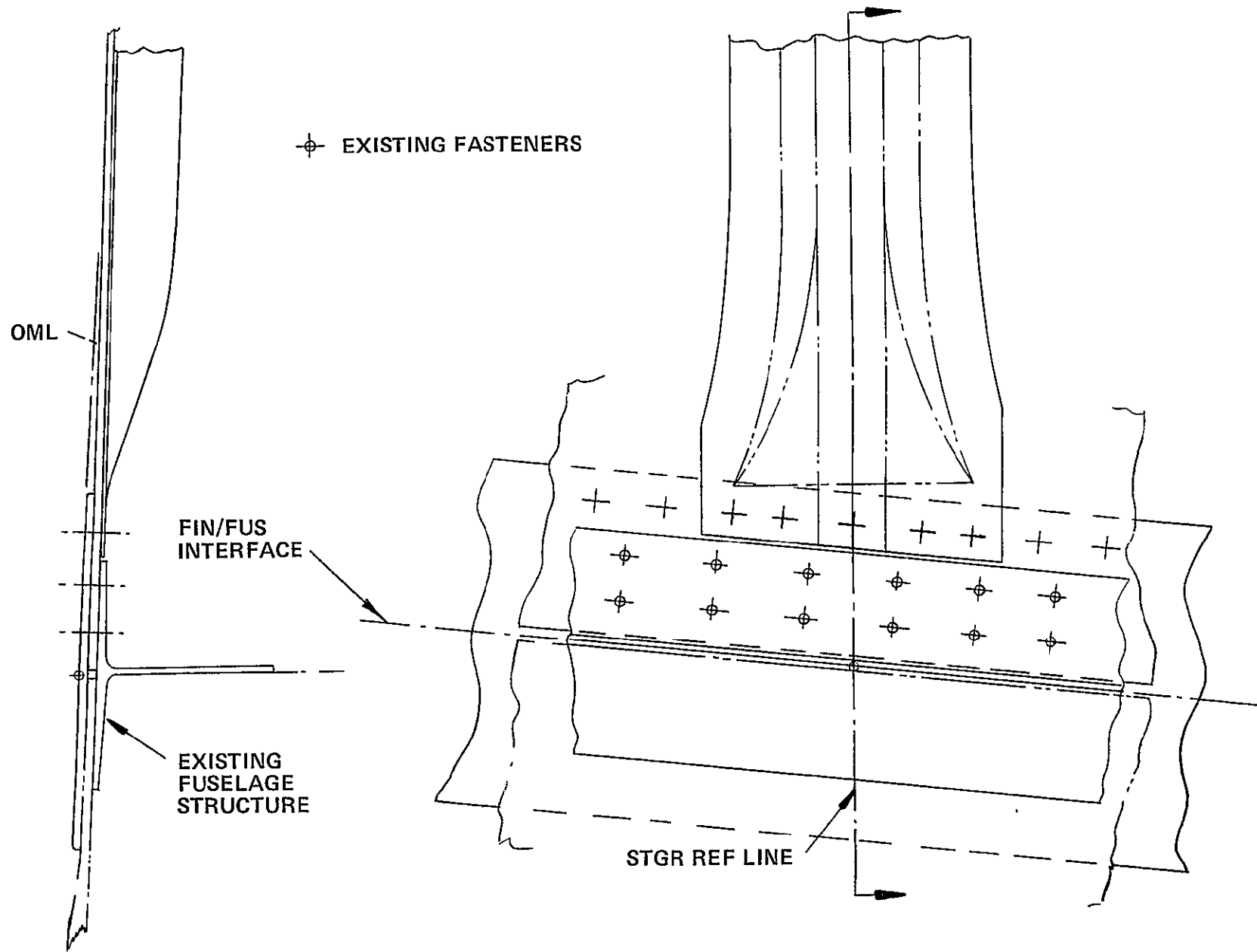


Figure 16. Stiffener Runout



TABLE 4. HAT SECTION STIFFENER CONFIGURATION COMPARISON

	CASE A		CASE B		CASE C		CASE D		
	mm	(in.)	mm	(in.)	mm	(in.)	mm	(in.)	
Dim a	} See Figure 12	38.1	(1.50)	38.1	(1.50)	38.1	(1.50)	50.8	(2.00)
Dim b		76.2	(3.00)	101.6	(4.00)	76.2	(3.00)	101.6	(4.00)
Dim W		151	(5.94)	175.4	(6.94)	151	(5.94)	152.4	(6.00)
Area mm <sup>2</sup> (in <sup>2</sup> )		478.7	(0.742)	640	(0.992)	478.7	(0.742)	613.5	(0.951)
Weight kg (lb) Skin + Stiffeners		130.9	(288.5)	148.1	(326.6)	150.8	(332.4)	161.8	(356.6)
Cost Stiffeners Only		\$4158		\$4115		\$4761		\$5385	

The cover panels will be of single-piece construction incorporating all the interfacing requirements of the metal version. The present design intent is to vary the spanwise thickness of the skin in three constant thickness areas. (See Figure 17.) Variations in chordwise thickness were discarded because of layup complexities with attendant higher costs. The primary layup of the skins will be a combination of +45-degree and 0-degree graphite. Final sizing has not been determined and will be dependent on further analysis and testing.

The preferred hat section stiffened panel (ref. concept 5, Table 3) along with the preferred honeycomb panel configuration (ref. concept 2B, Table 3) are compared on a cost, weight, and risk basis to the aluminum baseline in Table 5. The cost and weight figures reflect updating to incorporate the effects of lightning protection and additional design refinements. The hat stiffened concept was recommended and subsequently approved as the configuration to be utilized for Phase II, Detail Design. The recommended configuration is shown in Figure 18.

#### 2.1.1.2 Spars

The front and rear spars are very similar in design and interfacing requirements, and thus the design trade-off studies conducted on one are directly applicable to the other. The spar design is dictated to a large extent by existing geometry and several interface requirements. The front spar must accommodate the fuselage mating joint, HF antenna installation, dorsal closure assembly, interchangeable leading edge panels, and the tip installation. The rear spar also accommodates the fuselage mating joint and tip installation and additionally provides the rudder hinge and actuator

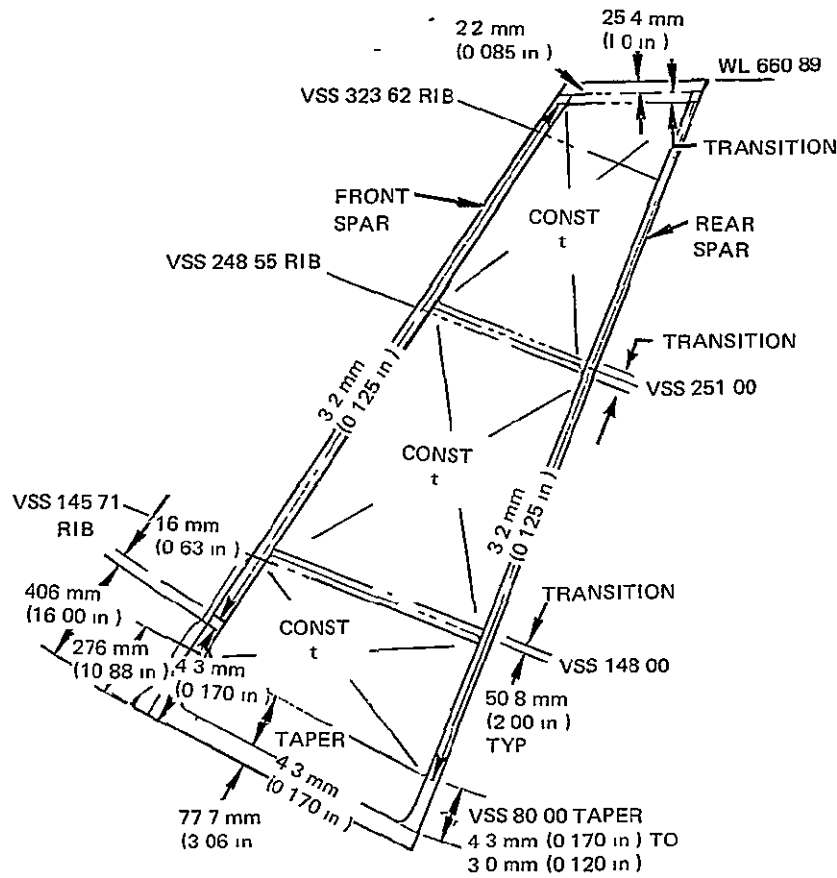


Figure 17. Spanwise Cover Thickness Variation

TABLE 5. COVER PANEL COMPARISON

Item	Cover Configuration		
	Aluminum Baseline	Hat Stiffened	Honeycomb
Weight - kg (lb)	208.8 (460.4)	176.3 (388.7)*	182.9 (403.2)*
Cost (Cover Only)	\$17 427	\$16 428	\$18 959
Risk	None	Low	High

\*Includes 7.7 kg (17 lb) for lightning protection

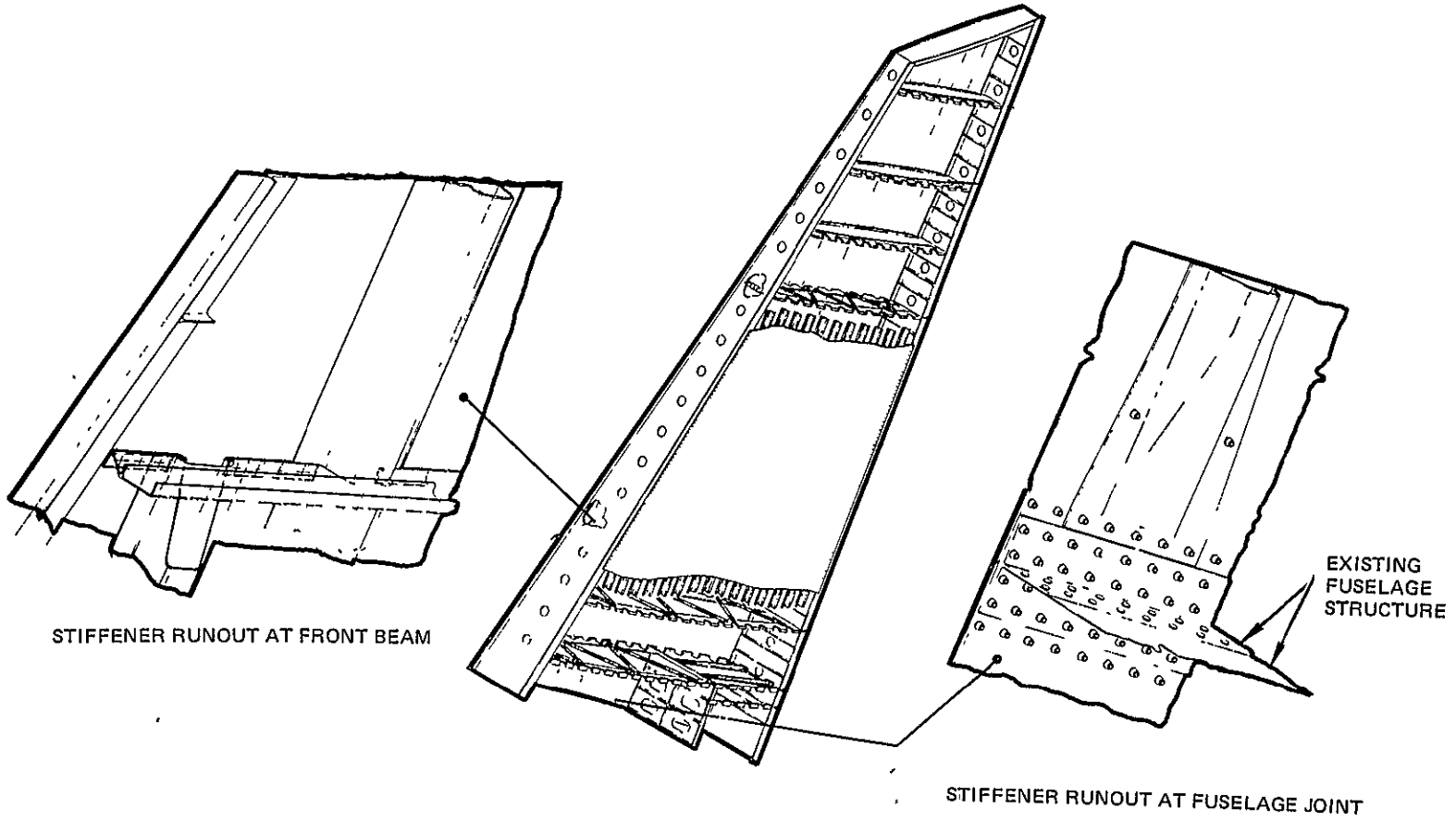


Figure 18. Hat Stiffened Cover Concept

support and mounting provisions for the trailing edge panels. Electrical and hydraulic functional attachment requirements must also be met. Both spars will require assembly/inspection access holes in the spar webs between the ribs.

Three basic concepts were initially considered for the design and fabrication of the spars -- a sine wave web, an integrally stiffened configuration, and a miniwich design. The three concepts are shown in Figure 19. The sine wave concept, while offering high structural efficiency, was eliminated early due to problems associated with access holes, rib closeout attachment, and interfacing with the existing fuselage/fin splice structure.

The integrally stiffened concept initially was an all graphite design; however, during the course of the trade-off studies, several hybrid versions were evaluated. The integrally stiffened rear spar concept depicted in Figure 20 is a one-piece assembly having an overall length of 7.620 m (300 in.) and varying in width from 0.589 m (23.2 in.) at the root to 0.196 m (7.7 in.) at the tip. The front spar is similarly constructed, however it is slightly smaller having a total length of 6.96 m (274 in.). The concept shown has integrally molded web stiffeners, rib attachment angles, and caps and is cocured in a single stage bonding operation.

Several variations of this design were considered, and their effect on weight and cost were evaluated. The additional evaluations included stiffener cross sectional variables (Figure 21), stiffener spacing (2 versus 3 per rib

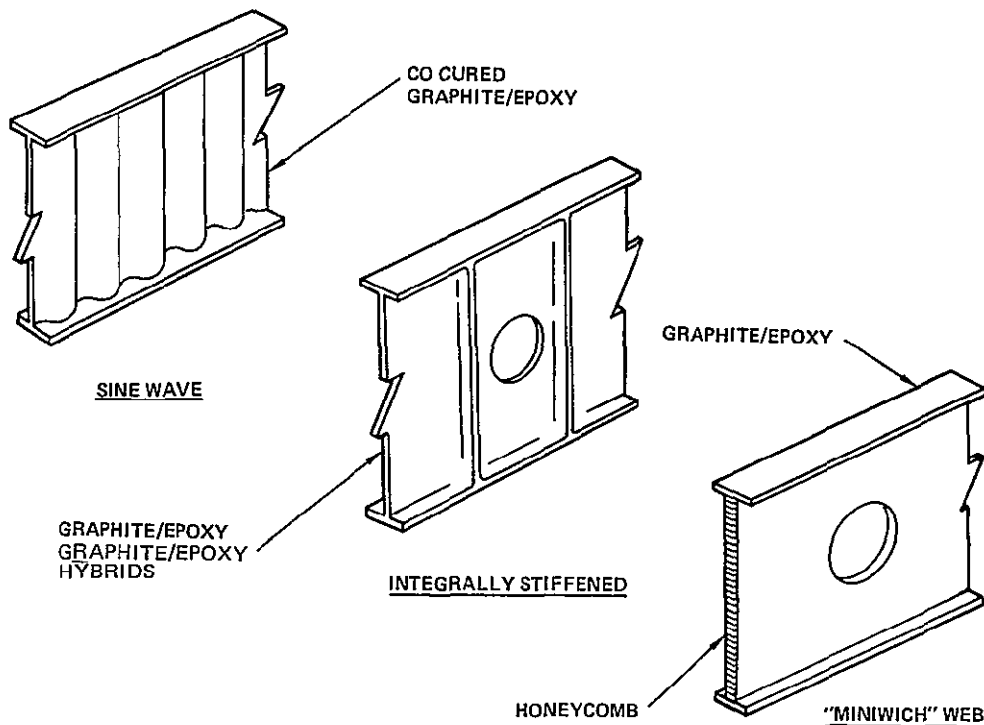
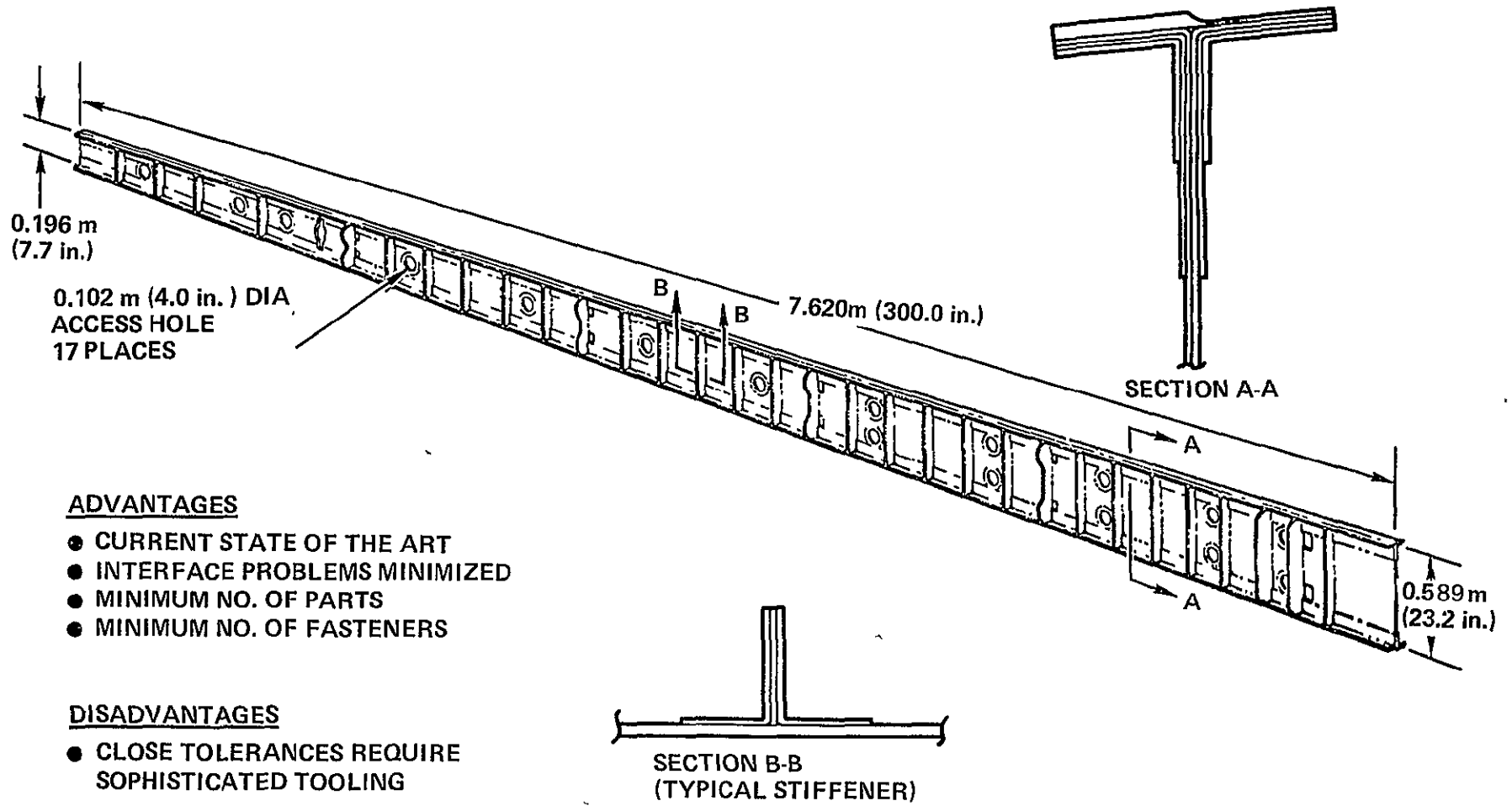


Figure 19. Study Concepts-Spars

REAR SPAR



ADVANTAGES

- CURRENT STATE OF THE ART
- INTERFACE PROBLEMS MINIMIZED
- MINIMUM NO. OF PARTS
- MINIMUM NO. OF FASTENERS

DISADVANTAGES

- CLOSE TOLERANCES REQUIRE SOPHISTICATED TOOLING

REPRODUCIBILITY OF THE ORIGINAL PAGE IS POOR

Figure 20. Integrally Stiffened Spar Design

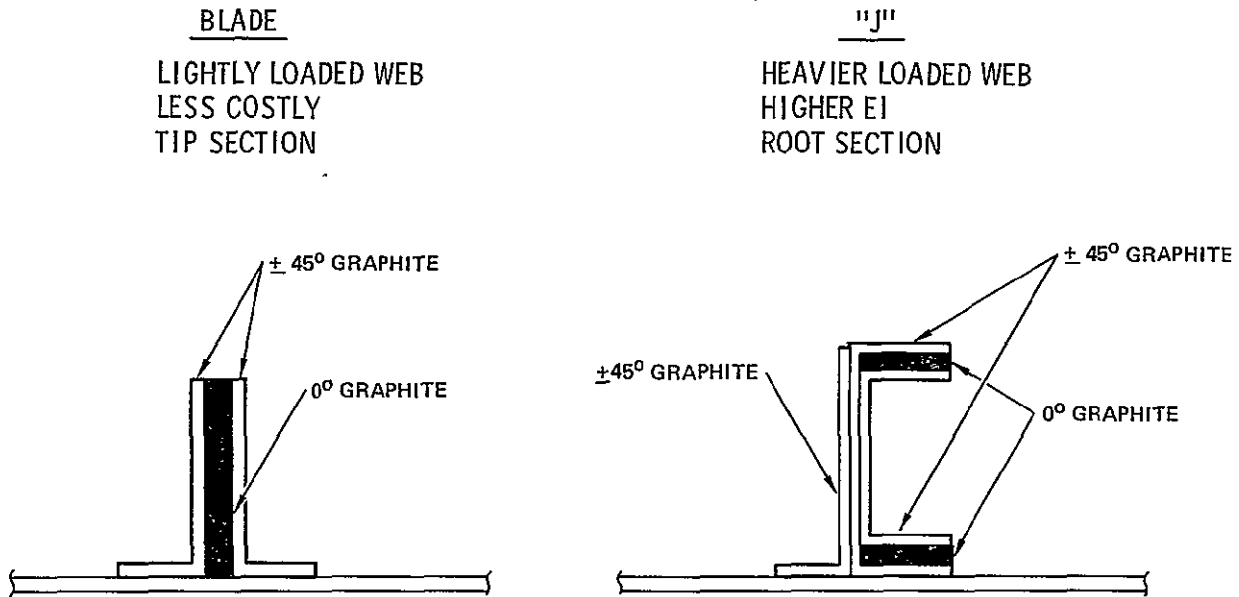


Figure 21. Spar Stiffener Configuration

bay), mechanical attachment of aluminum stiffeners, and secondary bonding of precured angle stiffeners. Initial indications are that the close tolerances required for location of the hinge rib attachment angles will lead to a compromise design that includes a combination of integral stiffeners and mechanically attached angles. The final spar definition will be determined during the detail design activities of Phase II.

The miniwich design configuration is shown in Figure 22. This concept is similar to the integrally stiffened laminate design except that a thin honeycomb core is utilized in the web area which eliminates the requirement for additional web stiffeners. Various core materials were considered including corrosion resistant aluminum, Nomex, and fiberglass, with preference given to the nonmetallic cores to minimize potential corrosion problems. The simplified method of construction and reduction of composite material in the webs makes this configuration highly desirable for potential cost and weight reductions. However, the problems of incompatibility with fuselage and leading and trailing edge structure, fastener and access hole potting requirements, and particularly potential moisture absorption increase the overall risk factors associated with this design.

A weight and cost summary of the matrix of spar design variables is shown in Figure 23 and compared to the existing metal design. The weight and cost results shown here represent only the most promising design from each distinct category. It can be seen that all the designs offer substantial weight savings over the metallic design while fabrication costs are held fairly constant.

REAR SPAR

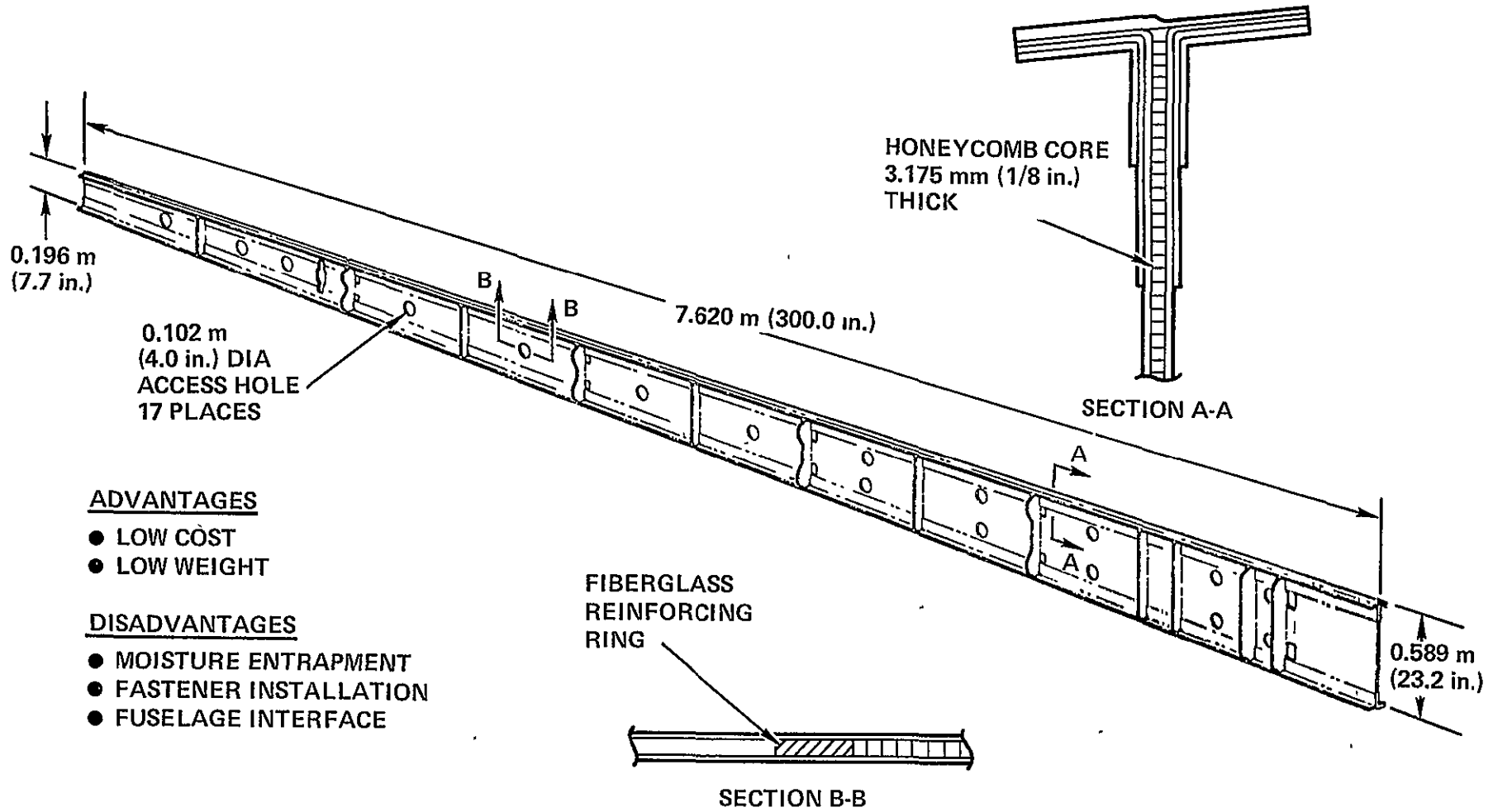
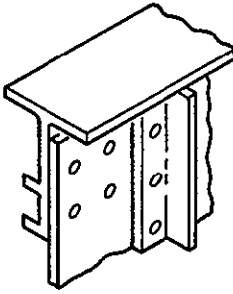


Figure 22. Miniwich Spar Design

CONFIGURATION				
	ALL GRAPHITE/ EPOXY  (a)	GRAPHITE/EPOXY  FIBERGLASS CENTER (b)	GRAPHITE/EPOXY  KEVLAR CENTER (c)	GRAPHITE/EPOXY  FIBERGLASS HONEYCOMB
METAL DESIGN	INTEGRALLY STIFFENED CONCEPTS			MINIWICH
WEIGHT (TOTAL FRONT AND REAR SPAR) – kg (lb)				
85.9 (189.4)	59.3 (130.8)	61.4 (135.3)	57.1 (125.8)	51.5 (113.5)
*COST (TOTAL FRONT & REAR SPAR) – \$				
10 491**	10 726	9833	10 022	8744

\*PROJECTED UNIT AVERAGE PRODUCTION COSTS (MATERIALS AND LABOR) FOR 250 UNITS.

\*\*AUXILIARY SPAR COST NOT INCLUDED.

Figure 23. Spar Weight and Cost Summary



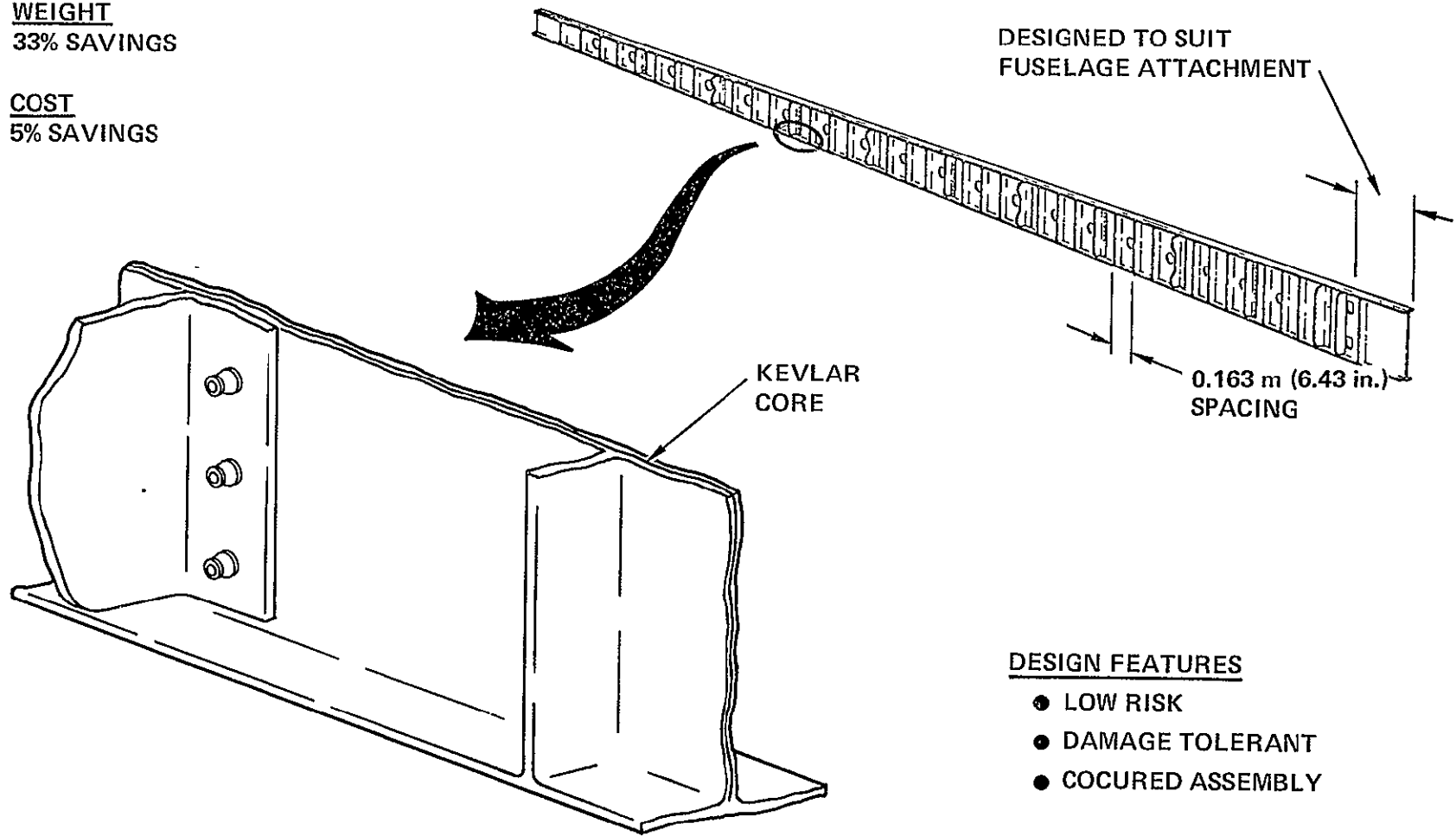
Table 6 is a summary of the factors considered in the selection of the solid web spar design. Both concepts were evaluated on a competitive basis and were judged to be equal in many of the consideration factors. Additionally, both concepts offer attractive weight savings and costs competitive to those of the metal spars. The final concept recommended was influenced primarily by the potential of environmental problems which might occur with the miniwich design. Although the miniwich design appears lighter and less costly than the solid laminate design, it was recommended that for the spars the better selection is the solid web concept for both the front and rear spars. The selected design is shown in Figure 24.

TABLE 6. L-1011 ACVF SPAR CONCEPT SELECTION CONSIDERATIONS

Factor Considered	Solid Web Stiffened	Miniwich Honeycomb Web
Structural Complexity Fatigue Endurance Fracture Control Tooling Requirements Inspectability Repairability Producibility	Concepts Judged Approximately Equivalent	
Weight Saving (From metal baseline)	33%	40%
Production Cost (Compared to baseline)	95%	84%
Risk Factors <ul style="list-style-type: none"> <li>● Volatile Entrapment</li> <li>● Environmental Resistance</li> </ul>	None  Good	Potentially High  Potentially Poor

WEIGHT  
33% SAVINGS

COST  
5% SAVINGS



DESIGN FEATURES

- LOW RISK
- DAMAGE TOLERANT
- COCURED ASSEMBLY

Figure 24. Selected Spar Configuration

### 2.1.1.3 Ribs

Figure 25 shows the locations of the rib structure based on a nominal 0.635 m (25 in.) spacing. The metal baseline structure utilized a nominal 0.432 m (17 in.) spacing. The hinge rib locations of the metal baseline governed the spacing of the composite fin rib structure. The trade-off study conducted in this report involves eleven ribs from vertical stabilizer station VSS 90.19 through VSS 323.62. Four basic rib structural concepts were selected for study: truss, miniwich web, stiffened web, and corrugated web. The corrugated web rib design proved to be too costly from a tooling standpoint, could not provide the required access for assembly and inspectability, and was eliminated. Five typical ribs were chosen for each sizing analysis from which the remaining rib's weight/costs were obtained by ratioing of rib areas based on the nominal rib dimensions at each given VSS.

The five typical ribs chosen to size each configuration were: VSS 90.19 (actuator/hinge shear-web stub-rib), VSS 97.199 (actuator/hinge combined shear-web, truss-web configuration), VSS 145.71 (major hinge rib), VSS 121.45 (major intermediate rib), and VSS 299.97 (upper hinge rib).

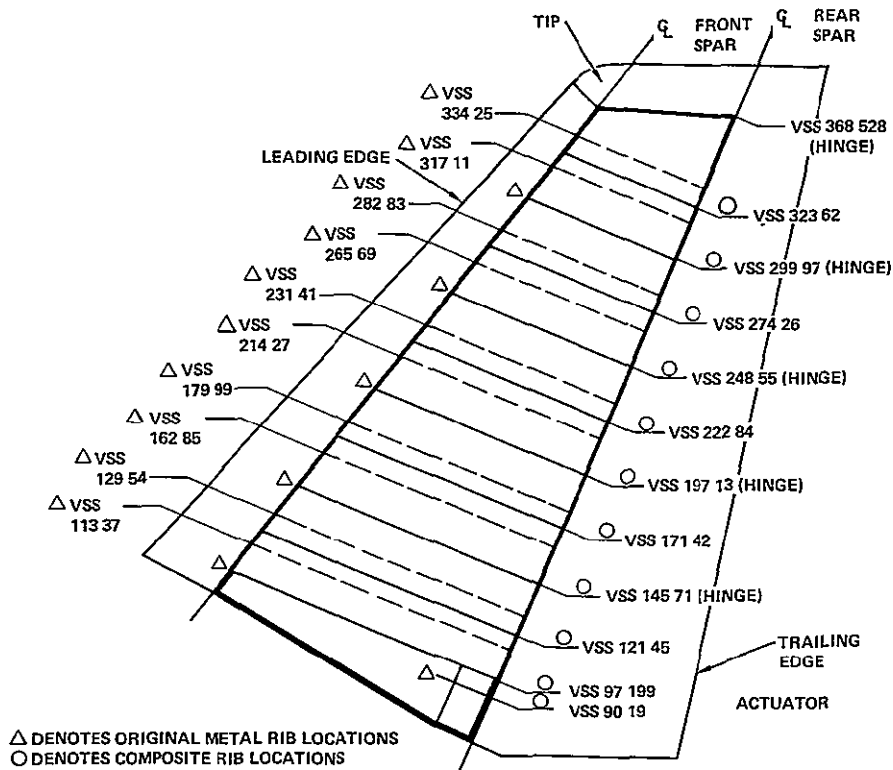


Figure 25. Fin Rib Locations

The most cost/weight effective rib design concepts from the proposal study were used for this trade study, i.e., (1) graphite/epoxy cap with aluminum cruciform diagonal truss, (2) graphite/epoxy cap and solid laminate shear web with integral stiffener, and (3) graphite/epoxy cap with miniwich core/graphite/epoxy facesheets web. Figures 26 through 31 illustrate the basic configurations considered.

The design requirements of accessibility for assembly, inspectability, and maintenance/repair precluded the use of any solid web design configurations for the lower seven ribs. Only the three upper most ribs were sized for a solid web design. Stub rib VSS 90.19 is a composite substitution shear web design and also precludes the use of cutouts for the same reasons.

Since a stiffened skin concept was used as a baseline design for this trade study, all rib concepts have provision for rib attachment to the skins by means of angle clips. These areas were included in the total cap weight based on the cutouts/stiffener location/configuration defined.

Honeycomb sandwich rib.- The honeycomb sandwich concept for the lower seven ribs (excluding stub rib VSS 90.19) provides access for assembly and inspection. In addition, integral stiffeners were added to prevent core shear/crushing from local loads induced by a man's weight during assembly and/or maintenance operations.

The upper three ribs do not require access through the ribs. The required access is provided by cutouts in the front and rear spars. However, a rough sizing conducted on these ribs for lightening holes found that the manufacturing costs incurred owing to the greater complexity negated any potential weight savings.

Stiffened web ribs.- The stiffened web rib concept was based on an integrally molded stiffener web-cap configuration to reduce part count. A solid laminate web was considered with and without access for the lower seven (excluding VSS 90.19) and upper three rib designs respectively.

Table 7 provides a summary of the rib configuration weights for VSS 90.19 through VSS 323.62. It can be seen from this summary table that on the basis of weight, the use of graphite/epoxy caps with aluminum cruciform diagonals for the lower seven ribs, graphite/epoxy caps with stiffened solid laminate webs for VSS 90.19 and VSS 97.19 (where applicable in the rear portion of the rib only) and graphite/epoxy caps with miniwich honeycomb core and graphite/epoxy facesheets for the remaining three upper ribs were recommended.

#### 2.1.1.4 Selected ACVF Configuration

During the conduct of the trade-off studies for the covers, spars and ribs, close coordination was maintained between the three design organizations to assure that the candidate configurations were all compatible when integrated into a complete fin box assembly and would meet the required program objectives. The selected configuration and the preferred concepts for the covers, spars and ribs are depicted in Figure 32.

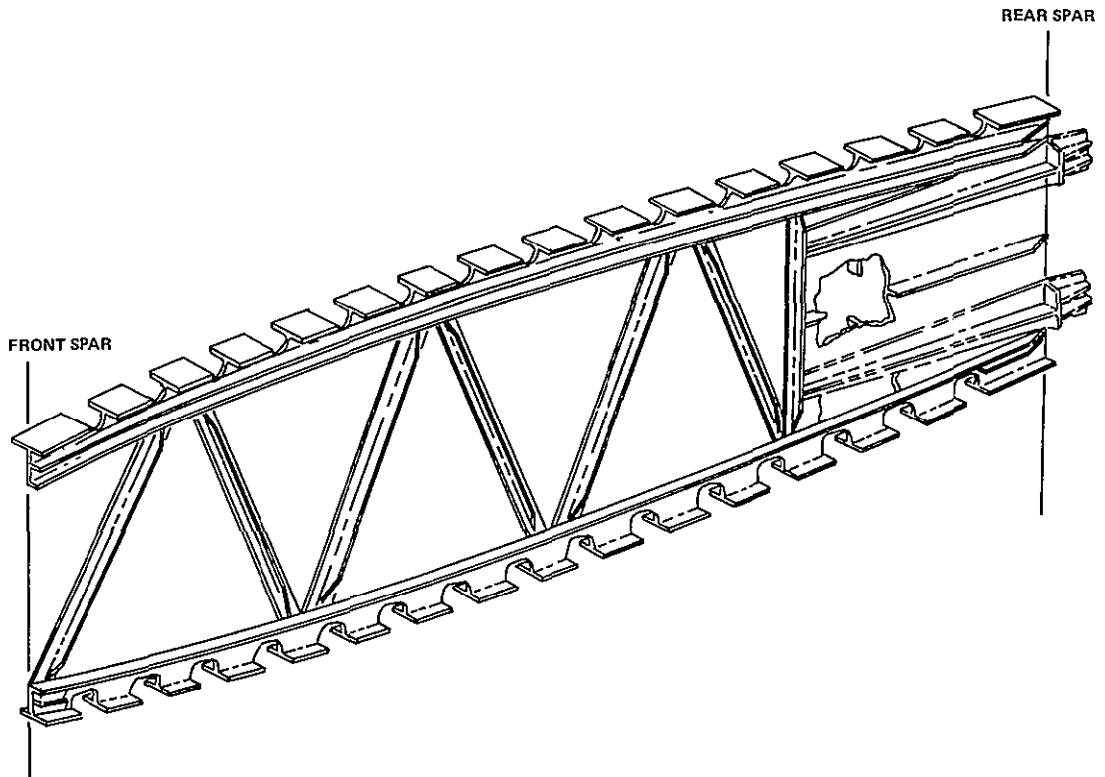


Figure 26. Hinge/Actuator Rib Concept (Type A)

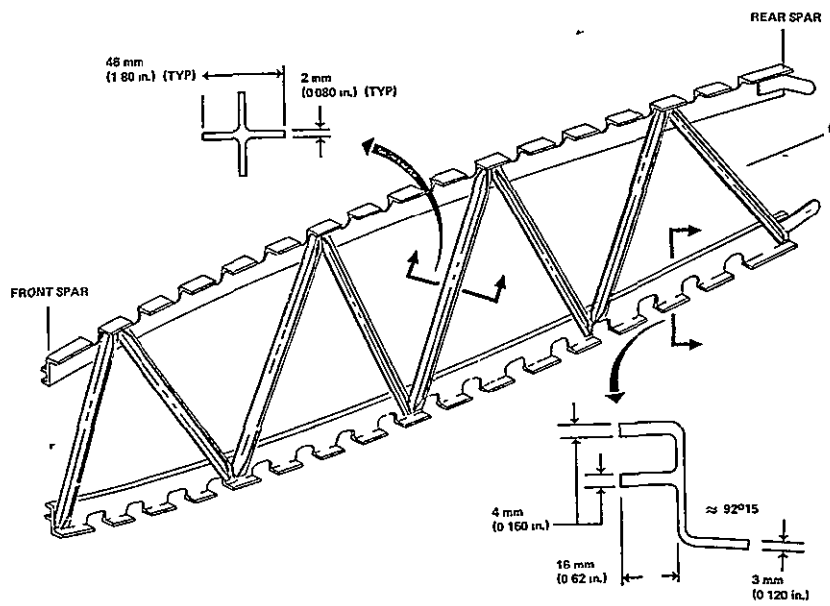


Figure 27. Hinge Rib Truss Concept (Type B)

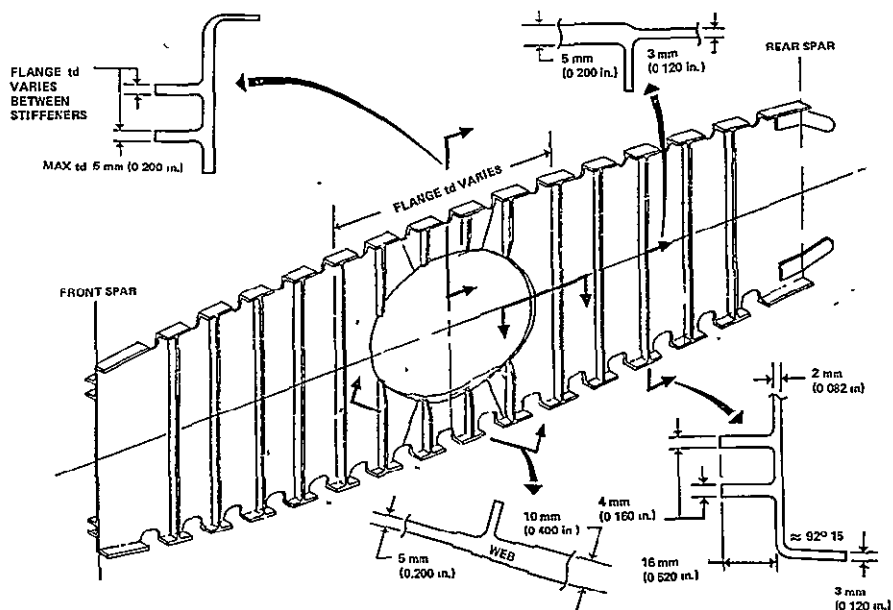


Figure 28. Hinge and Intermediate Stiffened Web Rib Concept for Lower Seven Ribs (Type C)

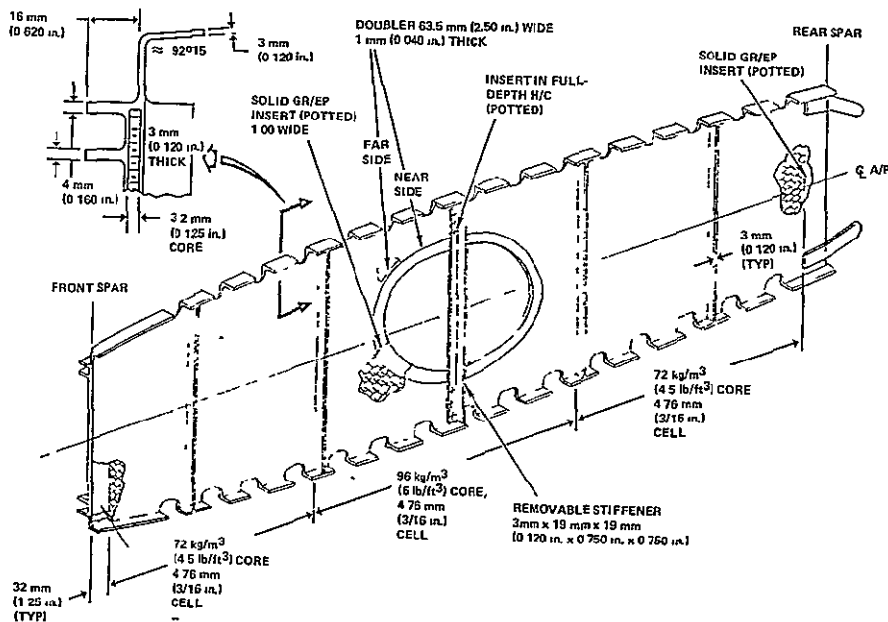


Figure 29. Hinge and Intermediate Miniwich Rib Concept for Lower Seven Ribs (Type D)

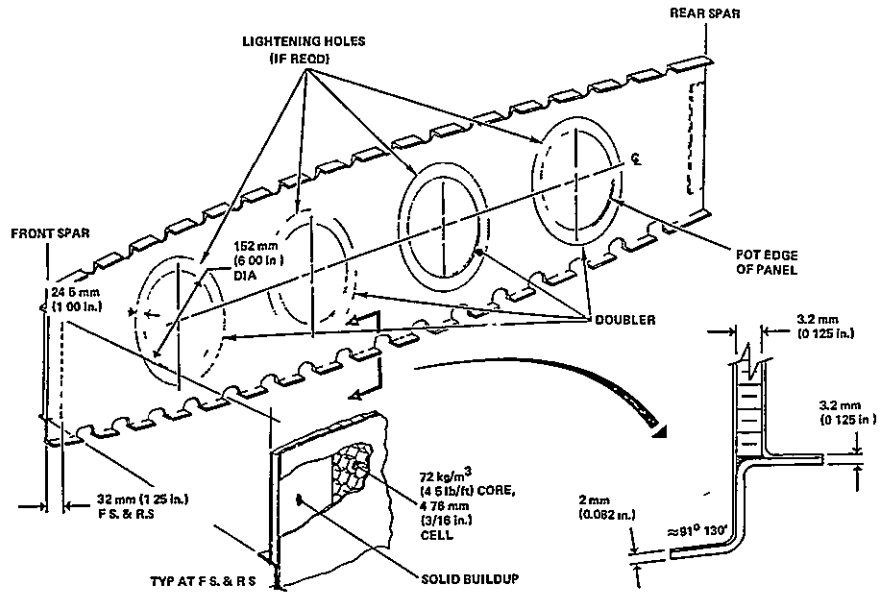


Figure 30. Hinge and Intermediate Miniwich Rib Concept for Upper Three Ribs (Type E)

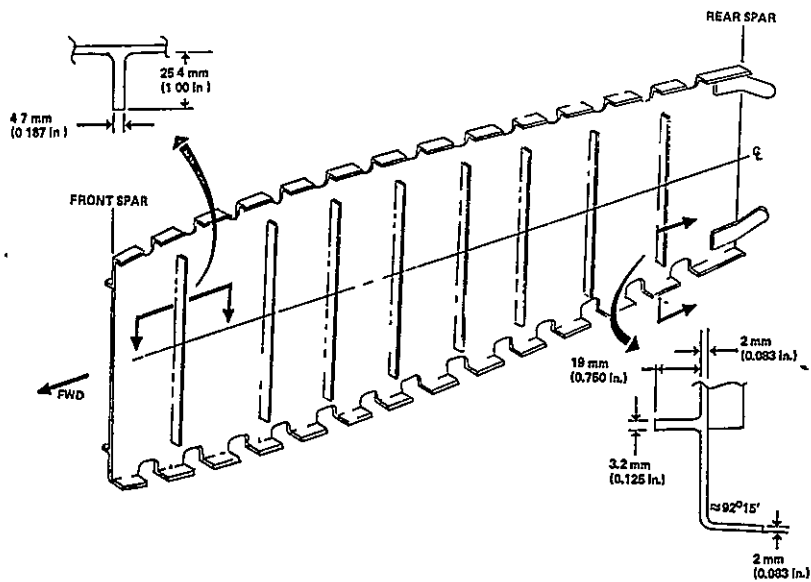


Figure 31. Hinge and Intermediate Stiffened Web Rib Concept for Upper Three Ribs

TABLE 7. L-1011 COMPOSITE VERTICAL FIN - RIB WEIGHT TRADES SUMMARY - SI UNITS

Vert Stab. Sta Rib Type	90.190 Actuator	97.199 Actuator	121.45 Interr	145.71 Hinge	171.42 Interm	197.13 Hinge	222.84 Interm	248.55 Hinge	274.26 Interm	299.97 Hinge	323.62 Interm
Truss Construction (1)	NA	(A)	(B)	(B)	(B)	(B)	(B)	(B)	(B)	(B)	(B)
Cap		4.20	3.13	2.84	2.76	2.49	2.32	2.15	2.00	1.77	1.65
Web, Truss, Filler		4.28	2.19	2.20	1.70	0.83	0.73	0.68	0.49	0.43	0.37
Fasteners		0.37	0.12	0.14	0.10	0.10	0.10	0.09	0.07	0.07	0.07
Total Rib Weight - kg		8.85	5.44	5.18	4.56	3.42	3.15	2.92	2.56 <sup>(5)</sup>	2.27 <sup>(5)</sup>	2.09 <sup>(5)</sup>
Maniwich Construction	NA	NA	(D)	(D)	(D)	(D)	(D)	(D)	(E)	(E)	(E)
Cap			2.76	2.60	2.44	2.28	2.05	1.95	0.88	0.79	0.71
Web Filler			3.06	2.71	2.31	2.03	1.69	1.46	1.06	0.96	0.66
Fasteners			0.20	0.20	0.18	0.17	0.15	0.14	-	-	-
Total Rib Weight - kg			6.02 <sup>(L)</sup>	5.51	4.98 <sup>(L)</sup>	4.48 <sup>(L)</sup>	3.89 <sup>(L)</sup>	3.55 <sup>(L)</sup>	1.94	1.75	1.37
Solid Web Construction	(A)	(2)	(2)	(C)	(2)	(2)	(2)	(C)	(2)	(E)	(2)
Cap	0.78			2.89				2.17		1.88	
Web, Filler	2.15			4.16				2.40		1.68	
Fasteners	0.30			-				-		-	
Total Rib Weight - kg	3.23			7.35				4.56 <sup>(6)</sup>		3.56	
Optimum Rib Weight (kg)	3.23	8.85	5.44	5.18	4.56	3.42	3.15	2.92	1.94	1.75	1.37

NOTES

- (1) Concept type, i.e., (A), (B), etc. (See Figures 26 through 30.)
- (2) Weights not calculated due to larger manufacturing costs and average weight penalty shown at VSS 145.71
- (3) Total composite rib weight = 11.81 kg  
 Total metal rib weight = 59.24  
 Total weight saved = 17.43 kg = 29.4%

- (4) Projected from ratioing weight of rib at VSS 145.71.
- (5) Projected from ratioing weight of rib at VSS 222.84.
- (6) Projected from ratioing weight of rib at VSS 145.71.

ORIGINAL PAGE IS  
OF POOR QUALITY



TABLE 7. L-1011 COMPOSITE VERTICAL FIN - RIB WEIGHT TRADES SUMMARY - CUSTOMARY UNITS

Vert Stao Sta Rio Type	90.190 Actuator	97.199 Actuator	121.45 Intern	145.71 Hinge	171.42 Intern	197.13 Hinge	222.84 Intern	248.55 Hinge	274.26 Intern	299.97 Hinge	323.62 Intern
Truss Construction (1)	NA	(A)	(B)	(B)	(B)	(B)	(B)	(B)	(B)	(B)	(B)
Cap		(9.26)	(6.91)	(6.27)	(6.08)	(5.50)	(5.12)	(4.74)	(4.40)	(3.90)	(3.64)
Web, Truss, Filler		9.12	(1.83)	(4.86)	(3.75)	(1.83)	(1.61)	(1.50)	(1.07)	(0.94)	(0.82)
Fasteners		(0.82)	(0.26)	(0.31)	(0.23)	(0.22)	(0.23)	(0.19)	(0.16)	(0.16)	(0.16)
Total Rib Weight-lb		(19.51)	(12.00)	(11.44)	(10.06)	(7.55)	(6.96)	(6.43)	(5.63) <sup>(5)</sup>	(5.00) <sup>(5)</sup>	(4.62) <sup>(5)</sup>
Manwich Construction	NA	NA	(D)	(D)	(D)	(D)	(D)	(D)	(E)	(E)	(E)
Cap			(6.08)	(5.74)	(5.38)	(5.02)	(4.53)	(4.30)	(1.93)	(1.74)	(1.57)
Web, Filler			(6.75)	(5.98)	(5.21)	(4.48)	(3.72)	(3.21)	(2.34)	(2.11)	(1.46)
Fasteners			(0.11)	(0.42)	(0.39)	(0.37)	(0.33)	(0.31)	-	-	-
Total Rib Weight-lb			(13.27) <sup>(4)</sup>	(12.14)	(10.98) <sup>(4)</sup>	(9.87) <sup>(4)</sup>	(8.58) <sup>(4)</sup>	(7.82) <sup>(4)</sup>	(4.27)	(3.85)	(3.03)
Solid Web Construction	(A)	(2)	(2)	(C)	(2)	(2)	(2)	(C)	(2)	(E)	(2)
Cap	(1.72)			(6.38)				(4.78)		(4.15)	
Web, Filler	(4.74)			(9.84)				(5.28)		(3.70)	
Fasteners	(0.66)			-				-		-	
Total Rib Weight-lb	(7.12)			(16.22)				(10.06) <sup>(6)</sup>		(7.85)	
Optimum Rib Weight (3)	(7.12)	(19.51)	(12.00)	(11.44)	(10.06)	(7.55)	(6.96)	(6.43)	(4.27)	(3.85)	(3.03)

## NOTES

- (1) Concept type, i.e., (A), (B), etc (See Figures 26 through 30)
- (2) Weights not calculated due to larger manufacturing costs and average weight penalty shown at VSS 145.71.
- (3) Total composite rib weight = (92.22) lb  
 Total metal rib weight = (130.60)  
 Total weight saved = (38.38) lb = 29.1%

- (4) Projected from rationing weight of rib at VSS 145.71
- (5) Projected from rationing weight of rib at VSS 222.84
- (6) Projected from rationing weight of rib at VSS 145.71

### 2.1.2 Weight Status

The program weight objectives are to realize a 20-percent weight saving compared to the metal design and to utilize at least 40-percent composite material in the redesign. The current weight status for the selected configuration is shown in Table 8. A weight savings of 19.5% [75.8 kg (167.2 lb)] is predicted including a 13.2 kg (29 lb) growth allowance, and composite material utilization is currently predicted to be 82.4 percent of the redesigned fin box weight. A summary of weight changes since the first quarterly weight status report (ref. 1) is presented in Table 9, and a weight-time history for the composite fin is provided in Figure 33.

### 2.1.3 Cost Status

Currently projected production/maintenance costs for the ACVF are shown in Table 10. The production cost estimate is 58 163 dollars as a result of a decision to cost the graphite at 20 dollars a pound instead of 15 dollars a pound as in the First Quarterly Report (ref. 1). The costs shown are based on a cumulative average of 250 aircraft and include only material and production labor costs, plus a quality assurance factor of 10 percent for metal and 15 percent for composites. Composite material costs include a 35-percent scrap/usage factor. The labor wraparound rate is 25 dollars an hour and a 76-percent learning curve is used. All costs are quoted in 1975 dollars.

### 2.1.4 Test Specimen Design

Two test specimens representing the cover panel to fuselage joint area were designed and fabricated. The initial hat section specimen incorporated a flared hat section transition at the joint end and a 30° scarf cut at the opposite end (see Figure 34). The hat was mounted on a 152 mm (6 in.) wide skin layup which was mechanically fastened to aluminum loading plates. The aluminum members at the joint were identical to the current airplane design. The first specimen although exceeding design requirements failed away from the joint area. The second specimen design was modified by strengthening away from the joint to preclude this type of failure. The testing results are documented in the Concept Evaluation Tests section.

### 2.1.5 Loft and Interface Drawings

The basic loft line drawings and cover trim definition drawing have been released. These two drawings define the skin trim interface and apply to both the sandwich and stiffened skin concepts.

The vertical stabilizer Basic Design Requirements Interface drawing (Drawing No. 1606603) and the loft data required for definition of rib

TABLE 8. WEIGHT STATUS REPORT

Item	Metal Design Total Weight		Target Weight		Composite Design Total Weight		Composite Mat'l Wt.		Weight Change	
	kg	(lb)	kg	(lb)	kg	(lb)	kg	(lb)	kg	(lb)
Covers	208.8	(460.4)	163.3	(360.0)	157.7	(347.6)	157.7	(347.6)	-3.1	(-6.8)
Spars	88.9	(196.0)	60.1	(132.4)	60.0	(132.4)	57.0	(125.8)	+5.7	(+12.6)
Ribs	70.8	(156.3)	53.7	(118.5)	56.0	(123.5)	30.2	(66.5)	-4.9	(-10.7)
Assembly Hardware	16.1	(35.4)	10.3	(22.7)	14.9	(32.9)	-	-	+5.3	(+11.7)
Protective Finish	4.4	(9.6)	4.4	(9.6)	4.4	(9.6)	-	-	-	-
Lightning Protection	-	-	7.0	(15.5)	7.0	(15.5)	-	-	-	-
Design Growth Allowance	-	-	-	-	13.2	(29.0)	13.2	(29.0)	-	-
Total Fin Predicted										
Delivery Weight ~ lb	389.0	(857.7)			313.2	(690.5)	258.1	(568.9)	+3.0	(+6.8)
Weight Saving ~ lb					75.8	(167.2)				
Percent Weight Saved					19.5%					
Percent Composite Material							82.4%			
Total Fin Current Indicated										
Weight ~ lb	389.0	(857.7)	298.8	(658.7)	300.0	(661.5)	244.9	(539.9)		
[Predicted Less Growth]					22.9%		81.6%			
Total Current Indicated Weight less Metal Components not Redesigned										
	374.4	(825.4)			285.4	(629.2)			23.8% Weight Saved	

Weight Basis: 95% EST, 5% CALC, 0% ACT

⚠ Total metal design weight less weight of components not redesigned

⚠ Based on redesigned metal components

TABLE 9. SUMMARY OF WEIGHT CHANGES

Item	Weight Change ~ kg (lb)				Remarks
	Total		Composite		
	kg	(lb)	kg	(lb)	
Covers	+6.1	(+13.2)	+6.1	(+13.2)	Extend stiffener flange width to provide for fastener installation
	+4.3	(+9.6)	+4.3	(+9.6)	Increase stiffener spacing to provide clearance for rib to skin fastener installation
	-11.6	(-25.6)	-11.6	(-25.6)	Revised buckling analysis to incorporate edge fixity constraints
	+1.0	(+2.2)	+1.0	(+2.2)	Revised weight estimate based on stress analysis and miscellaneous changes
	-0.8	(-1.7)	-0.8	(-1.7)	Eliminate remaining Kevlar from inside surface of skin (below VSS 90.19)
	-4.9	(-10.7)	-4.9	(-10.7)	Reduce Kevlar thickness on outer surface of skin by utilizing "120" or "220" style in lieu of "281" style
	+2.8	(+6.2)	+2.8	(+6.2)	Revise stiffener spacing to incorporate an additional stiffener per side
Spars	+5.7	(+12.6)	+5.7	(+12.6)	Revised weight estimate and decision to incorporate hybrid solid stiffened web design
Ribs	-6.7	(-14.8)	+7.1	(+15.7)	Composite design actuator ribs in lieu of metal
	+1.8	(+4.1)	+5.9	(+13.0)	Revised weight estimate and miscellaneous changes
Assembly	+5.3	(+11.7)	0		Utilize steel nuts and collars in lieu of aluminum to prevent galvanic action
Total	+3.0	(+6.8)	+15.6	(+34.5)	

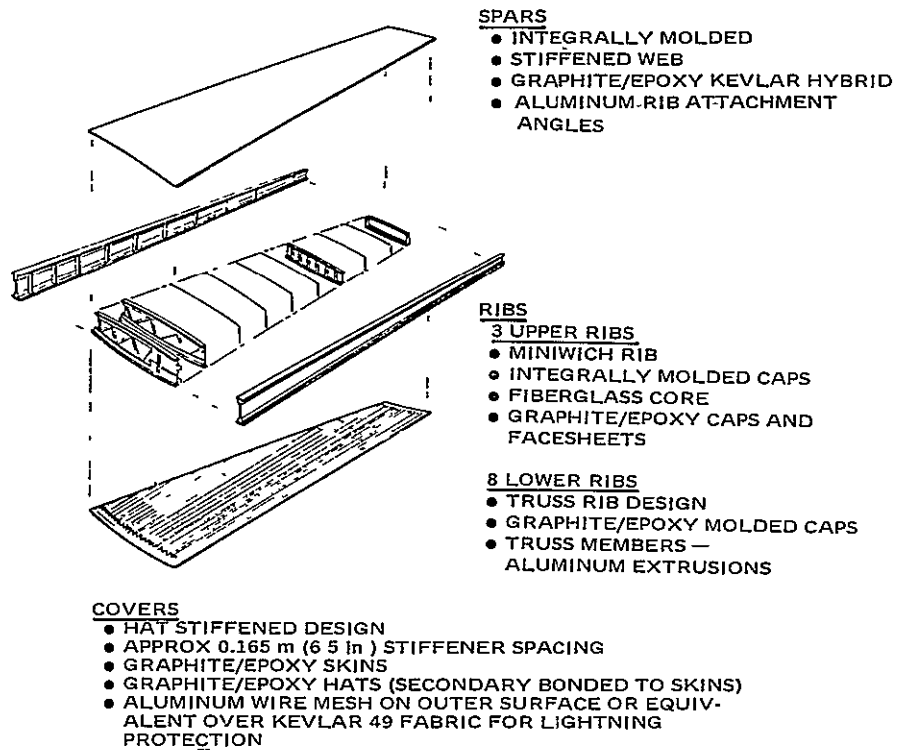


Figure 32. Advanced Composite Vertical Fin Configuration

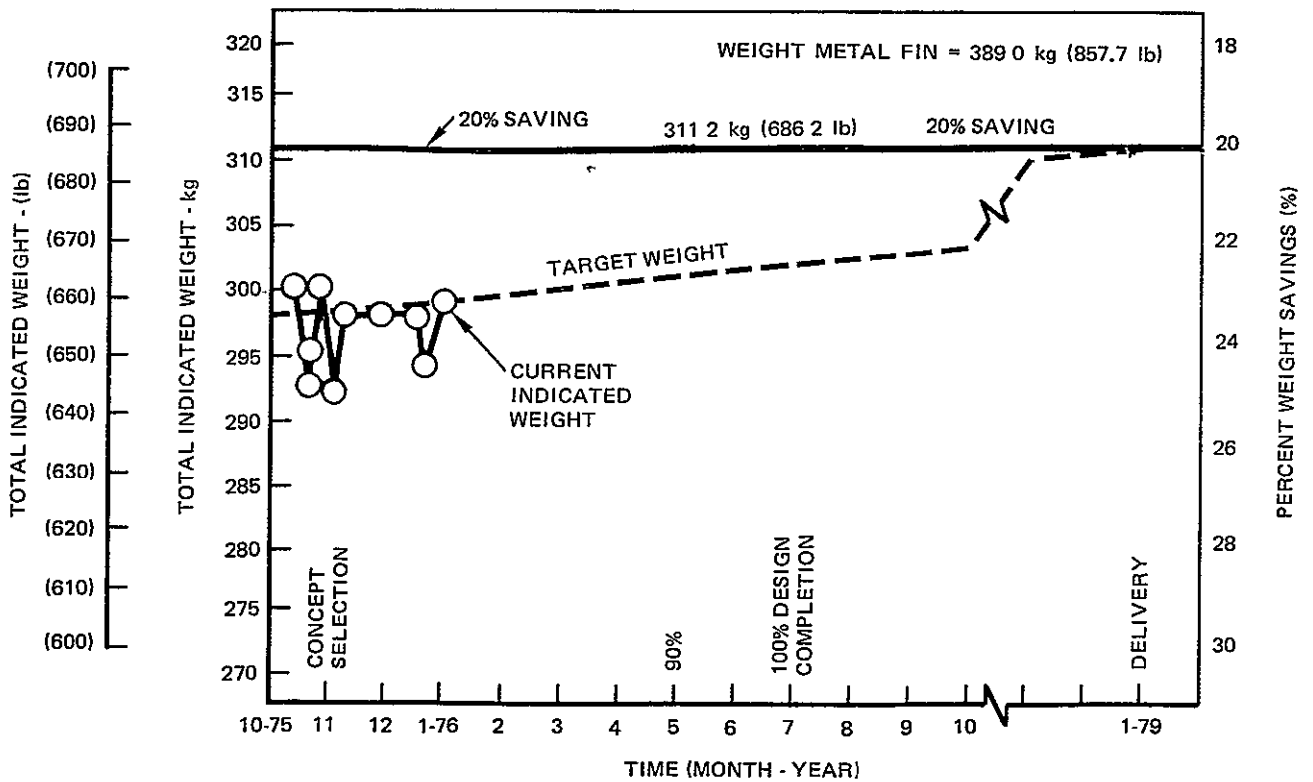


Figure 33. Weight-Time History

TABLE 10. PROJECTED PRODUCTION/MAINTENANCE COST

(Based on Cumulative Average of 250 Aircraft)

Component	Metal Fin			ACVF		
	Labor	Material	Total	Labor	Material	Total
Skin Covers (L/R)	14 467	2 960	17 427	5 400	12 807	18 207
Spars (Fwd/Aft)	9 274	1 217	10 491	7 739	3 347	11 086
Aux Spar	382	42	424	382	42	424
Actuator Ribs	2 707	270	2 977	1 573	432	2 005
Hinge Ribs	2 288	185	2 423	2 894	593	3 487
Intermediate	4 355	388	4 743	3 451	810	4 261
Upper Closure Ribs	854	49	903	854	49	903
Rib Spar Fittings	283	301	584	283	301	584
Assembly	17 185	5 752	<u>22 937</u>	13 375	3 831	<u>17 206</u>
Total	51 745	11 164	<u>\$62 909</u>	35 951	22 212	<u>\$58 163</u>
Maintenance	* 180 M/H Per A/C Per Year			* 180 M/H Per A/C Per Year		
Inspection						
Repairing						
Costs			<u>\$ 4 500.00</u>			<u>\$4 500.00</u>
*Based on 3000 flight hours per year						



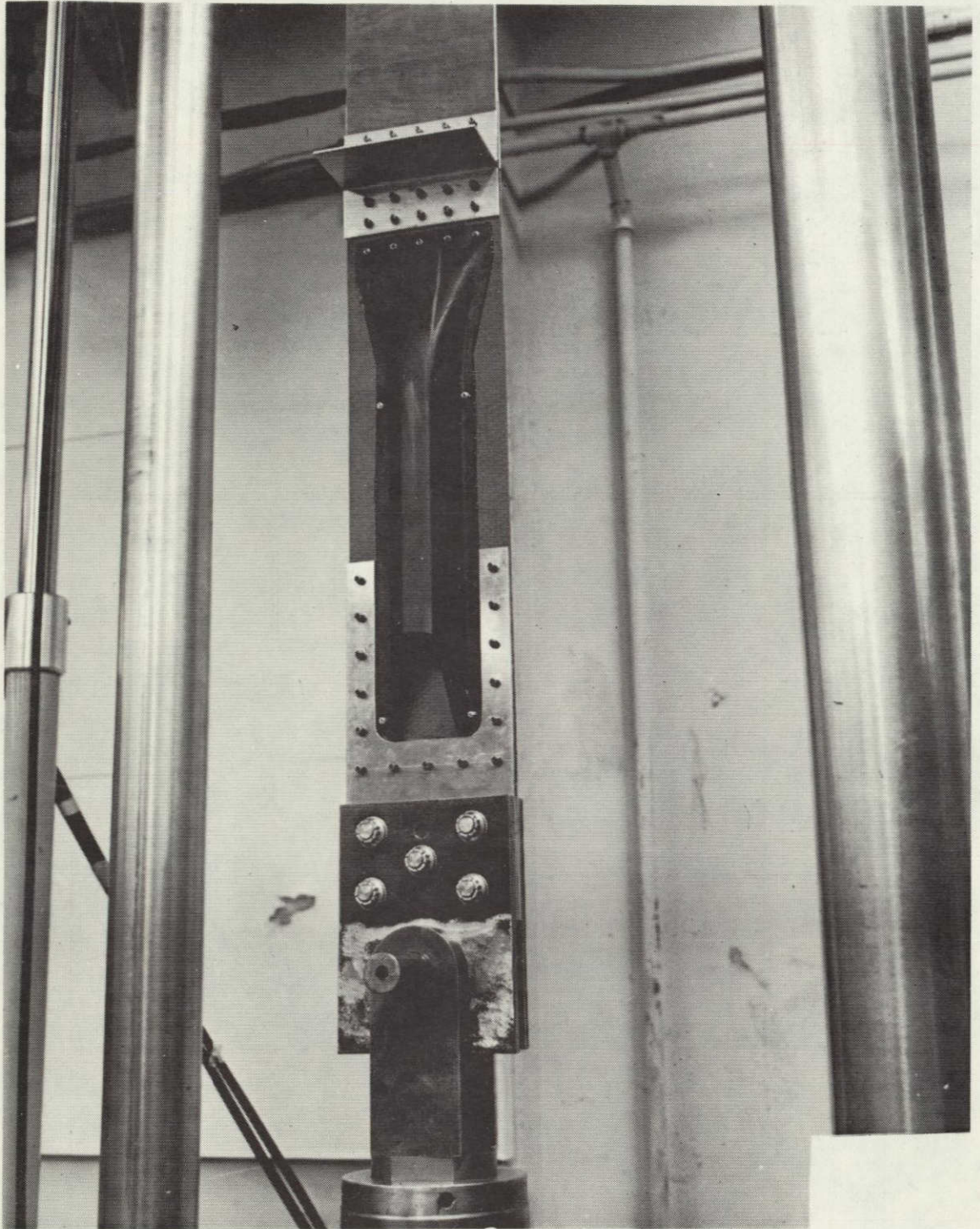


Figure 34. Hat Section Specimen

contours have also been released. These data generated at Lockheed's computer graphics unit will facilitate the assessment of the impact of tolerances and tooling concepts on assembly interfaces.

The primary purpose of the Vertical Stabilizer Interface Drawing is to provide the information necessary to assure that the composite fin will be physically and functionally interchangeable with the existing metal design. To this end, the drawing will provide the following information:

1. identification of the surrounding structure and the establishment of critical and noncritical features which must be accommodated to meet the interchangeability requirements.
2. identification of existing functional systems and their relationship to the fin structure.
3. identification of nonflight related items that are essential for manufacturing, transport, and/or assembly (hoisting provisions, alignment and symmetry points, etc.).
4. establishment of basic fin dimensional relationships, i.e., rib and stringer locations, that are required for coordination between the three design organizations (Lockheed-California Company, Lockheed-Georgia Company, and LAAD).

Additionally, the replacement of the metal fin with the composite fin will create a thermal mismatch between the existing aluminum (leading edge, fuselage, and rudder) adjacent structure. The most severe case of thermal mismatch will occur spanwise along the rudder hinge line interface. Hinge number 2 at RS 85.86 reacts all loads parallel to the hinge axis. Hinge number 7 is located at the tip approximately 6.8 m (22.5 ft) away. The differential expansion/contraction at the operational temperature extremes between the number 2 and number 7 hinges is 8.1/12.2 mm (0.32/0.48 in.) respectively for the expansion/contraction. The problem will be further evaluated and a design solution established during the Phase II detail design activities.

## 2.2 STRUCTURAL ANALYSIS

For the analysis of advanced composite structures a strong interface is required between all participating groups. This is particularly true where design and stress are concerned, as the material is engineered as well as the structure. An analysis flow chart is shown in Figure 35.

The structural analysis subtask includes the trade-off analysis, the initial preparation of the NASTRAN model, and the preparation of the Ancillary Test Plan and the FAA Certification Plan. It also includes much of the work in establishing the design criteria such as fatigue and fail safe requirements.



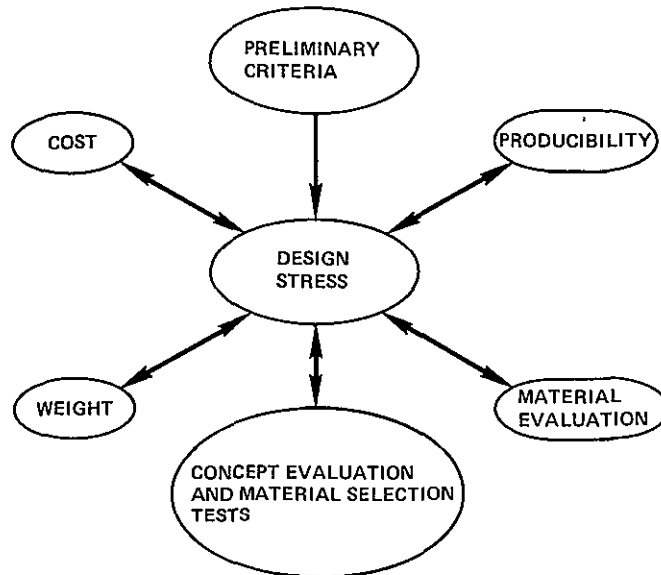


Figure 35. Structural Analysis Flow Chart

### 2.2.1 Analytical Approach

For the trade-off studies the internal loads used were basically those used for the 211 375-kg (466 000 lb) gross weight L-1011 airplane. In general the loads used attempted to represent the maximum internal loads for any model of the L-1011 currently available. These internal loads had been computed using finite element models by the Lockheed FAMAS system.

For the ACVF finite element analysis the NASTRAN system is being used. Much of the detail analysis of advanced composite structures has been automated on the Conversational Programming System (CPS) which is a remote terminal system. This system was used extensively in Phase I. In Phase II, CPS will be augmented by use of the Direct Computer Access System (DCAS) which allows editing and submittal to the batch processing mode.

### 2.2.2 Preliminary Design Allowables

To assure uniformity during the Phase I trade-off studies, preliminary design allowables were established which were suitable for linear laminate characterization programs. These allowables are shown in Table 11.

These particular values are an amalgamation of properties achievable with laminates using T300 graphite with either 400K (260°F) or 450K (350°F) curing resin systems. While they are not statistically based design allowables, it is anticipated that B basis allowables for a specific T300/epoxy

TABLE 11. PRELIMINARY DESIGN PROPERTIES FOR DRY GRAPHITE/EPOXY FOR LINEAR PROGRAMS

Stiffness	E1 (TENS/COMPR)	GPa (msi)	137.9 (20)
	E2 (TENS/COMPR)	GPa (msi)	8.96 (1.3)
	G	GPa (msi)	4.48 (0.65)
	NU		0.21
Longitudinal	TENSION $F_L^{tu}$ EPSU (1,1)	MPa (ksi) mm/m ( $10^{-3}$ in/in)	1172 (170) 8.5
	COMPR $F_L^{cu}$ EPSU (1,2)	MPa (ksi) mm/m ( $10^{-3}$ in/in)	1034 (150) -7.5
Transverse	TENSION $F_T^{tu}$ EPSU (2,1)	MPa (ksi) mm/m ( $10^{-3}$ in/in)	44.8 (6.5) 5
	COMPR $F_T^{cu}$ EPSU (2,2)	MPa (ksi) mm/m ( $10^{-3}$ in/in)	89.6 (13) -10
In-Plane Shear	$F_{LT}^{su}$ EPSU (3,1)	MPa (ksi) mm/m ( $10^{-3}$ in/in)	68.9 (10) (+)15.4
Thermal Expansion	ALFA (1)	$\mu\text{m}/(\text{m}\cdot\text{K})$ ( $10^{-6}$ in/in/ $^{\circ}\text{F}$ )	0.54 (0.3)
	ALFA (2)	$\mu\text{m}/(\text{m}\cdot\text{K})$ ( $10^{-6}$ in/in/ $^{\circ}\text{F}$ )	27.0 (15.0)
Physical Properties	THICKNESS	mm (in.)	0.1321 (0.0052)
	DENSITY	$\text{Mg}/\text{m}^3$ ( $\text{lb}/\text{in}^3$ )	1.605 (0.058)

resin combination will not result in laminate properties which are significantly lower than those obtained with these properties.

As a preliminary design policy for determining laminate strengths by material characterization programs, the following criteria were established:

1. No ply failure in the filament direction is permitted at ultimate load.
2. No in-plane shear or transverse failure is permitted in any ply at design limit load.
3. Account must be taken of the reduction in laminate ultimate tensile and compressive strengths due to stress concentrations from holes. This can be calculated from semi-empirical data or using the factors shown for cutouts in the Advanced Composite Design Guide (ref. 2).

Laminate allowables were computed using the Lockheed HYBRID program which is a stepped failure analysis using bilinear ply level stress-strain data; and the RI/LAAD AC50 program which is a linear program which computes carpet plots.

The effects of the environment on the unidirectional ply properties were estimated. A first-order estimate of the influence of the moisture/temperature environment is shown in Table 12. The percent reductions in properties were based upon an evaluation of three data sources:

1. The screening test results for T300/5209 discussed under Task 2.
2. The qualification and acceptance test results for T300/5209 discussed under Task 2.
3. The data on AS/3501 published in ref. 3.

The negative values shown in Table 12 in parentheses represent increases in strain for transverse compression and shear. These estimated reduction factors are applied to the room temperature dry properties to obtain wet (approximately 1 percent moisture by weight) properties at 322K (120°F) temperature for preliminary design purposes.

It should be noted that these factors are estimated from tests of T300/5209 and T300/934 with moisture contents of 0.32 percent to 0.74 percent tested at 344K (160°F) and tests of AS/3501 with a moisture content of 1.9 percent and interpolated to 322K (120°F).

The L-1011 aircraft design specification stipulates that the extreme temperature for structural design shall be 344K (160°F) (apart from internal heat sources) to account for hot soaking. The maximum temperature can occur at midday during hot days only on horizontally exposed surfaces on the ground, and temperatures of vertical surfaces such as the fin are normally somewhat

TABLE 12. PRELIMINARY ESTIMATE OF ENVIRONMENTAL REDUCTION FACTORS

		REDUCTION*
Stiffness	E1	0
	E2	25%
	G	25%
	NU	10%
Longitudinal	$F_L^{tu}$	0
	$\epsilon_L^{tu}$	0
	$F_L^{cu}$	14%
	$\epsilon_L^{cu}$	14%
Transverse	$F_T^{tu}$	32%
	$\epsilon_T^{tu}$	10%
	$F_T^{cu}$	18%
	$\epsilon_T^{cu}$	(-10%)
Shear	$F_{LT}^{su}$	18%
	$\epsilon_{LT}^{su}$	(-10%)
*Reduction factors used to convert room temperature dry properties to 322K (120°F) wet (approximately 1 percent moisture) properties.		

cooler because the solar radiation is less. Furthermore, the loads during ground handling are much less than the flight loads. The maximum structural temperature during flight is 322K (120°F) from sea level to 915 m (3000 ft) altitude, and the temperature drops off rapidly above 915 m (3000 ft). The sea level design flight conditions which apply significant loads to the structure occur at a velocity of 110 m/s (215 KEAS), and the air flow cools the structure below 322K (120°F). Consequently, the use of material properties at 322K (120°F) is conservative. It would be even more conservative to use material properties at 344K (160°F) for design in lieu of 322K (120°F).

The estimated environmental wet/hot reduction factors were applied to the room temperature dry allowables. The basic design properties for tension compression and shear were computed using these reduced ply-level properties in the HYBRID program. Buckling properties were computed using a general purpose buckling program called COMAIN. The calculated reductions for two typical laminates are shown in Table 13.

It can be seen that the effects on fiber dominated properties are minimal, while the effects on matrix dominated properties are more pronounced. In general the ACVF structure is not strength critical but buckling critical. Hence the effect of environmental factors on design weight are anticipated to be minimal.

It can also be seen from Table 13, that while in tension the modulus and strength of a laminate are degraded about equally, the same is not true for compression and shear. It can also be seen that the buckling and the modulus

TABLE 13. CALCULATED ENVIRONMENTAL EFFECTS ON LAMINATES

	Skin 25%0°/75%+45°	Spars and Crown 60%0°/40%+45°
Tension		
Strength	-5%	-2%
Modulus	-6%	-1%
Compression		
Strength	-19%	-16%
Modulus	-6%	-2%
Buckling	-2%	-2%
Shear		
Strength	-14%	-15%
Modulus	-2%	-4%
Buckling	-3%	-4%
<p>Computed with HYBRID and COMAIN using the preliminary estimate of environmental reduction factors.</p> <p>Conclusion: Negligible effect on surface design weight because it is designed by local buckling strength.</p>		

are not necessarily degraded the same. For an all  $0^\circ$  laminate, the compression modulus would be almost the same wet or dry. For an all  $\pm 45^\circ$  laminate the modulus degradation between dry and wet is about 23 percent.

The buckling is controlled by the unidirectional compression modulus. The degradation is small because the transverse properties have only a small influence on buckling. For an all  $0^\circ$  laminate, the buckling strength is degraded 5 percent due to moisture. For an all  $\pm 45^\circ$  laminate, the buckling degradation is 1.7 percent for a wet laminate. The reason for the difference between the modulus and buckling strength due to moisture can be seen in the equations shown below. Each term in each equation is affected to a different degree by moisture, so the total results are different.

The modulus derived from the A in-plane stiffness matrix is

$$E_x = \frac{A_{11} - \frac{A_{12}^2}{A_{22}}}{h}$$

and the buckling for a long simply supported panel from the D bending stiffness matrix is

$$N_x, cr \approx - \left( \frac{\pi}{b} \right)^2 \left[ D_{11} + 2 (D_{12} + 2 D_{66}) + D_{22} \right]$$

### 2.2.3 Design Criteria

As the ACVF is being designed to be installed on an existing airplane, it must be structurally and functionally compatible with the surrounding structure which is to be unchanged. Such a requirement limits the exploitation of the full benefits of advanced composites and of necessity reduces the configuration options.

As the ACVF may be removed after a certain number of years in service and be replaced by a metallic fin, all interfaces must be identical. It is thus important that load distributions must remain unchanged particularly at the root.

The bending stiffness (EI) and the torsional stiffness (GJ) must remain essentially unchanged so that the aeroelastic response does not change. To accomplish this, criteria of matching EI and GJ within +0 to +5 percent were

established. By adhering to the above criteria, the flutter integrity of the ACVF will be able to be proved by calculation and by limited testing, thus precluding the need for flutter model testing.

The requirements for Phase I state that no buckling will occur at ultimate load. However, since buckling analyses are generally conservative, a panel will not be beefed up if theoretical buckling occurs at 90 percent of ultimate load. While there is evidence that buckling is not detrimental to composite structures in shear or to some extent in compression, there is insufficient data and no post buckling analysis methods for composite structure are currently available. Buckling would therefore be an unacceptable risk at the present time.

There is experimental evidence that galvanic corrosion occurs when graphite and aluminum are placed in intimate contact. While many such cases occur on military aircraft and no problems have been encountered, such aircraft are designed for much shorter lives than commercial transports. The ground rule was established that all graphite/aluminum interfaces must be insulated with one ply of Kevlar 49 or fiberglass cloth.

As material properties are different for tension and compression, the laminate properties are dependent on the applied loads. The stress-strain curves for most composites in compression and shear are nonlinear, and in the case of Kevlar 49, the tension properties are also nonlinear. For the purposes of the HYBRID computer program, the stress-strain curves are idealized by two straight lines giving a bilinear curve. The slope of the initial line is the primary modulus, and the slope of the second line, the secondary modulus. The intersection of the two lines is called yield.

A sample run of HYBRID is shown in Figure 36. The laminate is  $\pm 45/0_4$  and the loading is uniaxial tension.

The input and output is described below:

- NM                      Number of materials
- EA(1,1,1)              Fiber direction moduli; primary tension and compression and secondary tension and compression
- EB(1,1,1)              Transverse moduli, same sequence
- G1(1,1)                Primary and secondary shear modulus
- MU(1)                 Poissons ratio
- ALA(1,1)              Thermal coefficients of expansion; fiber direction, transverse and shear
- EPT(1,1,1)            Tension strains  $\times 10^3$ ; fiber yield, transverse yield, fiber failure, and transverse failure

- EPC(1,1,1)    Compression strains  $\times 10^3$ ; yield and failure
- EPS(1,1)    Shear strain  $\times 10^3$ ; yield and failure
- N            Number of ply sets
- OP           Output option (1 prints input data tables)
- Dt           Temperature range from curing. Used only if residual thermal is to be included
- Th(1)       Ply set orientations
- T(1)       Ply set thicknesses
- M(1)       Material code
- NN(1)       Applied loads ratios  $N_x$ ,  $N_y$ ,  $N_{xy}$  and print out option, 1, prints all steps to total laminate rupture. After each failure, the laminate is maintained at the same strain and a redistribution is calculated before proceeding to the next step. With this option, the failure stress is not the final print out step. In this example, laminate failure occurs at failure of the  $0^\circ$  plies at 442.77 MPa (64 200 psi).

The output gives laminate properties and stresses and strains in the laminate axes, followed by the lamina stresses and strains in the lamina axes.

#### 2.2.4 Hat Stiffened Cover Analysis

For the trade-off analysis, it was decided to place certain constraints on the stiffener geometry. A fully optimized analysis invariably gives skin stiffener configurations which are totally impractical and can easily cloud the picture when trying to convert back to practical designs. Because of the necessity of maintaining a continuous rib cap as close to the surface as possible and because of the geometry of hinge fittings picking up the rib caps, a maximum stiffener height of 31.75 mm (1.25 in.) was established. The skins were basically designed to meet  $G_t$  requirements and  $E_t$  requirements along with the stiffeners. The stiffener spacing was then established based on local buckling analysis of the skins using a computer program COMAIN. These studies showed that the hat stiffened approach was better than the I stiffened approach.

Following the trade-off studies, the basic skin and stiffener layups for input into the NASTRAN model were determined. The cover was broken up into areas of constant stiffener spacing between the rib locations. The design loads were assumed to be constant over the respective areas and only axial  $N_x$  loadings and normal pressures were considered, as  $N_y$  loads were negligible and shears had little effect on buckling. The stiffener spacings and design



```

load(HYBRID,JKSN)STRMTH
x=9
NN
1
EA1(1,1,1)
21e6,20e6,21e6,15.65e6
EB1(1,1,1)
1.3e6,1.6e6,1.3e6,1.233e6
G1(1,1)
.66e6,.34e6
NU(1)
.21
ALA(1,1)
.3,14.4,0
EPT(1,1,1)
9.2,6,9.2,6
EPC(1,1,1)
7,11,9.3,17
EPS(1,1)
12.6,18
N
3
Op
1
Dt
0
Th(1)
45,-45,0
T(1)
.0312,.0312,.0208
H(1)
1,1,1
NN(1)
1,0,0,1

```

HYBRID760202  
\*\*\*\*\*

DeltaT; difference between cure and operating temp= 0

MATERIAL	EA1	EA2	EB1	EB2	NUAB	GAB1	GAB2	ALPHA A	ALPHA B
1	2.10E+07	2.10E+07	1.30E+06	1.30E+06	2.10E-01	6.60E+05	3.40E+05	3.00E-07	1.44E-05

MATERIAL	EAC1	EAC2	EBC1	EBC2
1	2.00E+07	1.56E+07	1.60E+06	1.23E+06

LAMINA	THICKNESS	THETA	MATERIAL
1	0.0312	45.00	1
2	0.0312	-45.00	1
3	0.0208	0.00	1

LIMIT STRAINS						
MATERIAL	eLt	eLc	eTt	eTc	eLT	
1	9.20E-03	-7.00E-03	6.00E-03	-1.10E-02	1.26E-02	

ULTIMATE STRAINS						
MATERIAL	eLt	eLc	eTt	eTc	eLT	
1	9.20E-03	-9.30E-03	6.00E-03	-1.70E-02	1.80E-02	

LAMINATE					
EX	EY	NUXY	GXY	ALPHA X	ALPHA Y
7.15E+06	3.69E+06	7.48E-01	4.25E+06	1.68E-07	3.10E-06
fx	fy	fxY	ex	eY	eXY
5.15E+04	0.00E+00	0.00E+00	7.21E-03	-5.39E-03	4.73E-11

Figure 36. Sample Run of HYBRID Computer Program

ORIGINAL PAGE IS  
OF POOR QUALITY

LAMINA	n	THETA	MATERIAL	fL	fT	fLT	eL	eT	eLT
1	45	1	1.93E+04	1.43E+03	-8.31E+03	9.07E-04	9.07E-04	-1.26E-02	
2	-45	1	1.93E+04	1.43E+03	8.31E+03	9.07E-04	9.07E-04	1.26E-02	
3	0	1	1.50E+05	-6.22E+03	3.12E-05	7.21E-03	-5.39E-03	4.73E-11	

YIELD IN DIRECTION 3 IN 45 PLY SET NO 1

YIELD IN DIRECTION 3 IN -45 PLY SET NO 2

LAMINATE	EX	EY	NUXY	GXY	ALPHAX	ALPHAY
	6.38E+06	3.21E+06	8.33E-01	4.25E+06	-3.41E-08	3.41E-06
	fx	fy	fxY	eX	eY	eXY
	6.42E+04	0.00E+00	0.00E+00	9.20E-03	-7.05E-03	5.59E-11

LAMINA	n	THETA	MATERIAL	fL	fT	fLT	eL	eT	eLT
1	45	1	2.29E+04	1.69E+03	-9.55E+03	1.07E-03	1.07E-03	-1.63E-02	
2	-45	1	2.29E+04	1.69E+03	9.55E+03	1.07E-03	1.07E-03	1.63E-02	
3	0	1	1.91E+05	-8.22E+03	3.69E-05	9.20E-03	-7.05E-03	5.59E-11	

YIELD IN DIRECTION 1 IN 0 PLY SET NO 3

FAILURE IN DIRECTION 1 IN 0 PLY SET NO 3

LAMINATE	EX	EY	NUXY	GXY	ALPHAX	ALPHAY
	9.62E+05	9.62E+05	8.88E-01	4.09E+06	1.27E-06	1.27E-06
	fx	fy	fxY	eX	eY	eXY
	8.85E+03	0.00E+00	0.00E+00	9.20E-03	-8.17E-03	2.79E-11

LAMINA	n	THETA	MATERIAL	fL	fT	fLT	eL	eT	eLT
1	45	1	1.09E+04	8.13E+02	-5.90E+03	5.16E-04	5.16E-04	-1.74E-02	
2	-45	1	1.09E+04	8.13E+02	5.90E+03	5.16E-04	5.16E-04	1.74E-02	
3	0	1	0.00E+00	0.00E+00	0.00E+00	0.00E+00	0.00E+00	0.00E+00	

LAMINATE	EX	EY	NUXY	GXY	ALPHAX	ALPHAY
	9.62E+05	9.62E+05	8.88E-01	4.09E+06	1.27E-06	1.27E-06
	fx	fy	fxY	eX	eY	eXY
	9.18E+03	0.00E+00	0.00E+00	9.53E-03	-8.47E-03	2.90E-11

LAMINA	n	THETA	MATERIAL	fL	fT	fLT	eL	eT	eLT
1	45	1	1.13E+04	8.42E+02	-6.12E+03	5.34E-04	5.34E-04	-1.80E-02	
2	-45	1	1.13E+04	8.42E+02	6.12E+03	5.34E-04	5.34E-04	1.80E-02	
3	0	1	0.00E+00	0.00E+00	0.00E+00	0.00E+00	0.00E+00	0.00E+00	

FAILURE IN DIRECTION 3 IN 45 PLY SET NO 1

FAILURE IN DIRECTION 3 IN -45 PLY SET NO 2

COMPOSITE FAILED  
HYBRID

Figure 36. Concluded

loads are shown in Figure 37. For the purpose of discussion, the basic analysis procedure for the cover area 7, the area extending from VSS 145.71 to VSS 197.13 and having a 0.183 m (7.20 in.) stiffener spacing, will be described. This area is shown in Figure 37.

#### 2.2.4.1 Basic Configuration

Each area was idealized as shown in Figure 38. The length L was 635 mm (25 in.) which corresponds to the distance between the ribs. Previous trade-off studies, considering a design with none, one, or two intermediate ribs, determined that one intermediate rib giving a 635 mm (25 in.) spacing was the most cost and weight efficient. Each panel was considered to be simply supported

Overall, the skin was allowed to taper spanwise and chordwise. Since the lower and aft sections of the fin box have the highest loadings, the  $\pm 45^\circ$  and  $0^\circ$  plies in the skin are allowed to drop off in number from the root to tip and from trailing edge to leading edge. It was determined because of fabrication considerations to add no new plysets from root to tip or from trailing edge to leading edge. For example, a taper of  $\pm 45_3/0_4/\pm 45_3$  to  $\pm 45_2/0_2/\pm 45_2$  would be allowed, but a taper of  $\pm 45_3/0_4/\pm 45_3$  to  $45_2/0_6/\pm 45_2$  would not, since in the latter case the number of  $0^\circ$  plysets has increased. The hat section was allowed to drop off  $0^\circ$  plies in the crown, but there was to be no tapering of the hat section as tool dimensions would remain the same along the hat section length.

A basic repeating skin-stiffener section in the panel area was used for analysis purposes and is shown in Figure 39. The web and flange have a  $(\pm 45/0/\pm 45)_s$  layup and the crown of the stiffener has a  $(\pm 45/0/\pm 45/0_N/2)_s$  layup. The section properties were determined by SECPRO, a computer program that determines section properties of sections built from composites.

The Kevlar outer plies were not considered during this phase of the analysis, but were added after the skin layup had been determined.

#### 2.2.4.2 Gt and Et Matching

In order to match the metal Gt, an initial estimate on the number of  $(\pm 45/\pm 45)$  ply sets in the skin was determined by

$$N_{45} = \frac{(Gt)_m}{4t G_{xy}}$$

ORIGINAL PAGE IS  
OF POOR QUALITY

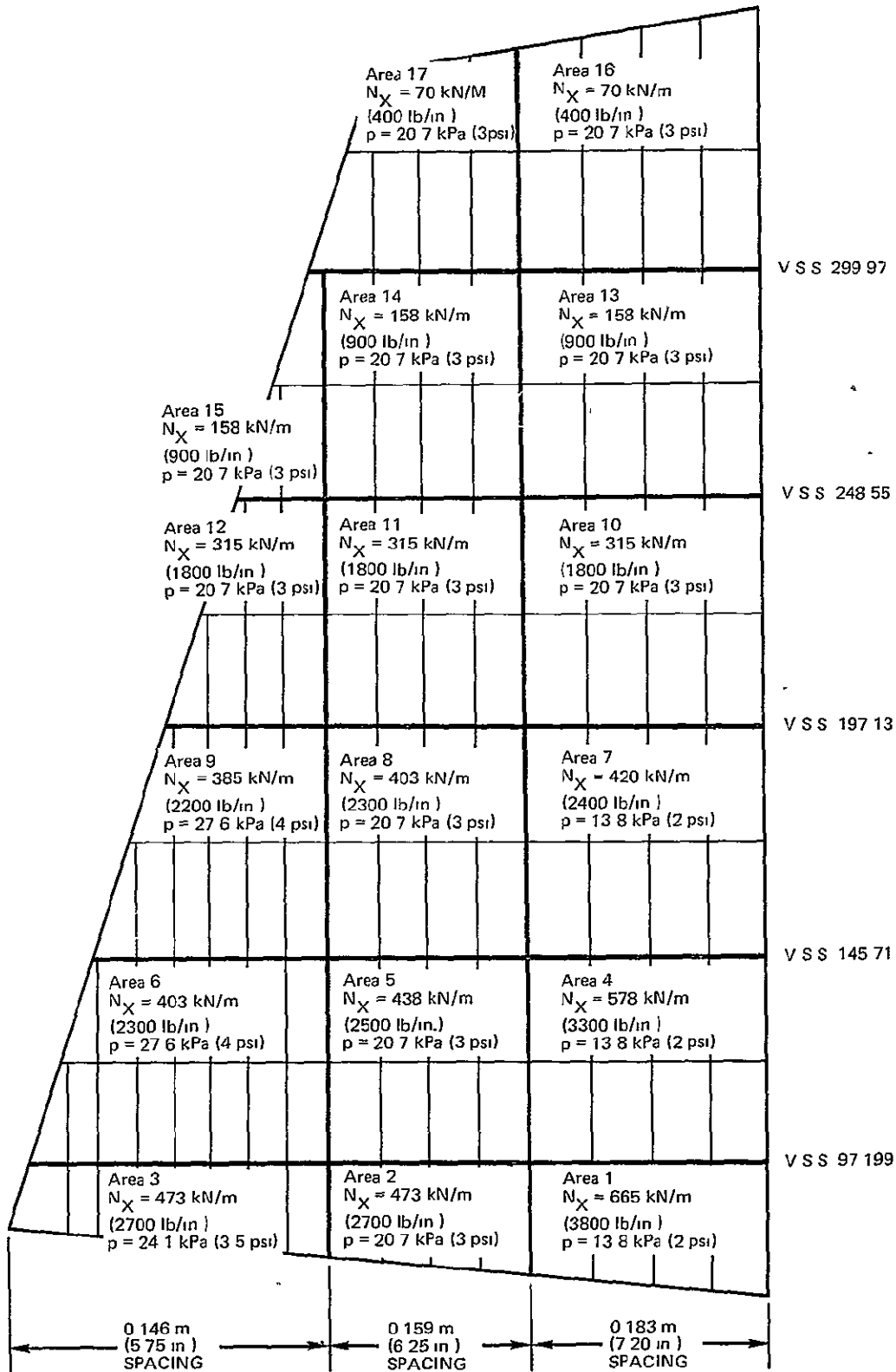


Figure 37. Design Loads and Stiffener Spacing

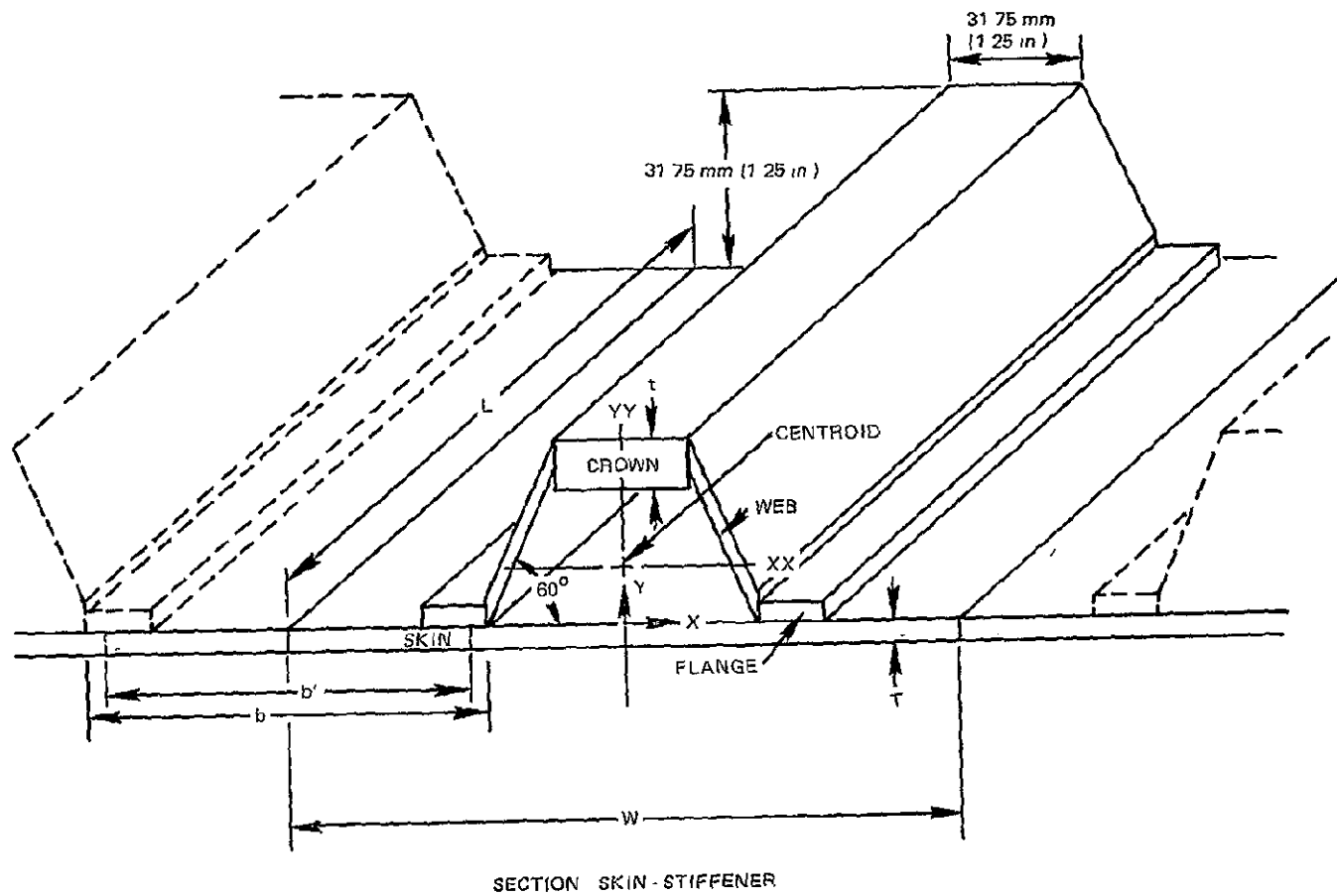


Figure 38. Typical Cover Area



where

$(Gt)_m$  = the metal  $Gt$

$t$  = thickness of one ply of composite

$G_{xy}$  = shear modulus of  $(\pm 45/\pm 45)$  layup

An initial estimate of the number of 0 degree plies in the skin was found by matching the composite and metal  $Et$  using

$$N_0 = \frac{(Et)_m}{E_x t}$$

where

$(Et)_m$  = the metal  $Et$

$E_x$  = Young's modulus of 0 degree layup

The total number of 0 degree plies  $N_0$  is distributed in the crown of the stiffener and the skin.

The initial layup determination for area 7 is shown in Table 14. Using the T300/5209 material properties, a material characterization computer program calculated a  $G_{xy}$  of 36.2 GPa (5.25 msi) for a  $(\pm 45)_s$  layup. Since panel stability depends heavily on the number of  $\pm 45$  plies, the calculated value of  $N_{45}$  was rounded up to 3 rather than down to 2. Young's modulus  $E_x$

TABLE 14.  $Gt$  AND  $Et$  MATCHING

VSS Location	Metal $Gt$ MN/m(lb/in $\times 10^{+3}$ )	$N_{45}$	Initial $N_{45}$	Metal $Et$ MN/m(lb/in $\times 10^{+3}$ )	$N_0$	Initial $N_0$
145.71 - 162.85	45.71 (261)	2.39	3	187.6 (1071)	10.3	5
162.85 - 179.99	45.71 (261)	2.30	3	183.9 (1050)	10.1	4
179.99 - 197.13	45.01 (257)	2.35	3	172.8 (987)	9.5	4

for the 0° layup in compression was 138 GPa(20 msi). Since the EI of the metal fin box was not to be exceeded, the value for  $N_0$  was rounded down. The total number of zeros was then distributed between the crown of the stiffener and the skin. The resulting initial layups for the crown and the skin are shown in Table 15.

The matching of the metal Et and the Et of a 0° layup, and then distributing the 0° plies in the skin and crown provide an initial composite skin-stiffener cross section with an EI close to the metal EI. The EI's for the 0.183 m (7.20 in.) wide composite sections at various VSS locations were calculated and compared to the EI's of the metal sections having the same width and location. The metal section centroids were taken to be 6.35 mm (0.25 in.) inboard of the skin mold line. Table 15 shows how the EI's of the skin-stiffener sections in area 7 were close to the metal EI's, but lower in value as desired.

### 2.2.4.3 Specific Configuration

Having an estimate of the basic layups for the skin-stiffener sections in a cover area available, an iterative procedure was begun to determine the specific layups. Using the design loads, the loads carried by the elements of the skin-stiffener section were calculated and then compared with strength and stability load limits.

Compressive and tensile strengths for uniaxial loading conditions were determined using the multilinear stepped failure analysis computer program HYBRID. The laminates were assumed to be flat infinite anisotropic composite plates under plane stress conditions. Strengths were determined for the skin, stiffener web, and stiffener crown elements.

TABLE 15. INITIAL SKIN AND CROWN INFORMATION

VSS Location	Skin Layup	Crown Layup	Metal EI MN·m <sup>2</sup> (lb·in <sup>2</sup> x10 <sup>+6</sup> )	Composite EI MN·m <sup>2</sup> (lb·in <sup>2</sup> x10 <sup>+6</sup> )
145.71 - 162.85	$\pm 45_3/0_5/\pm 45_3$	$\pm 45_2/0_5/\pm 45_2$	2.353 (820)	2.201 (767)
162.85 - 179.99	$\pm 45_3/0_4/\pm 45_3$	$\pm 45_2/0_6/\pm 45_2$	2.104 (733)	1.814 (632)
179.99 - 197.13	$\pm 45_3/0_4/\pm 45_3$	$\pm 45_2/0_5/\pm 45_2$	1.802 (628)	1.624 (566)



The column buckling load for the combined stiffener and skin section was determined using the Euler equation. For a simply supported column with constant cross section and in the elastic range, the critical load  $N_{x,cr}$  in kN/m (pounds per inch) width of  $W$  is

$$N_{x,cr} = \frac{\pi^2 c^2 (EI)}{L^2 W}$$

where  $c$  is the ratio of the column length  $L$  to the effective length  $L_e$ .

Compressive buckling loads were determined using the computer program COMAIN in which the panels are assumed to be orthotropic flat rectangular plates simply supported on all four sides. The loads were factored by 1.5 to account for edge restraint due to the stiffeners. Panel lengths were taken to be 635 mm (25 in.). An effective panel width  $b'$  between the stiffeners shown in Figure 38 was used where  $b'$  is equal to  $b-2r$  and  $r$  is the flange radius.

The stiffener section and skin are acted on by  $N_x$  loading. It was desired to determine the amount of the total loading carried by the skin, the crown of the stiffener, and the stiffener web. The amount of load carried by each of these elements was calculated as

$$N_{x,i} = \frac{N_x W}{b_i} \frac{E_i A_i}{\sum_{i=1}^6 E_i A_i}$$

where

$N_{x,i}$  = the axial load in element  $i$

$N_x$  = the total axial loading

$E_i$  = Young's modulus of element  $i$

$b_i$  = width of element  $i$

$A_i$  = area of element  $i$

$W$  = width of the skin-stiffener section

The pressure design load and the initial eccentricity of the applied  $N_x$  loading causes bending in the skin-stiffener section. Assuming an initially straight, simply supported elastic beam, the load in each element due to bending is

$$N_{x,i} = \frac{M_x E_i t_i y}{(EI)_x}$$

where

$y$  = distance from the neutral axis

$(EI)_x$  = the bending stiffness about the principle XX axis

$t_i$  = thickness of element  $i$

The load in each element has dimensions of kN/m (pounds per inch) width of element  $i$ . The moment  $M_x$  is a combination of effects due to pressure loading and the application of the load away from the neutral axis. The effect due to offset loading was assumed to be  $0.002 L W N_x$  where  $0.002L$  is the initial eccentricity which is based on a column length  $L$  of 635 mm (25 in.). The moment due to pressure loading is the maximum moment at the center of the beam length and is

$$M_x = p \frac{WL^2}{8}$$

where  $p$  is the pressure.

The load per element due to bending was, therefore, determined using

$$N_{x,i} = \left( p \frac{WL^2}{8} + 0.002 L W N_x \right) \frac{E_i t_i y}{(EI)_x}$$

The total applied  $N_{x,i}$  loading per element was then calculated by summing the amount of the total load carried and the load due to bending.

The results of a typical analysis during the iterative process to determine the specific element layouts for a skin-stiffener section in cover area 7 is shown in Table 16. The buckling load determination for the skin area between the stiffeners utilized the computer program PLBUCK, which is a version of COMAIN that determines the sign of the strain in the laminae and

TABLE 16. SKIN-STIFFENER ELEMENT LOADINGS

		Skin	Crown	Web
$N_x$ loading applied	kN/m (lb/in)		420 (2400)	
Pressure loading	kPa (psi)		13.79 (2)	
Column instability	kN/m (lb/in)		655.3 (3742)	
Layup		$[+45_3/0_2]_s$	$[+45_2/0_4]_s$	$[+45_2/0]_s$
Tensile Strength	kN/m (lb/in)	935.3 (5341)	1573.6 (8986)	503.6 (2876)
Compressive Strength	kN/m (lb/in)	767.9 (4385)	1362.2 (7779)	413.5 (2361)
Local Buckling Strength	kN/m (lb/in)	281.1 (1605)	3249.7 (18557)	657.2 (3753)
Applied $N_{x,i}$ Loading	kN/m (lb/in)	297.5 (1699)	612.6 (3498)	204.2 (1166)

then uses the appropriate tensile or compressive moduli to calculate the laminate A, B, and D matrices. The determination of the column buckling load, the section element loads due to the applied  $N_x$  loading, the section element loads due to bending, the total element loads, and section information was accomplished with SECP, a computer program which is a combination of the program SECPRO and the basic equations of the analysis to determine loads. The basic skin-stiffener section shown with skin layup of  $\pm 45_3/0_4/\pm 45_3$  and stiffener crown layup of  $\pm 45_2/0_8/\pm 45_2$  was the section chosen for cover area 7 as a result of the iterative process. It can be seen in Table 16 that the load in the skin is just above the calculated buckling load, since local buckling of the skin was allowed to take place just before ultimate load is reached.

A comparison of the metal and composite section EI's and Et's was again made, and the results are shown in Table 17. The values were within acceptable limits for the initial trade-off studies.

TABLE 17. EI AND Et COMPARISON

VSS Location	Metal Et MN/m (lb/in x10 <sup>+3</sup> )	Composite Et MN/m (lb/in x10 <sup>+3</sup> )	Metal EI MN·m <sup>2</sup> (lb·in <sup>2</sup> x10 <sup>+6</sup> )	Composite EI MN·m <sup>2</sup> (lb·in <sup>2</sup> x10 <sup>+6</sup> )
145.71 - 162.85	187.6 (1071)	164.3 (938)	2.353 (820)	2.052 (715)
162.85 - 179.99	183.9 (1050)	164.3 (938)	2.104 (733)	1.871 (652)
179.99 - 197.13	172.8 (987)	164.3 (938)	1.802 (628)	1.705 (594)

### 2.2.5 Honeycomb Cover Analysis

The honeycomb concepts considered are shown in Figure 7. The analysis of each concept was performed in sufficient depth to enable cost and weight estimates to be made, and EI and GJ calculations to be performed. In general the covers were buckling critical not strength critical. For these analyses, all panels were assumed to be simply supported, and panels were analyzed assuming orthotropic properties. Panel deflections under axial compression and pressure were also analyzed. These analyses were performed using the COMAIN computer program.

For the EI and GJ calculations the box section was idealized.

The EI was calculated as follows:

$$\text{Cover} \quad E \times t \times b \times 2 \times \left(\frac{h}{2}\right)^2$$

$$\text{Spar cap} \quad E \times A \times 2 \times \left(\frac{h}{2}\right)^2$$

Outer face sheet

$$52\,673 \times 1.524 \times 2362.2 \times 2 \times 284.48^2 = 30.69 \text{ MN}\cdot\text{m}^2 \\ (10.69 \times 10^9 \text{ lb}\cdot\text{in}^2)$$

Inner face sheet

$$52\,673 \times 1.524 \times 2108.2 \times 2 \times 254^2 = 21.84 \text{ MN}\cdot\text{m}^2 \\ (7.61 \times 10^9 \text{ lb}\cdot\text{in}^2)$$

Front spar caps

$$82\,733 \times 645.16 \times 2 \times 215.9^2 = 4.98 \text{ MN}\cdot\text{m}^2 \\ (1.73 \times 10^9 \text{ lb}\cdot\text{in}^2)$$

Rear spar caps

$$82\,733 \times 387.1 \times 2 \times 241.3^2 = 3.73 \text{ MN}\cdot\text{m}^2 \\ (1.30 \times 10^9 \text{ lb}\cdot\text{in}^2) \\ \Sigma = 61.24 \text{ MN}\cdot\text{m}^2 \\ (21.33 \times 10^9 \text{ lb}\cdot\text{in}^2)$$

Where  $\bar{h}$  is the mean distance from the skin to the box  $G_L$  and  $h$  is the distance from the spar cap centroid to the box  $G_L$ .

The EI of the metal fin box is  $58.00 \text{ MN}\cdot\text{m}^2$  ( $20.2 \times 10^9 \text{ lb}\cdot\text{in}^2$ ) so this value is acceptable.

The GJ was calculated by considering the fin box as an outer and inner box. The outer box included the outer face sheet of the cover and half the front and rear spar web thicknesses. The inner box consisted of the inner face sheet of the cover and the other half of the front and rear spar web thicknesses. Thus

$$GJ = \frac{[(2 \times 1.303)^2 + (2 \times 1.168)^2] 10^9}{\frac{4.445}{2038 \times 1.524} + \frac{0.406}{24\,130 \times 1.016} + \frac{0.457}{24\,130 \times 1.016}} \\ = 68.66 \text{ MN}\cdot\text{m}^2 \quad (23.92 \times 10^9 \text{ lb}\cdot\text{in}^2)$$

The measured GJ of the metal fin box was  $57.98 \text{ MN}\cdot\text{m}^2$  ( $20.2 \times 10^9 \text{ lb}\cdot\text{in}^2$ ). Thus the GJ is a little high but acceptable for trade-off purposes.

## 2.2.6 Analysis of Honeycomb Tip Runout

The honeycomb tip runout is illustrated in Figure 40. It is found that the maximum bending moment =  $64.79 (13.589 - 1.143) = 806.38 \text{ N}\cdot\text{m/m}$  ( $181.3 \text{ in}\cdot\text{lb/in}$ ). Assuming that this moment will act on the  $2.286 \text{ mm}$  ( $0.09 \text{ in.}$ ) thick end:

$$f_{b,\max} = \frac{\pm 806.38 \times 1.143}{2.286^3/12} = \pm 926 \text{ MPa} (\pm 134 \text{ ksi})$$

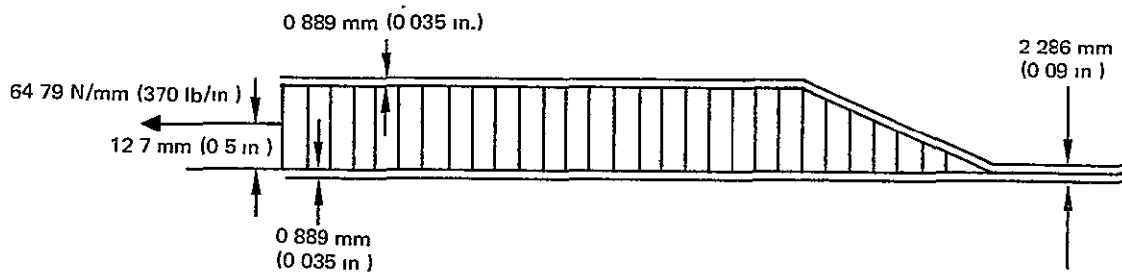


Figure 40. Honeycomb Tip Runout

Although this analysis is conservative, the bending stresses are considerably in excess of anything acceptable, and even if found to be tolerable statically the fatigue effects would be severe.

### 2.2.7 Spar Analysis

Trade studies were conducted on the spar webs and spar caps to determine the optimum configuration. A sample analysis of a web panel, stiffener, and spar cap located in the rear spar from VSS 171.42 to 197.13 is as follows:

The average shear flow in this bay is 0.1147 N/m (655 lb/in) ultimate. Using two panel stiffeners between ribs gives a panel spacing of  $655/3 = 0.218$  m (8.57 in.). The average width of the spar in this bay is 0.449 m (17.7 in.). The configuration of the web was chosen as 8 plies of  $\pm 45^\circ$  graphite/epoxy, and 7 plies of  $0^\circ$  181 style Kevlar 49. The Kevlar plies are located in the center of the web with 4 plies of  $45^\circ$  graphite/epoxy on each side to provide the highest buckling capability.

#### Web Sizing:

The allowable shear buckling was calculated using data from Figure 41 (reference 4).

$$D_{11} = D_{22} = 71.18 \text{ N m (630 lb}\cdot\text{in)}$$

$$D_{12} = 48.02 \text{ N m (425 lb}\cdot\text{in)}$$

$$D_{66} = 50.84 \text{ N}\cdot\text{m (450 lb}\cdot\text{in)}$$

$$\beta_s = 0.484, k_s = 8.95$$

$$N_{xy,cr} = 132.7 \text{ N/mm (756 lb}\cdot\text{in)}$$

$$\text{Buckling margin of safety} = \frac{132.7}{114.7} - 1 = +0.16 \text{ M.S.}$$

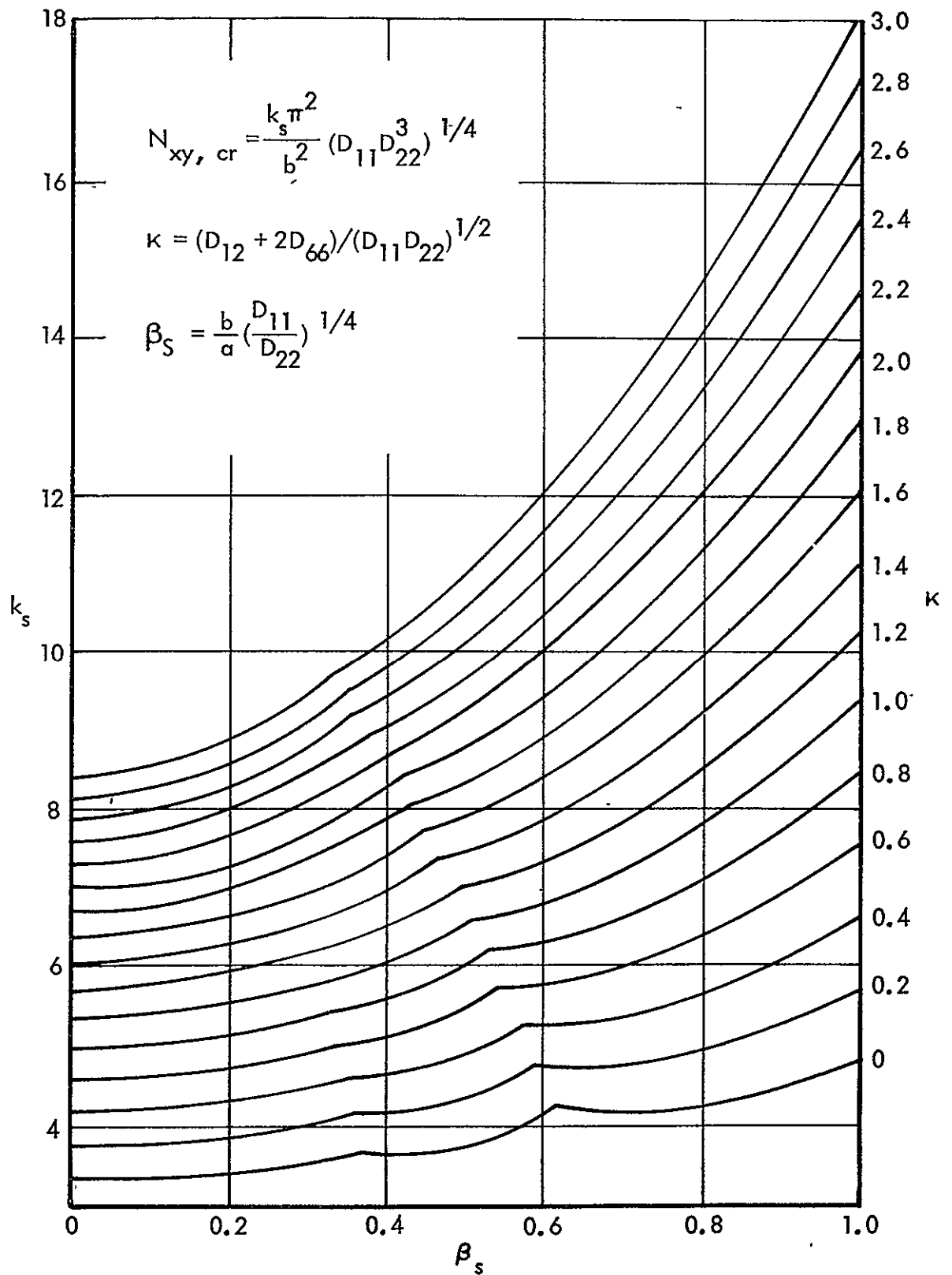


Figure 41. Shear Buckling Coefficients of Simply Supported, Orthotropic Plates

### Stiffener Sizing:

The spar web stiffeners were sized using the data from Table 9-20 of Reference 5.

$$a = 653 \text{ mm (25.71 in.)}$$

$$b = 449.58 \text{ mm (17.7 in.)}$$

$$\therefore a/b = 1.45$$

$$\gamma = 12$$

$$\begin{aligned} \therefore EI \text{ required} &= \gamma D_{11} a = 1271.175 \times 653 \\ &= 557.7 \text{ kN}\cdot\text{mm}^2 \\ &\quad (194 \times 10^3 \text{ lb}\cdot\text{in}^2) \end{aligned}$$

Using a tee stiffener as shown in Figure 42, the required number of plies are 16 of  $\pm 45^\circ$  and 9 of  $0^\circ$ . This yields an EI of  $589.3 \text{ kN}\cdot\text{mm}^2$  ( $205 \times 10^3 \text{ lb}\cdot\text{in}^2$ ).

$$\text{The margin of safety (EI)} = \frac{589.3}{557.7} - 1 = +0.06 \text{ M.S.}$$

### Spar Cap Sizing:

The rear spar cap load at VSS 171.42 is  $52.042 \text{ kN}$  ( $11\,700 \text{ lb}$ ). The tie cap cross section is as shown in Figure 43.

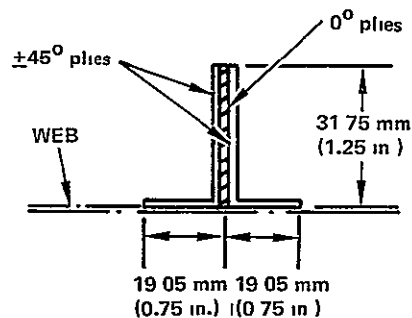


Figure 42. Spar Web Tee Stiffener



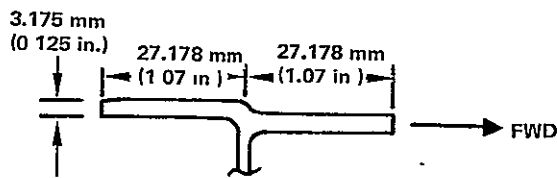


Figure 43. Spar Tie Cap Cross Section

The aft leg is 3.175 mm (0.125 in.) thick. This is set by constraints other than stress. Using 16 plies of  $\pm 45^\circ$  and 8 plies of  $0^\circ$  the thickness becomes  $24 \times 0.132 = 3.168$  mm (0.1257 in.). Assuming a 4.7625 mm (3/16 in.) fastener hole in the aft leg, the net section becomes  $(27.178 - 4.7625) \times 3.168 = 71.012$  mm<sup>2</sup> (0.11 in<sup>2</sup>). Using a net section allowable of 351.6 MPa (51 ksi) gives a load capability for this leg of  $351.6 \times 71.012 = 24.968$  kN (5620 lb). Using a configuration of 16 plies of  $\pm 45^\circ$  and 12 plies of  $0^\circ$  for the forward leg with the same size fastener hole yields a net area of  $(27.178 - 4.7625) \times 28 \times 0.132 = 82.847$  mm<sup>2</sup> (0.128 in<sup>2</sup>). This has an allowable net area section stress of 406.74 MPa (59 ksi). The allowable load in the forward leg is then  $406.75 \times 82.847 = 33.698$  kN (7580 lb).

$$\begin{aligned} \text{The total allowable load} &= 24.968 + 33.698 \\ &= 58.666 \text{ kN (13 189 lb)} \end{aligned}$$

The net section margin of safety is:

$$\frac{58.666}{52.042} - 1 = +0.13 \text{ M.S.}$$

At VSS 197.13 the rear spar load is 42.7 kN (9600 lb). Using the same shape and overall dimensions as at VSS 171.42, the aft leg is maintained at 3.168 mm (0.1247 in.) using a configuration consisting of 16 plies of  $\pm 45^\circ$  and 8 plies of  $0^\circ$  the allowable load is the same as before, i.e., 24.968 kN (5620 lb). Using the same 16 plies of  $\pm 45^\circ$  and 8 plies of  $0^\circ$  configuration for the forward leg yields a total allowable load of 49.936 kN (11 240 lb).

The margin of safety for the net section is

$$\frac{49.936}{42.700} - 1 = +0.17 \text{ M.S.}$$

The net section allowable data was taken from Figure 44 which comes from Reference 6.

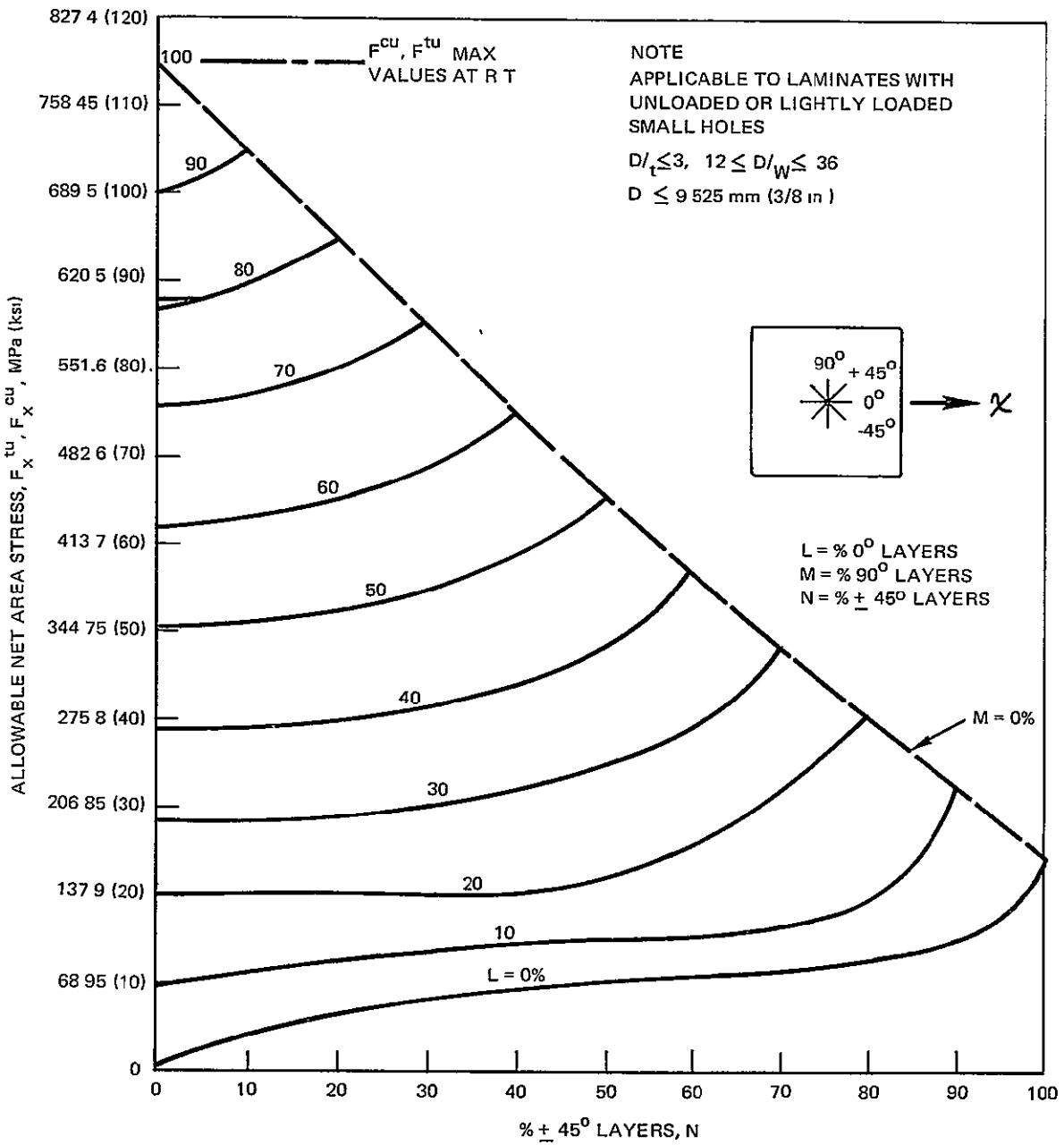


Figure 44. Design Net Strength of Graphite/Epoxy Laminates With Holes

## 2.2.8 Rib Analysis

For preliminary design the internal loads from the original analysis of the metal ribs were used. These loads were increased by a factor of 1.2 to account for any possible increase in loads for later models, and increased rib spacing.

The analysis presented here as a sample is for the rib at VSS 145.71 which is the lowest truss hinge rib. The primary loading is from the rudder hinge and this load is not expected to change, so the 1.2 factor was considered to be conservative.

The internal loads were originally computed using a 2D model which is shown in Figure 45. The rib caps were represented as beam elements and the truss members as axial elements. The loads in the beam elements and axial elements are given in Tables 18 and 19 respectively.

A similar model is planned for the composite ribs.

The rib cap and skin attachment flange in the metal L-1011 fin at VSS 145.7 are made from 7075-T6 aluminum sheet which is hydro-press formed. Basic sheet thickness is 1.27 mm (0.050 in.) but an additional 20.32 mm (0.8 in.) thick return flange reinforcement is mechanically fastened to approximately 685.8 mm (27 in.) of the aft end of the rib cap, as shown in Figure 46.

Based on the dimensions of this section, a preliminary graphite/epoxy design configuration (for VSS 145.7) for substitution was developed using the  $[0/45/90]_s$  basic layup 1.016 mm (0.04 in. thick). The following concept is an iterative result. The preliminary concept is shown in Figure 47.

For the idealized rib cap described in Figure 47, the P and M loads (axial and moment) are applied as in Figure 48. The maximum stress is

$$\sigma_{CAP} = \pm \frac{Mc_{MAX}}{I_{xx}} + \frac{P}{A} = \pm 0.509M + 6.481P$$

where M is in N.m, P is in kN, and  $\sigma_{CAP}$  is in MPa.

Increasing the P and M loads by a factor of 1.2 to conservatively account for the increased rib spacing in the ACVF, the maximum stress becomes

$$\sigma_{CAP} = \pm 0.611M + 7.777P$$

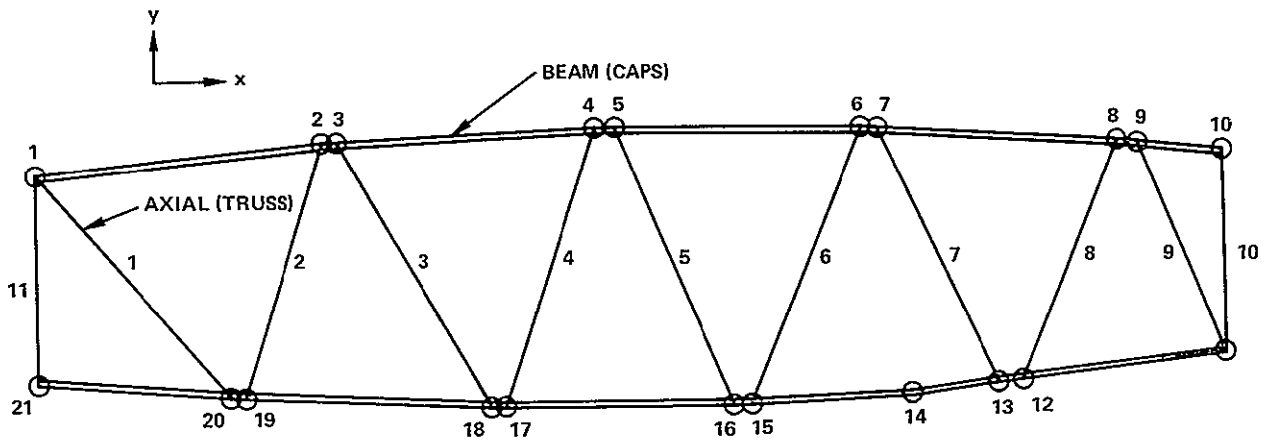


Figure 45. VSS 145.71 Hinge Rib 2D Model

where

$$\sigma_{\text{BENDING}} = \pm 0.611M$$

$$\sigma_{\text{AXIAL}} = 7.777P$$

Using the beam element loads from Table 20 for the hinge rib at VSS 145.71, the stresses in the elements due to the P and M loads are calculated (see Table 20).

Since beams 9 and 10 have tensile loads which exceed the given allowable, the cap was resized by adding 2.032 mm (0.08 in.) inserts as shown in Figure 49. The maximum stress in the cap following resizing is therefore defined by

$$\sigma_{\text{CAP}} = \pm \frac{Mc_{\text{MAX}}}{I_{xx}} + \frac{P}{A} = \pm 0.4752M + 6.444P$$

where M is in N.m, P in in kN, and  $\sigma_{\text{CAP}}$  is in MPa.

The stresses in beam elements 9 and 10 for the resized rib cap are shown in Table 21. Since beam element 9 has the maximum stresses, it will be used for the margin of safety check, where  $\sigma_{\text{allowable}} = 461.97\text{MPa}$  (67 000 psi). Using  $\sigma_1 = 374.18\text{MPa}$  (54 321 psi) and  $\sigma_2 = -328.06\text{MPa}$  (-47 642 psi), the

TABLE 18. BEAM ELEMENT LOADS

Beam No	N1	N2	$\sigma_{Max}^{(1)}$ MPa (psi)	Case No	$\sigma_{Min}^{(2)}$ MPa (psi)	Case No	$\sigma_{AXIAL} = \frac{(1)+(2)+(3)}{2}$ MPa	$\frac{A}{mm^2}$ (in <sup>2</sup> )	$P_{AXIAL} = (3) \times A$ kN (lb)	$\sigma_{BEND} = \frac{(1)-(2)(4)}{2}$ MPa	$2 \frac{I}{H}$ <sup>(5)</sup> mm <sup>3</sup> (in <sup>3</sup> )	$M = (4) \times (5)$ N · m (in-lb)
1	1	2	73 363 (10 640)	1	-63.128 (-9 156)	2	5.116 (742)	152 258 (0 236)	0 779 (175 1)	68 244 (9 898.0)	4522.8 (0.276)	308.62 (2 731.3)
2	2	3	43 465 (6 304)	4	-23.711 (-3 439)	1	9 877 (1 432.5)	152 258 (0 236)	1 504 (338.1)	33 584 (4 871.5)	4522.8 (0.276)	151.91 (1 344.5)
		$\nabla=1.2$										
3	3	4	80 944 (11 740)	2	-58.109 (-8 428)	1	11.418 (1 656)	152 258 (0 236)	1 738 (390.8)	69.005 (10 008.4)	4522.8 (0.276)	314.46 (2 783.2)
4	4	5	76.808 (11 140)	2	-52.628 (-7 633)	1	12.159 (1 763.5)	152 258 (0 236)	1 851 (416 2)	64.718 (9,386 5)	4522.8 (0.276)	292.71 (2 590.7)
5	5	6	66 231 (9 606)	4	-32 226 (-4 674)	1	17.002 (2 466)	152 258 (0 236)	2 588 (581.9)	49.229 (7 140.0)	4522.8 (0.276)	222 65 (1 970.6)
6	6	7	62.866 (9 118)	6	-25 269 (-3 665)	5	18.799 (2 726 5)	152 258 (0.236)	2 862 (643 5)	44 068 (6 391 5)	4522.8 (0 276)	199.32 (1 764 1)
7	7	8	64.749 (9 391)	6	-43.568 (-6 319)	5	10.590 (1 536)	292 257 (0.453)	3 095 (695 8)	54.158 (7 855 0)	8242.7 (0.503)	446.41 (3 951.1)
8	8	9	78.669 (11 410)	6	-62 425 (-9 054)	5	8 122 (1 178)	338 064 (0.524)	2 746 (617 3)	70 547 (10 232 0)	8291 9 (0 506)	584.97 (5 177 4)
9	9	10	99 70 (14 460)	1	-78.531 (-11 390)	5	10 583 (1 535)	338 064 (0.524)	3.578 (804 3)	89 115 (12 925 0)	8291 9 (0 506)	738.93 (6 540 1)
10	11	12	90.666 (13 150)	5	-71.637 (-10 390)	6	9.515 (1 380)	338 064 (0 524)	3 217 (723 1)	81 151 (11 770 0)	8291 9 (0 506)	672.89 (5 955.6)
11	12	13	59 778 (8 670)	5	-35.915 (-5 209)	6	11 931 (1 730.5)	338 064 (0.524)	4 034 (906 8)	47 846 (6 939.5)	8291 9 (0.506)	396 73 (3 511.4)
12	13	14	40.720 (5 906)	5	-15.672 (-2 273)	6	10 122 (1 468)	338 064 (0.524)	3.422 (769.2)	28 196 (4 089 5)	8291 9 (0 506)	233.80 (2 069 3)
13	14	15	69.154 (10 030)	3	-13 596 (-1 972)	2	27.778 (4 029)	152 258 (0.236)	4.229 (950.8)	41 375 (6 001 0)	4522.8 (0.276)	187 14 (1 656.3)
14	15	16	82 530 (11 970)	3	-42 789 (-6 206)	2	19.871 (2 882)	152 258 (0.236)	3 026 (680 2)	62.660 (9 088 0)	4522.8 (0.276)	283.40 (2 508.3)
15	16	17	92 872 (13 470)	1	-58 364 (-8 465)	2	17.254 (2 502 5)	152 258 (0.236)	2 627 (590 6)	75 618 (10 967 5)	4522.8 (0 276)	342.00 (3 027 0)
16	17	18	76 670 (11 120)	1	-58.923 (-8 546)	2	8.874 (1 287)	152 258 (0.236)	1 351 (303.7)	67 796 (9 833.0)	4522.8 (0.276)	306.63 (2 713.9)
17	18	19	86 667 (12 570)	1	-63.432 (-9 200)	2	11.618 (1 685)	152 258 (0.236)	1 769 (397 7)	75 049 (10 885 0)	4522.8 (0 276)	339 10 (3 001.3)
18	19	20	31 200 (4 525)	3	-11.018 (-1 598)	2	10 090 (1 463.5)	152.258 (0 236)	1 536 (345.4)	21 108 (3 061 5)	4522.8 (0 276)	95.46 (844 9)
19	20	21	99 147 (14 380)	2	-87.012 (-12 620)	1	6.067 (880 )	152 258 (0.236)	0 924 (207.7)	93 079 (13 500 0)	4522.8 (0.276)	420 98 (3 726.0)

TABLE 19. AXIAL ELEMENT LOADS

Axial No.	N1	N2	A1 ① mm <sup>2</sup> (in <sup>2</sup> )	A2 mm <sup>2</sup> (in <sup>2</sup> )	L = L' mm (in)	σ TENSION ② MPa (psi)	Case No.	P TENS = ① x ② kN (lb)	σ COMP ③ MPa psi	Case No.	P COMP = ① x ③ kN (lb)
1	1	20	97.419 (0.151)	97.419 (0.151)	566.67 (22.31)	62.853 (9 116.)	1	6.123 (1 376.5)	-57.909 (-8 399.)	2	-5.641 (-1 268.2)
2	2	19	97.419 (0.151)	97.419 (0.151)	519.43 (20.45)	26.841 (3 893.)	2	2.615 (587.8)	-32.343 (-4 691.)	3	-3.151 (-708.3)
3	3	18	97.419 (0.151)	97.419 (0.151)	591.57 (23.29)	12.776 (1 853.)	2	1.245 (279.8)	-19.250 (-2 792.)	3	-1.875 (-421.6)
4	4	17	97.419 (0.151)	97.419 (0.151)	572.52 (22.54)	24.214 (3 512.)	1	2.359 (530.3)	-20.836 (-3 022.)	4	-2.030 (-456.3)
5	5	16	97.419 (0.151)	97.419 (0.151)	586.23 (23.08)	31.633 (4 588.)	2	3.082 (692.8)	-29.875 (-4 333.)	1	-2.910 (-654.3)
6	6	15	97.419 (0.151)	97.419 (0.151)	577.09 (22.72)	41.534 (6 024.)	1	4.046 (909.6)	-41.169 (-5 971.)	2	-4.011 (-901.6)
7	7	13	97.419 (0.151)	97.419 (0.151)	561.59 (21.51)	56.082 (8 134.)	2	5.463 (1 228.2)	-60.233 (-8 736.)	1	-5.868 (-1 319.1)
8	8	12	97.419 (0.151)	97.419 (0.151)	561.59 (22.11)	66.603 (9 660.)	1	6.489 (1 458.7)	-71.361 (-10 350.)	2	-6.952 (-1 562.9)
9	9	11	97.419 (0.151)	97.419 (0.151)	444.50 (17.50)	92.252 (13 380.)	2	8.987 (2 020.4)	-95.768 (-13 890.)	2	-9.330 (-2 097.4)
10	1	21	303.87 (0.471)	303.87 (0.471)	403.86 (15.50)	51.049 (7 404.)	1	15.512 (3 487.3)	-50.173 (-7 277.)	2	-15.246 (-3 427.5)
11	10	11	303.87 (0.471)	303.87 (0.471)	403.86 (15.90)	50.759 (7 362.)	2	15.424 (3 467.5)	-45.954 (-6 665.)	3	-13.964 (-3 139.2)

\*\* Assume pin end column, L calculated from F.E.M. coordinates

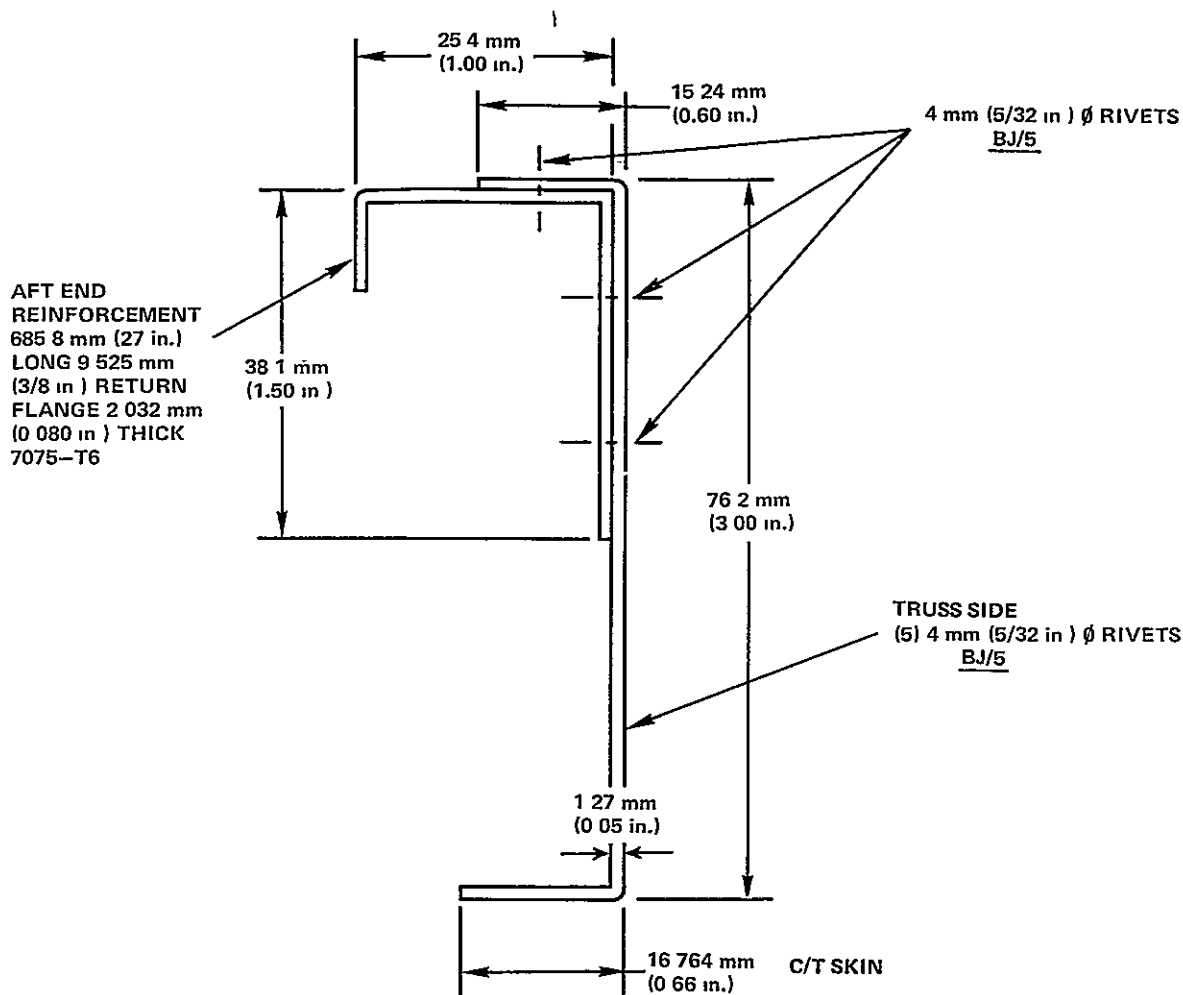


Figure 46. Metal Rib Cap Cross Section

respective margins of safety are found to be

$$\frac{461.97}{374.18} - 1 = 0.23 \text{ M.S.}$$

$$\frac{461.97}{328.06} - 1 = 0.41 \text{ M.S.}$$

Stability check for rib cap flange.- The uniaxial compression buckling allowable for the rib cap flange as idealized in Figure 50 is found using the method of reference 2 and is as follows:

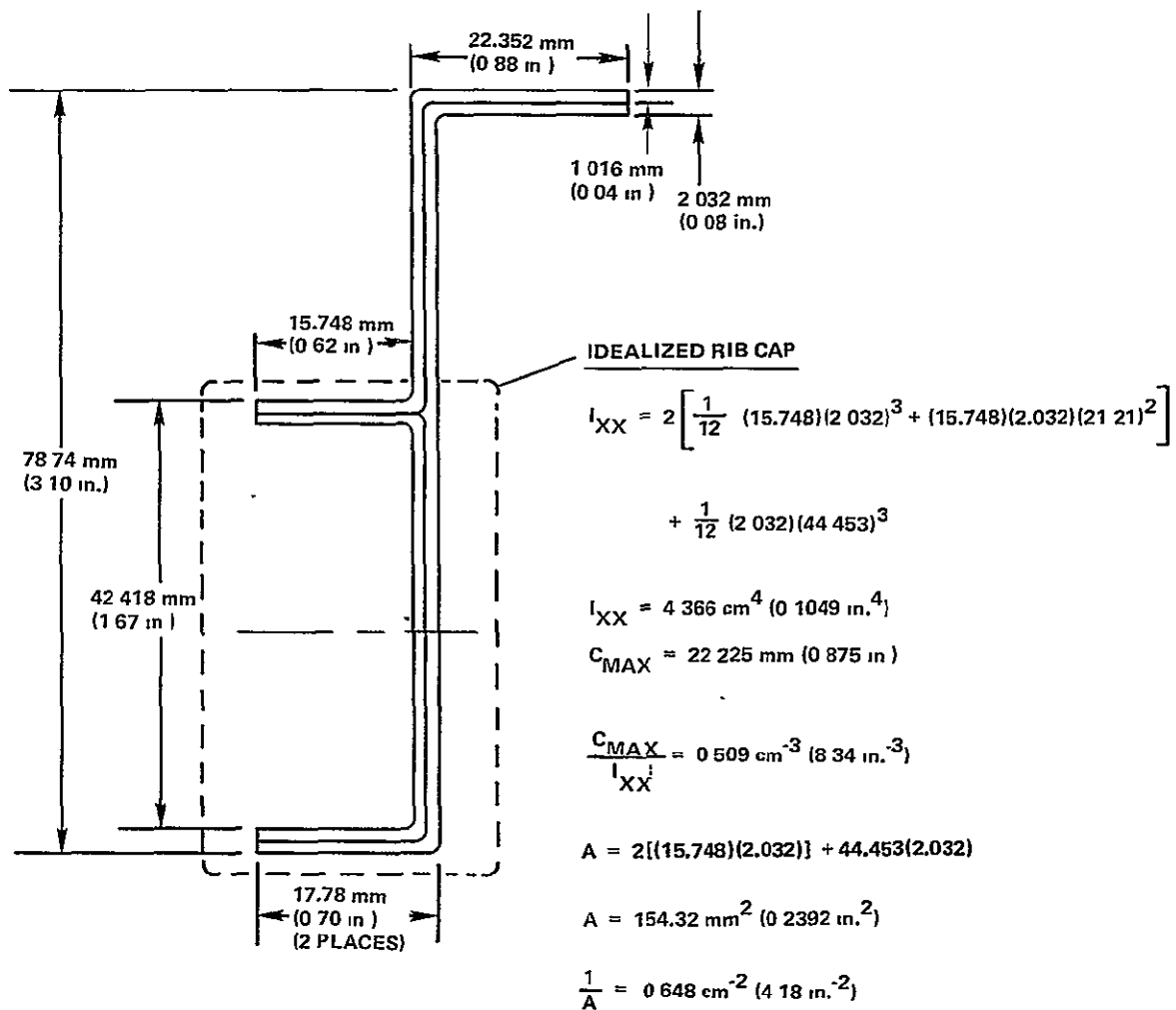


Figure 47. Preliminary Composite Rib Cap Concept

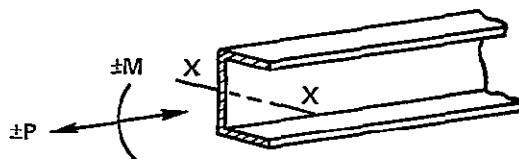


Figure 48. Rib Cap Load Application

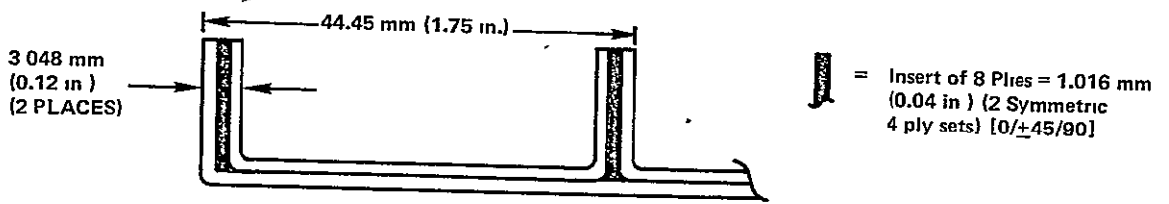


TABLE 20. BEAM ELEMENT STRESSES

BEAM NO.	P kN (lb)	7.777P MPa <sup>①</sup> (psi)	M N m (in·lb)	0.611M MPa <sup>②</sup> (psi)	$\sigma_1 = \text{①} + \text{②}^*$ MPa (psi)	$\sigma_2 = \text{①} - \text{②}^*$ MPa (psi)
1	0.779 (175.1)	6.056 (878.3)	308.65 (2 731.8)	188.50 (27 339.9)	194.56 (28 218.2)	-182.45 (-26 461.6)
2	1.504 (338.1)	11.693 (1 695.9)	151.91 (1 344.5)	92.774 (13 455.8)	104.47 (15 151.7)	-81.082 (-11 759.9)
3	1.738 (390.8)	13.516 (1 960.3)	314.46 (2 783.2)	192.05 (27 854.3)	205.56 (29 814.6)	-178.53 (-25 894.0)
4	1.851 (416.2)	14.394 (2 087.7)	292.71 (2 590.7)	178.77 (25 927.7)	193.16 (28 015.4)	-164.37 (-23 840.0)
5	2.588 (581.9)	20.124 (2 918.8)	222.65 (1 970.6)	135.98 (19 721.8)	156.10 (22 640.6)	-115.85 (-16 803.0)
6	2.862 (643.5)	22.255 (3 227.8)	199.32 (1 764.1)	121.73 (17 655.1)	143.98 (20 882.9)	-99.473 (-14 427.3)
7	3.095 (695.8)	24.063 (3 490.1)	446.41 (3 951.1)	272.64 (39 542.6)	296.70 (43 032.7)	-248.57 (-36 052.5)
8	2.746 (617.3)	21.349 (3 096.4)	584.97 (5 177.4)	357.25 (51 815.4)	378.60 (54 911.8)	-335.91 (-48 719.0)
9	3.578 (804.3)	27.816 (4 034.4)	738.93 (6 540.1)	451.28 (65 453.3)	479.10 (69 487.7)	-423.47 (-61 418.9)
10	3.217 (723.1)	25.008 (3 627.1)	672.89 (5 955.6)	410.95 (59 603.6)	435.96 (63 230.7)	-385.94 (-55 976.5)
11	4.034 (906.8)	31.361 (4 548.5)	396.73 (3 511.4)	242.30 (35 142.1)	273.66 (39 690.6)	-210.94 (-30 593.6)
12	3.422 (769.2)	26.602 (3 858.3)	233.80 (2 069.3)	142.79 (20 709.6)	169.39 (24 567.9)	-116.19 (-16 851.3)
13	4.229 (950.8)	32.882 (4 769.2)	187.14 (1 656.3)	114.29 (16 576.3)	147.17 (21 345.5)	-81.407 (-11 807.1)
14	3.026 (680.2)	23.524 (3 411.9)	283.40 (2 508.3)	173.08 (25 103.1)	196.60 (28 515.0)	-149.56 (-21 691.2)
15	2.627 (590.6)	20.425 (2 962.4)	342.01 (3 027.0)	208.87 (30 294.2)	229.30 (33 256.6)	-188.45 (-27 331.8)
16	1.351 (303.7)	10.503 (1 523.4)	306.63 (2 713.9)	187.27 (27 160.7)	197.78 (28 684.1)	-176.76 (-25 637.3)
17	1.769 (397.7)	13.754 (1 994.9)	339.44 (3 004.3)	207.30 (30 067.0)	221.06 (32 061.9)	-193.55 (-28 072.1)
18	1.536 (345.4)	11.945 (1 732.5)	95.461 (844.9)	58.301 (8 455.8)	70.246 (10 188.3)	-46.356 (-6 723.3)
19	0.924 (207.7)	7.183 (1 041.8)	420.98 (3 726.0)	257.10 (37 289.8)	264.29 (38 331.6)	-249.92 (-36 248.0)

\*  $\sigma_{\text{ALLOWABLE}} = 434.39 \text{ MPa (63 000 PSI)}$  [TENSION AND COMPRESSION FOR  $[0/\pm 45/90]_c$   
WHERE  $\sigma_1 = \text{TENSION}$  AND  $\sigma_2 = \text{COMPRESSION}$ ]

ORIGINAL PAGE IS  
OF POOR QUALITY



$$I_{XX} = 2 \left[ \frac{1}{12} (15\,748) (3\,048)^3 + (15\,748) (3\,048) (20\,70)^2 \right] + \frac{1}{12} (2\,032) (44\,45)^3$$

$$I_{XX} = 5\,607 \text{ cm}^4 \text{ (0.1347 in}^4\text{)}$$

$$C_{\text{max}} = 22\,23 \text{ mm (0.875 in.)}$$

$$\frac{C_{\text{max}}}{I_{XX}} = 0.396 \text{ cm}^{-3} \text{ (6.496 in}^{-3}\text{)}$$

$$A = 2[(15\,748)(3\,048)] + (44.45)(2\,048)$$

$$A = 1\,863 \text{ cm}^2 \text{ (0.2888 in}^2\text{)}$$

$$\frac{1}{A} = 0.537 \text{ cm}^{-2} \text{ (3.46 in}^{-2}\text{)}$$

Figure 49. Resized Composite Rib Cap

TABLE 21. STRESSES IN BEAM ELEMENTS 9 AND 10

Beam No	P (kN) (lb)		6 444 P MPa ① (psi)		M (in lb)		0 4752M MPa ② (psi)		$\sigma_1 = \text{①} + \text{②} *$ MPa (psi)		$\sigma_2 = \text{①} - \text{②} *$ MPa (psi)	
	kN	(lb)	MPa	(psi)	N·m	(in lb)	MPa	(psi)	MPa	(psi)	MPa	(psi)
9	3 578	(804.3)	23 057	(3 339.36)	738 93	(6 540.1)	351.121	(50 981.39)	374.18	(54 320.75)	-328.06	(-47 641.64)
10	3 216	(723.1)	20 724	(3 002.32)	672 89	(5 955.6)	319.74	(46 425.10)	340.464	(49 427.42)	-299.016	(-43 422.78)

\*\*See footnote Table 20

ORIGINAL PAGE IS  
OF POOR QUALITY

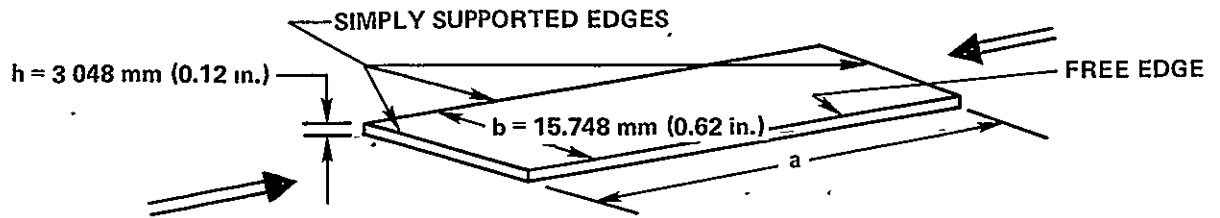


Figure 50. Idealized Rib Cap Flange

$$N_{x, CR} = \frac{h^3}{b^2} G_{xy} \quad \text{for } a/b = \infty$$

where

$$F_{x, CR} = \frac{N_{x, CR}}{h}$$

or

$$F_{x, CR} = \frac{h^2}{b^2} G_{xy}$$

For a  $[0/\pm 45/90]$  graphite/epoxy laminate,  $G_{xy} = 17.9 \text{ GPa (2.6msi)}$  and

$$F_{x, CR} = \frac{(3.048)^2}{(15.748)^2} (17\,900) = 671.56 \text{ MPa (97\,398 psi)}.$$

Using  $\sigma_2 = -328.06 \text{ MPa (-47\,642 psi)}$  from Table 21, the margin of safety is found to be

$$\frac{671.56}{328.06} - 1 = 1.05 \text{ M.S.}$$

Note that this preliminary sizing does not account for environmental and thermal effects, increased rib spacing, detailed design allowables or detailed loads or fail-safe considerations.

### 2.2.9 NASTRAN Model

The NASTRAN finite element model (FEM) was developed during Phase I. The model grid points, grid point coordinates, the element connection data, and the structural influence coefficients (SIC) unit load distributions have all been specified and checked out. Figure 51 shows a plot of the model structure, Figure 52 shows the grid point numbering system and Figure 53 shows the element numbering system. A summary of the ACVF critical load conditions is shown in Table 22. Columns 56 and 59 are the fatigue conditions.

The model grid network established for the composite fin is identical to the network used for the original analysis of the metal fin. This has permitted the direct respecification of the SIC unit load distributions used for the FAMAS model analyses of the metal fin and will result in the application of external loads in an identical manner to that for the metal fin. In addition, the modeling (element connections and sizing) of the metal leading edge structure, as well as the metal rudder will be identical to that used in the original design analysis.

The intermediate ribs are modeled at the same locations as the metal fin ribs and thus do not represent the proposed composite intermediate rib locations. The ribs in the NASTRAN model are modeled as equivalent shear webs not as trusses. A FEM simulates aerodynamic pressure loads as lumped loads at grid points, hence the internal loads at ribs are not representative of the true rib configuration. To model truss ribs, it would be necessary to have left and right surfaces modeled differently. This would complicate the model and still not give representative rib internal loads.

In order to achieve a better internal load distribution in the covers and spars and to allow direct comparison between the composite and metallic fin models, the decision was made to split the intermediate ribs into two at approximately 432 mm (17 in.) spacing. The actuator and hinge ribs are modeled in their correct location and do not include any lumped area from intermediate ribs.

It is intended to obtain internal rib loads from external pressure distribution and other applied loads from separate two dimensional models in the same manner as for the metallic fin.

The Lockheed version of NASTRAN is level 15.1 which has been modified by Lockheed particularly with regard to input and output simplification. When NASTRAN was assembled the capability of incorporating user developed elements was included. These elements are classed as dummy or DUM elements. The Lockheed developed anisotropic membrane element used for the covers and the spar webs is incorporated as the DUM 3 element. This element has been incorporated into the biaxially stiffened warped, anisotropic quadrilateral membrane. It is suitable for modeling stiffened or unstiffened metallic or composite panels. Stresses are output for both the stiffeners and the skin. Axial stresses are constant in the axial direction and vary linearly in the transverse direction. The shear stress is constant over the element.

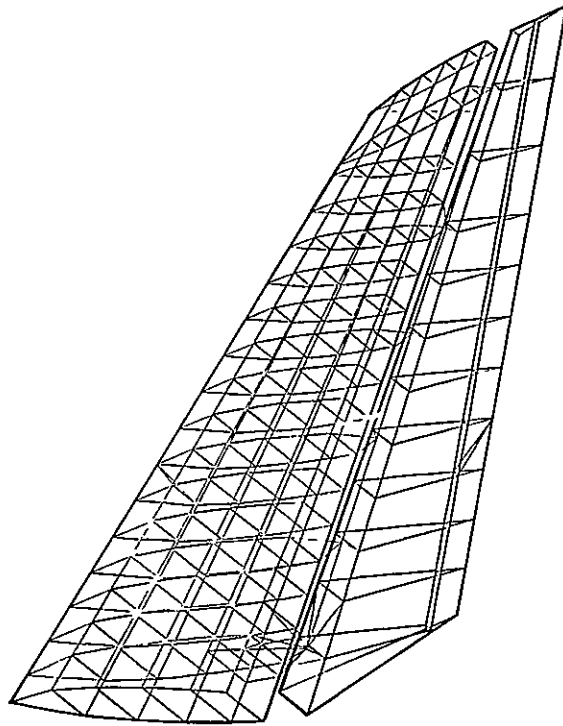


Figure 51. Fin Structural Model

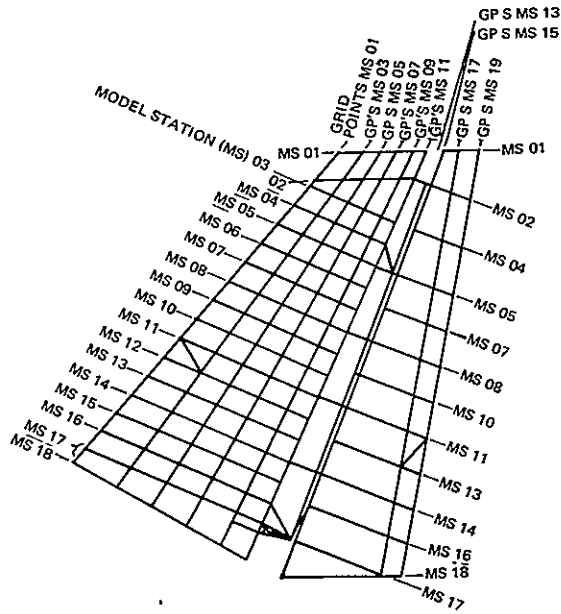


Figure 52. NASTRAN Model Left Surface



ELEMENT NUMBERS ARE DEFINED AS ELMSGP, WHERE EL IS THE ELEMENT GROUP NUMBER AND MSGP IS THE GRID POINT NUMBER LOCATED RELATIVE TO THE ELEMENTS IT DEFINES IS SHOWN BELOW.

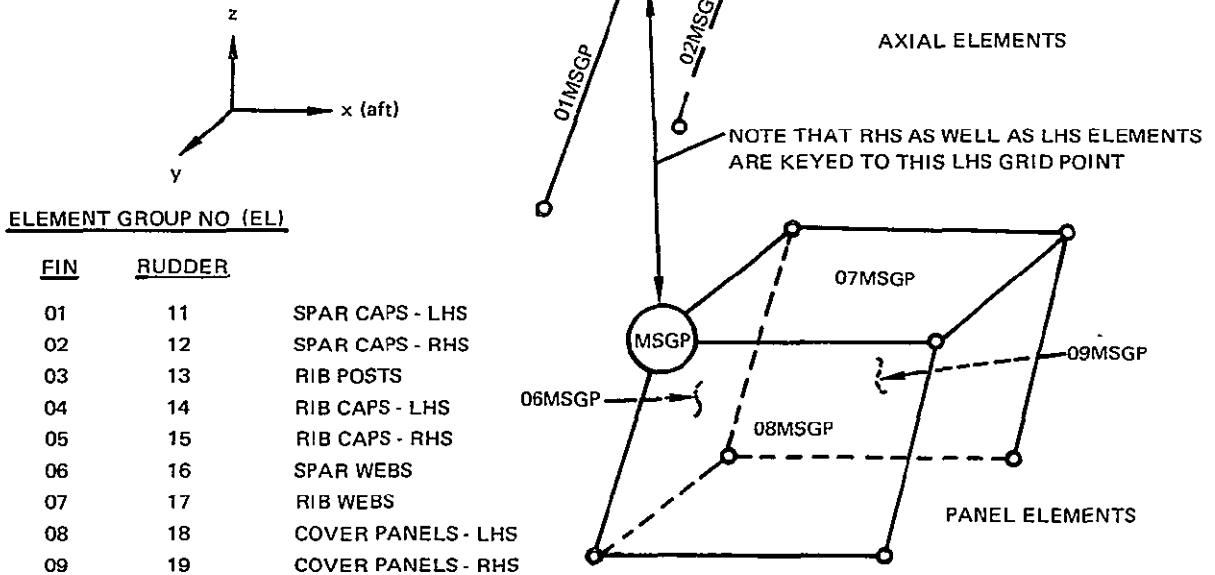


Figure 53. NASTRAN Model Element Numbering System

TABLE 22. CRITICAL LOAD CONDITIONS

Stacked Column	Condition	Condition Deser	GW		CG % MAC	V KEAS	M	h = (ft)	Comment
			kg	(lb)					
1	25133-1	V T Buffet	145 510	(320 790)	13 9	215	33	0 0	Static Buffet $\delta_{SP2} = -5.2^\circ$ , $\delta_{SP3,4,5,6} = -6.9^\circ$ $\delta_F = 15^\circ$
35	5424-1	V T Buffet	145 510	(320 790)	13 9	215	33	0 0	Static Buffet $\delta_{SP} = -2.6^\circ$ , $\delta_{SP3,4,5,6} = 3.45^\circ$ $\delta_F = 15^\circ$
56	4907-3	RM-2 <sup>(1)</sup>	211 378	(466 000)	28 7	250	38	0 0	Thrust - Off $\delta_F = 1^\circ$
59	4517/851	Dyn Lat. Gust	161 935	(357 000)	24 5	320	85	28 000	Max V T., $S_T$ , $M_x$ with Assoc $M_z$
73	3706-3	RM-2 <sup>(1)</sup>	191 419	(422 000)	32 0	250	38	0 0	System Failure Cond Thrust - Off

NOTE (1) RM-2 RUDDER MANEUVER - POINT IN TIME AT WHICH THE MAX SIDESLIP ANGLE OCCURS,  $\beta = \max$

REPRODUCIBILITY OF THE ORIGINAL PAGE IS POOR

0-2

The stiffener direction, spacing and properties are input directly, thus eliminating the need for lumped stiffeners. The skin material properties are defined by the [A] inplane stiffness matrix.

The output includes skin stresses, stiffener stresses, stiffener load and smeared skin loads. (Skin load plus smeared stiffener loading.)

Rib caps, rib posts, and the front and rear beam caps of the main box are modeled with NASTRAN ROD elements. NASTRAN SHEAR elements are used to represent the rib webs and trusses (in terms of equivalent shear panels). The leading edge and rudder structure are also modeled with NASTRAN ROD and SHEAR elements.

The fin model is coupled to the existing L-1011 fuselage afterbody model.

The NASTRAN model left surface is shown in Figure 52. This figure shows how the grid points are numbered. For example, the front spar and the root rib intersect at grid point 1803 and the rear spar and the root rib intersect at grid point 1811.

#### 2.2.10 FAA Certification Plan

The FAA Certification Plan outlines the procedure to be following in order to obtain certification. The main points of the plan are described in the following paragraphs.

Lockheed intends to obtain certification of the advanced composite vertical fin installed on L-1011 aircraft early in 1979. Certification will be based on satisfying both static strength and fail-safe requirements. Lockheed proposes to obtain certification by means of the following plan:

1. Substantiate the structural integrity of the ACVF by the following:
  - a. The pertinent criteria and loads documents will be reviewed. A criteria document will be prepared which will define the critical static and dynamic load conditions. It will also define the acoustic loads, the thermal and moisture environments, and the flutter requirements.  
  
The loads will be used in the first NASTRAN structural model run. After this run, the new structural influence coefficients will be evaluated and their effects on the loads will be investigated. From this investigation, the loads will be updated if necessary for the second NASTRAN run.
  - b. The static, fail-safe, and flutter analyses will be submitted to the Designated Engineering Representative (DER) for approval. The analyses will then be submitted to the FAA.

- c. A report which presents the analysis methods and design allowables to be used in the design of the composite vertical fin box structure will be submitted to the FAA for approval at an early stage in the program.
- d. A design criteria report will be prepared which will describe durability and damage tolerance requirements. It is intended to design the composite vertical fin to be damage tolerant to the repeated loads environment and to retain residual (fail-safe) strength adequate to withstand the damage and load levels to be defined in this report.
- e. A structural integrity control (SIC) plan will be prepared which will outline the steps to be taken to ensure the structural integrity of the composite fin box. This plan will be used to prepare the Structural Integrity Control Document during Phase II. The schedule of completion of component detail SIC plans will be provided in the overall SIC plan.
- f. A Quality Control Plan will be prepared which will outline the QA procedures. This plan and the Structural Integrity Control Plan are complementary.
- g. An Ancillary Test Plan will be prepared which will detail all tests except the ground test of a complete component. It will describe the number and type of all tests to qualify the material, to develop design allowables, and to verify design concepts for all critical areas. All coupon and subcomponent fatigue testing will be for four lifetimes and residual strength and static tests to failure will follow fatigue testing. These static test results will be compared with the results of static tests on articles which are not fatigued to determine the degradation, if any. A sufficient number of static and fatigue coupon tests will be performed to determine the effect of environmental factors (temperature and humidity) on mechanical properties.

In addition, the ancillary test program will be used to substantiate design details from a durability, environmental, and static strength viewpoint.

The schedule of all ancillary tests will be provided in the Ancillary Test Plan.

The FAA will be invited to witness fabrication and tests of all test specimens.

- h. A full-scale fin box will be ground tested. Fatigue testing for two lifetimes will be accomplished first, followed by static testing to ultimate and fail-safe testing. The testing procedures will be developed based on the results of the ancillary



test program. Information will also be available for defining the degree to which the loads and/or cycles would have to be increased to provide for environmental effects in the ground test of the full-scale ACVF.

2. Substantiate the flutter integrity of the composite configuration through a ground shake test and a limited flight flutter test program, during normal predelivery flight test.

### 2.3 PRELIMINARY ANCILLARY TEST PLAN

The preliminary plan for the ancillary test program for the L-1011 ACVF has been completed. The objectives of the program are to establish the structural integrity of the composite fin box under the normal operating environment of the L-1011 aircraft and to establish the requirements for testing of the full-scale test article.

The ancillary test program is designed to assess the effects of moisture, temperature, and fatigue on the surface laminates and subcomponents and to develop methods of simulating these effects in the full-scale test article. In addition, damage tolerance, fail safety, and repair procedures are to be evaluated and tested in order to establish the structural integrity of the fin and to aid in the preparation of a maintenance manual. The locations of the test specimens are shown in Figure 54. The circled numbers in this figure relates to the test item numbers shown in Table 25.

The ancillary test program has been divided into four major classifications:

- Material Qualification (Table 23) - These tests establish that the materials meet certain basic requirements of ACVF.
- Design Data (Table 24) - These tests provide the basic mechanical property data for the design and analysis of the ACVF structure.
- Concept Verification (Table 25) - These tests verify the design concepts used in critical portions of the ACVF structure.
- Fabrication and Assembly Procedure Verification (Table 26) - Fabrication and assembly of subcomponents for verification of processing and assembly procedures.

As the program progresses, the plan for the ancillary test program will be updated and modified to reflect changes resulting from prior test results and additional requirements which may appear.

ORIGINAL PAGE IS  
OF POOR QUALITY

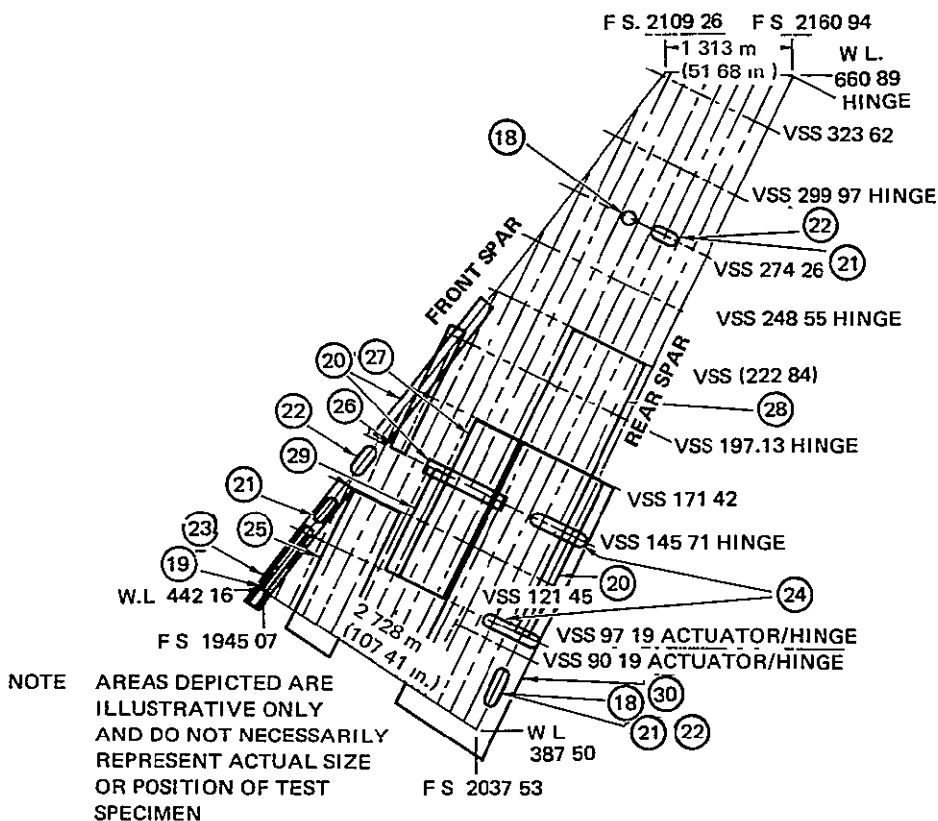


Figure 54. Development Test Coverage

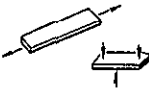
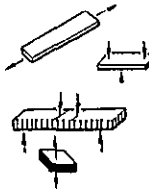
## 2.4 STRUCTURAL INTEGRITY AND QUALITY CONTROL PLANS

The design and fabrication of composite primary structure introduces variables not encountered in the design of metal structure. For composite structure, assurance that structural reliability and safety objectives are met requires an organized and systematic review of applicable variables and their influence on the structural integrity of each component.

### 2.4.1 Structural Integrity Control Plan

The L-1011 composite vertical fin will be designed to be fail-safe. To complement this fail safety, a structural integrity control plan will be implemented. This plan has many of the features of fracture control programs currently in use on metal aircraft structure. Emphasis is placed on tailoring the strength and durability assurance requirements on a part-by-part basis with proof testing being only one of many options. This approach is in line with the overall policies that have resulted in safe and durable

TABLE 23. MATERIAL QUALIFICATION - ANCILLARY TEST PROGRAM

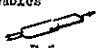

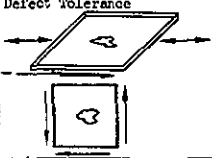
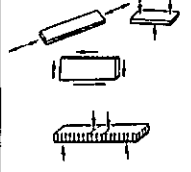
Test Item No	Description	Type of Test	Size		No of Spec	Material Requirements	Test Variables			Data	Instr	Purpose								
			mm	(in)			Wet Cond	Temperature	Others											
1A	Material Screening 	0° Flexure	12 7 x 76 2	(0 5 x 3)	40 20 20	8 165 kg (18 lbs) of graphite/ epoxy and 9 144 m (10 yards) of Kevlar 49- 281 cloth/ epoxy	Dry	RT, 344K (160°F)	(1) (2) (3) (4) (5) (6) (7) (8) (9) (10) (11) (12) (13) (14)	Stress, Modulus, Physicals	Extensometer	To determine environmental effects and to aid material selection								
		0° Short Beam Shear	6 35 x 16 13	(0 25 x 0 635)	40 20 20		Wet	344K (160°F)												
		45° Tensile	25 4 x 279 4	(1 x 11)	20 10 10		Skydr	RT												
		0° Tensile	25 4 x 279 4	(1 x 11)	20 10 10		Dry	344K (160°F)					Wet	344K (160°F)						
															Skydr	RT				
																	RT			
		Interlam Tension	25 4 x 25 4	(1 x 1)	20 10 10		Wet	344K (160°F)												
1B	(Thermal Warp)	Deflection Temperature	152 4 x 152 4	(6 x 6)	2					Defl Temp % Resin		To compare thermal response								
													1C	(Processing Variables)	Processing, Resin	203 2 x 609 6	(8 x 24)	2		
Interlam Shr	152 4 x 152 4	(6 x 6)	6																	
												Material Qualification 	0° Tensile	12 7 x 279 4	(0 5 x 11)	24	5 897 kg (13 lbs) of graphite/ epoxy, 6 401 m (7 yards) of Kevlar 49 cloth, 0 028 m <sup>3</sup> (12 board feet) of Alum Honeycomb, adhesive	Dry	RT, 219K (-65°F)	344K (160°F)
90° Tensile	25 4 x 558 8 sandwich	(1 x 22) sandwich	15	Dry	RT, 219K (-65°F)	344K (160°F)														
							45° Tensile	25 4 x 279 4	(1 x 11)	15	Wet									
0° Compression	25 4 x 558 8 sandwich	(1 x 22) sandwich	15	Dry	RT, 219K (-65°F)	344K (160°F)														
							0° Flexure	12 7 x 101 6	(0 5 x 4)	27	Wet									
0° Short Beam Shear	6 35 x 15 24	(0 25 x 0 6)	24	Dry	RT, 219K (-65°F)	344K (160°F)														
							Interlaminar Tension	50 8 x 50 8	(2 x 2)	9	Wet									
4	Cover, Honeycomb Sandwich Environmental Resistance	Face Tension	50 8 x 50 8	(2 x 2)	14							Dry				To determine effects of environment on C/R aluminum core and bond and evaluate Kevlar 49 cloth insulating barrier				
							Core Shear	76 2 x 203 2	(3 x 8)	12										
Sustained Load/Deflect																				
	5	Mechanically Fastened Joint Fatigue	Tension No-Load-Transfer	28 7 x 304 8	(1 13 x 12)	10		Press, Transition, Clearance Fits				To determine suitability of two graphite/epoxy materials for fatigue of mechanically fastened fin joints and effect of fastener fit on fatigue strength								
Tension, 4 Fastener Joint (High Load Transfer)													38.1 x 457 2	(1 5 x 18)	6					

Test Variables (1) Two Materials

(2) Hybrid

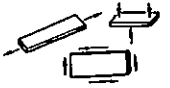
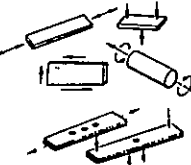
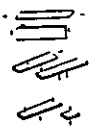


(3) Includes kevlar 49 Fabric Qualification

TABLE 24. DESIGN DATA - ANCILLARY TEST PROGRAM

Test Item No	Description	Type of Test	Size		No of Plies	No of Spec	Material Requirements	Test Variables			Data	Instrument	Purpose	
			mm	(in)				Wet Cond	Temp	Others				
11	Mechanical Joint Bearing Allowables 	Static Tension (Bearing)	25.4 x 203.2	(1 x 8,	(15 16, 18 24, 30)	87	51 256 kg (113 lbs) graphite/epoxy plus fasteners	Dry	RT	① ② ③ ④ ⑤	Stress Elongation	Extensometer	Bearing allowables Basic design data	
			50.8 x 204.8	2 x 12,		87		Wet	RT					
12A	Damage Tolerance 	Static Fracture, Fatigue & Crack Growth Impact	304 x 914.4	(12 x 36,		1	20 412 kg (45 lbs) graphite/epoxy	Dry	RT		Fracture toughness, crack growth rates, residual strength		Basic fracture and fatigue design data	
			381 x 203.2	1.5 x 8)		12		Dry	RT					
						12		Wet	RT					
						7		Dry	RT					
12B	Defect Tolerance 	Static Compression Shear	203.2 x 406.4	(8 x 16)	20	9	36 287 kg (80 lbs) graphite/epoxy 10 97 m (12 yards) Kevlar 49 cloth/epoxy	Dry	RT		Stress, strain defect growth rates		Determine critical stresses, delamination size, and defect growth rates	
			304.8 x 304.8	(12 x 12)		16		9	Wet					322K (120°F)
		Fatigue Defect Growth	203.2 x 406.4	(8 x 16)	20	9		Dry	RT					
			304.8 x 304.8	(12 x 12)		16		5	Wet					322K (120°F)
					5	Dry		RT						
					5	Wet		RT						
12C	Defect Repair	Static Compression Shear Fatigue	203.2 x 406.4	(8 x 16)	20	3		Wet	322K (120°F)		Stress		Verification of delamination repairs	
			304.8 x 304.8	(12 x 12)		16		3	Wet					322K (120°F)
			203.2 x 406.4	(8 x 16)		20		3	Wet					RT
			304.8 x 304.8	(12 x 12)		16		3	Wet					RT
								12						
13A	Graphite/Epoxy Ply Level Data 	0° Tension	12.7 x 279.4	(0.5 x 11)	6 12, 16	39	14 969 kg (33 lbs) graphite/epoxy prepreg, 0.109 m <sup>3</sup> (46 board feet) of alu honeycomb, adhesive	Dry	RT	① ② ③ ④ ⑤ ⑥ ⑦ ⑧ ⑨ ⑩ ⑪ ⑫	Stress/strain strength, moduli	Strain gages	Static design allowables and environment effects on basic properties	
		±45° Tension	25.4 x 279	(1 x 11)	6	15		Wet	RT, 219K (-65°F), 344K (-160°F)					
					12	20		Dry	RT					
					12	20		Wet	RT, 219K (-65°F), 322K (-120°F), 344K (160°F)					
		90° Tension	25.4 x 558.8	(1 x 22) sandwich	12	20		Dry	RT					
					12	20		Wet	RT, 219K (-65°F), 322K (120°F), 344K (160°F)					
		0° Compression	25.4 x 558.8	(1 x 22) sandwich	6	29		Dry	RT					
					6	20		Wet	RT, 219K (-65°F), 322K (120°F), 344K (160°F)					
		90° Compression	25.4 x 558.8	(1 x 22) sandwich	12	15		Dry	RT					
					12	15		Wet	RT, 219K (-65°F), 344K (160°F)					
		0° Interlaminar Shear	6.35 x 15.24 (0.25 x 0.6)		16	15		Dry	RT					
					16	20		Wet	RT, 219K (-65°F), 322K (120°F), 344K (160°F)					
0°/90° and ±45° Rail Shear	76.2 x 152.4	(3 x 6)	12	10	Dry	RT								
Thermal Expans	25.4 x 304.8	(1 x 12)	16	2	Dry	219K (-65°F) to 344K (160°F)								
				2	Wet	219K (-65°F) to 344K (160°F)								
				2										
					207									

ORIGINAL PAGE IS OF POOR QUALITY

TABLE 24. (Concluded)

Test Item No.	Description	Type of Test	Size		No of Plies	No of Spec	Material Requirements	Test Variables			Data	Instrument	Purpose	
			=	(in )				Wet Cond	Temp	Others				
13B	 Kevlar 49 Cloth/Epoxy Ply Level Data	0° Tension (Warp)	19 05 x 279 4	(0 75 x 11)	8	15	22 yards (20 12 m) of Kevlar 49 181 cloth/epoxy prepreg (114 lbs) (6 350 kg)	Dry	RT	(V5) (V6)	Stress/strain, strength, moduli	Strain gages	Design allowables and environmental effects on basic properties	
		±45° Tension	25 4 x 279 4	(1 x 11)	8	5		8	RT, 219K (-65°F), 344K(160°F)					
		90° Tension (Fill)	19 05 x 279 4	(0 75 x 11)	8	5		8	RT, 219K (-65°F), 344K(160°F)					
		0° Compression (Warp)	12 7 x 88 9	(0 5 x 3 5)	14	15		14	RT, 219K (-65°F), 344K(160°F)					
		90° Compression (Fill)	12 7 x 88 9	(0.5 x 3 5)	14	5		14	RT, 219K (-65°F), 344K(160°F)					
		0° Interlaminar Shear	6 35 x 15 24	(0 25 x 0 6)	14	5		14	RT, 219K (-65°F), 344K(160°F)					
		0°/90° and ±45° Rail Shear	76 2 x 406 4	(3 x 16)	8	15		8	RT, 219K (-65°F), 344K(160°F)					
		Thermal Expansion	25 4 x 304 8	(1 x 12)	8	10		8	RT					
								4	Dry/ Wet					219K(-65°F) to 344K(160°F)
								154						
		13C	 Laminate Data (Surfaces)	Tension	25 4 x 279 4	(1 x 11)		6 11, 18, 19	30					9 979 kg (22 lbs) graphite/epoxy 2 74 m (3 yards) of Kevlar 49 cloth/epoxy 0 045 m³ (19 board feet) of honeycomb adhesive
Compression	25 4 x 558 8			(1 x 22) sandwich (3 x 6)	6 11, 18, 19	25	30	RT						
In-Plane Shear	76 2 x 152 4			(3 x 6)	6 11, 18	25	15	322K (120°F)						
Interlaminar Shear	12 7 x 190 5			(0 5 x 0 75)	18, 19	15	10	RT						
Fatigue	25 4 x 279 4			(1 x 11)	18	5	10	322K (120°F)						
Combined Tension & Shear	762 x 304 8			(30 x 12) tube	18	5	5	RT						
						4	174	RT						
							174							
14	 Laminate Data (Spar & Rib)	Tension	25 4 x 279 4	(1 x 11)	20 32, 44	30	9 072 kg (20 lbs) graphite/epoxy 0 914 m (1 yard) of Kevlar 49 cloth/epoxy 0 040 m³ (17 board feet) of honeycomb adhesive	Dry	RT	(V1) (V2) (V3) (V4) (V5) (V6)	Stress/strain, strength, moduli	Extensometer and strain gages	Laminate static design property verification and effects of environment and holes on laminate properties for surfaces	
		Compression	25 4 x 558 8	(1 x 22) sandwich (3 x 6)	20 32, 44	25		24	RT					
		In-Plane Shear	76 2 x 152 4	(3 x 6)	8, 16	10		10	322K (120°F)					
		Flatwise Tension (Sandwich)	50 8 x 50 8	(2 x 2) sandwich	8	3		3	RT					
						3		125	322K (120°F)					
					125									
16	 Mechanical Joints Bearing Fatigue Tensile Bearing	Static Tensile Bearing	50 8 x 304 8	(2 x 12)	15 18, 24	50	45 36 kg (100 lbs) graphite/epoxy	Dry	RT	(V1) (V2) (V3)	Stress, elongation	Extensometer	Joint concept verification	
		Fatigue Tensile Bearing			30	50		RT						
						40		40	322K (120°F)					
						40		180						
17	 Bonded Joint	Static Tension	25 4 x 254	(1 x 10)	12	5	1 361 kg (3 lbs) graphite epoxy	Dry	RT		Shear strength	Extensometer	Bonded joint concept verification	
		Fatigue Spectrum				5		5	322K (120°F)					
						10		10	RT					
						30		30	322K (120°F)					
						55		55	322K (120°F)					

Test Variables: (V1) Thickness, (V2) Layup, (V3) Fastener Type/Size, (V4) Fiber Volume, (V5) Batch, (V6) Holes

TABLE 25. CONCEPT VERIFICATION - ANCILLARY TEST PROGRAM

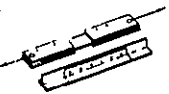






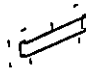
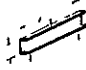





Item No.	Description	Type of Test	No Specimen	Test Variables		Size		Materials Required	Purpose of Test
				Condition	Temperature	mm	(in )		
2	A Spar Cap/Fuselage Joint 	Static Tension	5	Dry	297K (75°F)	101.6 x 152.4	(4 x 60)	4 536 kg (10 lb) graphite/epoxy	Evaluate concepts of flange and cap attachment
3	A Cover/Fuselage Joint 	Static Tension	6	Dry	297K (75°F)	177.8 x 762	(7 x 30)	13 608 kg (30 lb) graphite/epoxy	Evaluation of I section stiffened honeycomb and hat stiffened skins
18	A Rib Tension Joint 	Static Tension	6	Dry	297K (75°F)	50.8 x 152.4	(2 x 6)	13 517 kg (29.8 lb) graphite/epoxy	Verification of static and fatigue strength of rib and spar design details
			6	Wet	TBD				
		Fatigue	3	Dry	297K (75°F)				
			2	Wet	TBD				
	B Cap to Skin Joint 	Fatigue	10	Dry	297K (75°F)	50.8 x 304.8	(2 x 12)		
			5	Wet	TBD				
	C Cap to Web Joint 	Static Tension	10	Dry	297K (75°F)	152.4 x 304.8	(6 x 12)		
			10	Wet	TBD				
		Static Shear	2	Dry	297K (75°F)				
			2	Wet	TBD				
D Rib to Spar Joint 	Static Tension	5	Dry	297K (75°F)	152.4 x 304.8	(6 x 12)			
		5	Wet	TBD					
	Static Shear	1	Dry	297K (75°F)					
		1	Wet	TBD					
19	A Spar Cap to Fuselage Joint 	Fatigue	10	Dry	297K (75°F)	50.8 x 91.4	(2 x 36)	7 756 kg (17.1 lb) graphite/epoxy	Verification of fatigue strength of spar cap to fuselage joints
5	Wet		TBD						

TABLE 25. (Continued)

Item No	Description	Type of Test	No Specimen	Test Variables		Size		Materials Required	Purpose of Test	
				Condition	Temperature	mm	(in )			
20	A Rib Beam 	Static Combined Loads	1	Dry	297K (75°F)	508 x 1219 2	(20 x 48)	63 503 kg (140 lb) graphite/epoxy 15 876 kg (35 lb) kevlar 49/epoxy	Verification of the strength of ribs and spars in bending	
			1	Wet	TBD					
		Fatigue	1	Dry	297k (75°F)					
			1	Wet	TBD					
B	Spar Beam 	Static Combined Loads	2	Dry	297k (75°F)	609 6 x 1828 8	(24 x 72)			
			2	Wet	TBD					
21	A Rib Web 	Static Shear	1	Dry	297k (75°F)	508 x 1219 2	(20 x 48)	6 804 kg (15 lb) graphite/epoxy 0 9072 kg (2 lb) Kevlar 49/epoxy	Verification of static strength of rib and spar webs in shear	
			1	Wet	TBD					
	B Spar Web 		1	Dry	297k (75°F)	609 6 x 609 6	(24 x 24)			
			1	Wet	TBD					
22	A Rib Web 	Static Compression	2	Dry	297K (75°F)	152 4 x 508	(6 x 20)	4 990 kg (11 lb) graphite/epoxy 0 9072 kg (2 lb) kevlar 49/epoxy	Verification of static strength of rib and spar webs in compression	
			2	Wet	TBD					
	B Spar Web 		1	Dry	297K (75°F)	609 6 x 609 6	(24 x 24)			
			1	Wet	TBD					
23	A Front Spar Fuselage Joint 	Static Combined Loads	1	Dry	297k (75°F)	609 6 x 1828 8	(24 x 72)	61 235 kg (135 lb) graphite/epoxy 18 144 kg (40 lb) Kevlar 49/epoxy	Verification of static and fatigue strength of spar to fuselage joint design details	
			1	Wet	TBD					
		Fatigue	2	Dry	297K (75°F)					

94

REPRODUCIBILITY OF THE ORIGINAL PAGE IS POOR

TABLE 25. (Concluded)


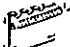






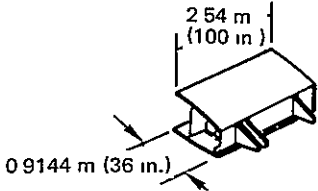
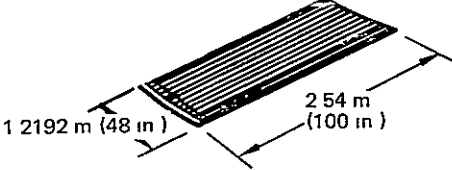
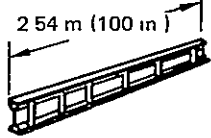
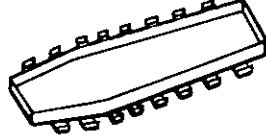
Item No	Description	Type of Test	No. Specimen	Test Variables		Size		Materials Required	Purpose of Test	
				Condition	Temperature	mm	(in )			
24	A Rudder Hinge Fitting 	Static Combined Loads	1	Dry	297K (75°F)	254 x 660.4	(10 x 26)	24.494 kg (54 lb) graphite/epoxy	Verification of static strength of rib design details	
			1	Wet	TBD					
	B Actuator Fitting 		1	Dry	297K (75°F)	304.8 x 685.8	(12 x 27)			
			1	Wet	TBD					
	C V597 Rib 		1	Wet	TBD	508 x 685.8	(20 x 27)			
			1	Dry	297K (75°F)					
Fatigue		1	Wet	TBD						
25	A Surface Attach to Fuselage 	Static Tension	1	Wet	TBD	546.1 x 1270	(21.5 x 50)	18.461 kg (40.7 lb) graphite/epoxy 0.6390 kg (1.4 lb) Kevlar 49/epoxy	Verification of static and fatigue strength of surface ace panels	
			Fatigue	1	Wet					TBD
			2	Dry	297K (75°F)					
26	A Stiffener Runout at Front Spar 	Static Tension	1	Dry	297K (75°F)	182.88 x 914.4	(7.2 x 36)	5.579 kg (12.3 lb) graphite/epoxy 1.614 kg (4 lb) Kevlar 49/epoxy	Verification of static and fatigue strength of surface panels	
			1	Wet	TBD					
		Fatigue	1	Wet	TBD					
			2	Dry	297K (75°F)					
27	A Surface Panel Stability 	Static Compression	1	Dry	297K (75°F)	1092.2 x 1905	(43 x 75)	27.760 kg (61.2 lb) graphite/epoxy 0.4536 kg (1.0 lb) Kevlar 49/epoxy	Verification of stability of surface panels	
			1	Wet	TBD					
28	A Surface Panel Fail Safety 	Fatigue	1	Dry	297K (75°F)	1092.2 x 1905	(43 x 75)	13.880 kg (30.6 lb) graphite/epoxy 1.361 kg (3 lb) Kevlar 49/epoxy	Verification of damage tolerance of surface panels	
29	A Stiffener/Skin with Interface Disbond 	Fatigue	1	Dry	297K (75°F)	132.88 x 914.4	(7.2 x 36)	2.223 kg (4.9 lb) graphite/epoxy 1.361 kg (3 lb) Kevlar 49/epoxy	Verification of damage tolerance of surface panels	
			1	Wet	TBD					



TABLE 26. FABRICATION AND ASSEMBLY PROCEDURE VERIFICATION —  
ANCILLARY TEST PROGRAM

ITEM NO.		DESCRIPTION	NO. SPECIMEN	PURPOSE
30	Subcomponent Box Beam Lower Aft Section		1	Validate design Critical region of fin Repair of Damage
31	Surface Subcomponent Fabricate		1 1	Validate fab. of surface structure 0.9144 m (36 in.) x 2.54 m (100 in.) panel for subcomponent box beam
32	Specimens for NASA Fabricate	COUPONS AND PANELS	3  715	Discussion specimens from prior tests  Material Properties
33	SPAR Subcomponent Fabricate		1	Validate fab. of spar structure for component box beam
34	Rib Subcomponent Fabricate		1 4	Validate fab. of rib structure for component box beam
35	Subcomponent Box Beam Assemble	SAME AS 30	1	Validate assembly of surfaces, rear spar, and ribs

commercial aircraft in the past and will lead to successful introduction of primary composite structure into commercial airline service.

Demonstration that static strength, durability, and fail-safe objectives are capable of being met for production hardware will be provided by component and full-scale tests and by related analyses. Demonstration that these objectives are met on each production composite vertical fin will be provided by implementing the quality control plan and the structural integrity control plan.

The structural integrity control plan establishes those actions that need to be applied in addition to those specified by the quality control plan to ensure that strength and durability objectives are met. The plan is responsive to special requirements that arise in individual parts or areas as a result of potential failure modes, damage tolerance and defect growth requirements, loadings and local configuration, inspectability, and as a result of local sensitivities to manufacture and assembly. The structural integrity control plan develops any special in-service inspection requirements that may be required to ensure that strength objectives are met throughout service use. This part-by-part review and planning will ensure that design, strength, and durability objectives are met by an adequate and cost-effective plan which is particularly suited for the part or area where it is to be applied. This assurance cannot be achieved by an overall criteria such as proof test or a single margin of safety.

The general flow of information and development of the structural integrity control plan is shown in Figure 55 and described below.

The structural integrity control plan will be implemented by review teams comprised of design/analysis, value and producibility, and quality assurance NDI representatives. The review teams will treat each part-of-area of the L-1011 composite vertical fin separately. While the structural integrity control may vary with each part/area, the major emphasis will be to provide evidence that the local structural integrity of each part produced is, in critical areas, equal to or in excess of the minimum required to obtain the strength and durability objectives as provided for in the design. It must also be proved to be within acceptable levels of variation from that demonstrated in the component and full-scale tests. Typical actions that will be implemented to achieve these objectives are:

1. Tabs for destructive evaluation of as-produced quality may be designed into the basic tooling adjacent to critical areas. Material cut from spar and rib webs for access holes can be used for destructive evaluation also.
2. Extension of tooling in major elements will be provided such as for the covers and spars. In addition, special fabrication instructions may be provided to ensure that the extended portion so produced will be representative of the basic structure of the

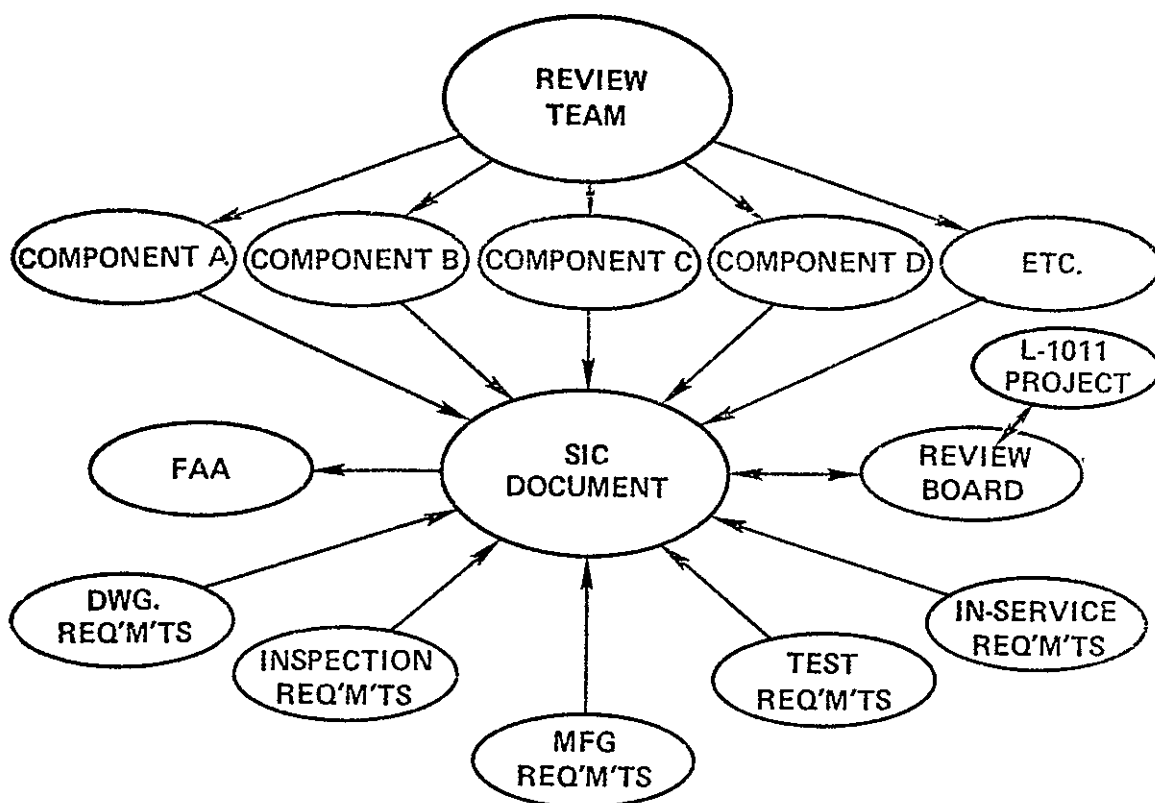


Figure 55. Structural Integrity Control Plan

component. Subsequent ultimate strength testing of the extension along with other destructive examinations will then be accomplished.

3. Methods for examination of plugs removed by hollow core drilling of select fastener holes will be developed. Testing will include resin/fiber volume ratio, selective peeling of layers, and examination using scanning electron microscopy (SEM) to evaluate adhesion between layers and between fiber and matrix.
4. Zoning of structure areas to define permissible void size locations, proximity to edges, etc.
5. Sampling and destructive testing of select members produced in number such as hat section stiffeners and perhaps web or rib elements.
6. Implementation of additional tests or analyses may be required for demonstrating the fail safety, durability, inspectability, sensitivity to manufacturing and fabrication tolerances, etc. These may also be required to substantiate adequacy of recommended structural integrity control procedures.

7. Proof testing of select subcomponents prior to assembly may be needed.
8. Requirements will be developed for in-service inspections of local areas because of peculiar features. Tests will be required to demonstrate the adequacy of these inspections by qualification of the inspection method and/or by demonstration of slow defect growth.
9. In-service monitoring of moisture will be conducted. This could include provision for tabs or elements to be removed and replaced at periodic intervals and used for evaluation of possible moisture buildup.

Iteration with detail design may be required to provide for reduced stress levels in select areas and/or detail design changes to improve inspectability or fail safety to implement the above.

#### 2.4.2 Quality Control Plan

Quality Assurance effort during Phase I centered around formulating a Quality Control Plan for the Advanced Composite Vertical Fin Program. The plan covers the activities of Lockheed-California Company as prime contract manager, Lockheed-Georgia Company, and Rockwell International Corporation, Los Angeles Aircraft Division as subcontractors and presents unique requirements pertaining to the L-1011 Advanced Composite Vertical Fin Program.

The plan outlines the tasks necessary to fulfill all the Quality Assurance requirements of the ACVF Program.

Key Quality Assurance requirements are:

- Review all contract documents and plan adequate Quality Assurance to ensure that all the engineering requirements are met.
- Maintain accuracy of measuring and testing equipment with traceability to the National Bureau of Standards.
- Establish and maintain accuracy of tooling to provide an assurance that each end product meets the dimensional requirements of the engineering drawings and that all interchangeability requirements are met.
- Establish procedure to assure that correct configuration is achieved; prepare and maintain complete documentation throughout the manufacturing and production phases to reflect the final product at time of delivery.

- Maintain surveillance to assure integrity of production work, of purchased material and of process control.
- Maintain adequate and accurate inspection records.
- Establish control and disposition of nonconforming material.
- Institute a responsive corrective action program.
- Schedule periodic independent audits by the government.
- Establish change control system of controlling documentation.

Several coordination meetings were held with FAA and NAVPRO inspection personnel to brief them on the program and establish guidelines for their involvement.

The Quality Assurance Laboratory performed acceptance tests on each batch of graphite material in accordance with the Quality Control Plan and applicable specifications. In addition, the QA laboratory performed qualification tests on the first batch of graphite/epoxy material. The laboratory established that the material (T300/5209) is in conformance with the specifications. All physical properties are being reported on Form 8634B Filamentary Laminate Static Property Data (organic matrix).

Preliminary NDI activity was started on test parts using ultrasonic through transmission with C-scan recordings.

## 2.5 CONCEPT EVALUATION TESTS

Tests were performed to evaluate the feasibility of the hat stiffened cover to fuselage joint. The primary purpose was to demonstrate that the joint loads could be carried before proceeding with the design.

The first specimen was fabricated using T300/934 as at that time the material system for the ACVF had not been chosen. The plan was to test specimens one using a 450K (350°F) cure resin system, and one using a 400K (260°F) cure resin system. The test specimen incorporated a hat section stiffener with a flared transition at the joint end and a 30° scarf cut at the opposite end. The stiffener was bonded to a 152 mm (6 in.) wide skin layup, which was then mechanically fastened to aluminum loading plates. The aluminum members at the joint were identical to the existing aircraft design.

The design ultimate load was 101.42 kN (22 800 lb). The specimen sustained a load of 144.12 kN (32 400 lbs). Figure 56 shows the load/stroke plot. The sudden drop in load at 126.77 kN (28 500 lb) occurred when the hat separated from the skin at the upper end away from the joint. Subsequent failure was in the mid section when the skin fractured under combined bending and tension.

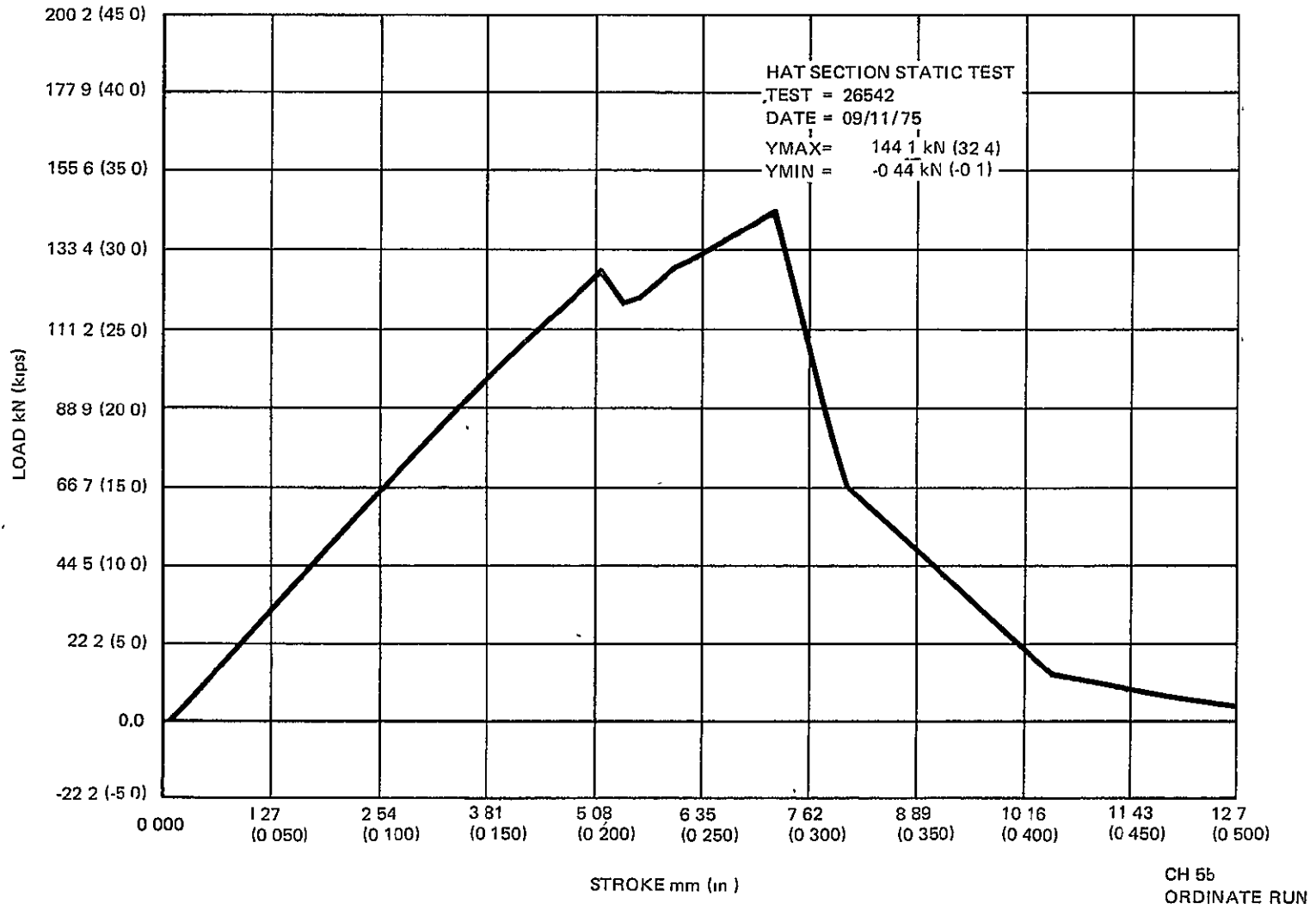


Figure 56. Joint Test Specimens

Subsequent to the testing of the first specimen, a second test article was designed and incorporated changes to preclude premature failure of the specimen away from the joint area. The stiffener was flared identical to the first at the joint; however, the opposite end was cut normal to the hat centerline and potted with fill material for approximately four inches. Additionally, 10 plies of doubler material were added for the last 152 mm (6 in.) of the stiffener. Additional mechanical fasteners were incorporated in the stiffener flange to skin away from the joint end. The aluminum plates utilized for loading the specimen were reduced in thickness to minimize loading eccentricities. This specimen was fabricated using T300/5209.

The runout configuration of the hat section has the basic hat section flaring out into a flat section of the fuselage joint so that all fibers are continuous into the joint area.

The second hat stiffener root joint section was tested in tension. The test was stopped when 71.172 kN (16 000 lb) of load had been applied and a popping sound was heard. The specimen setup is shown in Figure 57, the strain gage locations are shown in Figure 58 and strain gage plots are shown in Figure 59. Gages 1 through 5 represent channels 50 through 54 respectively. As shown in Figure 59, the hat stiffener was not picking up its share of load and one strain gage showed a sudden strain increase at 65.389 kN (14 700 lb).

The outboard end of the hat stiffener, which had been filled with syntactic foam to provide local shear rigidity and to transfer applied load from the skin into the crown of the hat was examined. Some thermal shrinkage cracks had appeared in this block during fabrication. However, examination now revealed that separations had occurred over a large part of the bond line between the filler block and the skin, and between the filler block and one side of the hat, which together with enlargement of a thermal crack, destroyed shear transfer capability of about a third of the filler block. This failure is believed to have been the source of the popping noise heard during the test. The strain gage records (Figure 59) indicate a simultaneous sudden increase in the skin load adjacent to the end attachment, in accordance with what would be expected when the bond to the filler block failed.

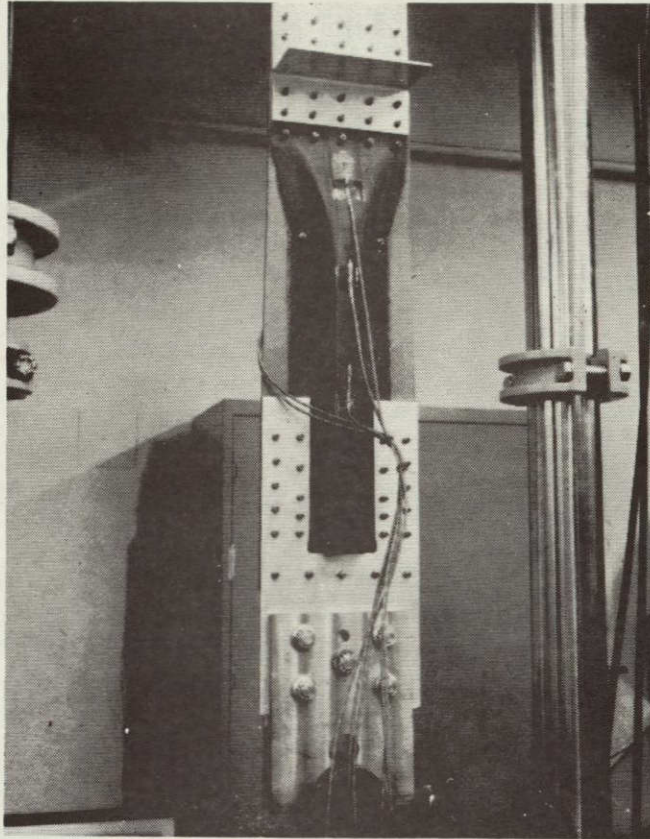


Figure 57. Stiffener Root Joint Tension Test

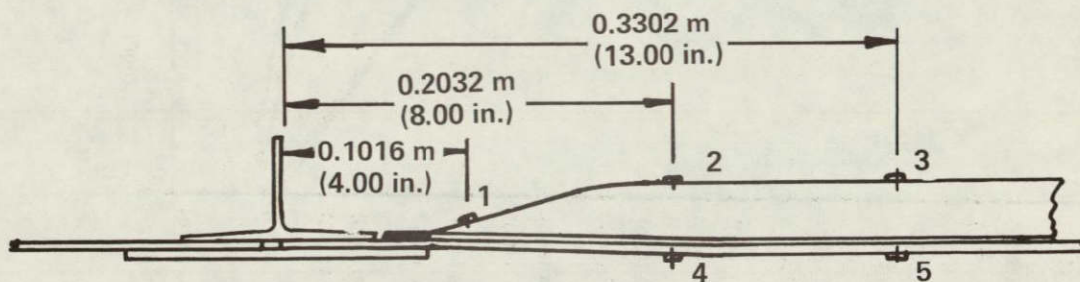


Figure 58. Location of Strain Gages



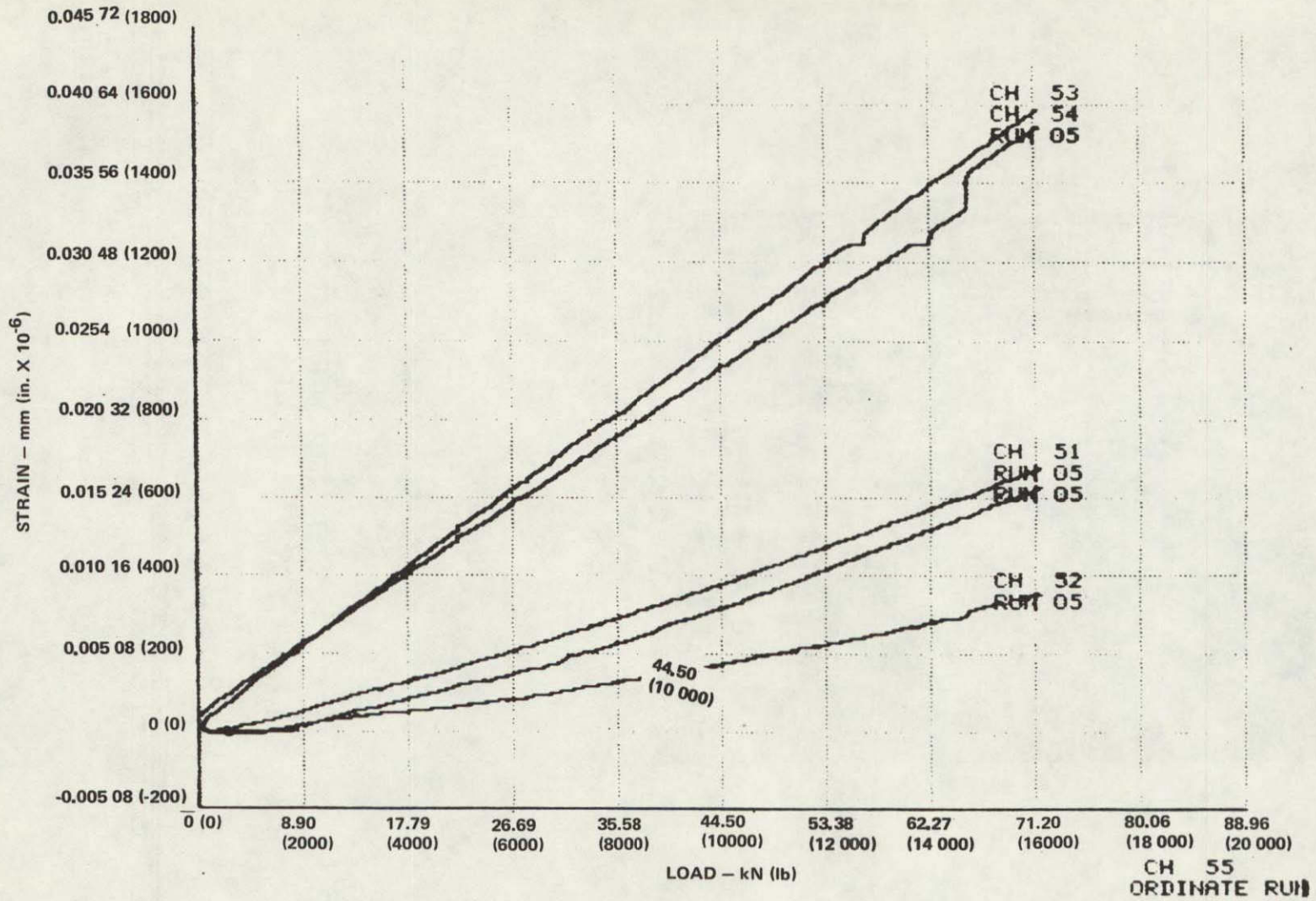


Figure 59. Tension Test Load Strain Gage Plots

### 3.0 TASK 2 MATERIAL SELECTION

#### 3.1 CANDIDATE MATERIALS

A list of candidate advanced composite materials was prepared based on aerospace industry usage and team (Lockheed and Rockwell) experience. The epoxies considered fall into two general classes based on the standard curing temperatures, 400K (260°F) and 450K (350°F). Each of the two classes have both advantages and disadvantages. The maximum fin temperature of 344K (160°F) is within the short-term capabilities of the 400K (260°F) curing resins. However, the long-term influence of humidity and temperature on 400K (260°F) curing resins has not been well characterized. If the 400K (260°F) curing resins have acceptable properties after environmental exposure, then the attributes of increased ductility, reduced thermal stresses, and fabrication/tooling advantages favor its use in lieu of the 450K (350°F) curing systems.

Candidate Materials considered are shown on Table 27 along with the availability of graphite and Kevlar 49 fabric preregs.

TABLE 27. CANDIDATE MATERIALS

Graphite/Epoxy Material (Supplier)	Graphite U.D. Tape	Graphite Fabric	Kevlar 49 Fabric (1)
● Graphite/epoxy unidirectional Tape Preregs 400K (260°F) Curing			
1. T300/5209 (Narmco)	X	X	X
2. T300/E715 (U S. Polymeric)	X	X	X
3. T300/E702 (U S Polymeric)	X	X	X
4. T300/SP288 (3M) or (CMC)	X		(3)
5. AS/CE345 (Ferro)	X	X	X
6. AS or T300/RAC6250 (Reliable)	X	X	X
● Graphite/Epoxy Unidirectional Tape Preregs 450K (350°F) Curing			
1. T300/934 (Fiberite)	X	X	X
2. AS/3501 (Hercules)	X		(2)
3. T300/5208 (Narmco)	X	X	X
4. T300/SP286 (3M) or (CMC)	X		(3)
5. T300/E759 (U S. Polymeric)	X	X	X
6. AS/CE9015 (Ferro)	X	X	X
7. AS or T300/RAC6350 (Reliable)	X	X	X
NOTE (1) Kevlar 49 will only be used as a hybrid with graphite and will be prepregged with the resin selected for the graphite			
(2) Hercules does not prepreg Kevlar 49 but Hexcel will prepreg Kevlar cloth with 3501 resin. (Hexcel did not quote for graphite prepreg.)			
(3) 3M does not prepreg Kevlar cloth.			

Most suppliers can prepreg graphite fabric and quoted such. However, no clear design/manufacturing requirement for graphite fabric has been identified to date. Fabric has a cost differential in excess of 20 percent and reduced mechanical properties. These must be offset by fabrication and cost reductions, and weight penalties must be acceptable before considering woven graphite for any part.

### 3.2. MATERIAL SELECTION - ANALYSIS AND TEST RESULTS

#### 3.2.1 Qualitative Analysis

The results of the qualitative screening of the candidate materials shown in Table 27 to the criteria discussed in the Material Evaluation and Selection Plan shown in appendix A are summarized in Table 28. The merit indices were assigned based on engineering judgment of the relative significance for each of the five parameters. Strength/stiffness and costs were judged most significant and were given maximum indices of 20 while the other parameters were given maximum indices of 10. Potential design strength reductions due to thermal residual stress effects reduced the indices of 450K (350°F) curing resins by 5.

TABLE 28. QUALITATIVE MATERIAL SCREENING

Resin Class	Prepreg	Usage	Production Experience	Data Availability	Strength/Stiffness	Costs	Merit Total
400 K (260°F) Curing	T300/5209	9	9	10	20	19	67
	T300/E715	4	8	8	20	17	57
	T300/E702	3	4	4	17	17	45
	T300/SP288	3	4	8	17	16	48
	AS/CE345	1	1	1	15	19	37
	AS/RAC6250	1	1	1	15	19	37
450K (350°F) Curing	T300/934	9	10	10	15	14	58
	AS/3501	10	9	10	13	15	57
	T300/5208	10	8	10	15	13	56
	T300/SP286	4	4	5	12	11	36
	T300/E759	3	3	2	12	12	32
	AS/CE9015	1	1	1	10	14	27
	AS/RAC6350	1	1	1	10	14	27

Since laminates with AS fibers have stiffnesses reduced by 5-10 percent (relative to T300 laminates) they were penalized by 2. The 450K (350°F) systems have incremental fabrication costs over 400K (260°F) systems due to

longer autoclave cure cycles and higher temperatures, and, consequently, the cost indices have been reduced by 5.

The greatest volume of material used within Lockheed Corporation is Fiberite's T300/934 due to its usage in production of the LMSC C4 missile. It is also being used by Rockwell for the space shuttle. The system with the next highest usage is Hercules' AS/3501, which has been used by all three team members. AS/3501 has been extensively used in Air Force composites programs. However, the California Company's experience with fabrication of AS/3501 has been unfavorable. The Georgia Company's elastomeric tooling program has used AS/3501 exclusively. Nationally, T300/5208 has the greatest usage. General Dynamics, LTV, and McDonnell/Douglas have used it extensively. All three contractors on this program have had some experience with T300/5208, but the Georgia Company experienced difficulty with voids in thick laminates of T300/5208. RI/LAAD is using it for their B-1 weapons bay door program. California Company's experience with U.S. Polymeric's T300/E715 and Kevlar 49/E715 has been favorable from both a producibility and structural standpoint. Georgia Company has had experience with a similar product: Narmco's T300/5209. Boeing selected T300/5209 for their 737 spoiler production program based on handling, overall quality, and QC experience after an extensive comparative fabrication (114 spoilers) effort. These spoilers are currently flying in a flight service evaluation program. LTV is also using T300/5209 in the substructure of the A7D wing and for the S-3A spoilers. Northrop has had good success with 3M's T300/SP288 in their low cost manufacturing program. Other systems considered include U.S. Polymeric's E759 450K (350°F cure) and E702 400K (260°F cure - highflow), Ferro's, and Reliable's epoxies; but they have seen limited aerospace usage.

The most data are available for T300/5208, AS/3501, T300/934, and T300/5209 - followed by T300/SP288 and T300/E715 (generated at the California Company). Long term (transport aircraft) environmental data is being generated for AS/3501 and T300/5209 under a NASA program, and other government agencies are generating environmental data for T300/5208 as well as other systems.

Based on the qualitative analysis T300/5209 and T300/934 were selected for quantitative analysis and screening tests. The runner-up materials for evaluation as backup systems are T300/E715 (or T300/SP288) for 400K (260°F) curing and AS/3501 (or T300/5208) for 450K (350°F) curing.

### 3.2.2 Screening Test Results

The material screening tests described in appendix A were performed on both T300/5209 (plus 5209/Kevlar 281 cloth for hybrids) and T300/934 (plus 934/Kevlar 281 cloth for hybrids).

The laminate physical property data are presented in Table 29. Thicknesses of the laminates were approximately 0.127 mm (5 mils) per graphite ply and 0.229 mm (9 mils) per Kevlar ply. The negative void content values for two of the laminates are believed to reflect a fundamental accuracy limitation

TABLE 29. PHYSICAL PROPERTIES

Material Identity	T300/934		T300/5209			GR/KEV HYBRID		
	0°	+45°	0° LTV Cure	0° Narmco Cure	+45°	Narmco PANEL	934	5209
Specimen ID	1MP 594	1MC 568 Y3	1MS 600	1MS 614	1MS 622	1459	1MP/MD 603	1MS/MT 626
Density, kg/m <sup>3</sup> (g/cc)	1600 (1.6000)	1594 (1.594)	1574 (1.574)	1561 (1.561)	1547 (1.547)	1570/1573 (1.570 - 1.573)	1515 (1.515)	1471 (1.471)
Resin Weight %	28.2	27.7	28.1	29.2	32.8	29.5 - 30.1	31.7	35.5
Graphite Weight %	71.8	72.3	71.9	70.8	67.2	70.5 - 69.9	50.6	44.7
Kevlar Weight %	-	-	-	-	-	-	17.7	19.8
Fiber Volume %	65.3	65.5	64.3	62.8	59.1	63.2	43.6/18.6	37.4/20.2
Void Volume %	-0.3	0.2	0.3	0.8	0.9	0 - 0.2	1.8	0.6
Thickness/Ply mm (Mils)	0.156 ±0.013 (6.13 ±0.5)	0.152 ±0.005 (5.97 ±0.2)	0.138 ±0.005 (5.44 ±0.2)	0.138 ±0.002 (5.42 ±0.1)	0.146 ±0.008 (5.76 ±0.3)	0.135 ±0.008 (5.3 ±0.3)	TOTAL 2.77 (109)	TOTAL 2.74 (108)
Moisture Weight Gain %	0.42	0.63	0.32	0.32	0.74		0.70	0.62
Skydrol Weight Gain %	0.06	-0.12	0.04	-0.01	-0.05		0.00	-0.06

Densities Used: T300 = 1760 (1.760), KEV = 1440 (1.440), 934 = 1287 (1.287) (Vs. 1300 (1.30) NOM), 5209 = 1250 (1.250) (Vs. 1235 (1.235) NOM)

108

REPRODUCIBILITY OF THE  
ORIGINAL PAGE IS POOR

associated with the void content analysis method. The accuracy of the method is limited to approximately  $\pm 0.5$  percent volume percent. The weight gain data for the water immersed specimens showed that the hybrid specimens gained a relatively larger amount of weight as a result of the exposure than did the graphite laminates exposed at the same temperature.

Samples treated with hydraulic fluid and then wiped with absorbent tissue to remove excess fluid showed up to a 0.06 percent weight gain whereas samples treated in the same way and then rinsed with methanol showed up to 0.12 percent weight loss. The significance of these weight changes could not be assessed since they are close to the limits of accuracy of the gravimetric method used.

The results of the interlaminar shear, flexure, interlaminar tension, and the  $\pm 45^\circ$  tension tests are summarized in Table 30. It should be noted that the flexure test used a constant 63.5 mm (2.5 in.) span that resulted in a span-to-depth ratio of less than the standard of 32.

It was observed that the interlaminar shear and 3-point flexure tests showed no significant differences in failure stresses between the phosphate ester immersed specimens and the control specimens tested at ambient. Also, there were no significant differences in failure stresses between the water soaked specimens and the controls tested at 344K (160°K).

For hybrid laminates, the 5209 resin system provided higher interlaminar tension values than the 934 system. However, because the two types of laminates were not processed in a comparable manner, direct comparison may be questionable. The results for the 934 system were unacceptable, and further investigation would be required to use it as a hybrid with Kevlar 49.

The bending modulus data for the 3-point flexure tests are also given in Table 30. These data show that the bending modulus was not affected by either 7-day immersion in distilled water or hydraulic fluid immersion.

The modulus and the ultimate stress values for the  $\pm 45^\circ$  tensile tests did not significantly change as a result of the 7-day environmental exposure, but the yield stress and the failure location were affected by the environmental exposure. In addition, the water immersed specimens for laminates of both resin systems (934 and 5209) had lowered yield strengths; in the case of the T300/5209 laminate, the yield stress was lower by 30 percent, and in the case of the T300/934 laminate, the yield stress was lower by 20 percent. For the  $\pm 45^\circ$  tensile tests the failure location varied almost randomly with the specimen and with the exposure conditions.

Figure 60 summarizes the mechanical properties comparison of the two resin systems. The dashed-lines indicate the standard deviation range. It shows that under the conditions used, the laminates with the 934 resin system had generally higher properties than the laminates with the 5209 resin. The principal exception, as previously noted, is the interlaminar tension tests.

TABLE 30. MATERIAL SCREENING TEST RESULTS

Material	T300/934		T300/5209								(T300 + KEV)/934		(T300 + KEV)/5209				
			EAV Cure Cycle				Narmco Cure Cycle										
Specimen Identification	IMP 594		1'S 600				1'NS 614				IMP/MD 603		1'NS/MT 626				
Resin/Graphite/Kevlar	28 2/71 8		28 1/71 9				29 2/70 8				31 7/50 6/17 7		35 5/44 7/19.8				
Voids	-0.3		0.3				0.8				-0.5		+0.6				
Density (kg/m <sup>3</sup> )(g/cc)	1600 (1.600)		1574 (1.574)				1561 (1.561)				1515 (1.515)		1471 (1.471)				
Wt Gain in Water Soak	0.42		0.32				0.32				0.70		0.62				
Wt Gain in Skydrol Soak	+0.05		+0.04				-0.01				0.00		-0.06				
Short Beam Shear Strength	F <sup>isu</sup> (MPa)		F <sup>isu</sup> (ksi)		F <sup>isu</sup> (MPa)		F <sup>isu</sup> (ksi)		F <sup>isu</sup> (MPa)		F <sup>isu</sup> (ksi)		F <sup>isu</sup> (MPa)		F <sup>isu</sup> (ksi)		
Controls - Tested at	R T	114	(16.6 ± 0.6)		89.6	(13.0 ± 0.4) <sup>(6)</sup>		86.9	(12.6 ± 0.8)		80.7	(11.7 ± 0.6)		62.7	(9.1 ± 0.3)		
Skydrol Soak - Tested at	R T	113	(16.4 ± 0.9)		88.3	(12.8 ± 0.6)		91.0	(13.2 ± 0.4)		75.2	(10.9 ± 0.3)		66.9	(9.7 ± 0.4)		
Water Soak - Tested at	344K (160°F)	91	(13.2 ± 0.5)		72.4	(10.5 ± 0.2)		65.5	(9.5 ± 0.2)		64.1	(9.3 ± 0.4)		51.7	(7.5 ± 0.4)		
Controls - Tested at	344K (160°F)	95	(13.8 ± 0.5)		77.9	(11.3 ± 0.3)		73.1	(10.6 ± 0.3)		68.3	(9.9 ± 0.8)		51.5	(7.9 ± 0.5)		
3- Pt Flexure (3.2 cm mom arm)	F <sup>bu</sup> (MPa)	F <sup>bu</sup> (ksi)	E <sup>b</sup> (GPa)	E <sup>b</sup> (msi)	F <sup>bu</sup> (MPa)	F <sup>bu</sup> (ksi)	E <sup>b</sup> (GPa)	E <sup>b</sup> (msi)	F <sup>bu</sup> (MPa)	F <sup>bu</sup> (ksi)	F <sup>bu</sup> (MPa)	F <sup>bu</sup> (ksi)	F <sup>bu</sup> (MPa)	F <sup>bu</sup> (ksi)			
Controls - Tested at	R T	1465	(212.5 ± 7.4)		114	(16.6 ± 0.5)			1355	(196.5 ± 4.8)		116	(16.8 ± 0.2)		1060	(153.8 ± 3)	
Skydrol - Tested at	R T	1367	(198.3 ± 7.2)						965	(140.0 ± 9.5)				1210	(175.5 ± 10.5) <sup>(4)</sup>		
Water Soak - Tested at	344K (160°F)	1298	(188.3 ± 6.6)		115	(16.7 ± 0.6)			1165	(168.9 ± 6.7)		115	(16.7 ± 0.3)		1069	(155.1 ± 2.0)	
Controls - Tested at	344K (160°F)	1326	(192.3 ± 4.7)		115	(16.7 ± 0.3)			1222	(177.3 ± 5.6)		113	(16.4 ± 0.3)		927	(134.4 ± 12.4)	
4- Pt Flexure (1.6 cm mom arm)	F <sup>bu</sup> (MPa)	F <sup>bu</sup> (ksi)	F <sup>bu</sup> (MPa)	F <sup>bu</sup> (ksi)	F <sup>bu</sup> (MPa)	F <sup>bu</sup> (ksi)	F <sup>bu</sup> (MPa)	F <sup>bu</sup> (ksi)	F <sup>bu</sup> (MPa)	F <sup>bu</sup> (ksi)	F <sup>bu</sup> (MPa)	F <sup>bu</sup> (ksi)	F <sup>bu</sup> (MPa)	F <sup>bu</sup> (ksi)			
Controls - Tested at	R T	1064	(154.3 ± 4.5)		1151	(167.0 ± 9.0)											
Skydrol - Tested at	R T	1119	(162.3 ± 11.1)		1211	(175.7 ± 7.7)											
Water - Tested at	344K (160°F)	1036	(150.3 ± 8.8)		963	(139.6 ± 7.4)											
Controls - Tested at	344K (160°F)	1213	(176.0 ± 8.2) <sup>(3)</sup>		1167	(169.3 ± 10.6) <sup>(3)</sup>											
Interlaminar Tension	F <sub>2</sub> <sup>tu</sup> (MPa)	F <sub>2</sub> <sup>tu</sup> (ksi)	F <sub>2</sub> <sup>tu</sup> (MPa)	F <sub>2</sub> <sup>tu</sup> (ksi)	F <sub>2</sub> <sup>tu</sup> (MPa)	F <sub>2</sub> <sup>tu</sup> (ksi)	F <sub>2</sub> <sup>tu</sup> (MPa)	F <sub>2</sub> <sup>tu</sup> (ksi)	F <sub>2</sub> <sup>tu</sup> (MPa)	F <sub>2</sub> <sup>tu</sup> (ksi)	F <sub>2</sub> <sup>tu</sup> (MPa)	F <sub>2</sub> <sup>tu</sup> (ksi)	F <sub>2</sub> <sup>tu</sup> (MPa)	F <sub>2</sub> <sup>tu</sup> (ksi)			
Controls - Tested at	R T	1.4-10	(0.2* to 1.5*)		17-22	(2.5** to 3.2***)											
Skydrol Soak - Tested at	R T	1.4-9	(0.2* to 1.3*)		12-22	(1.8** to 3.2***)											
Water Soak - Tested at	344K (160°F)	4.1-12	(0.6* to 1.7*)		12-17	(1.7* to 2.4***)											

All entries except Interlam tension are mean ± one std devn for 5 tests (unless number of tests is noted in parenthesis)

\*Failure at Kevlar graphite interface  
\*\*Interlaminar Failure in Graphite  
\*\*\*Adhesive bond Failure - Kevlar to loading block

TABLE 30. Concluded

Material	T300/934							T300/5209 (Narmco Cycle)						
Specimen Identification	140 569 Y3							14S 622						
Resin Content	27.7							32.8						
Void Content	0.2							0.9						
Density	1594 (1.594)							1547 (1.547)						
Wt Gain in Water Soak	0.63							0.74						
Wt Gain in Skydrol Soak	-0.12							-0.05						
Tension - 45° 12 Ply Specimens	$F_{tu}$ MPa	$F_{tu}$ ksi	$F_{ty}$ MPa	$F_{ty}$ ksi	$E_p$ GPa	$E_c$ msi	Failure Mode	$F_{tu}$ MPa	$F_{tu}$ ksi	$F_{ty}$ MPa	$F_{ty}$ ksi	$E_p$ GPa	$E_c$ msi	Failure Mode
Controls - Tested at R T	187.5	(27.2 ± 0.3)	146.2	(21.2 ± 0.7)	23.98	(3.42 ± 0.21)	3A, 2B	164.1	(23.8 ± 0.6)	100.7	(14.6 ± 0.3)	15.72	(2.28 ± 0.12)	ALL C(6)
Skydrol Soak - Tested at R T	186.9	(27.1 ± 0.2)	143.4	(20.8 ± 1.1)	23.58	(3.42 ± 0.40)	1A, 3B	157.2	(22.8 ± 0.4)	102.0	(14.8 ± 0.3)	15.85	(2.30 ± 0.06)	ALL C
Water Soak - Tested at 344K (160°F)	174.4	(25.3 ± 1.0)	91.0	(13.2 ± 0.4)	21.58	(3.13 ± 0.24)	1A, 2B, 2C	186.2	(27.0 ± 1.5)	52.4	(7.6 ± 0.3)	11.79	(1.71 ± 0.11)	ALL A
Controls - Tested at 344K (160°F)	171.7	(24.9 ± 0.5)	111.0	(16.1 ± 1.0)	22.06	(3.20 ± 0.52)	2A, 1B, 2C	199.3	(28.9 ± 0.4)	75.2	(10.9 ± 0.6)	13.24	(1.92 ± 0.10)	ALL C(4)
Conditioning Water Soak - 7 Days at 333K (140°F) tested at 344K (160°F) Skydrol Soak - 7 Days at 325K (125°F) tested at R T. $F_{ty}$ = 0.002 offset obtained from 50.8 mm (2 in) gage length mechanical extensometer placed at center of 152.4 mm (6 in) test length between tab reinforcements Each entry average of 5 tests except where number of tests indicated in parenthesis Failure Mode (A) In Midsection (B) Adjacent to end tab (C) partly or entirely under end tab														

REPRODUCIBILITY OF THE ORIGINAL PAGE IS POOR



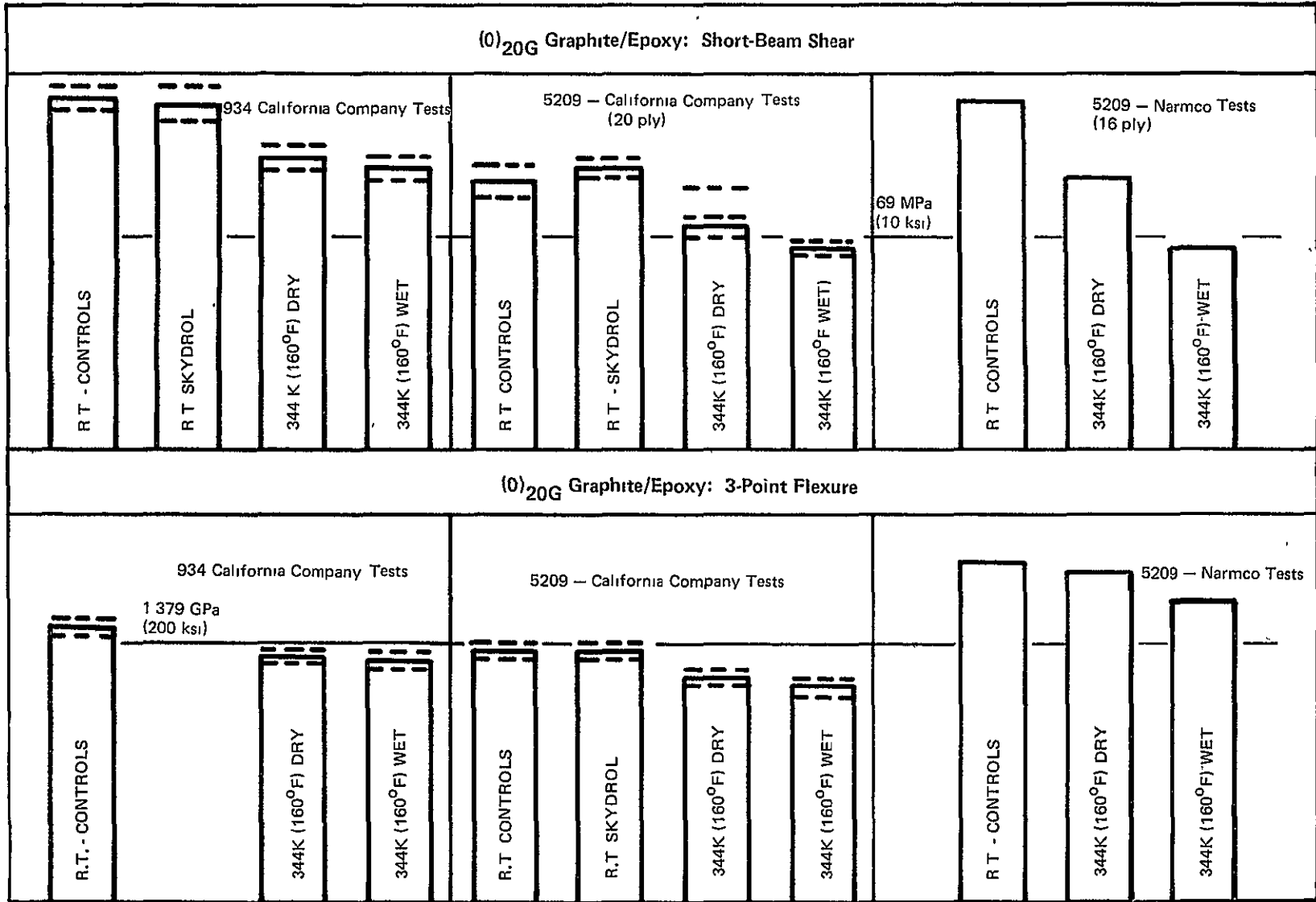


Figure 60. Mechanical Properties Comparison

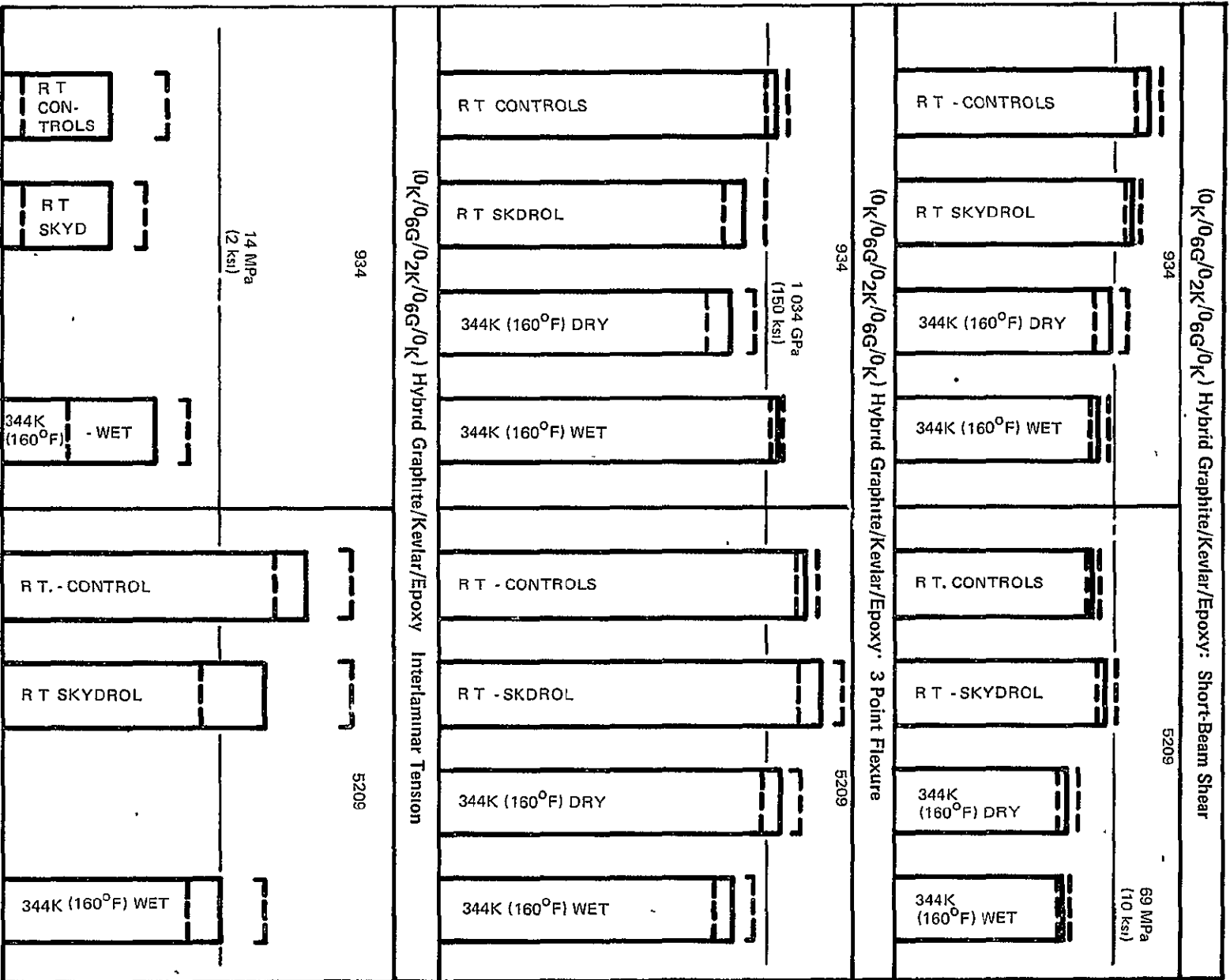


Figure 60. Continued.

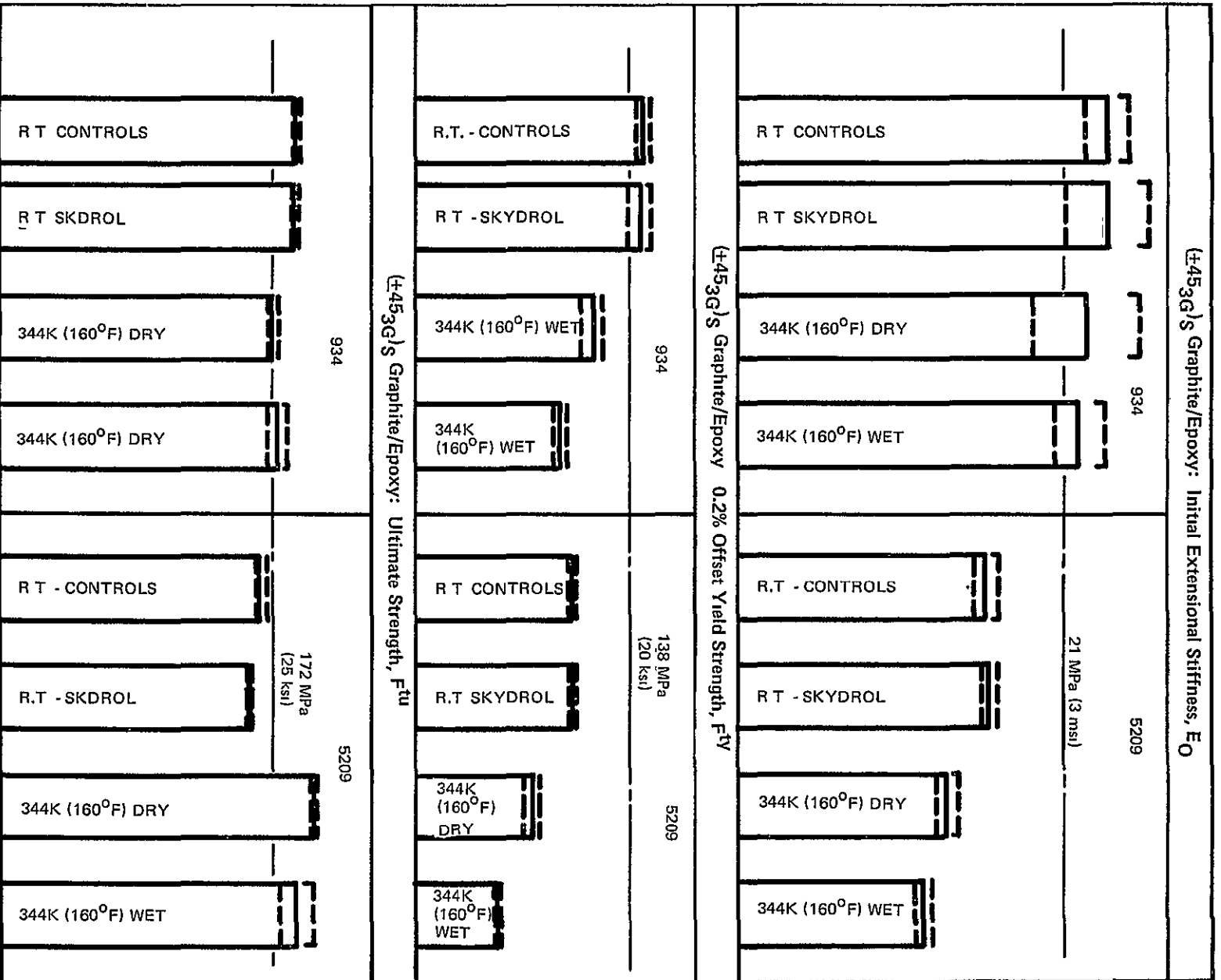


Figure 60. Continued.

Also shown are the results of Narmco short-beam shear and flexure tests of T300/5209 to similar requirements. The primary difference between the Narmco tests and the California Company tests are that Narmco used 16 plies instead of 20 plies. This probably accounts for the higher strengths. The one test ( $\pm 45^\circ$  tensile test, yield stress) which did detect a measurable effect from the water immersion indicated a somewhat greater percentage loss in strength for the 5209 laminate than for the 934 laminate.

Task 4a of the Material Screening Test Plan (Appendix A) is to evaluate and compare the fabricability of both materials. This verified that both materials can be formed satisfactorily to the compound shape of the hat-stiffener runout and that sound parts result with either the fast or slow heat-up rates.

The results of the Task 5 thermal expansion tests are shown in Figure 61. The difference between the flat temperature and room temperature, the coefficients of thermal expansion, the stiffness properties, and the  $[0_4/90_4]$  layup geometries were input to the LAMSTR computer program and resultant curvatures were calculated. The computed curvatures were within 5 percent of those measured. The curvature of the 934 panel was 44 percent greater than that of the 5209 panel.

The following conclusions resulted from the screening tests:

1. The laminate mechanical properties determined in this study were unchanged as a result of 7-day ambient exposure to phosphate ester hydraulic fluid.

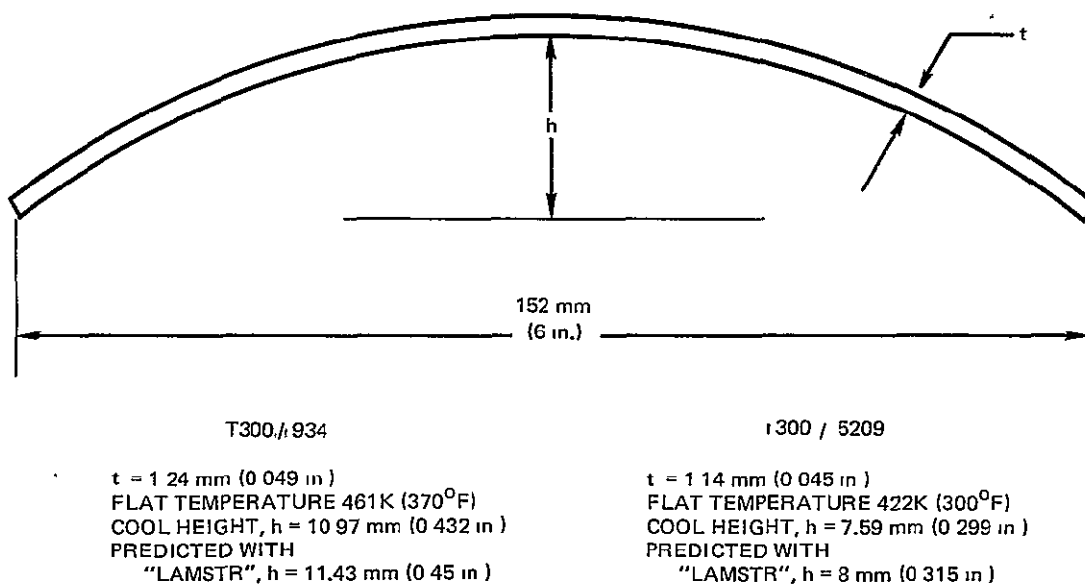


Figure 61.  $0_4/90_4$  Warp Panel Comparison

2. The amount of moisture absorbed into the laminates as a result of the 7-day distilled water immersion was essentially the same for the two resin systems used.
3. The hybrid laminates absorbed moisture at a more rapid rate than did the laminates which contained only the T300 graphite.
4. The magnitude of the weight gain resulting from immersion for 7 days in distilled water was approximately 0.3 to 0.7 percent of the total laminate weight (it is not believed that saturation conditions were achieved).
5. The weight changes resulting from a 7-day immersion in hydraulic fluid were on the same order as the limits of accuracy for the analysis method used.
6. Based on the test results obtained with the  $\pm 45^{\circ}$  tensile specimens, both resin systems were plasticized by the distilled water immersion conditioning with the 5209 resin laminates showing slightly more reduction in properties (on a percentage basis) than the 934. The plasticizing action did not reduce the ultimate strength values, but caused a reduction in the initial slope of the stress-strain curve and yield strength values. It also resulted in a change in the mode of failure for the 5209 specimens.
7. The 5209 resin system provided higher interlaminar tension values than the 934 resin for graphite/Kevlar-49 hybrid laminates; however, direct comparison is difficult because of differences in processing (e.g., prestaging for the 5209 Kevlar material vs no prestaging for the 934 Kevlar material).
8. For both resin systems, the interlaminar shear, flexure, and interlaminar tension tests indicated little effect on mechanical properties due to moisture effects.
9. Both 934 and 5209 process equally well for the requirements of the ACVF program.
10. The thermal expansion tests indicated that cross-ply laminates of T300/934 have a greater thermal residual stress than laminates of T300/5209.

A significant factor in comparing the two materials is the autoclave cure cycle. The cure cycles used for fabricating the screening test specimens are shown in Figure 62. It is recognized that in fabricating various pieces of hardware variations in cure cycles are required. However, it is evident that substantially more time and energy are required for curing 934 than for 5209. Two autoclave cures of 5209 can be completed in one shift compared to one for 934. This translates into a significant difference in cost when manpower is included.

### 3.4 Selected Material

The material selected for the ACVF program is Narmco T300/5209. This decision was based primarily on economic considerations, as the results of the qualitative material screening of 5209 and 934 resin systems showed the two systems to be comparable in most areas. Each system has its advantages and its disadvantages, but both are acceptable for the ACVF program.

The processing of both systems is satisfactory from tack, handling, and drape viewpoints. Some problems encountered during prebleeding tests and with poor adhesion of Kevlar 49 were considered to be solvable with more work and vendor cooperation.

Experiments with slow heat-up rates which are required for the elastomeric tooling concept showed 5209 to be satisfactory. Additional work is required by the Georgia Company to verify that sufficient rubber expansion can be achieved to supply the required pressure for curing.

Manufacturing at the California Company and RI/LAAD expressed preference for 5209 due to the lower cost of the shorter autoclave cycle (see Figure 62) and the possible reductions in tooling requirements. Stress also preferred the 5209 because of reduced residual thermal stresses.

The use of 400K (260°F) curing resin instead of 450K (350°F) curing resin can result in possible reductions in tooling requirements as follows:

1. The temperature of the tool side of a laminate tends to lag behind that of the bag side of the laminate, so there is a thermal gradient across the laminate thickness. If this gradient is too great, corrective measures (such as thermal insulating blankets) must be taken to prevent part warpage, etc. The lower temperature cure minimizes this gradient and can reduce (or eliminate) insulating blankets.
2. The difference in thermal expansion between the tool and the part must be accounted for in the tool design. The difference is less for the lower cure temperature. Under certain conditions, this can permit the use of aluminum instead of steel and result in reduced machining costs for a complex tool.
3. Tool warpage due to thermal gradients in the tool during cure must be minimized by tool design (e.g., by bracing). The magnitudes of thermal gradients are less for the lower cure temperature, and, consequently, the requirements for the tooling can be less.

It should be noted that reasons cited above are of a general nature and are not specific to the ACVF. Nothing is implied concerning differences in tooling costs because of different resin curing temperatures.

While recognizing that further testing and manufacturing development will be required, it was the consensus of the team that a 400K (260<sup>o</sup>F) curing system would be more beneficial to the program. Consequently the T300/5209 material system was selected.

The backup system tentatively selected was U.S. Polymeric's T300/E715, a 400K (260<sup>o</sup>F) curing system. This system will be subjected to the same screening tests used on the 5209 system to demonstrate equivalent environmental resistance. If it fails to demonstrate equivalent environmental resistance, its alternate, 3M's T300/SP288 will be tested.

#### 3.2.4.1 Material Specification

The status of the material and process specifications is shown in Table 32.

#### 3.2.4.2 Qualification of T300/5209

The QA Laboratory completed qualification testing of the graphite/epoxy prepreg material, Narmco Rigidite T300/5209, and established that the material conforms to Specification C22-1379/211. The qualification tests also constitute acceptance of batch number 1473. The test results are summarized in Table 33.

TABLE 32. STATUS OF MATERIALS AND PROCESSES ENGINEERING SPECIFICATION

Number	Subject	Dates	
		Master Scheduling	Release
C-22-1379 (Basic)	Graphite Fiber Nonwoven Tape and Sheet, Resin Impregnated, General Specification For	Released	
C-22-1379/211	Graphite Fiber Nonwoven Tape and Sheet, 2.413 GPa (350 ksi) Strength, 227.53 GPa (33 MSI) Modulus, 344K (160°F) Service, Epoxy Preimpregnated	Released	
C-22-1350/131	Epoxy Preimpregnated Intermediate Modulus Organic Fiber Fabric, Type 1, 400K (260°F) Curing, 344K (160°F) Service, for Hybrid Application	2-4-76	2-18-76
C-22-1350/132	Epoxy Preimpregnated Intermediate Modulus Organic Fiber Fabric, Type 2, 400K (260°F) Curing, 344K (160°F) Service, for Hybrid Application	2-4-76	2-18-76
LCM 30-1085B	Adhesive, Hat Stiffener to Skin and Wire Mesh Bonding	Released	
PB-X-XXX	Fabrication of Hat Stiffened Cover Assembly	TBD	TBD
LCM XX-XXXX	Wire Mesh	TBD	TBD
LCP 71-1073C	Preparation for an Installation of Mechanical Fasteners	TBD	TBD
PB 75-425D	Environmental Sealing of Model L-1011 Aircraft	TBD	TBD
PB 78-433B(1)	Application of Exterior Coating System for the L-1011 Aircraft	TBD	TBD
LCP 70-1092/1	Standard Repair Manual, L-1011	TBD	TBD
PB XX-XXX	Fabrication of Spars for L-1011 Vertical Fin	TBD	TBD
PB XX-XXX	Fabrication of Miniwich Ribs for L-1011 Vertical Fin	TBD	TBD
PB XX-XXX	Fabrication of Truss Ribs for L-1011 Vertical Fin	TBD	TBD
Status is preliminary. Certain existing documents may prove adequate with minor amendment. Consolidations may prove more cost effective.			



TABLE 33. QUALIFICATION TESTING RESULTS T300/5209

Fiber Properties					
Property	Unit	Requirement	Certificate Value		
Strand Breaking Strength	GPa (min) (psi) (min)	2.151 (312 000)	2.537 (368 000)		
Strand Modulus	GPa (psi x 10 <sup>6</sup> )	206.8 - 241.3 (30 - 35)	226.2 (32.8)		
Fiber Density	kg/m <sup>3</sup>	1 700 - 1 780	1 748		
Uncured Properties					
Property	Unit	Requirement	Test Results		
Volatiles Test Temp. 408K (275°F) Time at Temp. 10 ±2 min	% by wt max	2	0.48		
Uncured Resin Content	% by wt	41 ±3	41-42		
Flow 10 min. @ 408K (275°F) and 103.4K Pa (15 psi)	%	7 - 22	13-14		
Gel Time @ 408K (275°F)	min.	Report for Information Only	5 min. 15 secs		
Areal Weight	kg/m <sup>2</sup>	0.144 ±5	141 - 144		
Mechanical and Physical Properties					
Property	Unit	Test Temp K (°F)	Requirement △	Test Results	
				Min or (Max)	Average
Specific Gravity			1.51 - 1.59	1.55-(1.58)	1.568
Cured Fiber Volume	%		60 - 66	64.7-(66)	65.5
Water Absorption	% Max		0.1	(0.07)	0.04
Longitudinal Tensile Strength	GPa (min) (ksi) (min)	297 (75)	1.276 (185)	1.420 (206)	1.510 (219)
		218 (-67)	1.276 (185)	1.310 (190)	1.379 (200)
		344 (160)	1.172 (170)	1.282 (186)	1.372 (199)

TABLE 33. (Concluded)

Property	Unit	Test Temp K (°F)	Requirement △	Test Results	
				Min or (Max)	Average
Longitudinal Tensile Modulus	GPa (10 <sup>6</sup> psi) (min)	297 (75)	131 (19)	145 (21)	145 (21)
		218 (-67)	131 (19)	138 (20)	145 (21)
		344 (160)	124 (18)	145 (21)	145 (21)
Transverse Tensile Strength	MPa (ksi) (min)	297 (75)	48.3 (7.0)	55.2 (8.0)	61.4 (8.9)
		218 (-67)	55.2 (8.0)	64.4 (9.2)	68.2 (9.9)
		344 (160)	37.9 (5.5)	46.2 (6.7)	51.7 (7.5)
Transverse Tensile Modulus	GPa (10 <sup>6</sup> psi) (min)	297 (75)	7.6 (1.1)	11.7 (1.7)	11.7 (1.7)
		218 (-67)	8.3 (1.2)	13.8 (2.0)	14.5 (2.1)
		344 (160)	7.0 (1.0)	10.3 (1.5)	10.3 (1.5)
Transverse Tensile Strain at Failure	% (min)	297 (75)	(0.5)	(0.5)	(0.5)
±45° Tensile Strength	MPa (ksi) (min)	297 (75)	159 (23)	172 (25)	180 (27)
		218 (-67)	159 (23)	186 (27)	186 (27)
		344 (160)	159 (23)	186 (27)	193 (28)
		344 (160) WET △	145 (21)	165 (24)	172 (25)
±45° Tensile Modulus	GPa (10 <sup>6</sup> psi) (min)	297 (75)	13.8 (2.0)	13.8 (2.0)	15.2 (2.2)
		218 (-67)	9.0 (1.3)	10.3 (1.5)	11.7 (1.7)
		344 (160)	12.4 (1.8)	13.8 (2.0)	14.5 (2.1)
		344 (160) WET △	10.3 (1.5)	11.0 (1.6)	11.7 (1.7)
Longitudinal Compressive Strength	GPa (ksi) (min)	297 (75)	1.276 (185)	1.662 (241)	1.751 (254)
		218 (-67)	1.310 (190)	1.917 (278)	2.020 (293)
		344 (160)	1.310 (180)	1.434 (208)	1.551 (225)
Longitudinal Compressive Modulus	GPa (10 <sup>6</sup> psi) (min)	297 (75)	131 (18.0)	133 (19.3)	140 (20.3)
		218 (-67)	131 (18.0)	138 (20.1)	143 (20.8)
		344 (160)	131 (18.0)	136 (19.8)	143 (20.8)
Longitudinal Flexural Strength	GPa (ksi) (min)	297 (75)	1.448 (210)	1.613 (234)	1.751 (254)
		218 (-67)	1.517 (220)	1.931 (280)	1.958 (284)
		344 (160)	1.172 (170)	1.565 (227)	1.655 (240)
		344 (160) WET △	1.069 (155)	1.248 (181)	1.303 (189)
Longitudinal Flexural Modulus	GPa (10 <sup>6</sup> psi) (min)	297 (75)	131 (19)	131 (19)	138 (20)
		218 (-67)	131 (19)	131 (19)	138 (20)
		344 (160)	124 (18)	131 (19)	138 (20)
		344 (160) WET △	117 (17)	124 (18)	131 (19)
Longitudinal Short Beam Shear Strength	MPa (ksi) (min)	297 (75)	90 (13)	97 (14)	103 (15)
		218 (-67)	110 (16)	117 (17)	117 (17)
		344 (160)	69 (10)	76 (11)	83 (12)
		344 (160) WET △	55 (8)	62 (9)	69 (10)
Cured Thickness Per Ply	mm (in)		0.119 - 0.140 (0.0047 - 0.0055)	0.124 - 0.135 (0.0049 - 0.0053)	0.130 (0.0051)

△ Average of 3 determinations for fiber volume, specific gravity and water absorption. Average of 5 measurements for cured thickness per ply. Values for all other tests are minimum individual of a set of 5 determinations for qualification tests.

△ After seven days immersion at 325K (125°K)

## 4.0 TASK 3 - FABRICATION

### 4.1 PRODUCIBILITY CONSIDERATION STUDIES

Extensive producibility technology studies were involved in the selection of materials, design concepts, tooling and fabrication processes to achieve a cost competitive composite fin box structure. These producibility technologies are described for each component segment as follows:

#### 4.1.1 Skin Cover Concepts

##### 4.1.1.1 Ortho Grid Blade Stiffened Skin Cover

The fabrication approach for this concept is the cocuring of an integrated assembly of prebled details (blade - rib cap - skin) utilizing preshaped rubber mandrel blocks and an outer skin female mold tool (see Figure 63). The complete assembly is vacuum bag and autoclave pressure cured. The rubber blocks provide the transverse pressure needed when curing the blade stiffeners and rib caps.

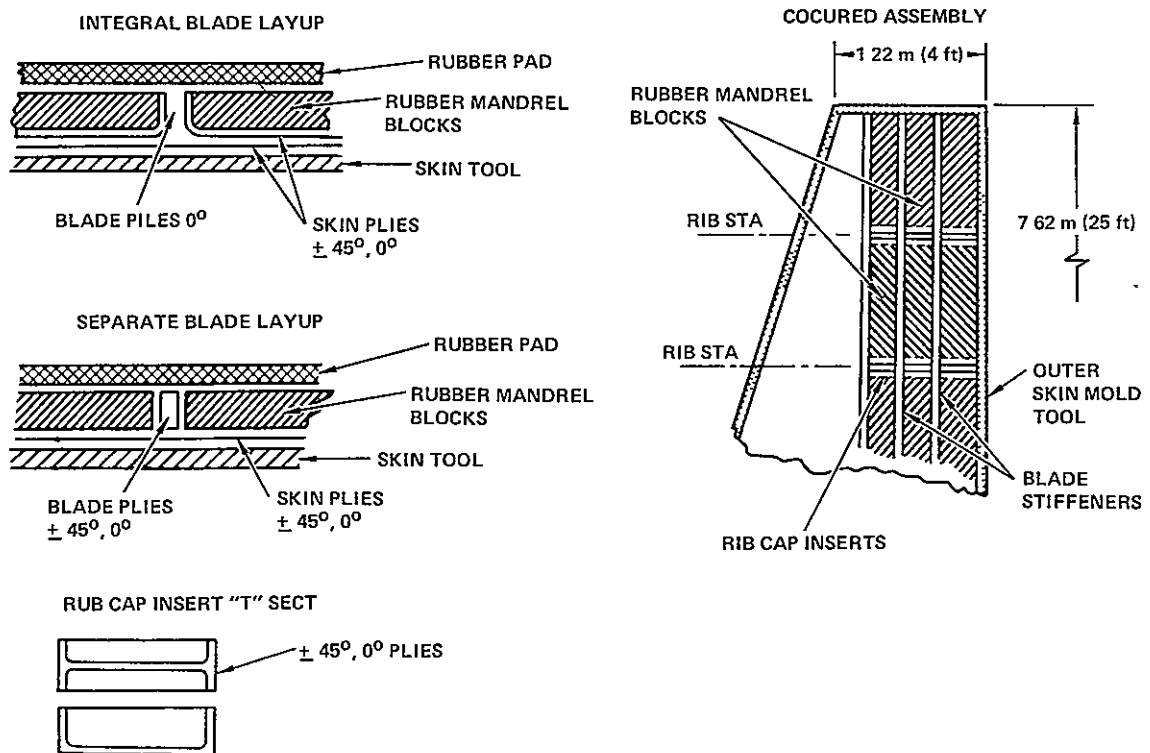


Figure 63. Ortho Grid Blade Stiffened Skin Cover

The California Company has made some stiffened skin panels approximately 1.22 m by 1.22 m (4 ft by 4 ft) using this process. Also, internal IRAD work has been done to characterize the various rubber compounds and to determine the limitations and constraints.

One of the problems that can occur with this approach is misalignment of blades and rib cap inserts during the cure cycle caused by nonuniform rubber block expansion. Rubber characterization data has shown variation in width, length, and thickness shrinkage during repeatable cure cycles and also degradation of the rubber after 30 or more cure cycles. Another problem is the difficulty in scaling up the process to accommodate the full size skin cover which measures 2.9 m by 7.62 m (9.5 ft by 25 ft). Autoclave equipment that will heat the tool mass and part in a uniform manner during the cure cycle for skin panels of this size must be provided to prevent nonuniform rubber mandrel expansion.

A proposed solution to overcome these difficulties is to cure the rib inserts, assemble by shimming, and then to secondarily bond them in place at each rib station. This would minimize the possibility of rib station misalignment. New rubber compounds are needed to provide uniform expansion rates, increased thermal conductivity, and production repeatability for at least 100 cycles must be developed.

This fabrication process still requires extensive scale-up development to achieve dimensional requirements and process repeatability. In addition, large production runs will be necessary to offset the initial tooling and fabrication development costs.

#### 4.1.1.2 A-Frame Section Stiffened Skin Cover

One approach in fabricating the A-frame section configuration is to vacuum bag and autoclave cure the part utilizing a four segment tool as shown in Figure 64. The A-frame section is fabricated from five separate ply layup segments of graphite/epoxy prepreg. Segment sections 1 (see Figure 64) are layed up in the flat and then cut to the developed widths. The filler is a 0° graphite/epoxy prepreg rope made to a specific diameter to fill in the intersection corners.

Laying these segments on the mating tool surfaces is a difficult operation especially in the 7.62 m (25 ft) lengths, since interface alignment of the laminate segments and tool surfaces must be maintained. Fabrication of this length stiffener will involve complex alignment and clamping devices.

Upon completion of the layup in the tool, the bleeder cloths and vacuum bag are applied and the completed assembly is autoclave cured. Edge bleeding is the recommended method of resin removal using this approach.

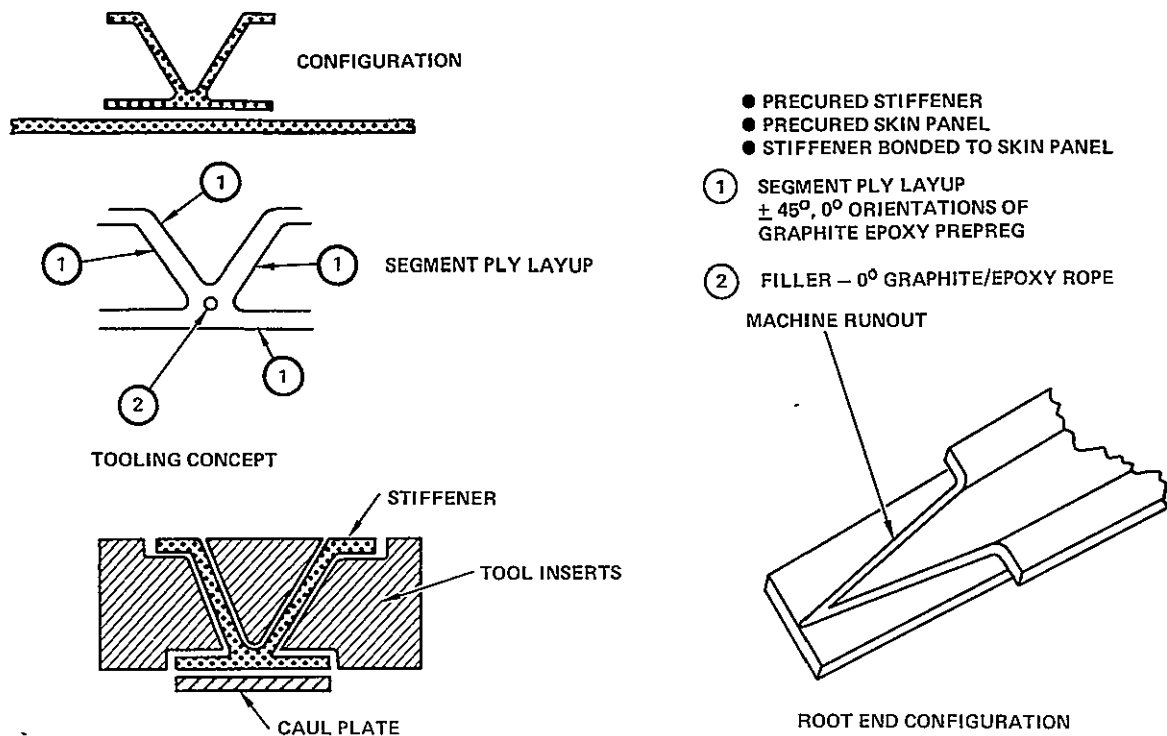


Figure 64. A-Frame Section Stiffened Skin Cover

Another approach that utilizes this tool and obtains improved fiber/resin ratio control is to prebleed the ply layup segments in the flat, and then, using a heat gun, form the segments on the tool surfaces. The detail layups and tool segments are assembled and autoclave cocured (without bleeder cloths) into an integral section shape.

The pultrusion process is a possible lower cost and more efficient approach for this stiffener configuration. However, considerable development effort is required to construct a (4) segment tool and maintain the wall thickness tolerances of the laminate during the pultruding operation.

The pultrusion of various types of stiffener configurations has been discussed with several suppliers of pultrusion products. In general, the most difficult problem to resolve is the pultrusion of  $\pm 45^\circ$  laminate surface covered with scrim cloth (104 fiberglass) and/or  $0^\circ$  plies in order to pultrude through the die orifices.

Both the prepreg and the wet resin systems have been investigated for use in the pultrusion process. Also, the use of heat dies and microwave curing methods have been studied.

### 4.1.1.3 I-beam Section Stiffened Skin Cover

The fabrication approach to the I-beam section stiffener as seen in Figure 65 is similar to that considered for the A-frame section stiffener. Seven separate prepreg laminates are used to fabricate this section configuration. Several I-beam section stiffeners and floor posts have been fabricated by the prepreg plus edge bleeding process utilizing tools similar to the concept shown in Figure 65.

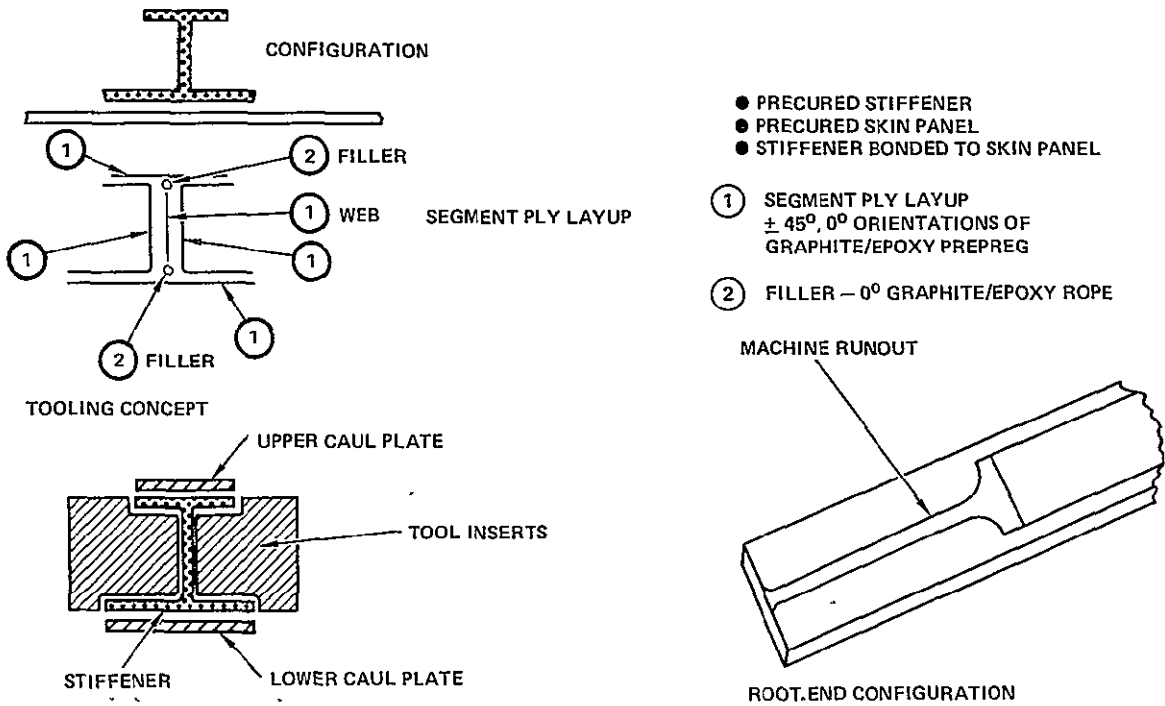


Figure 65. I-Beam Section Stiffened Skin Cover

However, since the cost of hand layup was found to be expensive, the pultrusion process is being investigated. If the problems described previously in the discussion of the A-frame section can be resolved, the pultrusion process has possibilities of being a more economical approach. Pultrusion tooling for the I-beam section is simpler than that for the A-frame section stiffener, however, the flow of the prepreg material through the die will require development to achieve uniform wall thickness.

#### 4.1.1.4 Hat Section Stiffened Skin Cover

The hat section stiffener is the simplest approach to fabrication and tooling in comparison to the A-frame and I-beam stiffener configurations. Only one basic male and/or female tool is necessary to fabricate this stiffener configuration utilizing the hand layup approach. Three ply layup segments are used in this configuration.

Figure 66 depicts the male tool approach. Elevated temperature pre-bleeding is required to assure good resin content control, to prevent fiber wash, and to minimize bridging at the flange radius. The final cure is

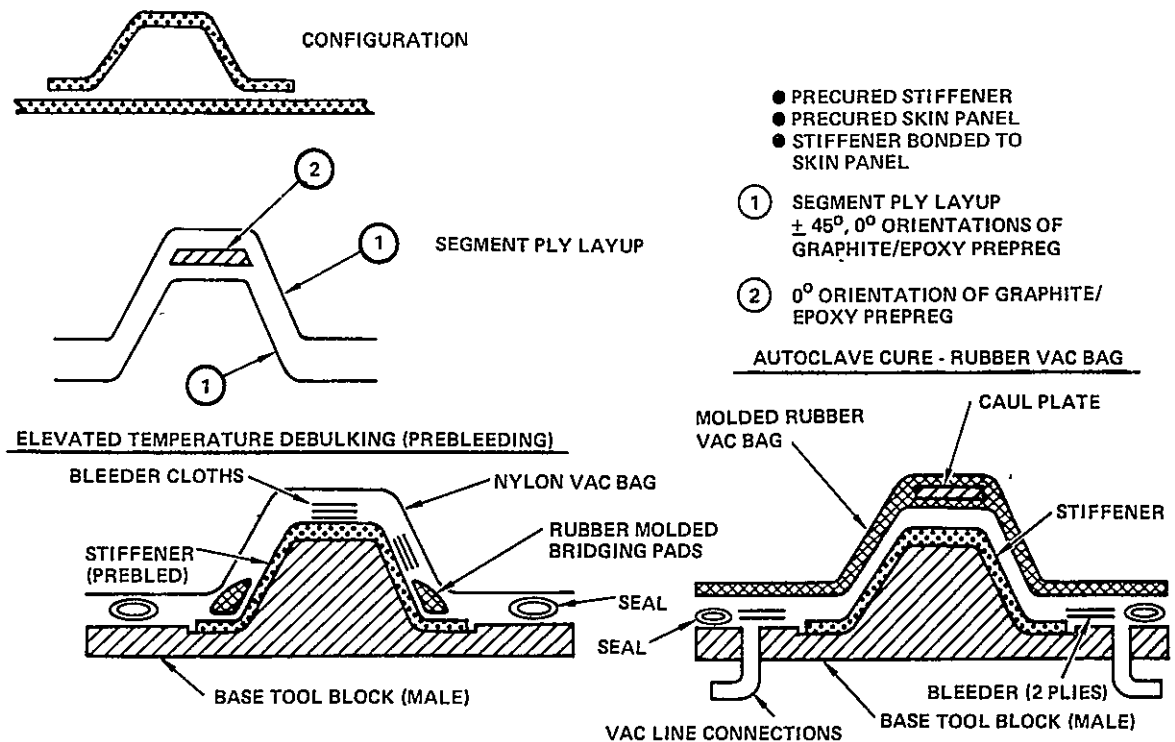


Figure 66. Hat Section Stiffened Skin Cover - Male Tool Concept

achieved by using a precision molded rubber bag during the autoclave cure to obtain uniform wall thickness and dimensional configuration.

Several hat section stiffeners have been made by this process for the root end joint test program.

The female tool approach is illustrated in Figure 67. This approach utilizes three tools: male layup block, female tool block and an expandable rubber mandrel.

In this approach, the prepreg segment ply layups are first assembled on the male tool layup block. It is then transferred into the female base tool block where the molded rubber mandrel is inserted into the tool. In order to control the resin bleed out, metal bleeder tubes are molded in the rubber mandrel. These are readily removed after each cure cycle and are heat cleaned.

The thermal expanding rubber mandrel will provide uniform pressure distribution on the laminate surface, and this process should improve the dimensional repeatability of the sectional shape. In addition, this female mold process requires one autoclave cure cycle to fabricate the stiffener.

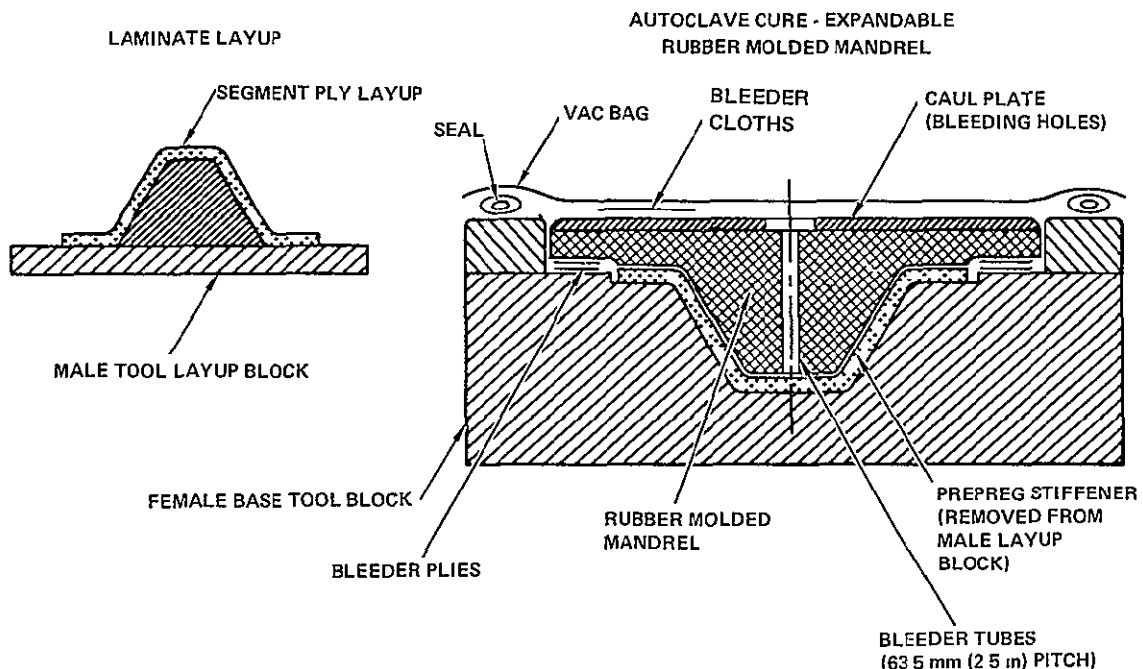


Figure 67. Hat Section Stiffened Skin Cover - Female Tool Concept



RI/LAAD has utilized this rubber mandrel process approach to fabricate the sine wave spars and ribs for the B-1 vertical stabilizer.

The hat section configuration has good potential for the pultrusion process to reduce the fabrication cost. It is a simpler configuration to pultrude than either the A-frame and/or I-beam section stiffener. An IRAD program has been initiated to develop the pultrusion concept using prepreg material plus microwave curing.

#### 4.1.1.5 Hat Section Stiffened Skin Cover - Root End Flare Out

Three flare out configuration approaches have been proposed for the hat section stiffener joint termination. These are shown in Figure 68 as: molded transition, machined run out, and secondary bonded reinforcement.

The molded transition configuration has been selected to be used to develop a fabrication process. The flare out transition shape has been modified to facilitate the layup and drape of material with a minimum of

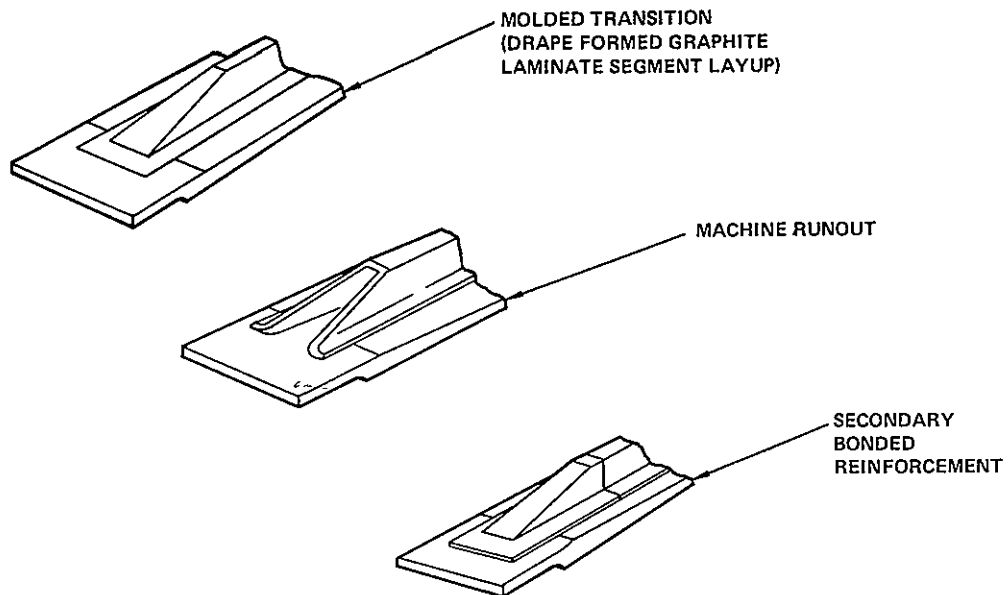


Figure 68. Hat Section Stiffened Skin Cover - Root End Flare Out

fiber disorientation by placing the  $0^\circ$  ply between the  $\pm 45^\circ$  plies in the segment laminate layups. This has resolved the  $0^\circ$  ply disorientation and separation during layup. Also, the use of a heat air gun during the segment ply layup in the transition area has resolved the problem of fiber wrinkling and disorientation by softening the resin as the fibers are ironed onto the compound contour.

A successful hat section molded transition specimen has been fabricated by this process procedure and was utilized for the fuselage joint test.

The machine runout and secondary bonded reinforcement flare out configurations have not been developed because of structural and weight considerations.

#### 4.1.1.6 Honeycomb Skin Cover - Continuous Core

The fabrication approach to this honeycomb skin cover design concept is to use a female bonding fixture tool containing alignment jigs for the root insert as shown in Figure 69. The female tool surface is used to layup the skin surface panels.

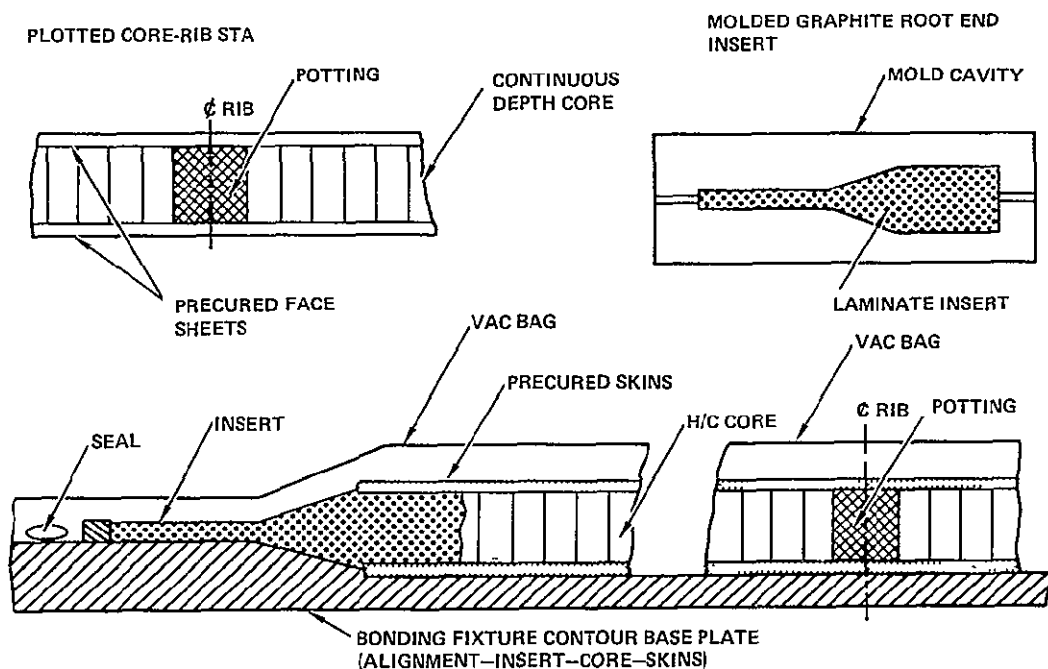


Figure 69. Honeycomb Skin Cover - Continuous Core

The skin panels are precured and adhesive bonded to the fiberglass honeycomb core and the root end insert. The insert is made in a separate mold tool by compacting the graphite prepreg into the mold and curing in an autoclave and/or a large heated platen press.

Potting at the rib stations for fastener attachments is precured in place prior to the bonding of the face skins. Also, the periphery tapered honeycomb core edges of the skin cover are closed off using prepreg doublers cocured to the face skins and the core during the bonding cycle.

There are several problems associated with this fabrication approach that need careful attention. The honeycomb core will require close tolerance machining 0.122 mm (+ .005 in.) for mating to the root end insert. The molding of the root end insert requires a precision mold tool to achieve close tolerance thickness control. An alternate would be to mold and then finish machine to the dimensions required, which involves an expensive extra operation.

At the rib stations, an expanding type of potting compound that expands and cures during the bonding cycle is used. This process requires development to prevent over or under expansion which can lead to porous potted areas and/or skin disbond.

#### 4.1.1.7 Honeycomb Skin Cover - Runout at Rib Station

The tooling and fabrication approach for panels with runouts at the ribs is the same as for the continuous core honeycomb skin cover and root end insert. At the periphery tapered core edges and at the rib station runouts, prepreg doublers that are cocured during the bonding cycle are used. (See Figure 70.)

One of the problems associated with this approach is that the tapered runouts at the rib stations under autoclave pressure 586 to 690 kPa (85 to 100 psi) may cause the edge core to collapse if a 30° slope or less is not maintained. This also holds true for the skin edge periphery honeycomb core slope.

If the 30° slope is not feasible, an alternate method is to pot all tapered edges to prevent core collapse. This method results in a considerable weight increase.

The problems, solutions, and development that have been discussed in the honeycomb skin cover concepts shown in Figures 69 and 70 have evolved

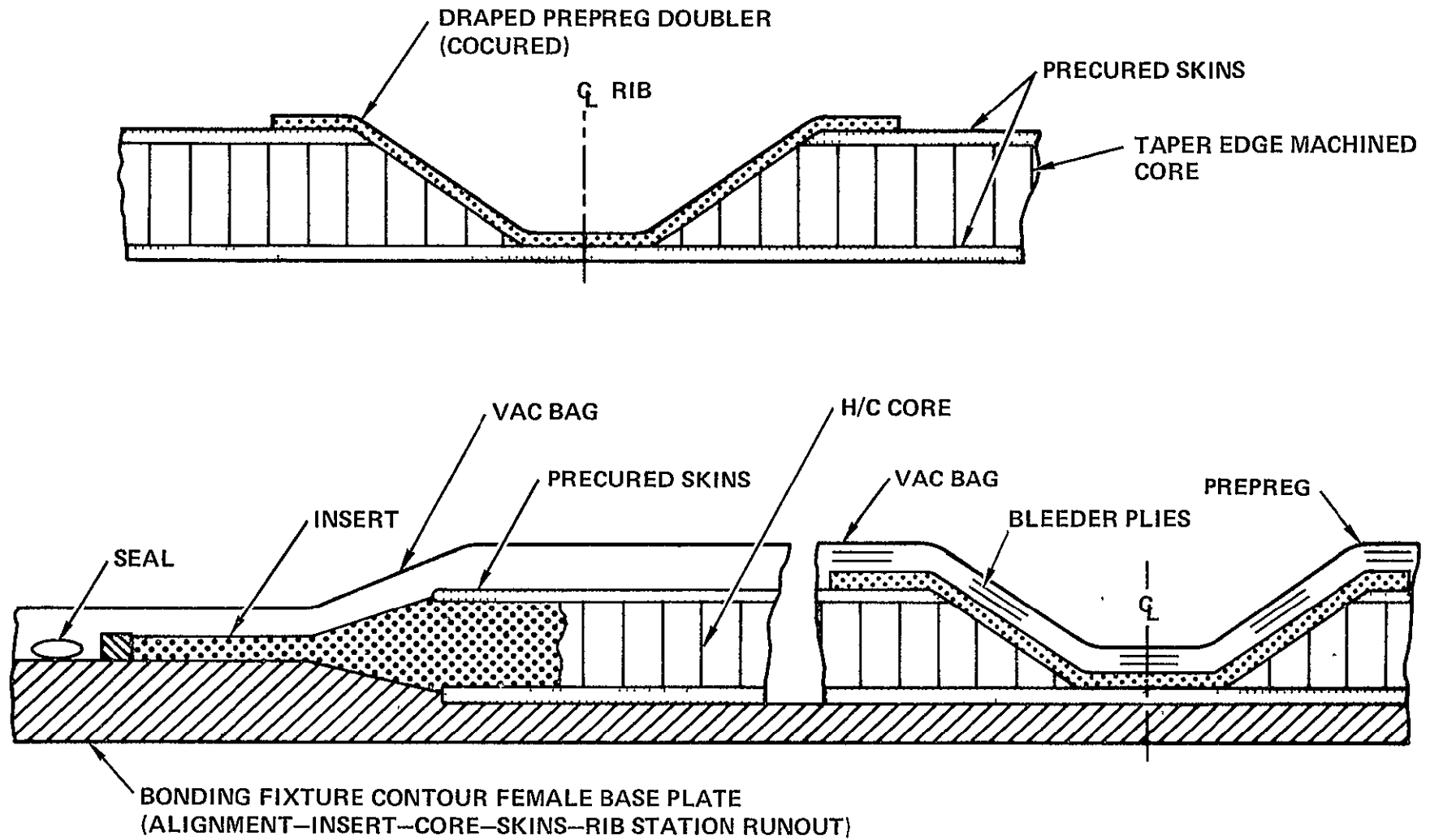


Figure 70. Honeycomb Skin Cover - Runout at Rib Station

from the experience obtained during tooling and the fabrication of the P-3 composite sandwich floor beams, L-1011 spoiler, and the L-1011 aileron skin panel.

#### 4.1.2 Spar Concepts

From manufacturing producibility considerations, both front and rear spars will be cocured as integral spar assemblies using the thermal expandable elastomeric mold process. The tool complexity is essentially the same for the various spar configurations investigated in the design concept studies. Tooling costs do not influence concept selection.

#### 4.1.3 Rib Concepts

The fabrication approach for the internal truss rib caps and miniwich ribs is a springboard from the B-1 vertical stabilizer practices which use castable ceramic cauls, silicone rubber layup/pressure members, and positive autoclave pressure control. Prepreg developed blanks will be tape machine layups. These blanks will be prebled and the patterns of the rib configurations cut out from the blanks. The various rib designs are the product of close design/manufacturing interface to ensure producibility, low cost, and low risk. The low part-count principle is reflected in integral fabrication approaches for truss rib caps and miniwich ribs. The Rockwell 305mm (12-inch) tape-laying machine will be used for rib fabrication. To avoid wrinkling problems prebleeding practices are to be employed.

##### 4.1.3.1 Baseline Tooling Concept for Miniwich Ribs

The integral cocure fabrication approach for the miniwich ribs utilizing the picture frame holding tool is shown in Figure 71. Stiffened webs were originally conceived as integrally stiffened details fabricated in press by expanding rubber process against controlled pressure. Stiffeners will probably change to secondarily attached details for reasons of cost and logistics interference of other program requirements for press usage.

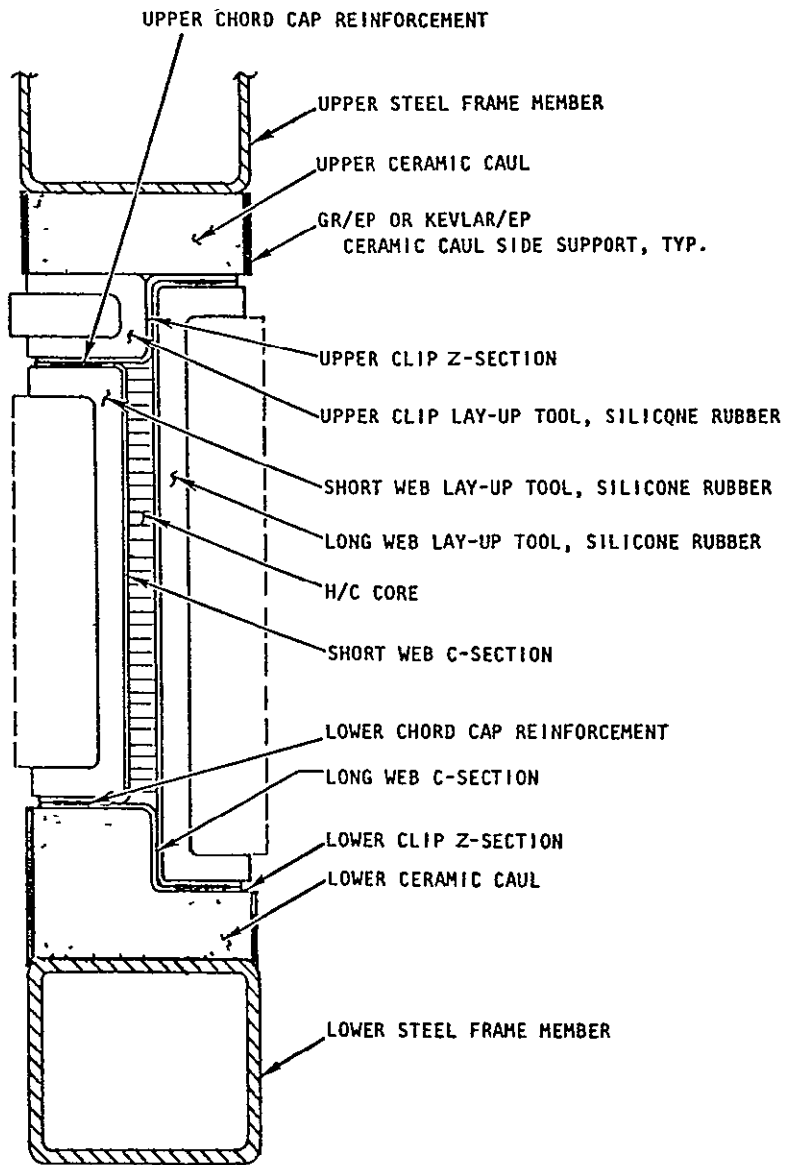


Figure 71. Baseline Tooling Concept-Miniwich Ribs

#### 4.1.3.2 Baseplate Tooling Concept for Truss Rib Caps

The baseplate approach considered is presently preferable for truss rib caps (see Figure 72) and is lower in cost than the picture frame holding tool shown in Figure 71. Since the holding of total rib depth dimension tolerances is not required for truss rib caps, the upper and lower rib caps are to be fabricated simultaneously. The typical process plan is described as follows:

##### Composite cap details.-

- Machine lay multiply blanks
- Stack/debulk/prebleed
- Stamp out required patterns
- Assemble prepreg details on respective tool members
- Bag and cure
- Trim with aid of overpress templates

##### Cruciform aluminum diagonals.-

- Machine upper and lower standing legs
- Burr
- Clean and anodize

##### Assembly.-

- Locate and cleco assemble rib caps and diagonals
- Drill, ream, and radius prep for fasteners
- Burr
- Apply sealant
- Install fasteners wet
- Clean and identify
- Weigh assembled part
- Final inspection
- Package and ship

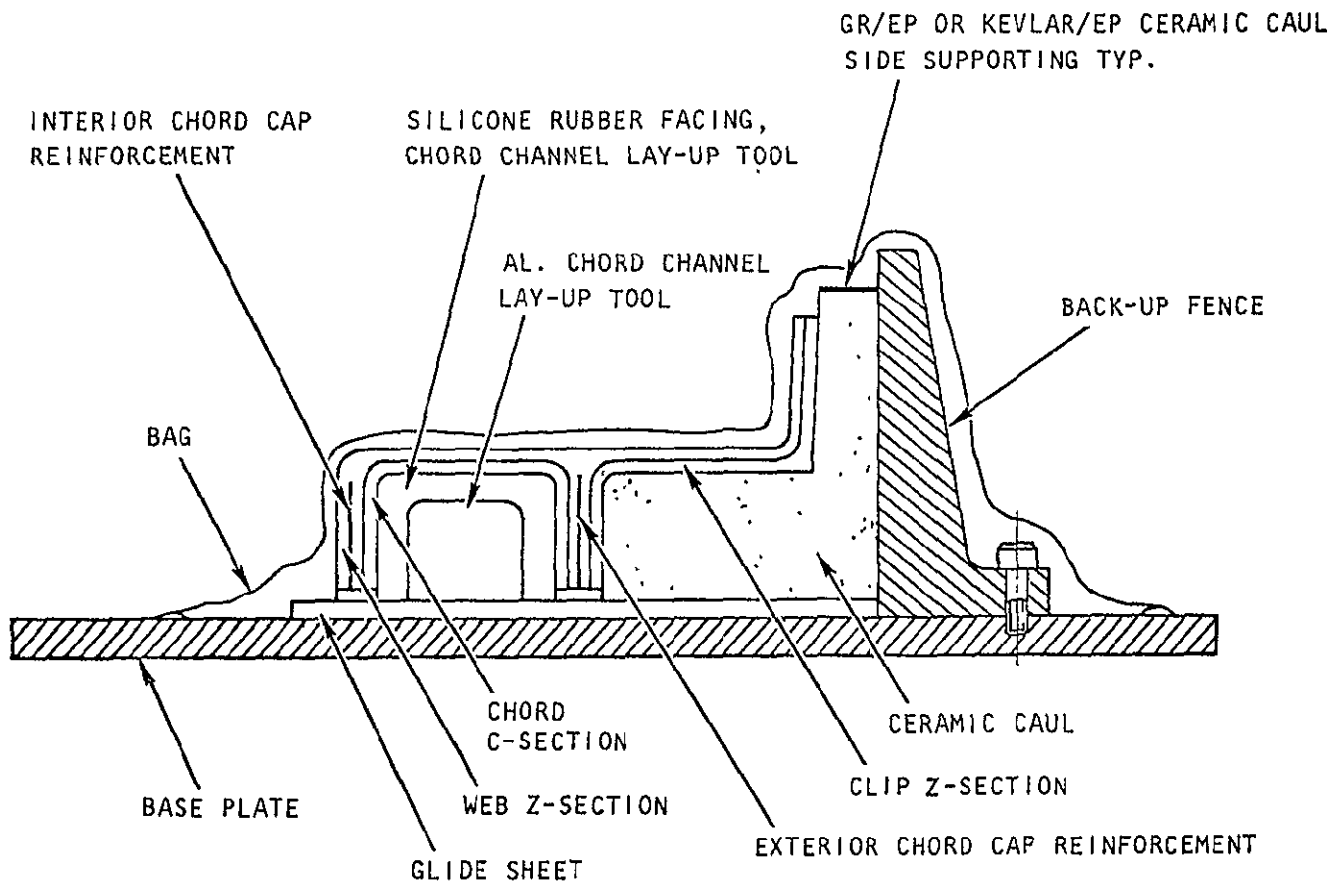


Figure 72. Baseplate Tooling Concept-Truss Rib Caps



#### 4.1.3.3 Producibility Rating, Rib Configurations

Producibility ratings are based on best current judgments. Access considerations played a major role in arriving at judgments.

Ratings shown in Table 34 are stated for the producibility aspects only. These do not include cost and accessibility aspects which should also enter into the final choice.

It was determined at that time that overall, the miniwich rib without access holes was the lowest cost design. However, this design concept was not viable for the first six ribs because of accessibility requirements, so the truss rib aluminum diagonals were recommended.

The manufacturing cost estimates for rib VSS 145.71 shown in Table 35 are based on a quantity of ten ribs. The data listed in the column (titled Previous Estimate) was based on the initial trade studies. The data in the column (titled Present Estimate) is data that was developed during Phase I.

### 4.2 PRELIMINARY FABRICATION PLANS

The producibility considerations have already played a key role in the selection of design concepts with potential for low cost. The basic features of the preliminary fabrication plans are:

- Simplicity in fabrication is a major objective for achieving low cost, using advanced manufacturing methods such as net molding to size, draping, forming broadgoods, and cocuring components.
- Broadgoods dispensing machines will be used for the rapid layup of covers and spars using unidirectional and bidirectional prepreg materials in widths ranging from 305 mm to 610 mm (24 inches to 42 inches). Semiautomatic tape laying machines will be used for the layup of laminates for ribs.
- Existing large autoclaves and shop facilities are to be fully exploited.

#### 4.2.1 Skin Covers

The fabrication plan for the skin covers (Figure 73) includes the use of a broadgoods dispensing machine to layup wide prepreg plies. The prepreg and wire mesh screen is laid up on the female contoured bond fixture. Incremental plies for reinforcing pads and other elements are laid up in a similar manner and cut to shape. The cover elements are assembled on the bond fixture, debulked, and autoclave cured. Dimensional thickness control of the peripheral lands and rib stations of the covers will be facilitated by use of interface surface caul plates, bleeder systems, and cure cycle pressure envelopes.

TABLE 34. PRODUCIBILITY RATING, RIB CONFIGURATIONS

Rib Configuration	Complexity	Inspect-ability	Repair-ability	Maintain-ability
Truss, aluminum diagonals	2	1	2	2
Miniwich w/o access hole	2	3	2	3
Miniwich w/ access hole	3	3	2	3
Stiffened web w/o access hole	3	3	2	2
Stiffened web w/ access hole	4	2	3	2
1 - Highest				

TABLE 35. MANUFACTURING ESTIMATES, RIB VSS 145.71 (10 RIBS)

Rib Configuration	Labor Hours <sup>(1)</sup>	
	Previous Estimate	Present Estimate
Truss, aluminum diagonals	59.1	63.7
Miniwich w/o access hole	38.24	52
Miniwich w/ access hole	-	111.15
Stiffened web w/o access hole	103.3	110.3
Stiffened web w/ access hole	-	165.5
1) Includes 15% Manufacturing Engineering Planning, Scheduling, and Order Release Support, and 15% Q&RA		

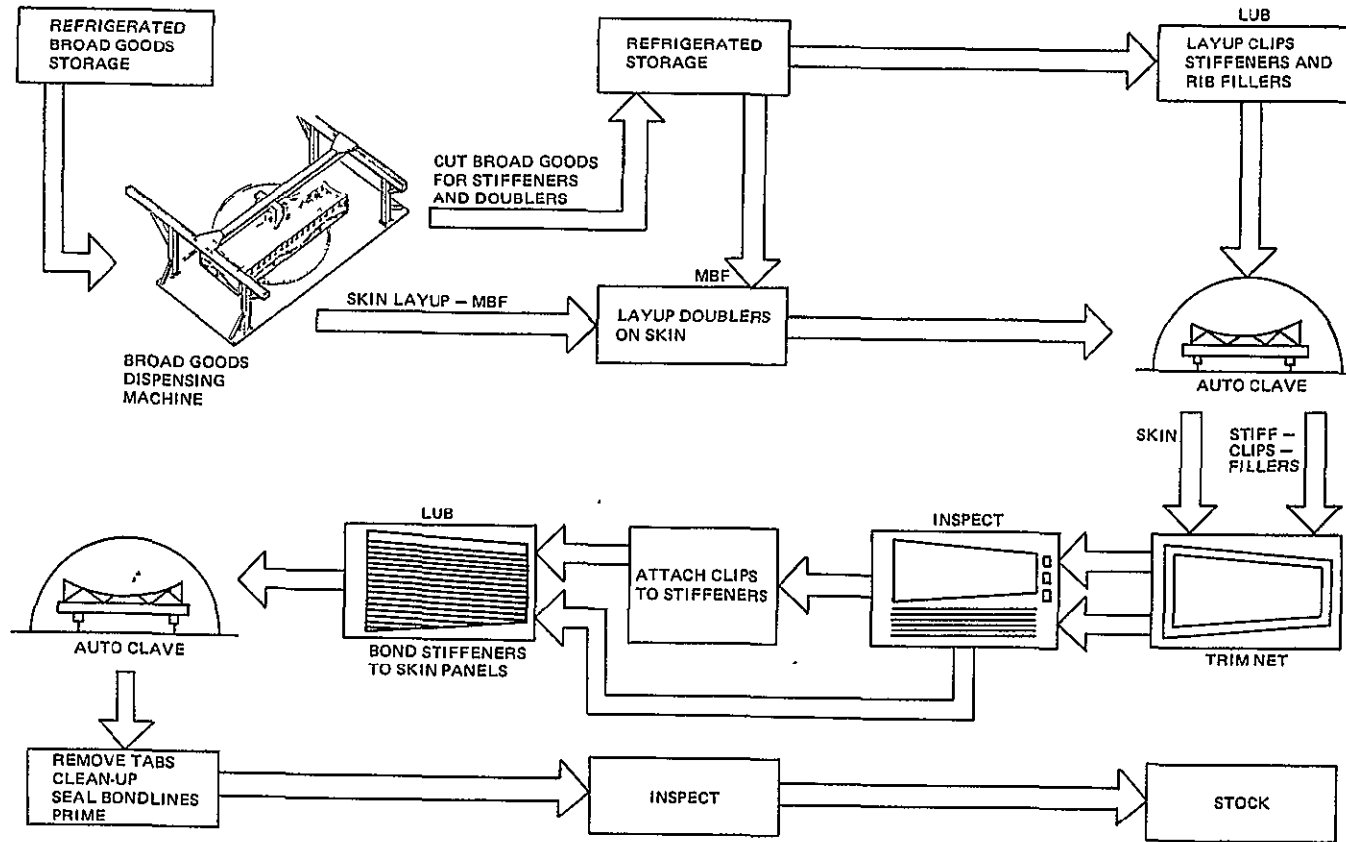


Figure 73. Cover Fabrication

#### 4.2.2 Spars and Ribs

Fabrication Flow Chart plans for the spars and truss ribs are shown in Figures 74 and 75 respectively. Female tools will be used to achieve assembly tolerance requirements. Most of the development effort on the elastomeric molding process for spars and ribs has been accomplished under IRAD and Air Force Contract studies. The main development effort in Phase II will be the application of this process to long parts. The thermal mismatch of the tooling and the composite part will be compensated for dimensionally in tool design.

#### 4.3 ASSEMBLY

Assembly costs for the composite box are projected to be considerably lower than those for the metal box. As assembly is the largest single item in manufacturing labor cost, it is a prime concern in developing the structural concepts.

The major assembly sequence for the box is shown in Figure 76. The substructure is drilled, and mechanically fastened in the assembly fixture. The covers are then located, drilled, and mechanically fastened. Accessibility for the assembly of the last cover is achieved through multiple hand holes in the spars and through the large truss ribs. To preclude corrosion, the primary fastener will be titanium (6 AL-4V) alloy Hi-Tigue with A286 steel collars. The straight-shank, close-tolerance fasteners will be installed in close-fitting holes tentatively with  $-.0254$  mm to  $+.0762$  mm ( $-0.001$  to  $+0.003$  in.) tolerance range. All joints will use faying-surface sealant and fasteners will be installed wet. A Lockheed IRAD program has evaluated a variety of fasteners installed in graphite/epoxy laminated plates for corrosion resistance. When subjected to a salt-water test titanium fasteners show excellent corrosion resistance.

Preset power feed and speed Quackenbush or Spacematic drilling motors with carbide drills such as Metal Removal master carbide drill B-t point and carbide and/or diamond coated pilot countersinks and/or combination carbide drills will be used. These precision drills eliminate reaming operations and reduce assembly costs. Backup blocks will be used to prevent delamination.

#### 4.4 TEST SPECIMEN FABRICATION

##### 4.4.1 Skin Covers

###### 4.4.1.1 Hat Stiffener Root End Joint T300/934 Resin System

Two main problems were involved in developing successful hat stiffened test specimens: (1) determining a suitable shape configuration for the stiffener area incorporating transitions from a hat section shape to the

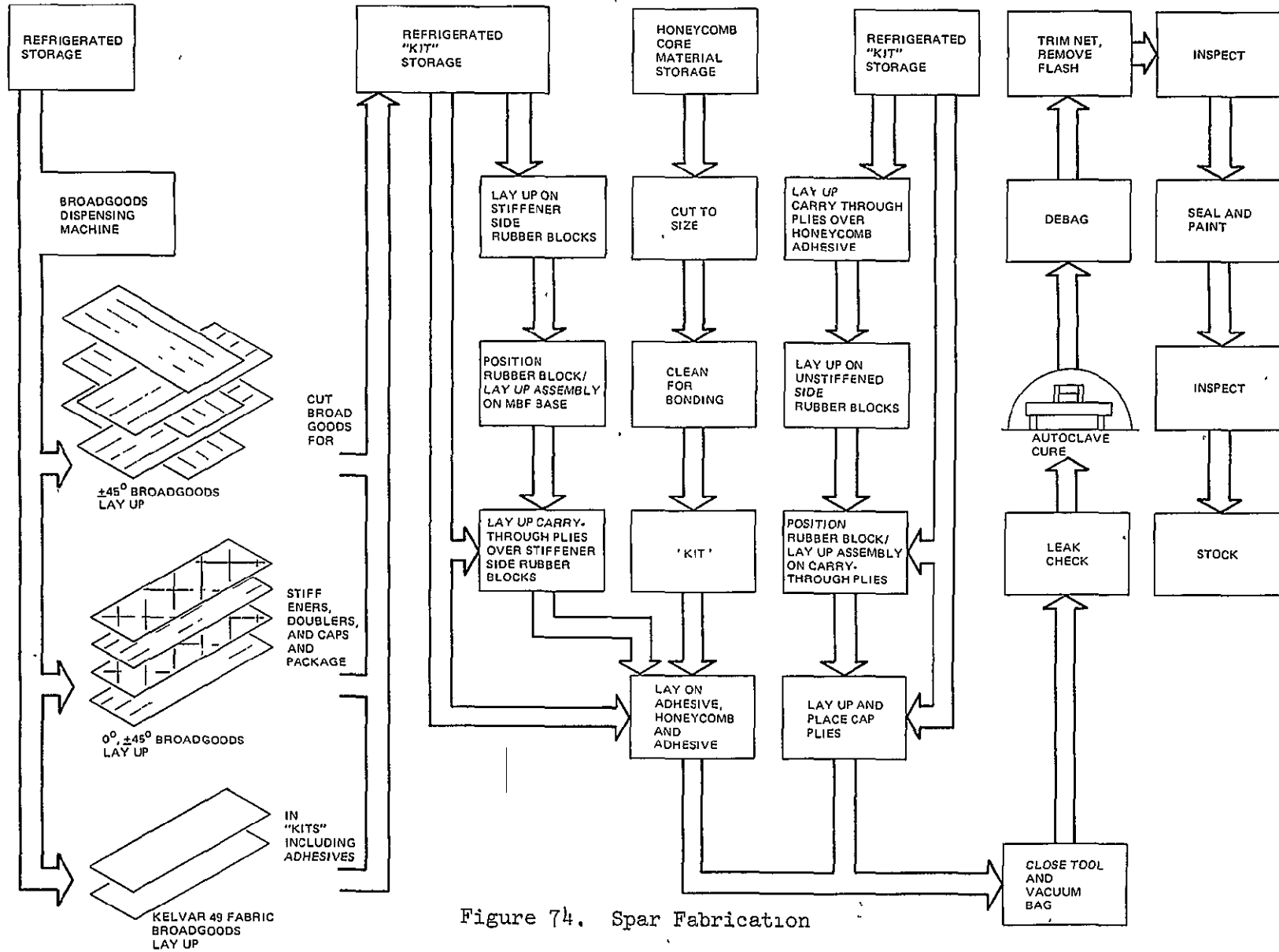


Figure 74. Spar Fabrication

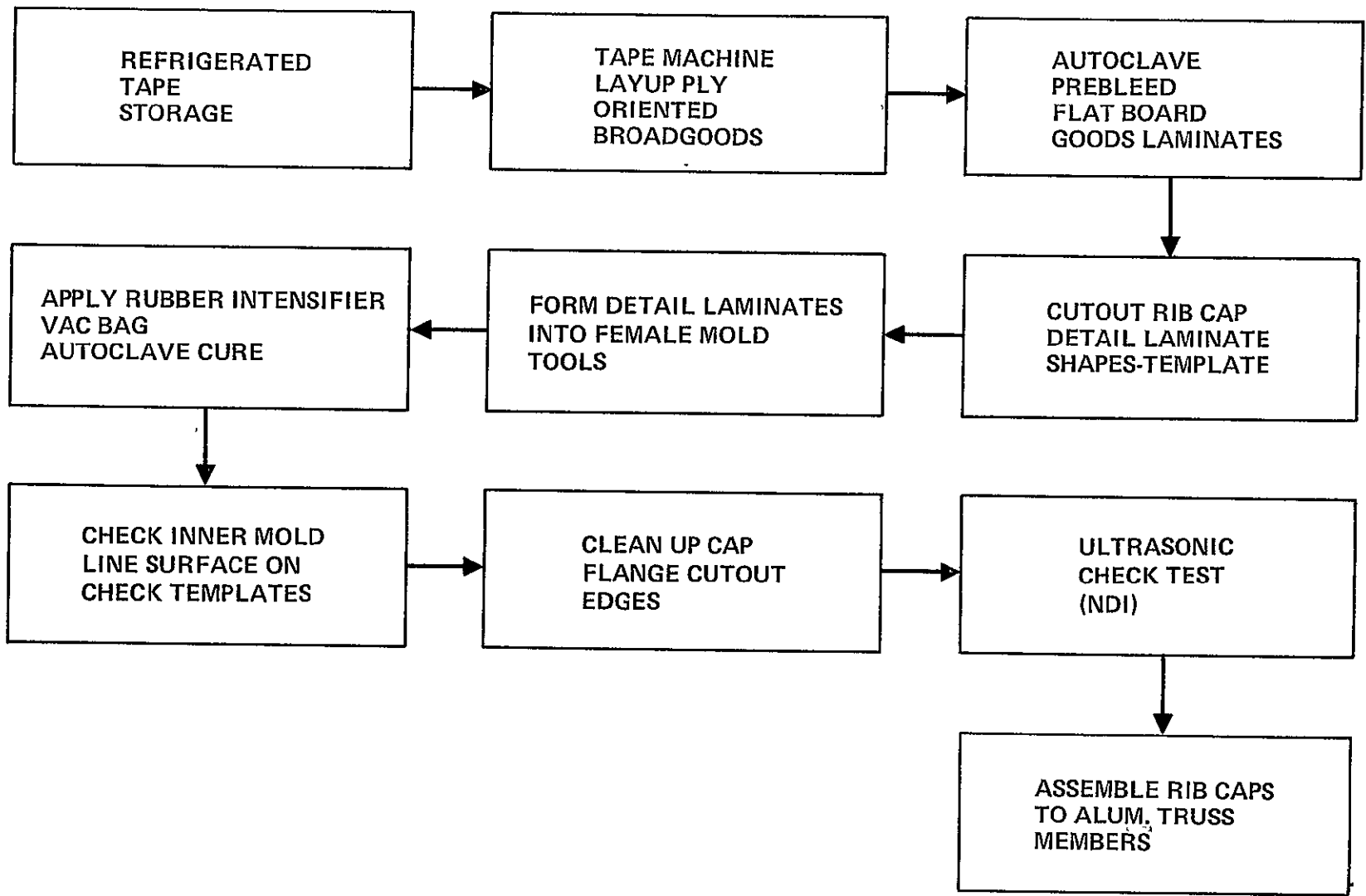


Figure 75. Truss Rib Cap/Clip Fabrication

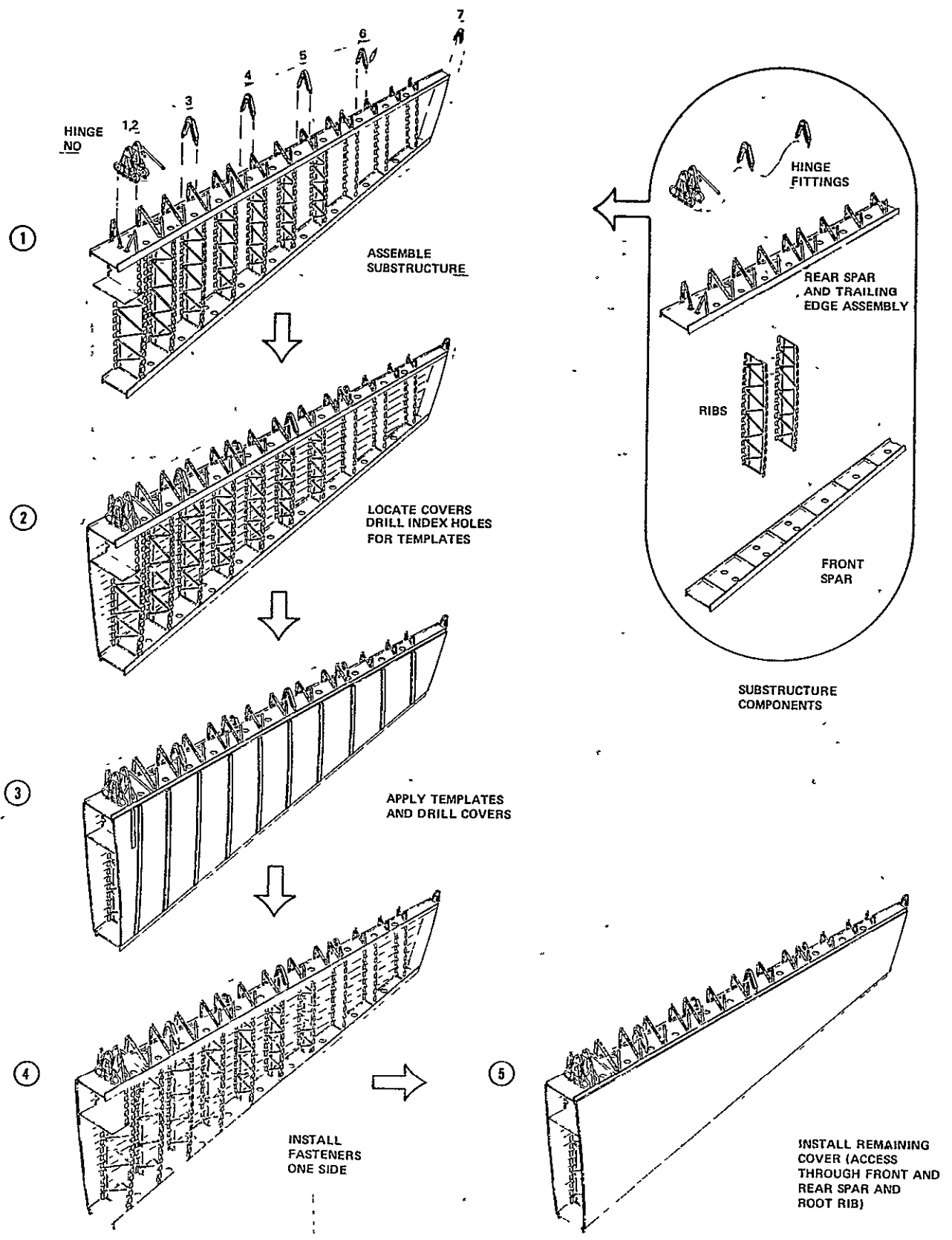


Figure 76. Composite Vertical Fin Box Assembly Sequence

flared end of the hat, since a smoothly faired shape was required to provide a wrinkle-free part with minimum distortion of fiber direction; (2) determining a suitable fabrication method to maintain uniform cross-sectional thickness and the related fiber-resin ratio as specified for the hat stiffener. The dimensional control problem arises primarily because of excess resin in the prepreg tape (approximately 40 percent by weight) which must be bled out of the laminated part during the molding process to provide a resin content below 30 percent by weight. Methods were required for two material systems, T300/934 (450K) (350°F cure) and T300/5209 (400K) (260°F cure).

The basic tools were designed and fabricated to make the hat stiffened test specimens. They are identified as listed below and are shown in Figure 77.

<u>Tool No.</u>	<u>Description</u>
C-2-75-T1	Hat Stiffener Mold
C-2-75-T2	Skin Mold
C-2-75-T3	Bonding Fixture
C-2-75-T5	Formed Silicone Rubber Pressure Bag

The hat stiffener mold was made from mahogany fastened to a base plate of aluminum. Mahogany was used to facilitate reworking of the mold shape as development progressed.

It was determined at an early stage of development that laminated parts made by the conventional bag molding process must be prebled and compacted prior to final cure in order to achieve adequate control of laminate thickness and the specified fiber-resin ratio in the end product. The fabrication processes developed to fabricate a successful test article are briefly described below. These processes will serve as the basis for full scale production development of the hat section stiffener.

The hat section stiffener was laid up in three stages. The part incorporates 10 plies of graphite in rib and flange areas and 20 plies in the cap area. Three flat laminates were prepared. Two laminates incorporating 5 plies each and one laminate consisting of 10 plies for the cap area were made. These multiple-ply lay-ups were then draped over the mold to form the complete laminate as specified. A heat gun assist was required in the transition area.

The laminate was then prebled and compacted using the following method: Bleeder material - Mockburg paper; Bleeder ratio - 1 ply Mockburg to 4 plies graphite. The bleeding heat and pressure cycle consisted of heating to 366K (200°F) at 3.3 to 5.5K (6° to 10°F) per minute under a pressure of



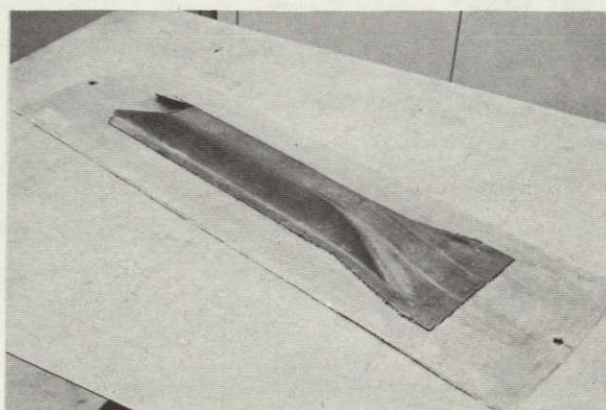
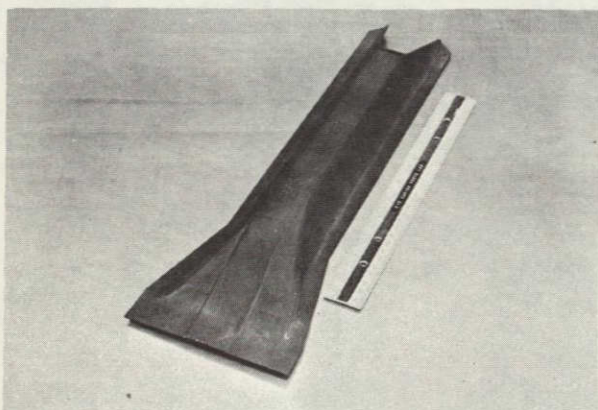
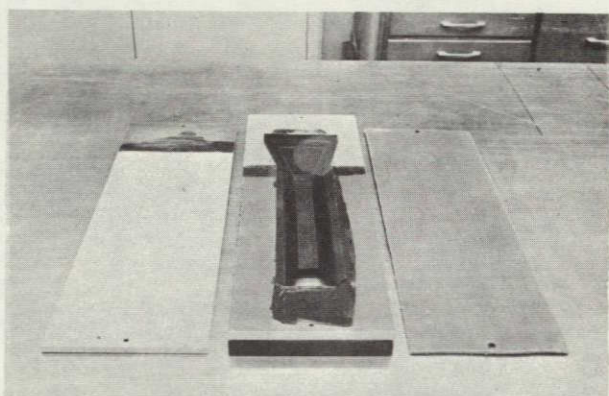
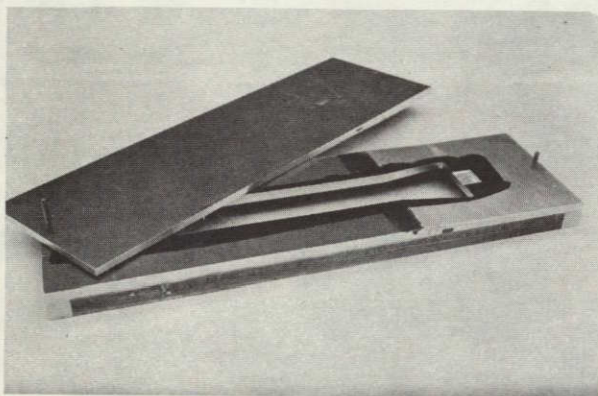
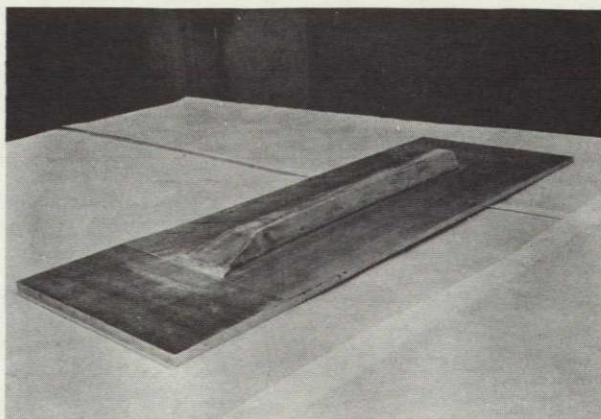
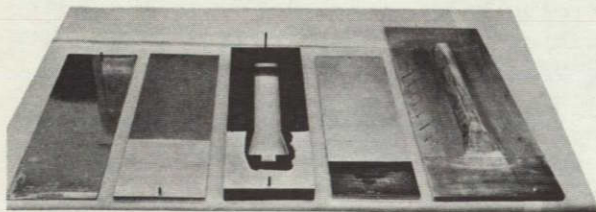


Figure 77. Hat Stiffener Tooling

full vacuum plus 70.0 kPa (10 psi). The part was held between 366K (200°F) and 378K (220°F) for 15 minutes under pressure, and was then rapidly cooled under pressure to 389K (150°F).

The final cure was accomplished with a precision formed silicon rubber bag and no bleeder using the following cycle:

- Apply full vacuum and heat to 394K (250°F) at 2.2-3.3K (4-6°F) per minute.
- At 394K (250°F), apply 690 kPa (100 psi) pressure and hold for 30 minutes.
- Heat to 450K (350°F) at 2.2-3.3K (4-6°F) per minute and hold for 2 hours.
- Cool under pressure to 339K (150°F).

The laminated part fabricated by the above method did not vary over  $\pm 0.127$  mm ( $\pm 0.005$  in.) from average thickness of each segment and resin content ranged from 30 to 33 by weight percent. The test part skin material consisting primarily of Kevlar 49, 281 fabric was laminated by the conventional bag molding method. A small amount of resin was bled from the part to assure removal of air.

The hat stiffener was then bonded to the skin using FML37 epoxy adhesive film, 2.87 kPa (0.06 lb/ft<sup>2</sup>), and BR123 epoxy primer on faying surfaces. Bonding was done at 345 kPa (50 psi) bondline pressure and 394K (250°F) temperatures for one hour.

The assembled part met design load requirements when tested as described elsewhere in this report. The part in various fabrication stages and the completed assembly are shown in Figure 77.

#### 4.4.1.2 Hat Stiffener Root End Joint T300/5209 Resin System

The tooling used to fabricate this specimen was basically the same as that used for the T300/934 specimen fabricated during the first quarter. The type of bleeder used, prebleeding heat and pressure cycle, and the final cure cycle were necessarily different because of the lower cure temperature of the 5209 resin, 400K (260°F). These processes are described below for the hat section and skin components of the test specimen.

The hat section laminate was prebled and compacted using a layup system consisting of porous armalon (teflon-coated glass cloth) placed next to the part, followed by one ply of 120 glass cloth, and then a required number of 181 glass cloth plies. The number of 181 glass cloth plies was determined by requiring 1 ply of 181 for every 2 plies of graphite/epoxy. The bleeding heat and pressure cycle was accomplished in an autoclave with a nylon film pressure bag and is as follows:

- Apply full vacuum plus 586 kPa (85 psi) pressure.
- Heat to  $358 \pm 2.75\text{K}$  ( $185^\circ \pm 5^\circ\text{F}$ ) at 4.95 to 6.05K ( $9^\circ$  to  $11^\circ\text{F}$ ) per minute.
- Hold at 358K ( $185^\circ\text{F}$ ) for 5 minutes.
- Release positive pressure and cool to 339K ( $150^\circ\text{F}$ ) under vacuum pressure only.

Final cure was done in an autoclave with a precision formed silicon rubber bag and no bleeder. The following cycle was used:

- Apply full vacuum plus 586 kPa (85 psi) pressure.
- Heat to 400K ( $260^\circ\text{F}$ ) at 2.75-5.5K ( $5^\circ$ - $10^\circ\text{F}$ ) per minute.
- Hold at 400K ( $260^\circ\text{F}$ ) for 15 minutes.
- Cool to 339K ( $150^\circ\text{F}$ ) under pressure.

For the skin component, the graphite portion of this laminate was prebled by using a method identical to that used for the hat section. Prior to final cure, the outer plies of Kevlar 49 281 fabric were prestaged at 366K ( $200^\circ\text{F}$ ) for 10 minutes with no pressure or bleeder. The purpose of this operation was to prevent excessive flow and bleeding of resin in the final cure of the total laminate.

The final cure was accomplished in an autoclave with a nylon film bag and no bleeder by using the same cure cycle as was used for the hat section. The hat stiffener was bonded to the skin with the same bond fixture and adhesive that was used for the T300/934 specimen.

The fabrication of T300/5209 graphite/epoxy sheet laminate requires the use of bleeder plies placed above the prepreg material to absorb the excess resin during the autoclave curing cycle. The customary practice which conforms with the supplier's recommendations is to use approximately one ply of 181 (or 1581) weave glass cloth for each two plies of Narmco T300/5209 prepreg tape in order to provide the proper bleeding action and obtain a finished laminate having the proper resin content and density.

The skin cover structure currently proposed for the L-1011 ACVF utilizes as many as 34 plies of prepreg to obtain approximately 4.76 mm (3/16 in.) thickness in the thickest regions of the root. The thickness is tapered to less than half this value over the span to a minimum of 15 plies by dropping off plies as required. In fabricating such a panel, strict adherence to the 1 to 2 ratio of glass cloth bleeder plies to prepreg plies would require care and

tailoring in production that would increase cost. Questions were therefore raised regarding just how critical is the number of bleeder plies in producing variations in resin content in the finished panel.

Tests were run to determine whether the use of an excess number of bleeder plies resulted in an unacceptable variation in resin content of the finished graphite/epoxy panel representative in thicknesses and layups of the design proposal for the ACVF skin cover. Two test panels each 0.356 by 0.305 m (14 by 12 in.) in size representing, respectively, the ACVF skin thickness and layup at extreme inboard and outboard stations were fabricated. The same number of bleeder plies, namely, the number appropriate for the thicker (inboard) design, was used for both panels. One ply of 120 glass cloth was placed next to the laminate and 17 plies of 121 glass cloth were placed above. The thinner, finer weave 120 cloth provides a smoother finish and is counted as 1/2 bleeder ply.

Other details of the two panels were identical. The prepreg material used in fabrication came from the same roll of tape, and the panels were processed side by side under one vacuum bag in the same autoclave run. Corprene edge dams were utilized around each specimen.

The autoclave cure cycle used for the T300/5209 resin system is as follows:

- Apply full vacuum.
- Heat to 353K (175<sup>o</sup>F) at 2.2-3.3K (4<sup>o</sup>-6<sup>o</sup>F) per minute
- Hold at 353K (175<sup>o</sup>F) for 30 minutes.
- Apply 586-690 kPa (85-100 psi) pressure and vent vacuum bag to air at 138 kPa (20 psi).
- Heat to 400K (260<sup>o</sup>F) at 2.2-3.3K (4<sup>o</sup>-6<sup>o</sup>F) per minute.
- Hold at 400K (260<sup>o</sup>F) for 90 minutes.
- Cool to 333K (140<sup>o</sup>F) under pressure.

Resin content, fiber volume, and density determinations were made on specimens cut from the finished test panels. The characteristics of the two test panels are presented in Table 36.

The results indicated that in the thicknesses and layups tested, the resin content of the finished T300/5209 skin cover panel was not affected by use of bleeder plies of the ratio in excess of one bleeder ply to two plies of prepreg. There apparently was little wicking action in the bleeding process. Out of 17 bleeder plies of 181 glass cloth provided, 16 were saturated in the case of the 34-ply test panel, and 8 in the case of the 15-ply test panel.

TABLE 36. BLEEDER PLY TEST PANEL CHARACTERISTICS

	Panel A	Panel B
Panel Layup	$[(0_2/+45)_4/0]_S$	$[0_2/+45/0/+45/0_{1/2}]_S$
Number of Plies	34	15
Number of Bleeder Plies Used	17-1/2	17-1/2
Number of Bleeder Plies Saturated	16-1/2	8-1/2
Finished Panel Thickness	4.420 mm (0.174 in.)	2.03 mm (0.080 in.)
Average Ply Thickness	0.130 mm (0.0051 in.)	0.15 mm (0.0053 in.)
Resin Content - wt %	27.6	29.7
Density - kg/m <sup>3</sup> - (gm/cc)	1556.0 (1.5660)	1572.9 (1.5729)
Fiber Volume - %	64.5	63.2

## 5.0 TASK 4 - TOOLING DEVELOPMENT

### 5.1 TOOLING CONCEPTS

From the results of the producibility consideration studies and the preliminary manufacturing plans evolved the proposed tooling concepts for the skin covers, spars, ribs and assembly. These tooling concepts are described in the following flow charts illustrating the planned tooling configurations:

#### Skin Covers

- The cover fabrication tool types shown in Figure 78 display the broad goods dispensing machine, mold bond layup fixture, layup blocks (flat and stiffener details), saw and assembly fixtures, and lifting accessors.

- Spars

Spar fabrication tool types are shown in Figure 79. This prescribes the tooling breakdown sequence of the tool base and rubber blocks. Also shown are the materials utilized in the tool and the spar component.

- Figure 80 shows a cross section of the basic tool illustrating the autoclave assist thermal expansion elastomeric tooling for the rubber/steel mandrel segments.

#### Ribs

- Figure 81 depicts the general manufacturing flow and the tooling types at each process station to fabricate the miniwich rib detail. An autoclave assist elastomeric expansion system, as shown in Section A, is utilized to provide the pressure on the laminate during the cure cycle.
- Tooling for the truss rib fabrication is explained in the flow chart Figure 82. Rib cap tabs are precut to contour shape in the flat and finish molded in the female tool.
- The autoclave assist elastomeric expansion system is also used to fab the rib cap details. A rib subassembly fixture is required to install the aluminum extruded cruciform truss members.

#### Assembly - Box Structure

- The existing L-1011 aileron assembly fixture will be modified to receive and locate the composite component segments. One of the important modifications will be to develop the drilling templates to utilize the spacematic machines which have power feed and speeds.

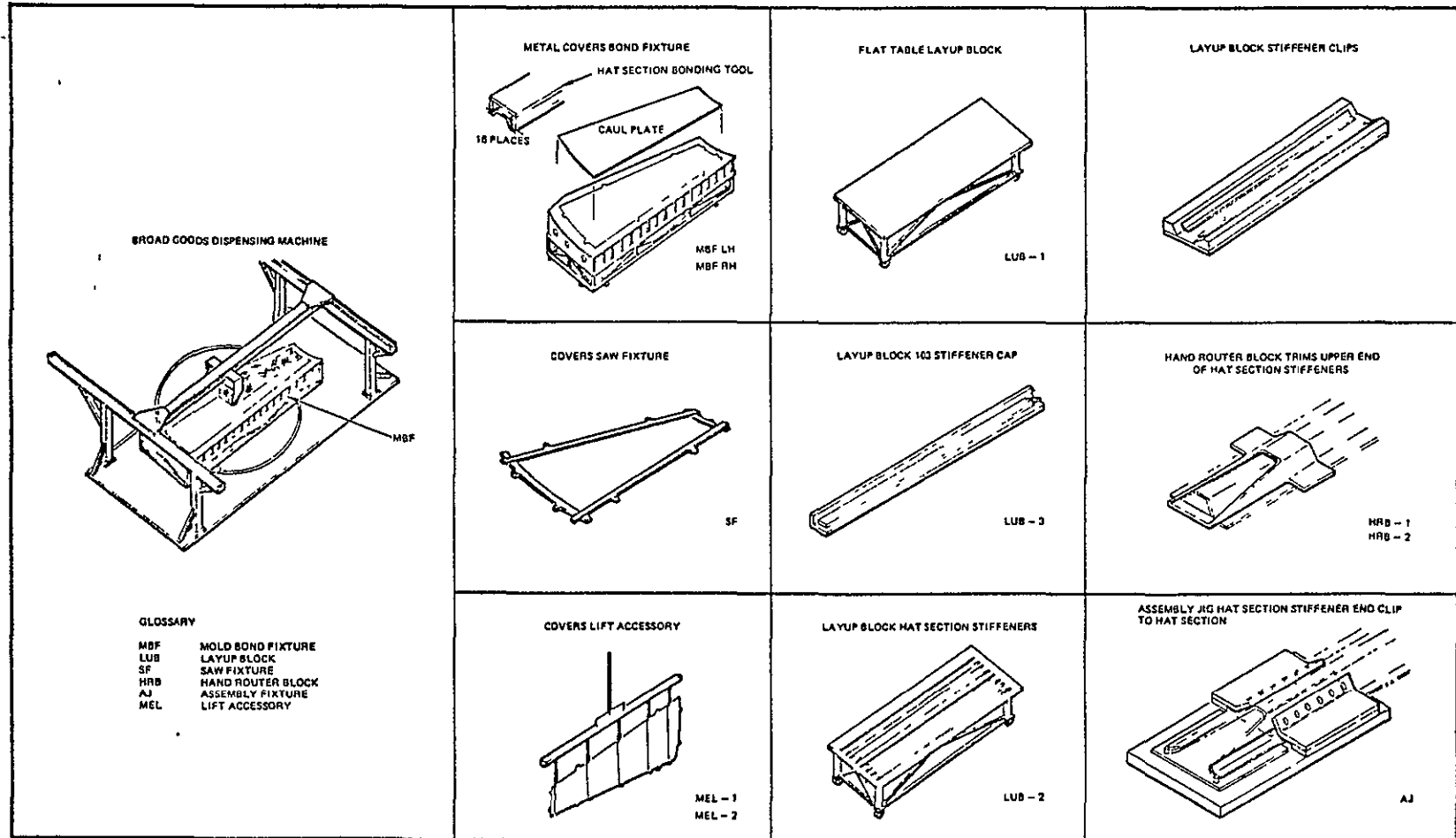


Figure 78. Cover Fabrication Tool Types

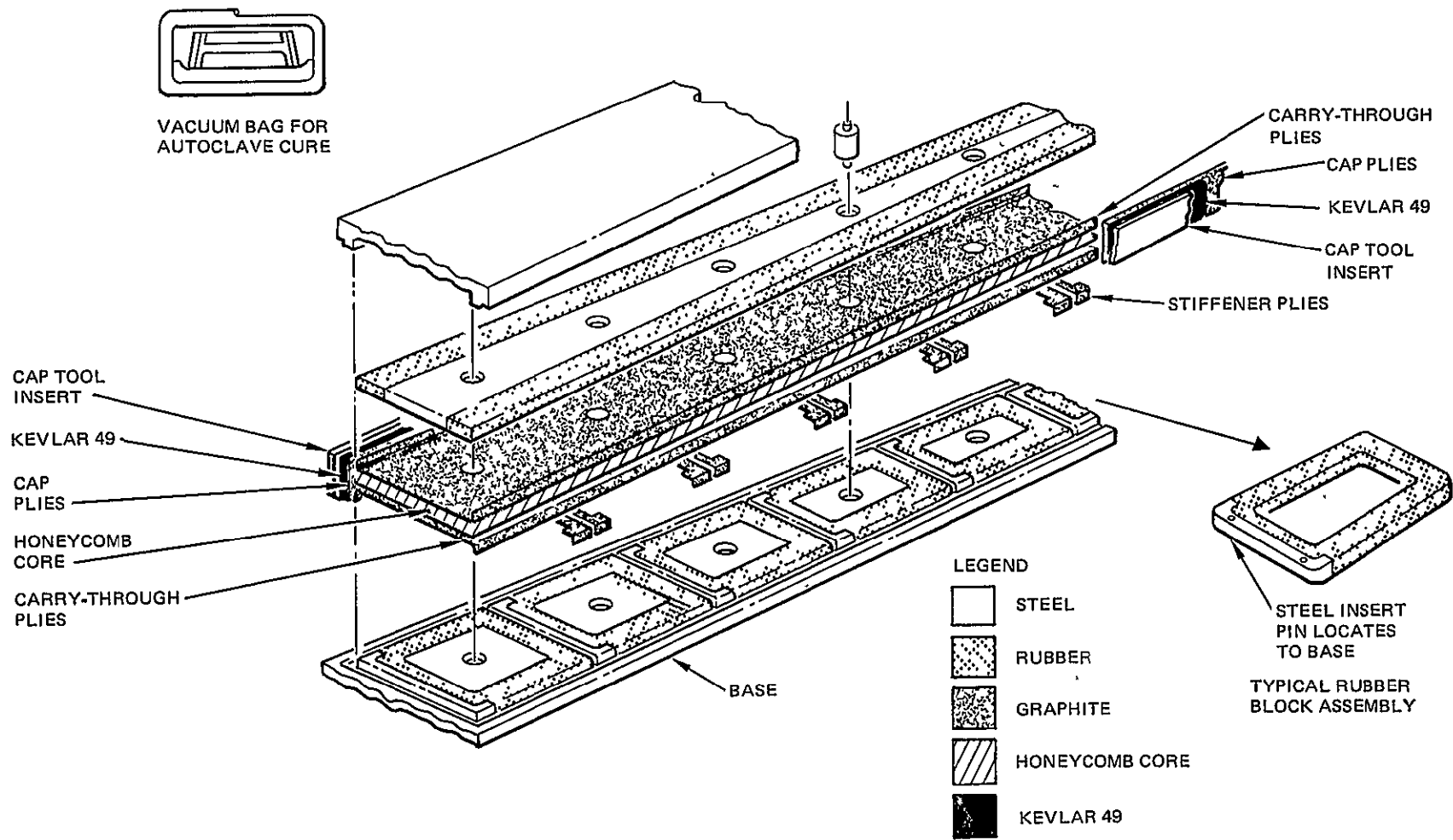


Figure 79. Spar Fabrication Tool Types



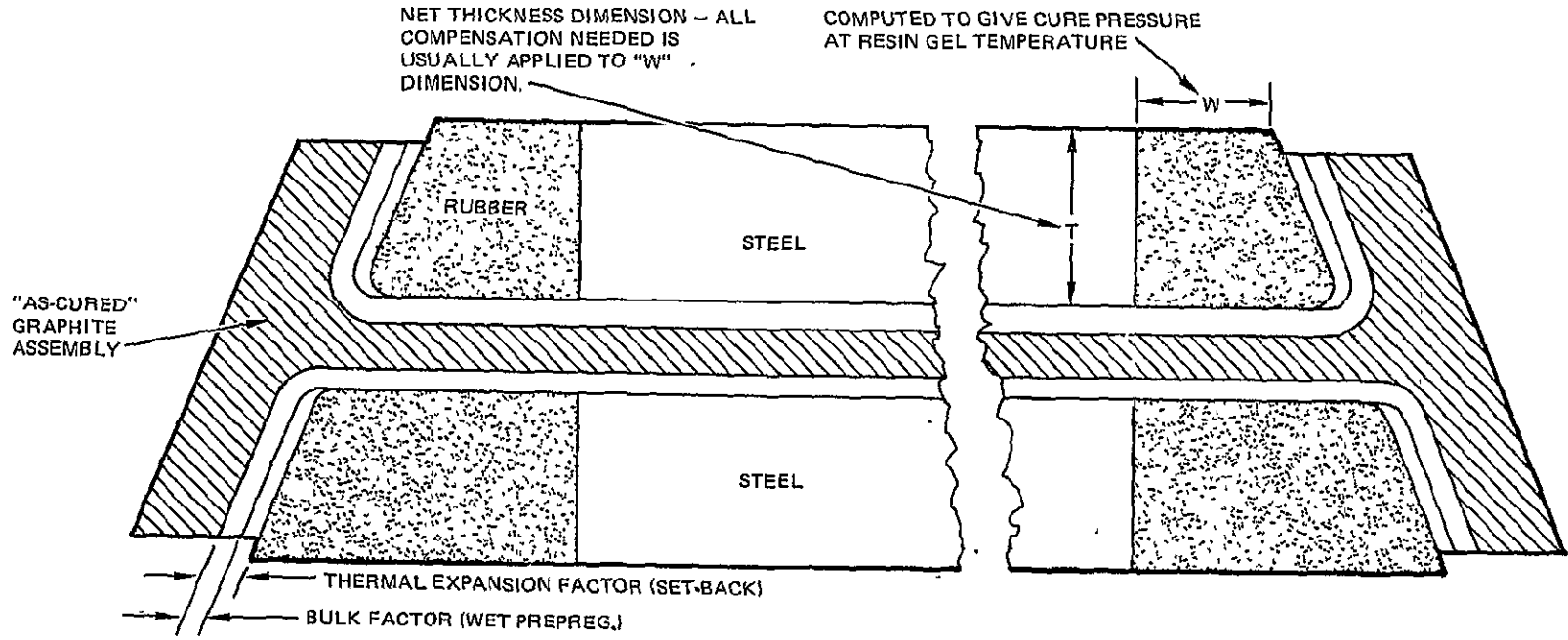


Figure 80. Thermal Expansion of Elastomeric Tooling for Spars

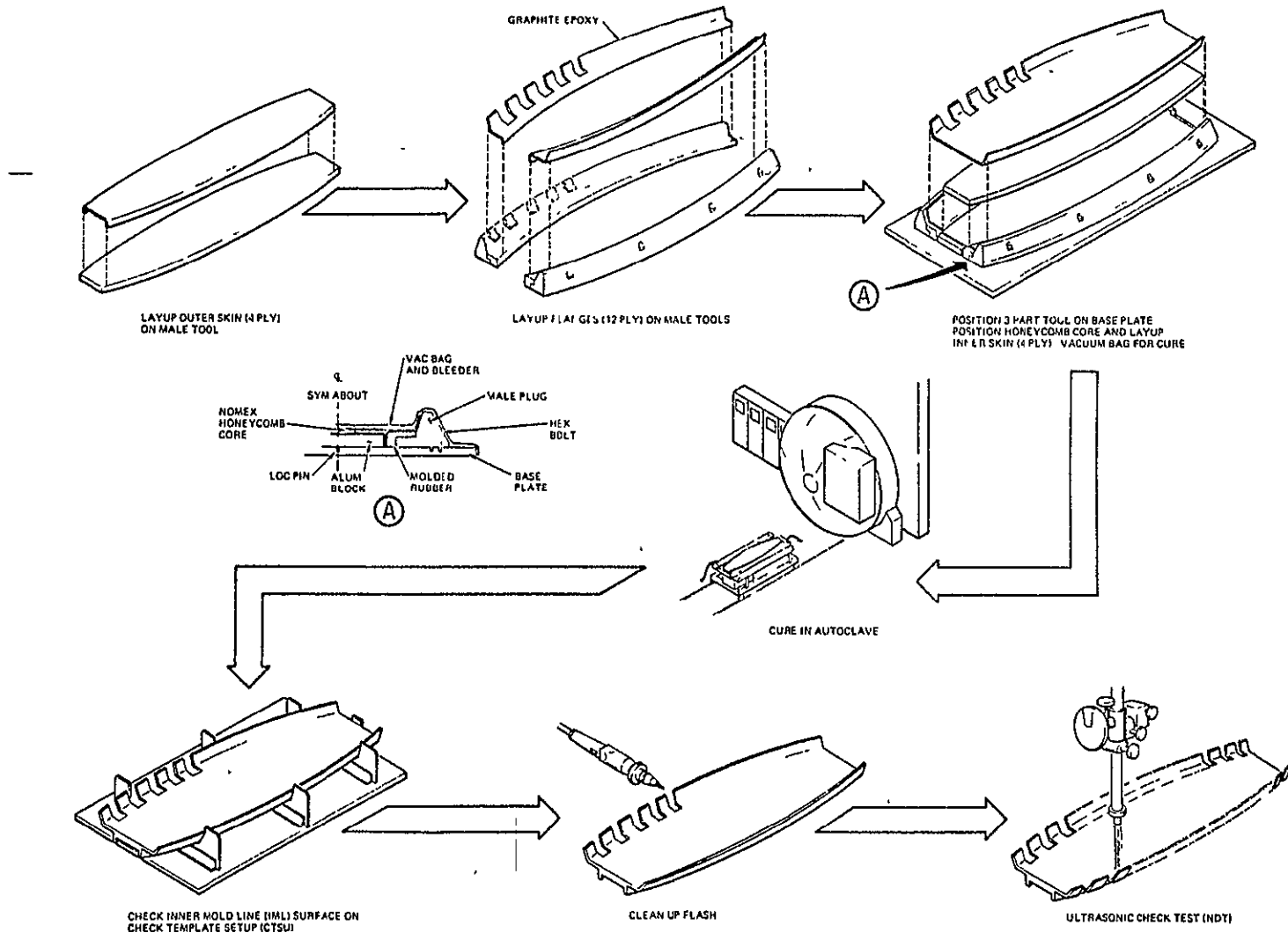


Figure 81. Miniwich Rib Fabrication Tool Types

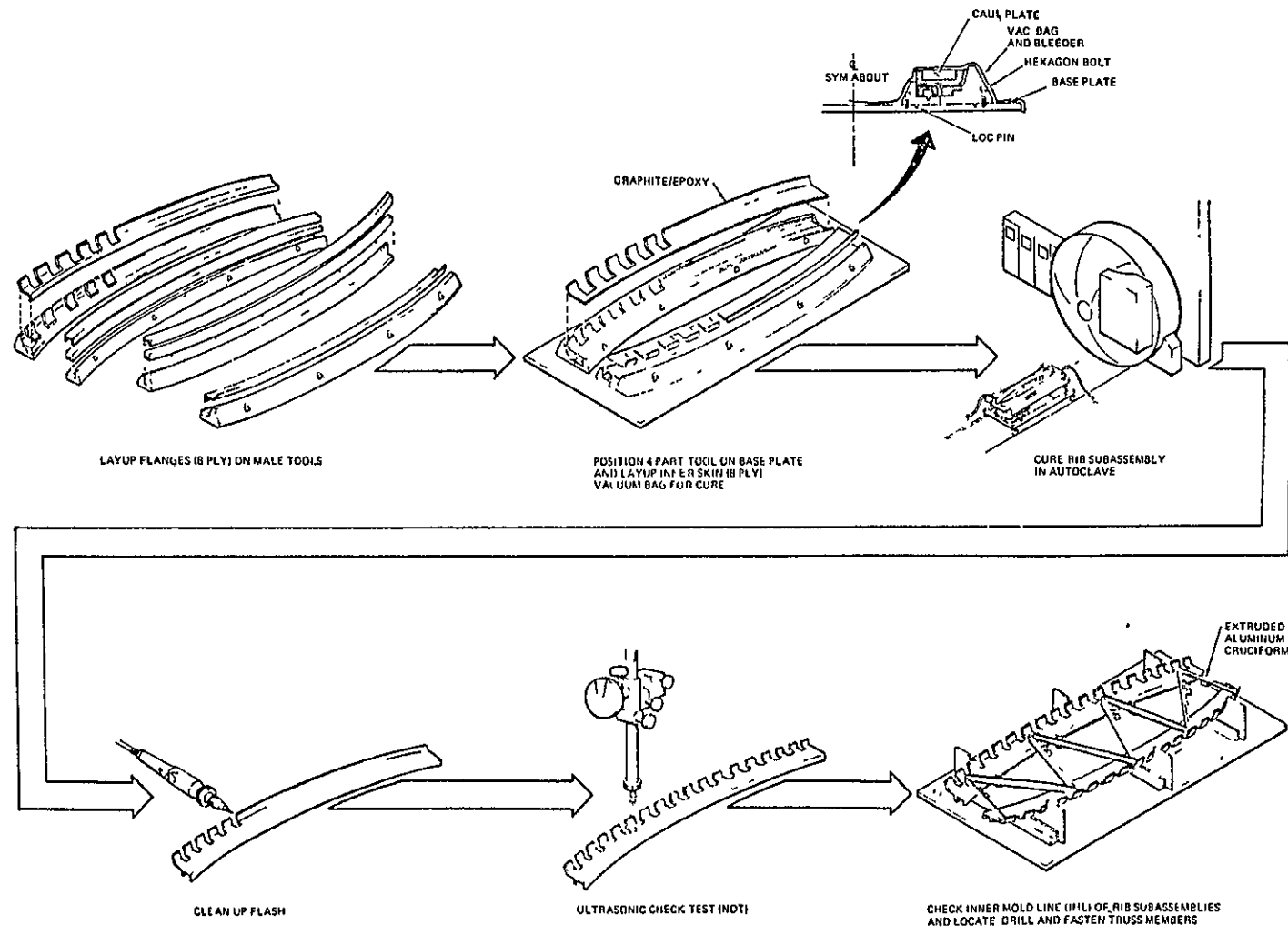


Figure 82. Truss Rib Fabrication Tool Types

This powered drilling method is required to produce close tolerance quality holes in composite materials. Figure 83 shows the changes required in the tooling assembly and the type of spacematic templates for drilling precision holes.

## 5.2 TOOL DESIGN AND FABRICATION

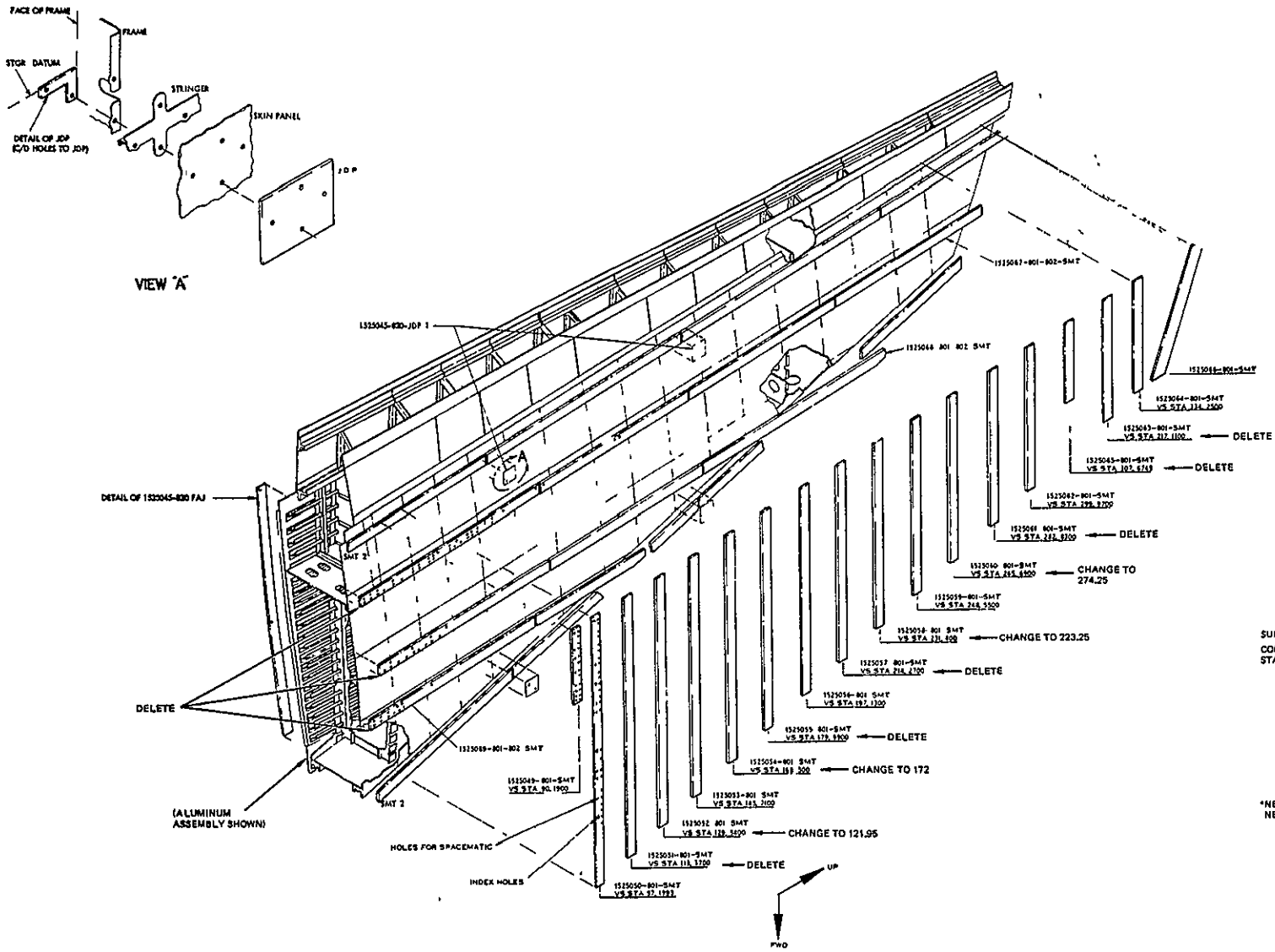
During this Phase I period, manufacturing branches pursued a series of tasks to prepare for the implementation of Phase II. Some of the main tasks are listed:

- Specification for the tool steel (ASTM "A36" hot rolled steel annealed) were determined and issued to the subcontractors. This will provide uniform continuity for the thermal expansion interface for all component details. Thermal expansion of steel is close to the expansion of  $\pm 45$  graphite/Kevlar composite materials.
- Manufacturing research organizations have conducted material evaluation and processes development tests and fabricated concept evaluation specimens.
- Manufacturing planning has participated in preplanning of Engineering jobs and developed operation sheet formats.
- Tooling has commenced with tool designs for long leadtime tools.
- Manufacturing engineering has prepared detailed area and equipment plans.
- The source book which sets up requirements for the delivery assemblies from the Georgia Company was completed.
- Ancillary test specimens were reviewed to determine tooling types.

### 5.2.1 Skin Covers

#### 5.2.1.1 Limited Production Tooling Plan

The design concept of the full size limited production tools will evolve from and be verified by design and fabrication of the subcomponent tools and fabrication of the subcomponent. Control media used for the subcomponent tool will also be used for the full size tools. Existing procedures provide for collecting costs for each tool built at Lockheed. This is done by issuing a tool order for each tool to be built and posting charges to the tool order number. Manufacturing research will support the tooling development effort during design and fabrication.



SUMMARY  
COMPOSITE ASSEMBLY RIB  
STATIONS ARE -

90 100 (HALF RIB)
97 100
*121.95
145 71
*172 00
197 13
*223.25
248 55
274 25
299 97
334 25

\*NEW LOCATIONS - REQUIRE  
NEW TEMPLATES

Figure 83. Drilled Tooling Modification for Composite Assembly

Flat table layup block design.- A flat layup table shown in Figure 84 will be fabricated for use with the broadgoods layup tool. It will be used for layup of broadgoods from which doublers and hat section material can be cut. It can be used to layup the skin in the flat and subsequent draping into the contoured skin mold.

Layup block for the hat section stiffeners.- Several hat section tools will be mounted on one table as shown in Figure 85. Hats will be laid up using broadgoods in multiple layers. Layup table will be used for bagging and will be placed in the autoclave.

Skin bonding tool design for the first stage - bond skin assembly and second stage bond skin and stiffener assembly.- Two skin bonding tools will be built, one for the left hand skin and one for the right hand skin (See Figure 86). Because of the shallow contour of the tool, it is planned to layup the graphite directly on the tool surface. The tools will be configured to fit under the broadgoods dispensing tool. These tools will be used for both curing of the basic skin and, with addition of appropriate tool locating details, the bonding of the hat sections to previously cured skin in a secondary operation. Provisions will be made on the surface for process control coupons.

Basic design concept for the broadgoods dispensing layup tool.- The broadgoods layup tool shown in Figure 87 is essentially a device for transporting a roll of graphite prepreg so that the roll can be unwound on to the skin tool or on to a flat table. The roll carrier is moved along a rail by hand and the proper ply orientation is achieved by positioning the tool or table under the carrier.

Ancillary test hat section stiffened panel configurations and fabrication planning procedures.- To define the concepts which will be used to fabricate the ancillary test specimens, Production Design Outlines will be used. These outlines will be developed before the final drawing is released and will describe the tooling and manufacturing plan and identify related documents which control fabrication. Operations sheets will be prepared for each test specimen. These will list materials and tools to be used, the detailed fabrication procedure to be followed, and will provide entries for recording of processing data. These sheets also provide for inspection at appropriate points in the process. Manufacturing Research in conjunction with Production will fabricate the ancillary test specimens. This will acquaint Production personnel with the techniques required for the remainder of the program.

Subcomponent procedures for box beam skins test specimen.- Production Design Outlines and Operations Sheets for the subcomponent skins will be prepared as for the ancillary test specimens. Production personnel will fabricate the skins with Manufacturing Research assistance.

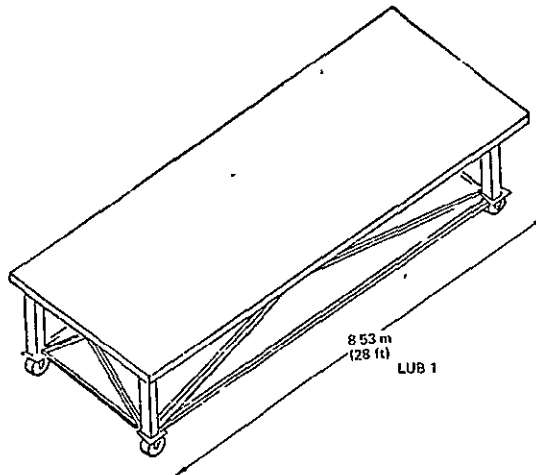


Figure 84. Flat Table Layup Block

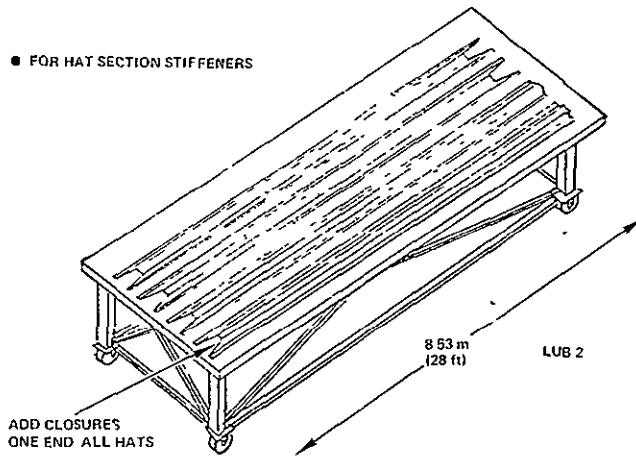


Figure 85. Layup Block

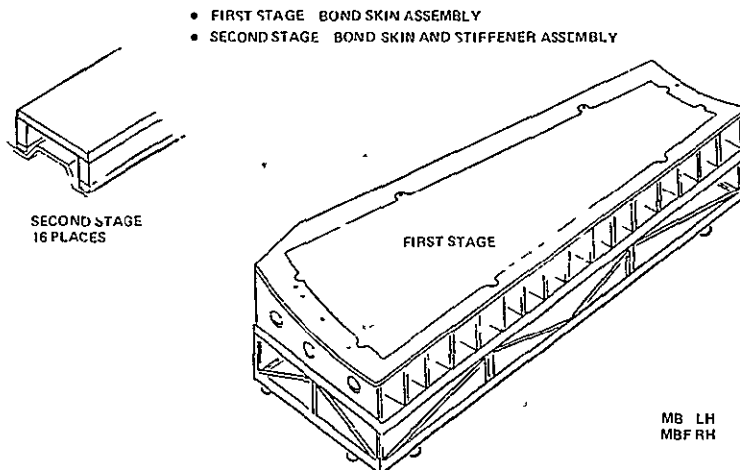
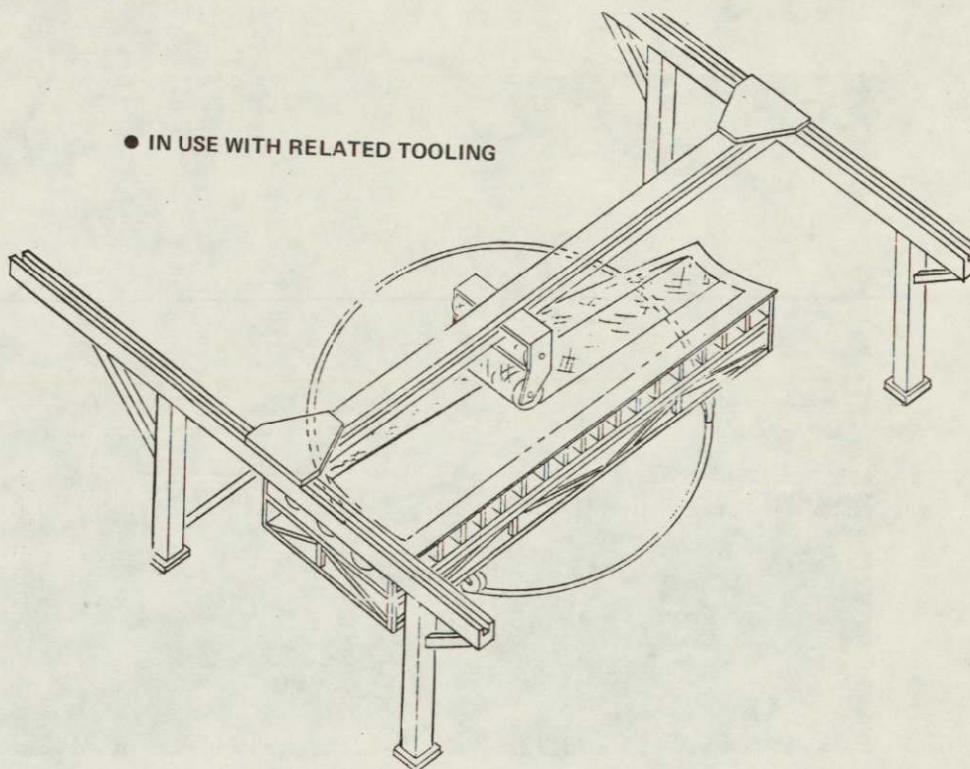


Figure 86. Skin Bonding Tool



● IN USE WITH RELATED TOOLING

Figure 87. Broad Goods Layup Tool

Hat section stiffener development. - Tools for a 2.7 m (9 ft) - long hat section, a hat section closeout, and a typical skin panel were fabricated, and parts were molded on these tools in order to verify concepts and develop fabrication methods.

The male hat section tool is shown in Figure 88 and the bag and bleeder arrangement is shown in Figure 89. To obtain the desired fiber-to-resin ratio in the cured laminate, three plies of bleeder cloth were used overall with two additional plies over the thicker cap area.

The uniform section obtained by this process can be seen in Figures 90 and 91. The hat section exhibited no distortion except for a slight axial twist which could be easily removed by light finger pressure.

The following sequence was used to lay up the five basic inner plies/10 cap strip plies/five basic outer plies construction of the hat.

- Lay up two innermost basic plies on flat table, transfer to tool, drape over tool, and smooth down with tedlar squeegee.
- Lay up remaining three plies, transfer to tool, position on previous plies, and smooth down.



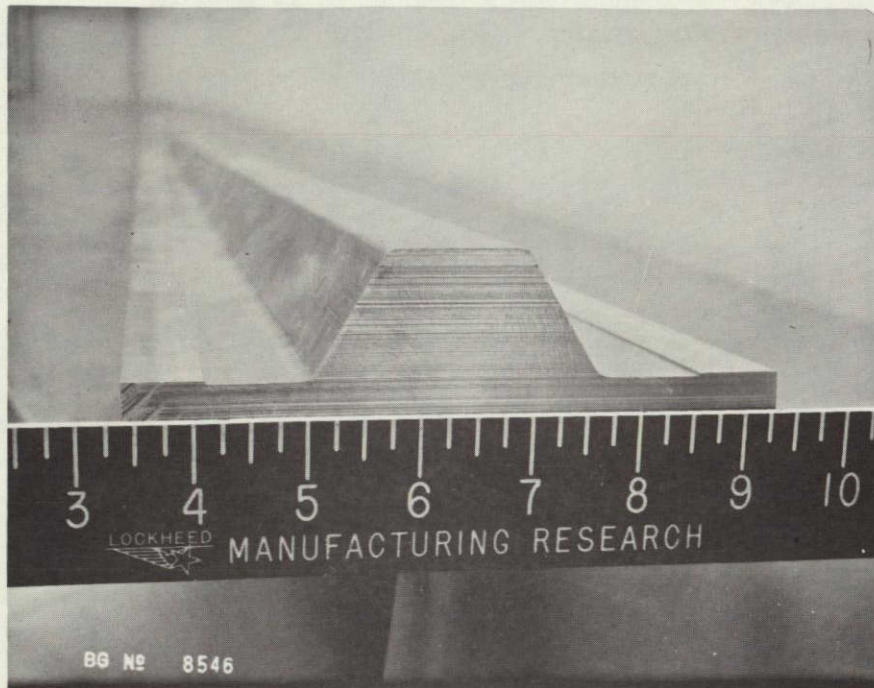


Figure 88. Aluminum Hat Tool

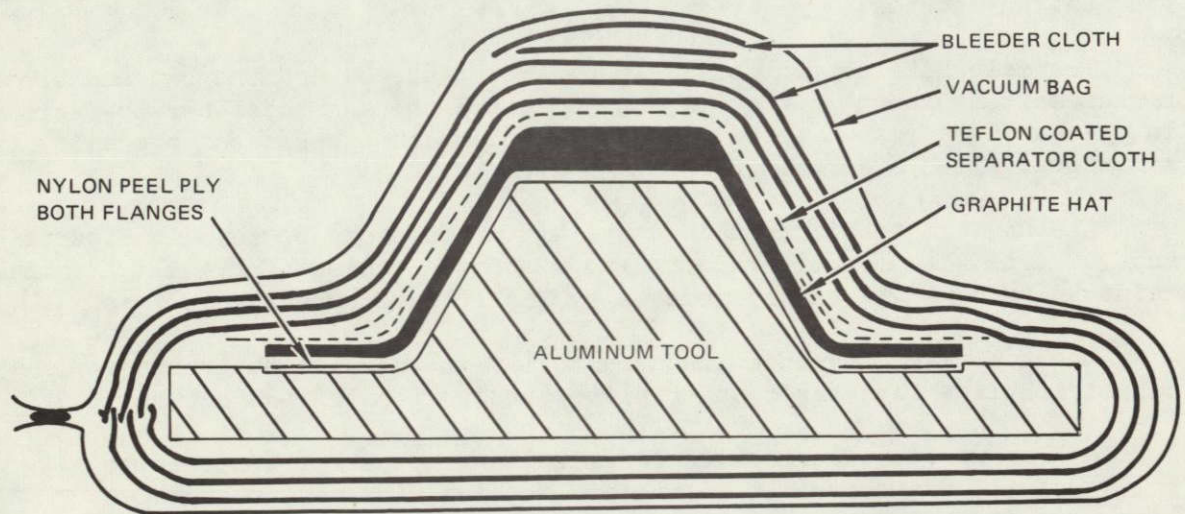


Figure 89. Bag and Bleeder Arrangement for Hat Section

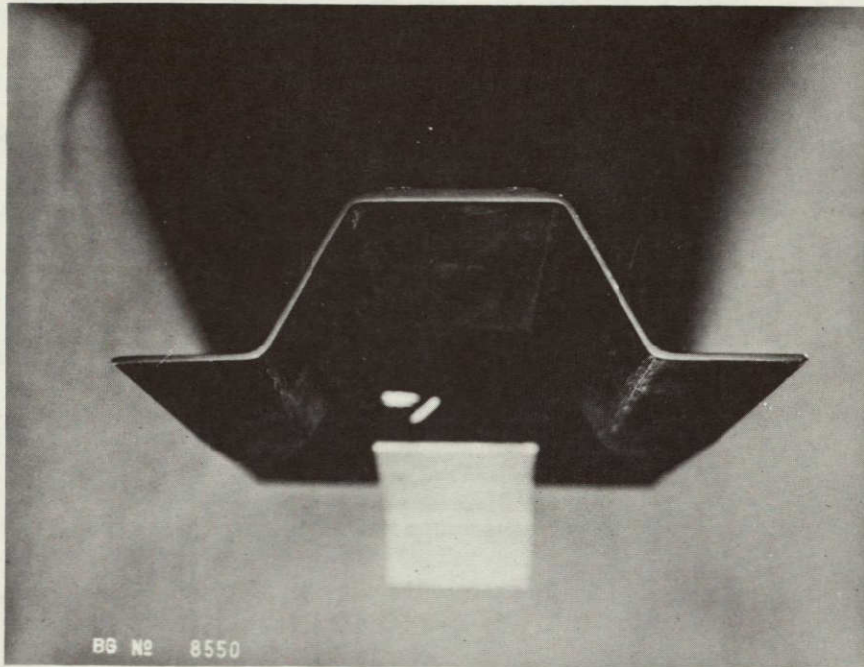


Figure 90. Cured Hat Section

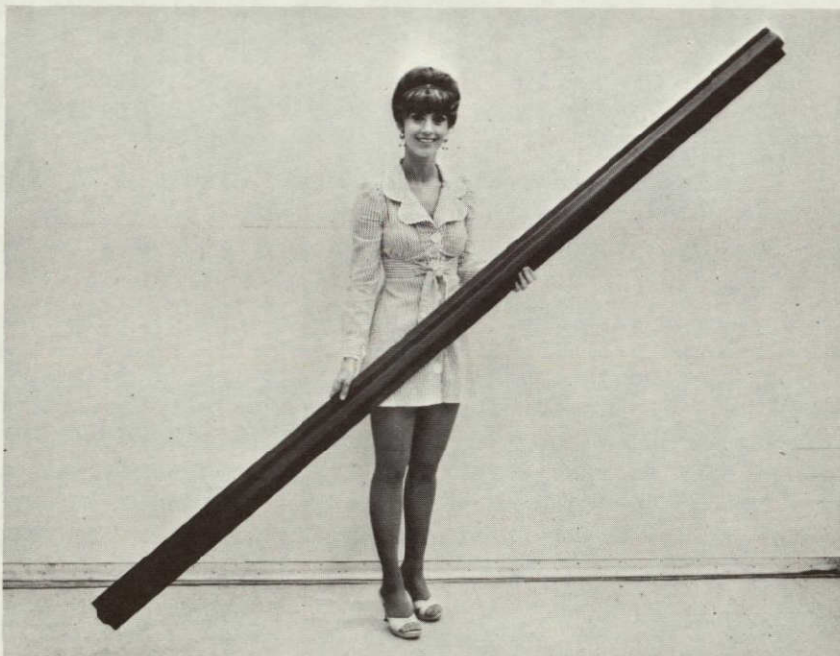


Figure 91. Hat Stiffener for Fin Cover



- Lay up 10 plies for cap strip on flat table, transfer to tool, center carefully on previous layup, and smooth down.
- Continue as in first two steps to lay up five outer plies.

To assure that the bond surfaces of hat flanges remain clean until layup of hat and skin for bonding, peel ply (nylon taffeta) is placed on the tool prior to layup of hat laminate. During cure of the hat, sufficient resin flows from the prepreg into the peel ply to assure adhesion until it is removed. Figure 92 shows the peel ply partially removed from the cured hat section.

Hat closeout development.- Development of fabrication methods for the hat section closeout was conducted on separate tooling. Figure 93 shows the closeout tool made according to the design concept under investigation at the time. This tool was subsequently joined to the basic hat section tool shown in Figure 88.

Several development pieces are shown in Figure 94. It was found that the same bleeding method and cure cycle could be used for both the hat and closeout, thus assuring that the hat and closeout could be made integrally. Figure 95 shows such a hat during layup. The first five plies have been worked down over the tool and trimmed, and the 10 plies of unidirection cap filler have also been laid down. Tedlar (clear) and teflon (white) strips visible in Figure 95 were laid in to permit development of QA inspection techniques for the hat. Figure 96 shows the completed hat.

An 0.43 m (18 in.) wide section of graphite laminate representative of the skin (except for contour) from VSS 100 to VSS 190 has been molded. It includes a 4-ply thickness transition on the inner skin and is shown in Figure 97. It was molded with a Style 281 Kevlar cloth outer facing on a 0.0635 mm (.025 in.) thick steel plate to simulate the full-size tool. The finished part showed no distortion and exhibited a smooth surface on the bag side and is being used for hat-to-skin bonding development.

Hat-to-skin bonding development.- All hat-to-skin bonding development has been done with 3M Company AF-55 adhesive, 0.293 kg/m<sup>2</sup> (0.06 lb/ft<sup>2</sup>). A typical bonding development specimen is shown in Figure 98. A desired objective of this bonding development, in addition to meeting the structural requirements, is to perform the bonding without special bonding fixtures; that is, apply the bonding pressure directly to a flexible bag which serves as the pressure diaphragm. Although not all bonding testing is complete, the following procedure for hat-to-skin bonding appears to give satisfactory results:

- Remove peel ply from skin and hat flange bond surfaces. Cut adhesive to suit and assembly hat, adhesive, and skin. (For development studies hat is held in place with a small piece of tape at each end.)



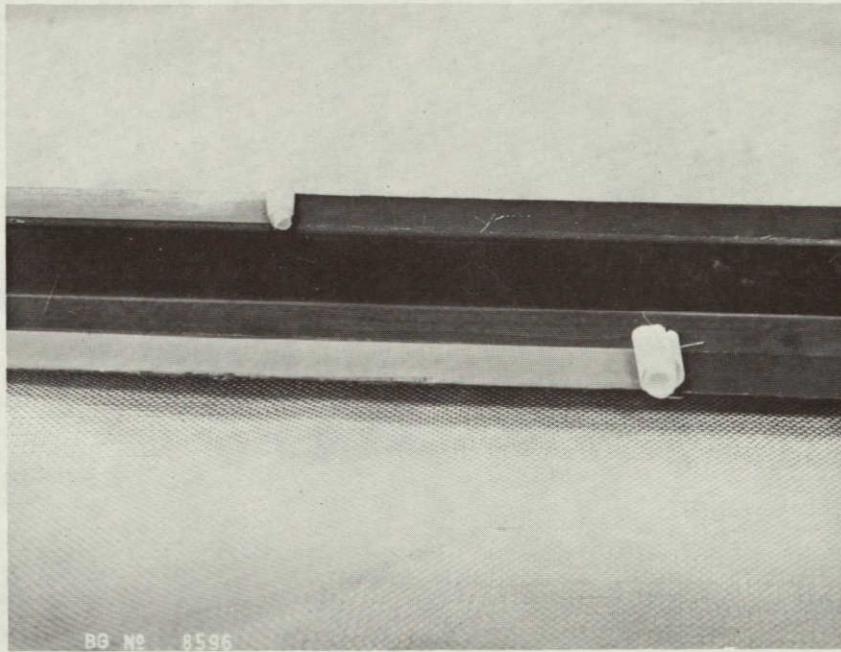


Figure 92. Bond Surface of Hat Flanges  
(Nylon Peel Ply Partially Removed)

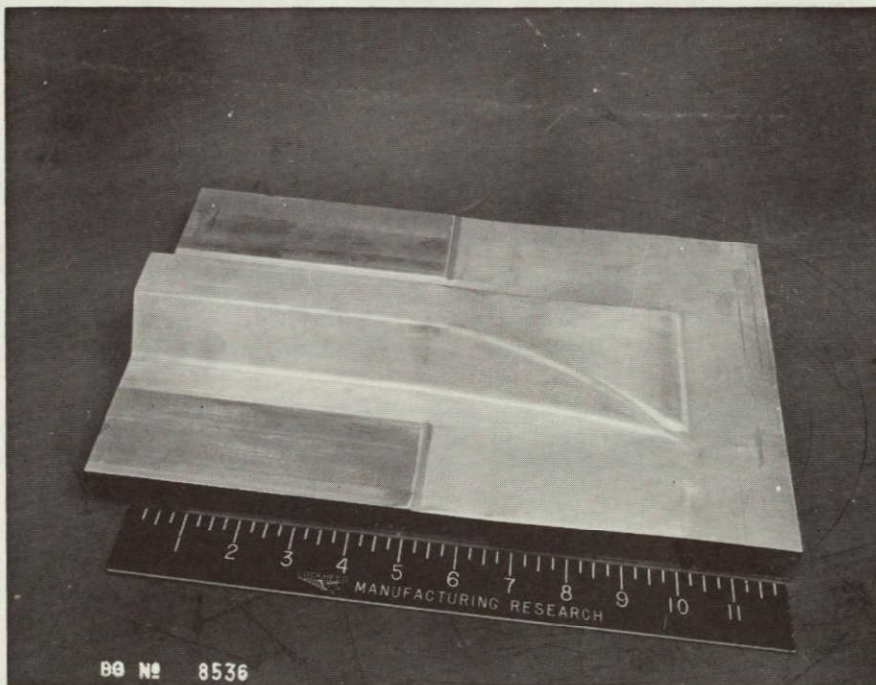


Figure 93. Hat Section Closeout Tool

REPRODUCIBILITY OF THIS  
ORIGINAL PAGE IS POOR

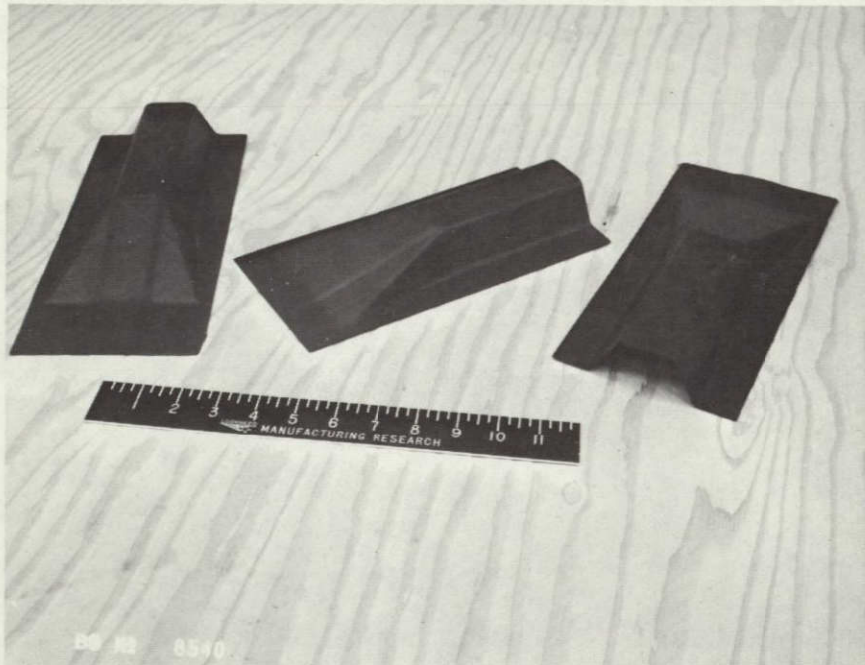


Figure 94. Hat Section Fabrication Development

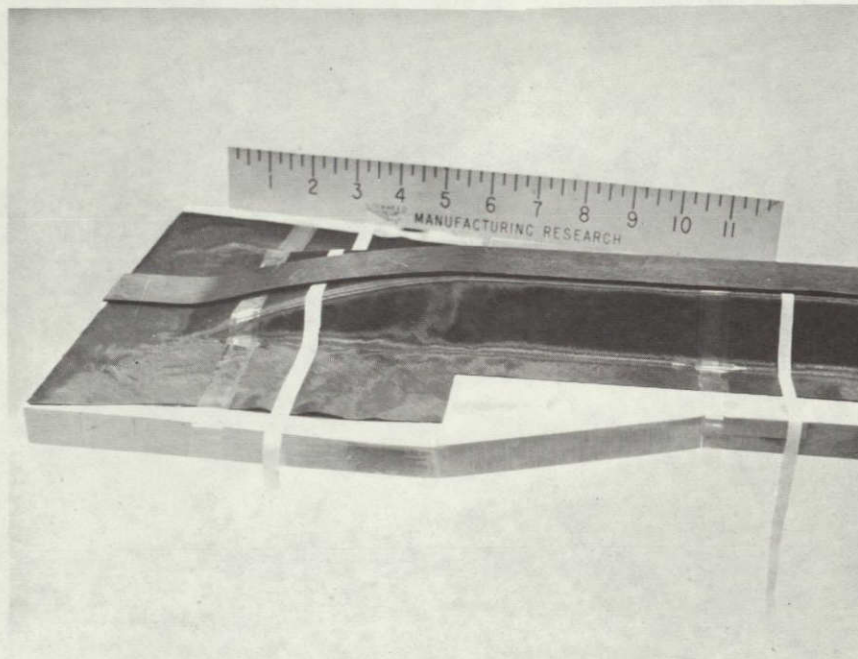


Figure 95. Fabrication of Hat Section with Integral Closeout



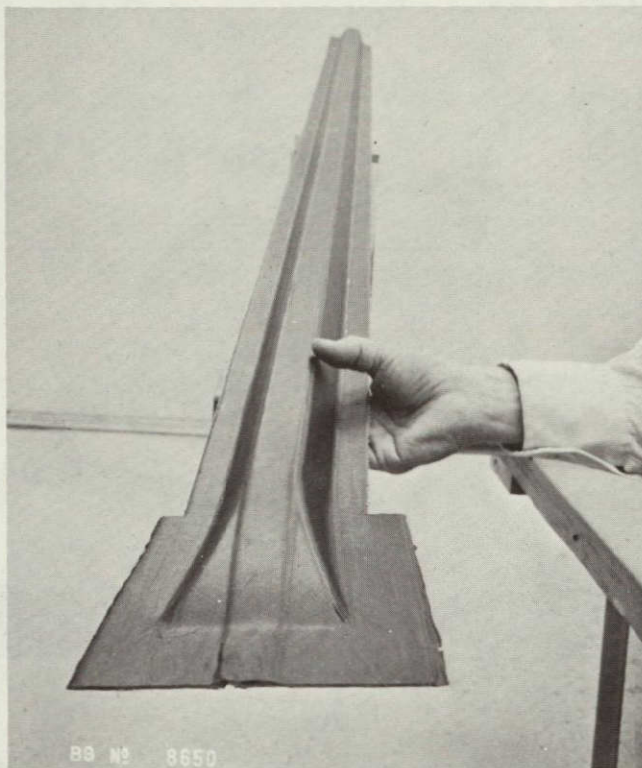


Figure 96. Hat Section with Integral Closeout

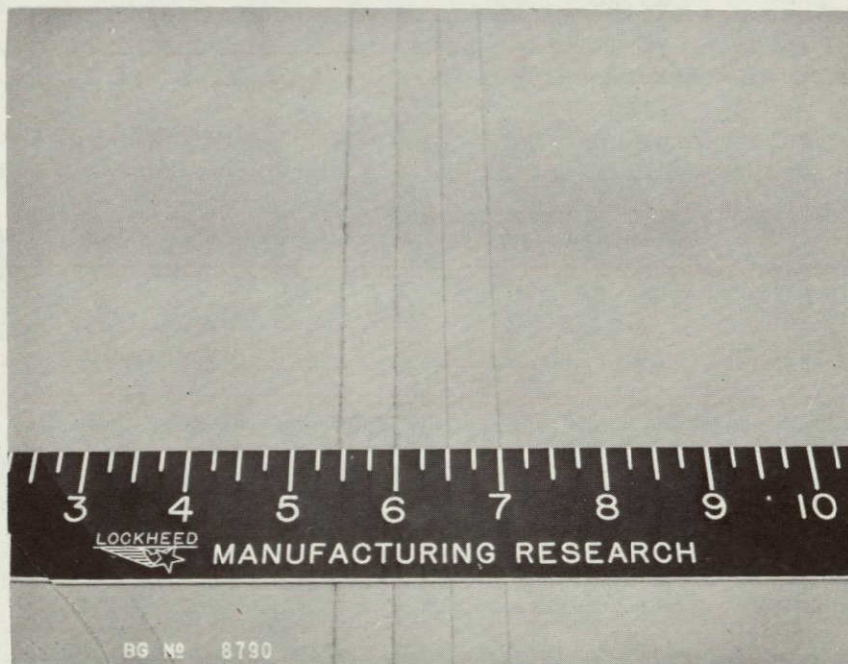


Figure 97. Four-Ply Thickness Transition Area on Inner Surface of Skin. (Gray appearance due to peel ply.)

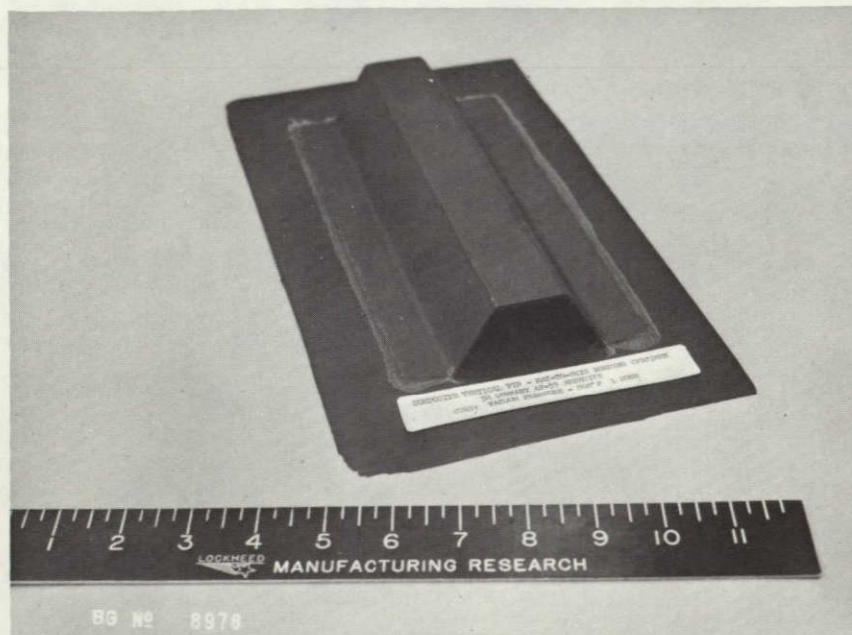


Figure 98. Typical Bonding Development Specimen

- Place one ply of 181 glass cloth as bleeder around entire assembly after positioning thermocouple at bond line. Seal assembly in vacuum bag (Vac-Pac) and install it in autoclave.
- Apply full vacuum and check for leaks. Apply 138 kPa (20-psi) autoclave pressure, venting the vacuum to atmosphere at 103 kPa (15-psi) autoclave pressure. Raise temperature of part 2.2K - 3.9K ( $4^{\circ}$  -  $7^{\circ}$ F) per minute to 394-400K ( $250^{\circ}$  -  $260^{\circ}$ F), holding this temperature for 1 hour. Cool under pressure to 333K ( $140^{\circ}$ F).

#### 5.2.2 Spars

Manufacturing and tooling considerations for the front and rear spars are shown in Figure 99. All vertical forces required to mold spars are from autoclave bag pressure. Heat is also provided by the autoclave. All horizontal forces required are provided by rubber expansion. Hand holes to provide access for fin box assembly are molded into web.

- The hand hole reinforcement shear web test specimen is described in Figure 100. The drawing shows the latest hand hole configuration, utilizing collar type reinforcement.



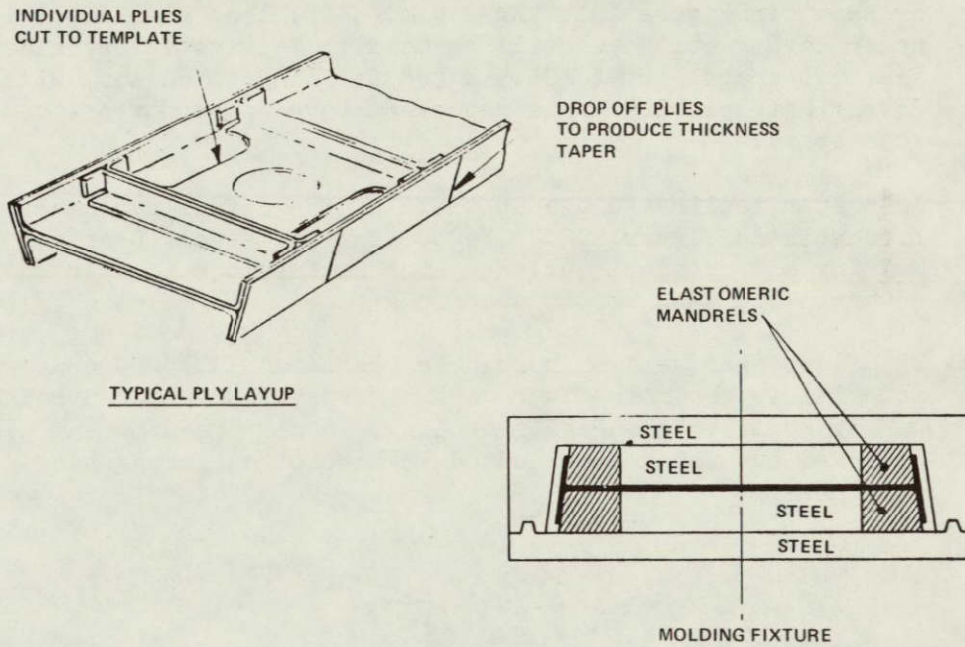


Figure 99. Manufacturing and Tooling Considerations - Spars

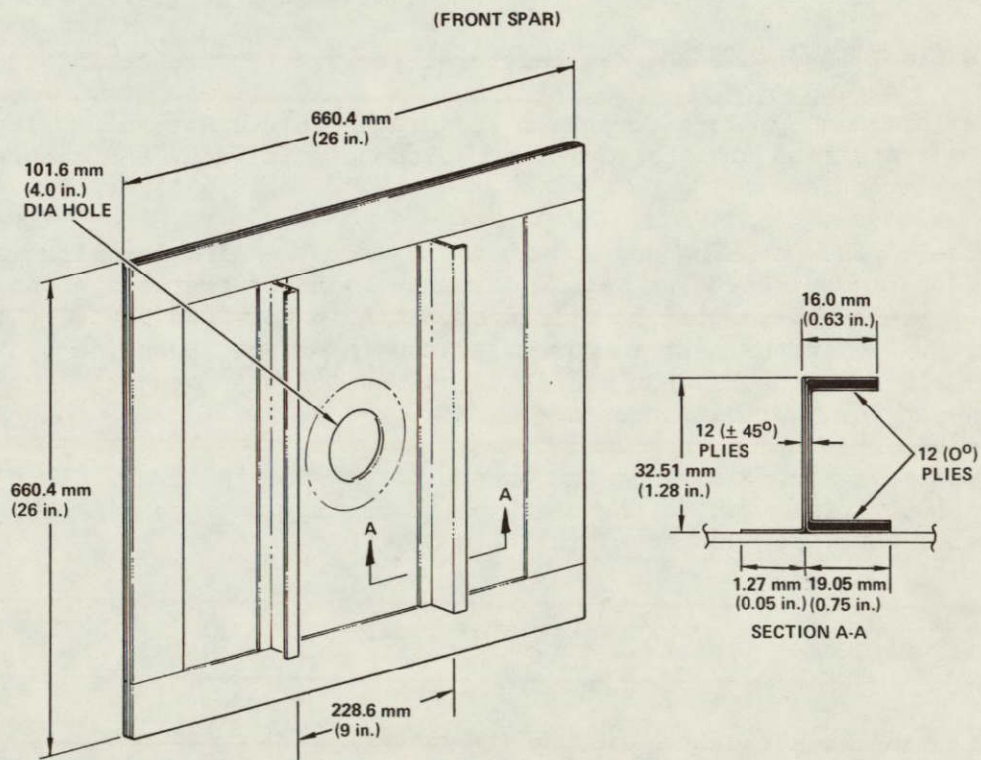


Figure 100. Hand Hole Reinforcement Shear Web Test Specimen



- The IRAD tooling (over all design) concept for the rear spar is shown in Figure 101. An 2.4 m (8 ft) long steel tool is under construction and will be used to fabricate approximately six test spars - up to 25.5 m (84 ft) long. The tool will investigate problem areas representative of both front and rear spars.
- IRAD spar tooling (close up view) of the detail parts are presented in Figure 102. The tooling has steel inserts for molding all critical surfaces such as fuselage to spar and cover to spar and rib to spar interfaces.
- The first spar section molded in graphite T300/5209 composite material is shown in Figure 103. Warpage of web occurred but was overcome by changes in tooling. Some core dimpling also occurred but was not evaluated for effect on strength or stiffness.

### 5.2.3 Ribs

Manufacturing and tooling feasibility studies for the truss, miniwich, and stiffened web ribs are itemized as follows:

- Tooling approaches for the truss, miniwich, stiffened web designs
- Tool improvements for sealer/release and ceramic cauls
- Processing plans for bleed and drape cycle, pattern development, transition area problems, H/C closeout miniwich, and cocure compatibility.

The revised tooling and assembly flow for the miniwich ribs is illustrated in Figure 104. The main difference from the previous planned approach is that the rib tabs will be molded as a single edge and routed to contour definition after the part is cured. Close interface chordwise width tolerances of the rib cap ribs between the hat section stiffener spacing is the main reason for the fabrication change.

Revision to the tooling and assembly flow for the truss ribs, shown in Figure 105, is similar to the miniwich in routing out the rib tabs to contour after the part has been cured in the tool.

## 5.3 FINAL ASSEMBLY

In Figure 106, the basic final assembly fixture and a step by step planned assembly approach for the composite detail hardware components are shown. Several investigations are underway to establish the best drilling practices consistent with the simple assembly sequence presented in Figure 76.

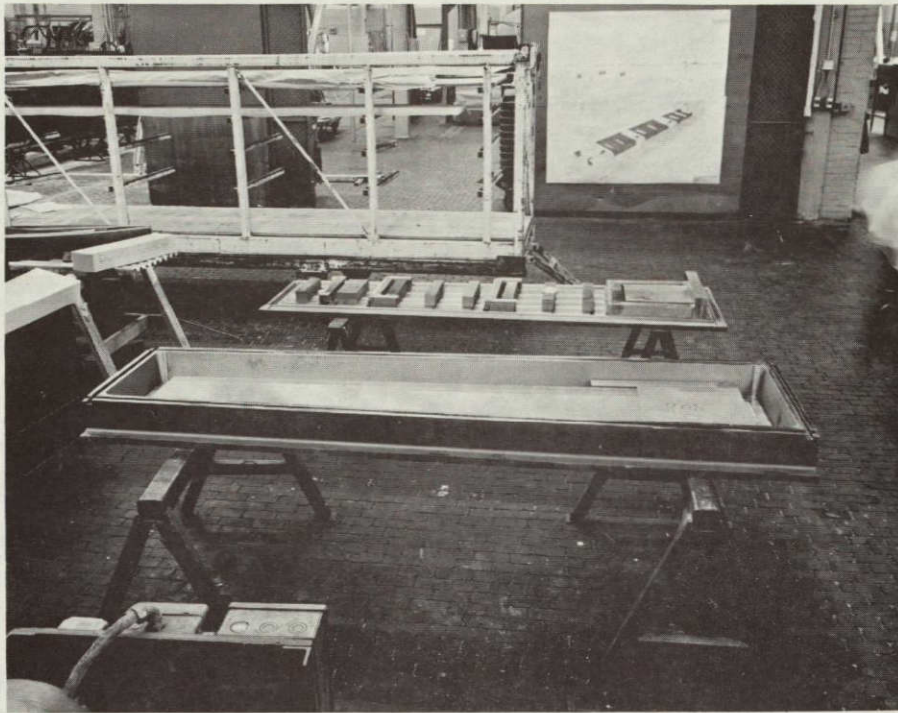


Figure 101. Prototype Spar Tool

REPRODUCIBILITY OF THE  
ORIGINAL PAGE IS POOR

REPRODUCIBILITY OF THE  
ORIGINAL PAGE IS POOR



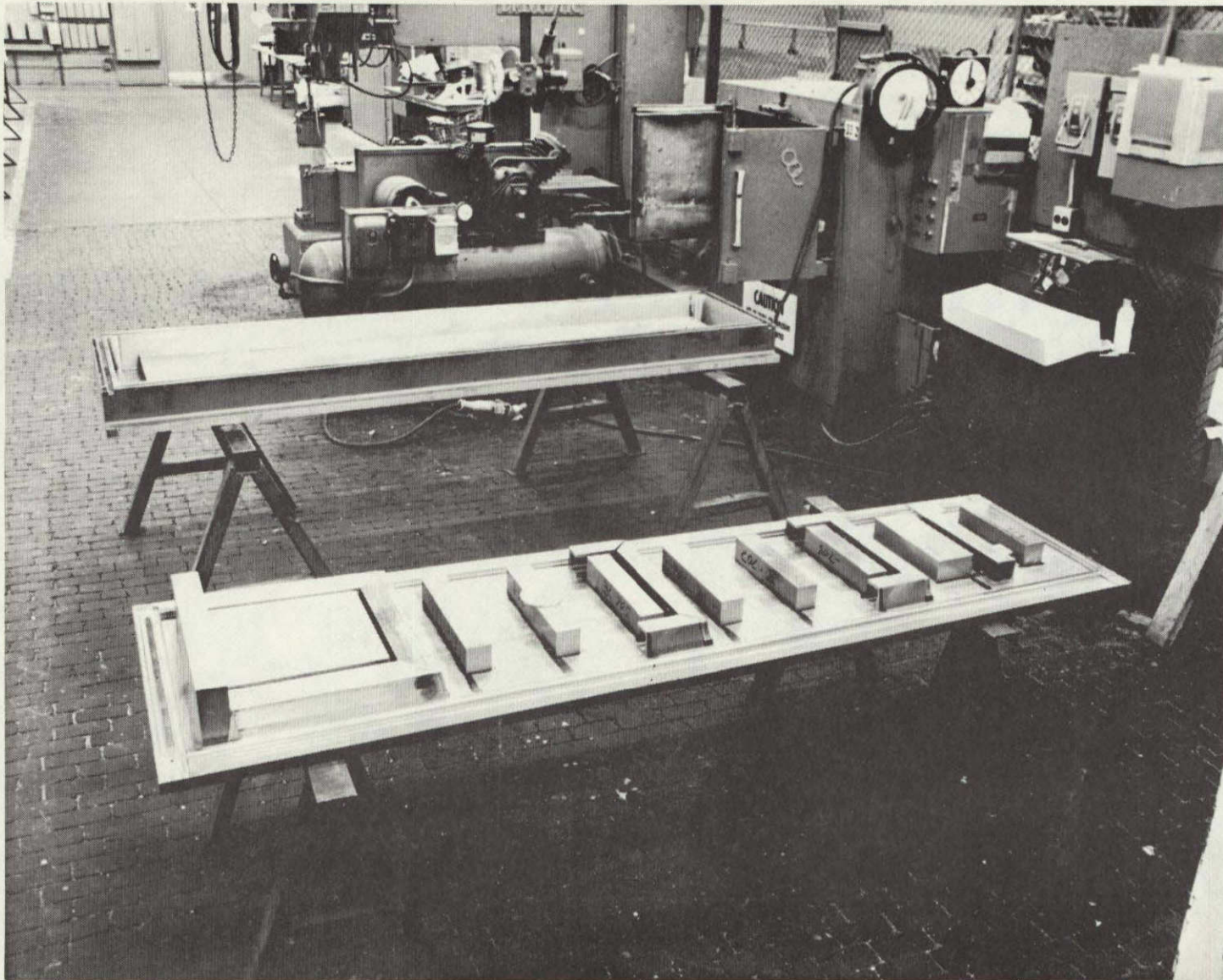


Figure 102. Spar Tooling



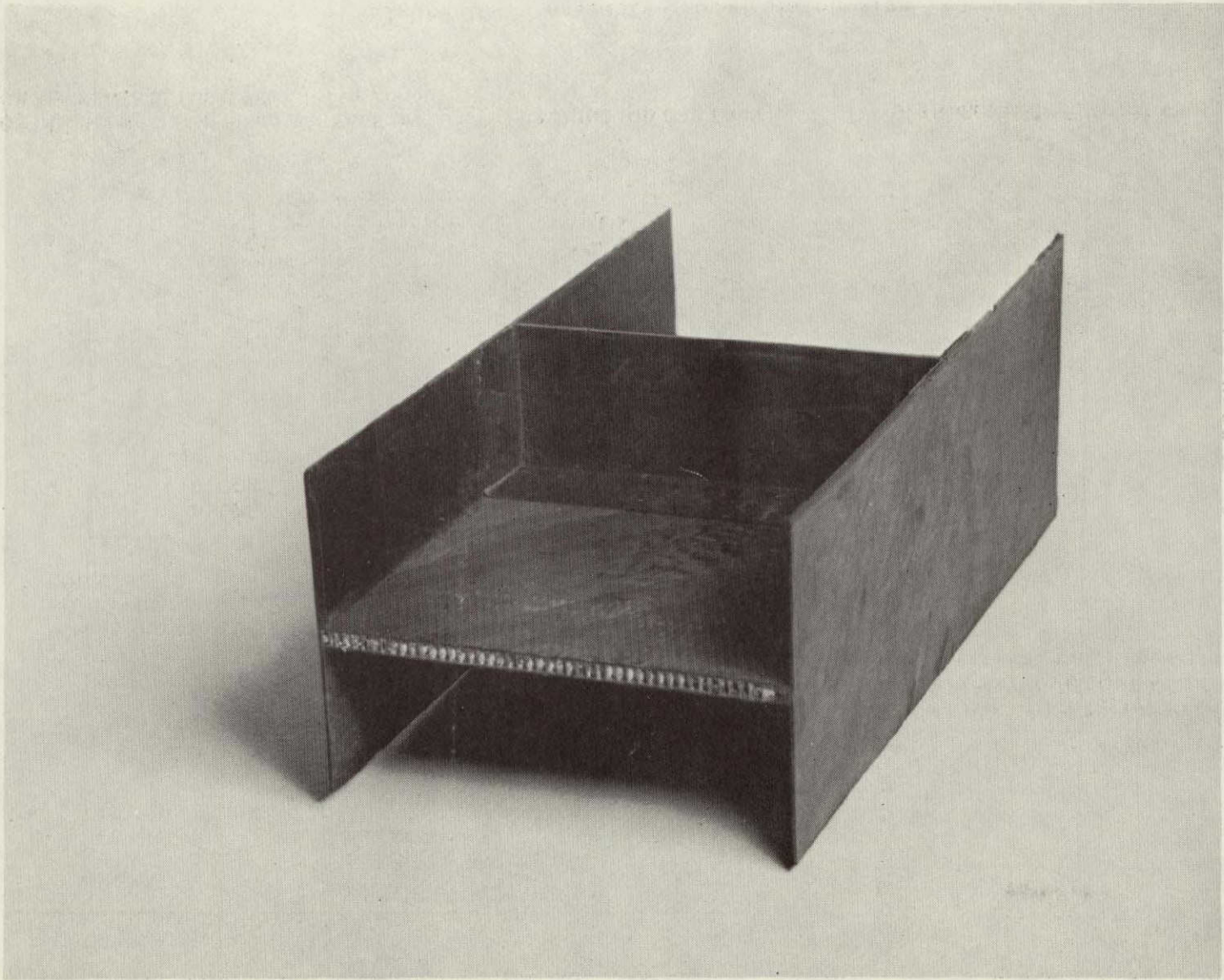


Figure 103. First Molded Spar Section



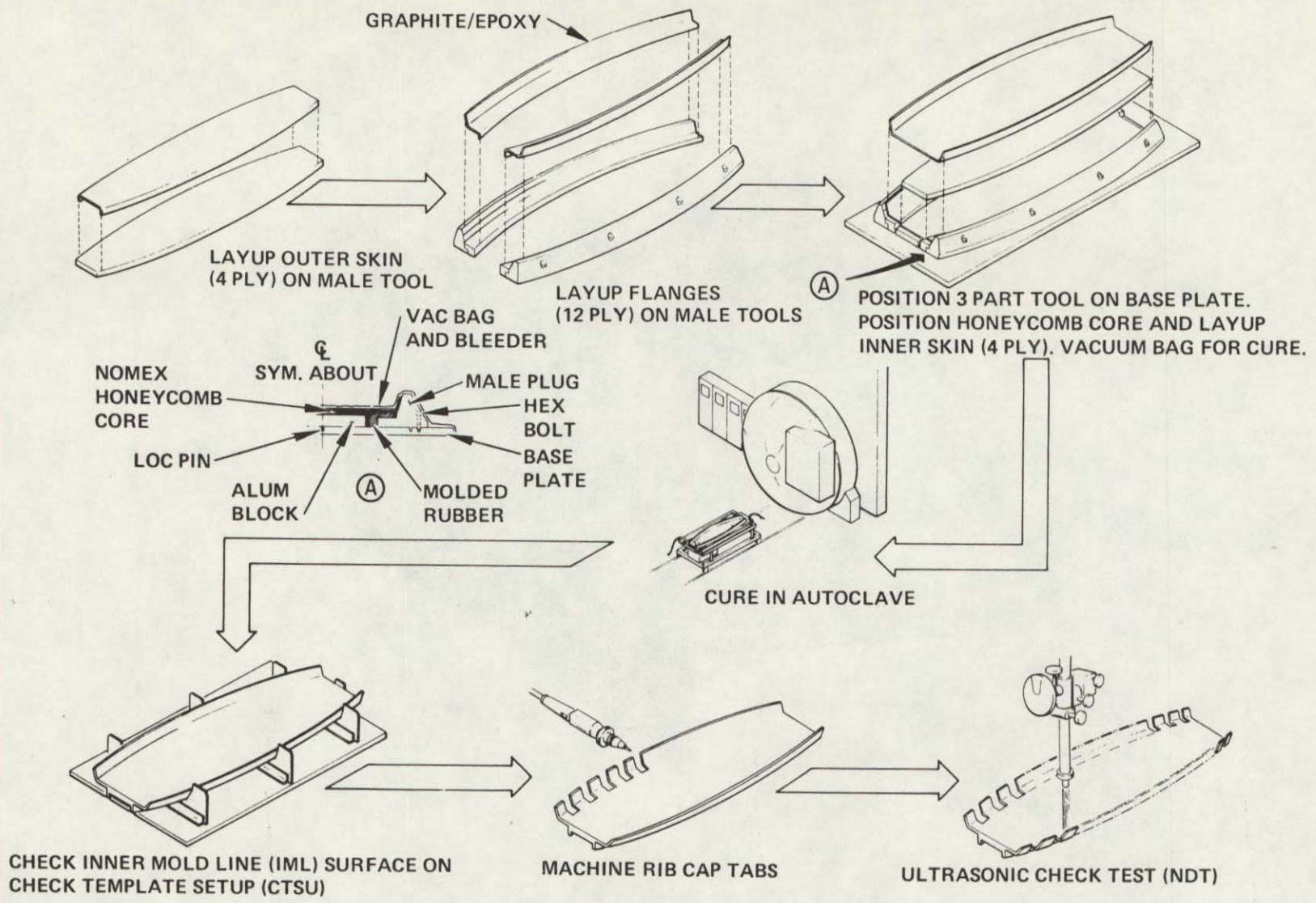


Figure 104. Assembly Flow-Miniwich Ribs

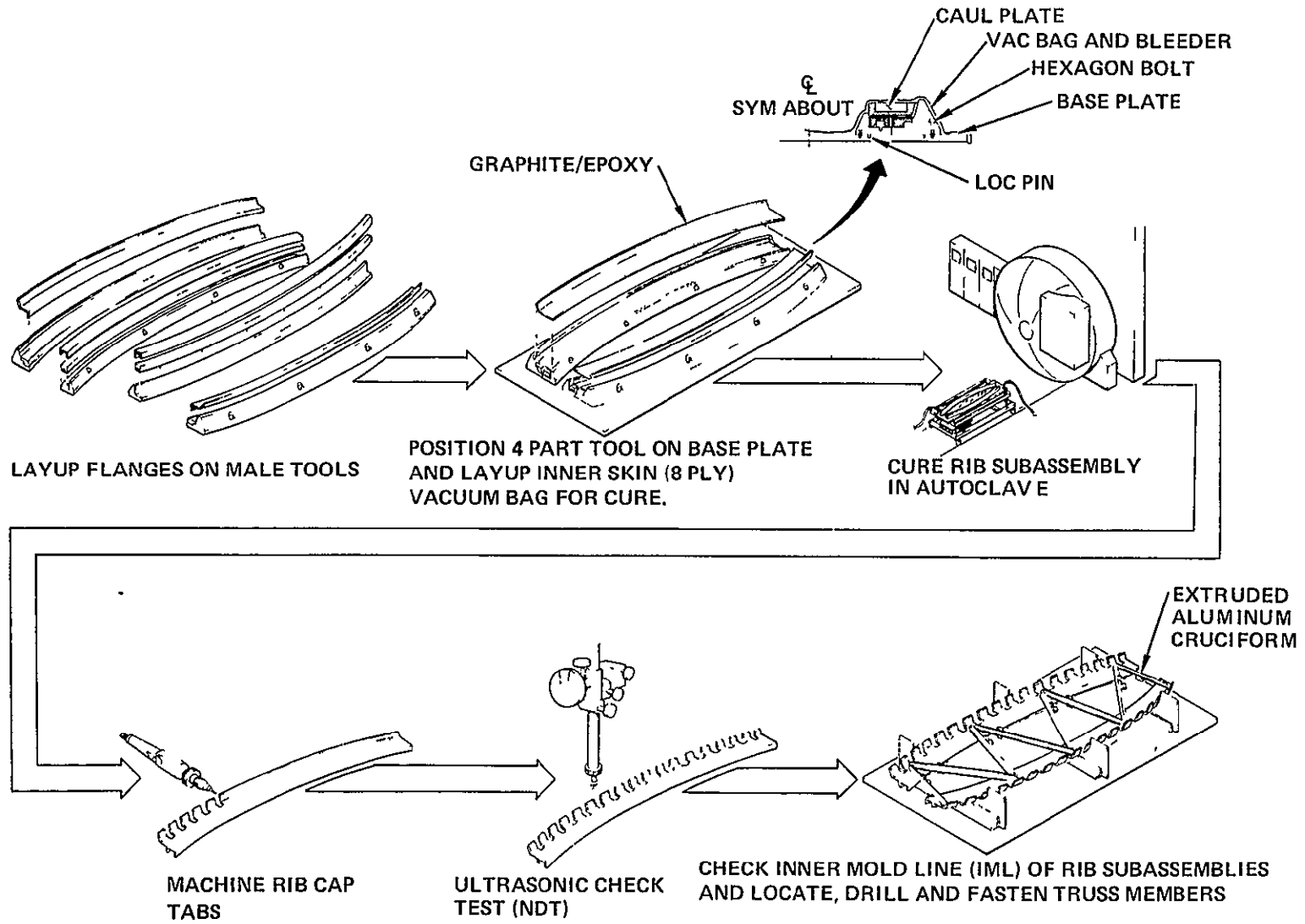
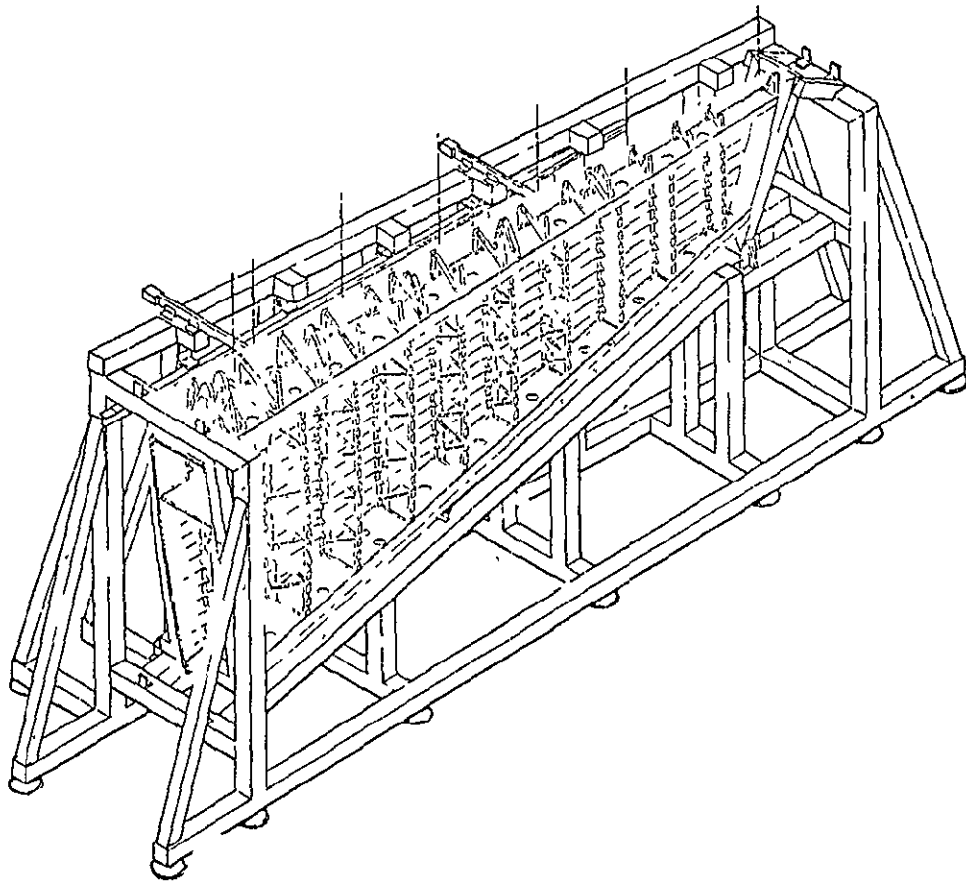


Figure 105. Assembly Flow-Truss Ribs



1. LOCATE F/S
2. LOCATE RIBS
3. LOCATE T/E ASSY
4. ASSEMBLE SUBSTRUCTURE
5. LOCATE L.H. COVER  
DRILL ATTACH HOLES  
& REMOVE
6. LOCATE R.H. COVER  
DRILL ATTACH HOLES  
& INSTALL FASTENERS
7. INSTALL L.H. COVER  
(ACCESS THRU ROOT RIB  
& SPAR ACCESS HOLES)

Figure 106. Final Assembly Fixture

## 6.0 PRELIMINARY DESIGN REVIEW (PDR)

A PDR was held for the Government on 12 November 1975 at the Lockheed-California facility in Burbank, California. Attendees at this review included personnel from NASA-Langley Research Center, FAA, USAF, and NAVPRO, Burbank, as representatives of the Government, Lockheed-California, Lockheed-Georgia, and RI/LAAD personnel. The PDR was held for the Government so that they may assess the work progress and the projected program outlook. The PDR presented a review and assessment of the recommended ACVF configuration and its evolution from conceptual and trade studies; design activities and success in achieving a low-cost, light-weight, reliable design; analysis and test plans for evolving and finalizing design; material procurement activities; material specifications and conformance with specifications; manufacturing activities and plans; and the status and outlook of the sprogram with respect to schedules and budgets. All of the data presented at the PDR is included in this report.



## APPENDIX A. MATERIAL SELECTION AND EVALUATION PLAN

- Objective - The objective of this plan was to select an advanced composite material system for the ACVF that would meet the program requirements from the standpoint of quality, reproducibility, and cost.
- Approach - The approach used in this plan is shown in the flow chart in Figure A-1 and consists of the following elements:
  - Requirements - Establish advanced composite material requirements for the ACVF relative to environmental considerations, design, structures, producibility, costs, and other factors.
  - Qualitative analysis - Collect and evaluate available data for graphite and Kevlar/epoxy prepregs relative to the ACVF requirements.
  - Quantitative analysis - Perform screening tests as required to resolve questions left unanswered by the available data.
  - Selection of advanced composite material system(s) - Select primary and backup material systems that best satisfy the program requirements.

Other materials such as adhesives, honeycomb cores, coating, etc. will be selected during preliminary design to meet specification requirements.

### A.1 REQUIREMENTS

#### A.1.1 Environmental

The material systems must perform satisfactorily under all environments experienced by the L-1011 vertical fin. The environments include:

- Temperature - 219K (-65°F) to 344K (160°F) as specified in reference 7. The 344K (160°F) is a ground soak condition. The maximum flight temperature is 322K (120°F).
- Humidity - Up to 100 percent relative humidity.
- Hydraulic fluid - The lower portion of the aft spar is adjacent to the hydraulic actuators. While the structure is not normally exposed to hydraulic fluids, it may be subject to temporary exposure due to leaks. The fluid consists of a 50/50 percent mixture of Chevron Hyjet III and Stauffer Aerosafe.

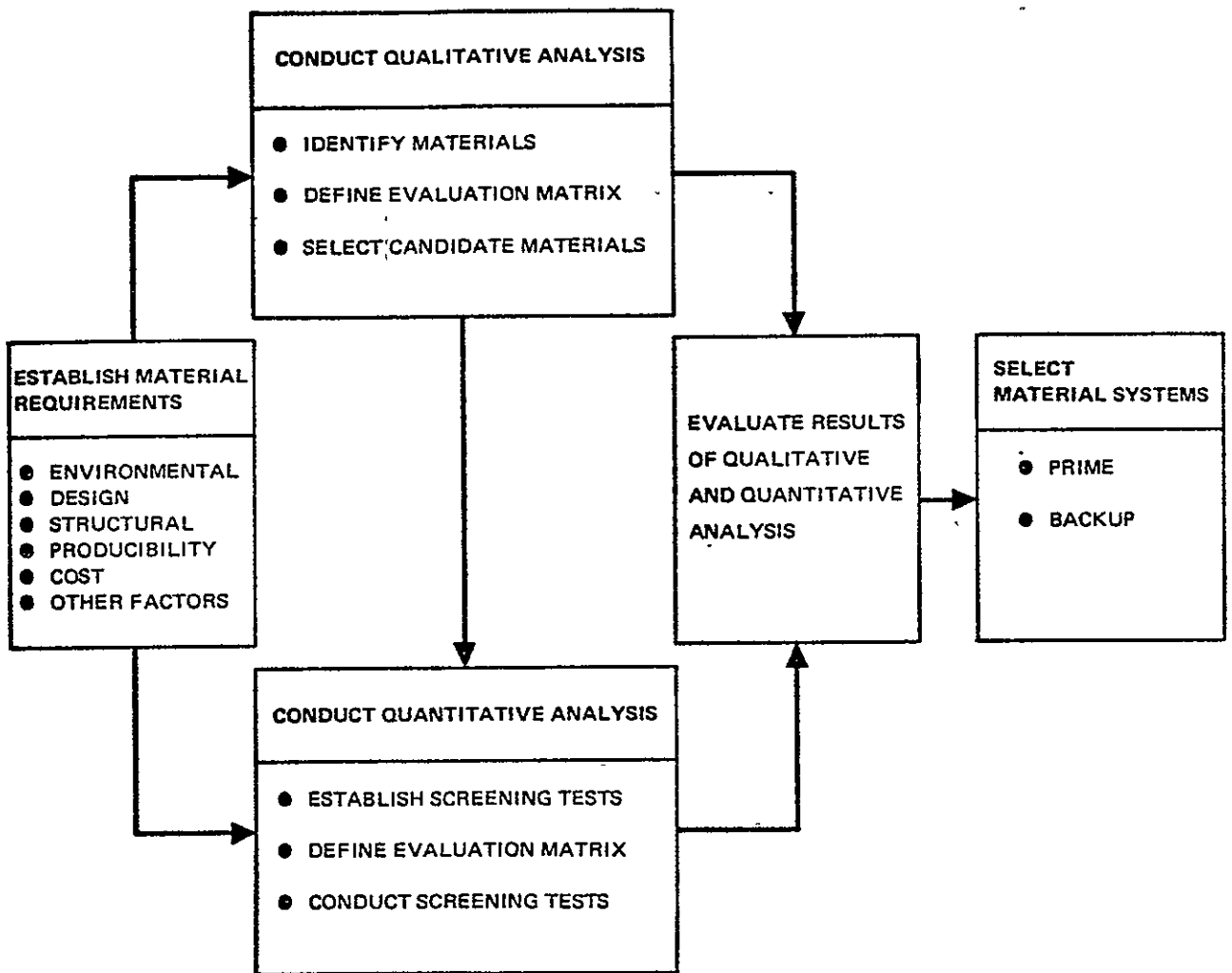


Figure A-1. Material Evaluation and Selection Plan Flow Chart

- Ultraviolet radiation - The surfaces exposed to sunlight will be painted to resist uv.
- Lightning - The surfaces of the vertical fin are subject to lightning sweep and will be protected by a surface treatment such as aluminum mesh or equivalent.
- Rain and hail erosion and foreign object damage (FOD) - The surfaces are in a vertical plane and are exposed to limited rain and hail erosion, and polyurethane paint should provide adequate protection. The location of the vertical fin minimizes FOD from runways and handling.

#### A.1.2 Design

The proposed design calls for Kevlar 49 fabric on the surfaces both as a corrosion-inhibiting barrier between the graphite and the lightning protection and to protect the graphite against damage from low-energy impact. Consequently, resins must be compatible with both graphite and Kevlar 49. The proposed design also calls for honeycomb sandwich construction for the upper rib webs. To prevent corrosion of the core, nonmetallic (HRP type) cores will be used with graphite/epoxy faces.

#### A.1.3 Structural

The materials must retain relatively high specific strengths and stiffnesses when subject to the design environmental conditions. The materials should have minimum data scatter, consistently cure to fiber/resin ratios that provide a good balance of properties and that are readily achievable with normal production processes, have characterization data available, and have minimum thermal residual stresses.

#### A.1.4 Producibility

Resin must be compatible with projected manufacturing processes (spars/ribs use a modified elastomeric molding process; skins use standard autoclave cure and bonded stringers, RI/LAAD plans to use an automatic tape machine for ribs) and must provide satisfactory fiber/resin ratio control, shelf life, tack, drape, handleability, machinability, bleeding characteristics, flow control, and cure cycle (gelation) characteristics.

### A.1.5 Costs and Other Factors

The requirement is to minimize system cost including material procurement, handling, and processing costs. Other factors include industry usage, experience among team members, and compatibility between Kevlar and graphite pre-pregs. It is considered desirable that the primary graphite/epoxy system has been, or is being, used on a government funded program so that fabrication and service experience data is available.

## A.2 QUALITATIVE ANALYSIS

The initial evaluation and qualitative screening will be accomplished by comparing the several materials with the requirements stated above. Its objective is to narrow the field of materials to enter the screening test program. The available data and experience among the team members and the industry will be examined to answer the following questions:

- Usage - Is the material being used on other government funded programs?
- Production Experience - Has hardware been successfully fabricated by team members and/or industry?
- Data Availability - Is characterization, design, and long-term (transport aircraft) environmental data available?
- Strength/Stiffness - Within the L-1011 environment (including humidity and temperature), what are the relative strengths and stiffnesses? This includes relative thermal residual effects.
- Costs - What are the raw material and relative fabrication costs?

A detailed analysis of the materials considered relative to these questions will be conducted. Merit numbers based on engineering judgment of the relative significance for each of the five parameters will be assigned each fiber/resin material. These will be tabulated. The materials with the two highest merit scores for both the 400K (260°F) and the 450K (350°F) curing classes will be selected for the screening test program. One will be designated prime and the other designated backup for each class. An alternate backup material will be selected where deemed advisable.

## A.3 QUANTITATIVE ANALYSIS

Since the primary purpose of the material screening tests is to choose between resin systems (rather than to obtain design allowables), the tests

are selected to compare relative influence of critical environments at minimum test costs and within schedule constraints. The most critical (see under Requirements) are moisture at maximum temperature 344K (160°F), and hydraulic fluid soak. These primarily affect the resin and resin/fiber bond. This can be best measured by compression in the fiber direction, interlaminar shear, and interlaminar tension. A flexure test loads half of the plies in compression and is a relatively inexpensive qualitative test to distinguish changes in resin properties.

The greatest unresolved issue relates to the relative environmental resistance of the 400K(260°F) and 450K (350°F) curing resins in the L-1011 environment. That is, will the 400K (260°F) resins perform satisfactorily, or is it necessary to use a 450K (350°F) resin to maintain adequate strength under the environmental conditions experienced by the L-1011?

Since the proposed structure consists of both all graphite and graphite/Kevlar hybrids, the test coupons will be cut from panels of the following configuration: 0<sub>20G</sub> and (0<sub>K</sub>/0<sub>6G</sub>/0<sub>2K</sub>/0<sub>6G</sub>/0<sub>K</sub>).

The intent of the structural tests is to assess the relative effect of the environments on the properties. The intent of the process variable tests is to evaluate and compare the fabricability of the materials. It will also verify that sound parts result when parts similar to the surfaces are fabricated by several methods. Additionally, manufacturing research will conduct a supplemental program to verify the processes. A number of larger size surface panels will be fabricated and tested to verify the recommended curing characteristics such as temperature and pressure applications. Resin flow, density, and resin control properties will be evaluated.

The other part of the quantitative analysis concerns the thermal residual stresses due to the temperature differential from the cure temperature to the operational temperature. This results in transverse cracking (matrix crazing) under certain loading conditions. Since there is greater differential for 450K (350°F) curing resins than for 400K (260°F) curing resins, it is expected that they will craze at lower stress levels. Typical laminates will be analyzed to determine the magnitude of these stresses and their effect on the design. Unsymmetrically laminated plates will also be tested thermally to quantify this effect.

#### A.4 SELECTION PROCEDURE

The results of the screening test for both the structural/environmental and fabricability tests will be evaluated. The structural comparison between materials will include both the absolute magnitudes and relative environmental effects on the interlaminar shear, flexural, and interlaminar tension strengths. Additionally, the relative thermal residual stresses will be quantified for typical laminates. These data will be used to modify or confirm the merit numbers for the production and strength/stiffness column of the evaluation matrix. The material with the highest score will be selected as the primary

material, and its runner up within the same resin class will be selected as backup. If there are overriding fabrication reasons for selecting a material from the other class for a particular component, the one with the highest score and the one with next highest score will be considered as alternates.

#### A.5 MATERIAL SCREENING TEST PLAN

The primary purpose of the screening tests is to enable a value judgment to be made between the 400K (260°F) and 450K (350°F) curing resin classes.

- Task 1: Fabricate three test panels of each resin system with the following configurations:
  - a. (0<sub>20G</sub>) (subscript G for graphite tape)
  - b. (0<sub>K</sub>/0<sub>6G</sub>/0<sub>2K</sub>/0<sub>6G</sub>/0<sub>K</sub>) (subscript K for Kevlar 49 281 fabric)
  - c. (±45<sub>3G</sub>)<sub>S</sub>
  - d. Run chemical and micro analyses to determine resin and void content.
- Task 2: Cut a. and b. panels into 20 each of the following specimens:
  - Flexure: 12.7 mm (0.5 in.) x 76.2 mm (3 in.)
  - Interlaminar Shear: 6.35 mm (0.25 in.) x 16.13 mm (0.635 in.)
  - Interlaminar Tension: 25.4 mm (1 in.) x 25.4 mm (1 in.)  
(Configuration b. only)

Adhesively bond metallic clevis to each face of the interlaminar tension specimens (configuration b. only). USE FML37 adhesive with both resin specimens. Identify each specimen by material and layup configuration. Cut panel 3 into 20 each of the following specimens (with fiberglass tabs).

  - Tension: 25.4 mm (1 in.) x 279.4 mm (11 in.)
- Task 3: Condition one-fourth of the coupons by immersion in water at 325K (125°F) for seven days and one-fourth of the coupons in hydraulic fluid at room temperature for seven days. The conditioning should be timed to permit testing within 24 hours of removal from bath, and the coupons should be kept in plastic bags to prevent drying between conditioning and test. Measure moisture weight gain.



- Task 4: Consists of four subtasks (Table A-1):

a. Process Variables:

1. Layup length of hat stiffener using existing male tool ( $\pm 45_G/0_{3G}$ )<sub>S</sub>. Check handleability, drapability, and tack.
2. Layup 152 mm (6 in.) x 152 mm (6 in.) panel ( $0_K/\pm 45_G/0_G/0_K$ )<sub>S</sub>. Prebleed one side and autoclave cure. Check thickness, resin content, and void content.
3. Layup 152 mm (6 in.) by 152 mm (6 in.) panel ( $0_K/\pm 45_G/0_G/\pm 45_G/0_K$ )<sub>S</sub>. Autoclave cure bleeding one side. Check thickness, resin content, and void content.
4. Check results of (3) with a 0.55K (1°F) to 1.11K (20°F)/min autoclave heatup rate.

- b. Control test at room temperature of the graphite  $\pm 45^\circ$  tensile coupons and both all graphite and graphite/Kevlar hybrid in  $0^\circ$  flexure, interlaminar tension, and interlaminar shear for both

TABLE A-1. TEST SUMMARY FOR TASKS 4b, c, d, AND e

Test Type	Material Conf.	Task Number, Condition, and Number of Coupons per Material				Total Tests Per Resin Material
		4b R.T. Dry	4c R.T. Skydrol	4d 344K (160°F) Wet	4e 344K (160°F) Dry	
$0^\circ$ Flexure	A. Graphite	5	5	5	5	20
	B. Hybrid	5	5	5	5	20
$0^\circ$ Interlaminar Shear	A. Graphite	5	5	5	5	20
	B. Hybrid	5	5	5	5	20
Interlaminar Tension	A. Graphite	-	-	-	-	--
	B. Hybrid	5	5	5	5	20
$\pm 45$ Tension	A. Graphite	5	5	5	5	20

Total number of tests is 240 for two resins.

resins (5 replicates each). The interlaminar tension test is applied only to the hybrid coupons.

- c. Room temperature test of the graphite  $\pm 45^\circ$  tensile coupons and both all graphite and graphite/Kevlar hybrid specimens preconditioned by one week immersion in hydraulic fluid at room temperature. Test both resins in  $0^\circ$  flexure, interlaminar tension, and interlaminar shear (5 replicates each). The interlaminar tension test is applied only to the hybrid coupons.
- d. Elevated temperature test 344K (160°F) of the graphite  $\pm 45^\circ$  tensile coupons and both all graphite and graphite/Kevlar hybrid specimens preconditioned by one week immersion in water 325K at (125°F). Test both resins in  $\pm 45^\circ$  tension,  $0^\circ$  flexure, interlaminar tension, and interlaminar shear (5 replicates each). The interlaminar tension test is applied only to the hybrid coupons.
- e. Elevated temperature test 344K (160°F) unconditioned (dry) specimens.

Note that instrumentation is not required for any of these tests. However, deflection versus load should be recorded for the flexure tests and an extensometer should be used to determine elongation versus load for the  $\pm 45^\circ$  tensile coupons.

- Task 5: Fabricate 152 mm (6 in.) by 152 mm (6 in.) panels of 0/90 configuration. Reheat in an oven several times to determine temperature at which panel becomes flat. Cool to room temperature and record height at center of panel to determine warp curvature.
- Task 6: A written test report is required.

**REPRODUCIBILITY OF THE  
ORIGINAL PAGE IS POOR**



## REFERENCES

1. Flight Service Evaluation of an Advanced Composite Empennage on Commercial Transport Aircraft, Quarterly Technical Report - No. 2 NAS 1-14000, Lockheed-California Company, 1 October 1975.
2. Air Force Materials Laboratory; Advanced Composite Design Guide - Volume II, Analysis, Third Edition, January 1973.
3. Verette, R.M.: Temperature/Humidity Effects on the Strength of Graphite/Epoxy Laminates; AIAA Paper No. 75-1011, August 1975.
4. Seydel, E.: Uber das Ausbeulen von rechteckigen, isotropen oder orthogonally - anisotropen platten bei Schubbeanspruchung. Ingenieur-Archiv, Vol. IV, Band 1933.
5. Timoshenko: and Gere:, Theory of Elastic Stability. Second Edition, 1961.
6. Graphite/Epoxy, Boron-Graphite/Epoxy Hybrid and Boron/Aluminum Design Allowables; AFML-TR-72-232, Grumman Aerospace Corporation, December 1972.
7. Structural Design Loads Criteria, L1011, LR 21611, Lockheed-California Company, August 1968.